

# **RPSEA**

# ***FINAL REPORT***

***07122.17.01***



## ***Geological Foundation for Production of Natural Gas from Diverse Shale Formations***

**Contract 07122-17**

**July 30, 2011**

Principal Investigator: Jack C. Pashin  
Title: Director, Energy Investigations Program  
Geological Survey of Alabama  
P.O. Box 869999, Tuscaloosa, AL 35406

## **LEGAL NOTICE**

**This report was prepared by the Geological Survey of Alabama as an account of work sponsored by the Research Partnership to Secure Energy for America, RPSEA. Neither RPSEA members of RPSEA, the National Energy Technology Laboratory, the U.S. Department of Energy, nor any person acting on behalf of any of the entities:**

- a. MAKES ANY WARRANTY OR REPRESENTATION, EXPRESS OR IMPLIED WITH RESPECT TO ACCURACY, COMPLETENESS, OR USEFULNESS OF THE INFORMATION CONTAINED IN THIS DOCUMENT, OR THAT THE USE OF ANY INFORMATION, APPARATUS, METHOD, OR PROCESS DISCLOSED IN THIS DOCUMENT MAY NOT INFRINGE PRIVATELY OWNED RIGHTS, OR**
- b. ASSUMES ANY LIABILITY WITH RESPECT TO THE USE OF, OR FOR ANY AND ALL DAMAGES RESULTING FROM THE USE OF, ANY INFORMATION, APPARATUS, METHOD, OR PROCESS DISCLOSED IN THIS DOCUMENT.**

**THIS IS AN INTERIM REPORT. THEREFORE, ANY DATA, CALCULATIONS, OR CONCLUSIONS REPORTED HEREIN SHOULD BE TREATED AS PRELIMINARY. REFERENCE TO TRADE NAMES OR SPECIFIC COMMERCIAL PRODUCTS, COMMODITIES, OR SERVICES IN THIS REPORT DOES NOT REPRESENT OR CONSTITUTE AN ENDORSEMENT, RECOMMENDATION, OR FAVORING BY RPSEA OR ITS CONTRACTORS OF THE SPECIFIC COMMERCIAL PRODUCT, COMMODITY, OR SERVICE.**

## **ABSTRACT**

Shale gas development is taking place in multiple Paleozoic formations in the Black Warrior basin and the Appalachian thrust belt of Alabama. The diversity of these formations, which range in age from Cambrian to Mississippian, provides an excellent opportunity to examine shale formations with a wide range of reservoir properties in varied geologic settings. To facilitate the development of shale gas reservoirs in the region, this study employs a systematic, multidisciplinary approach to the evaluation of shale reservoirs. Key geologic variables addressed are stratigraphy, sedimentation, structure, hydrodynamics, geothermics, petrology, geochemistry, gas storage, and permeability.

Stratigraphy and sedimentation are important because many of the fundamental characteristics of shale are determined in the original depositional environment. Alabama shale reservoirs were deposited in euxinic sedimentary basins that were influenced by the development of cratonic carbonate ramps and orogenic foreland basins. Numerous sedimentary processes were active in these basins, and secular variation of physical, geochemical, and biological processes resulted in complex stratigraphic architecture and heterogeneous reservoir quality, which are important considerations for shale gas development. Folding and faulting affect the geometry and continuity of reservoirs, and fracturing affects subsurface flow and the applicability of completion technology to shale formations. The Black Warrior basin and Appalachian thrust belt contain a spectrum of extensional and compressional tectonic structures, and these structures are expressed differently in each target shale formation.

Hydrodynamics and geothermics in the study area are influenced by recharge along the frontal Appalachian structures, as well as gas pressure in the interiors of deep geologic structures. Heterogeneous permeability in stacked geologic formations is a key determinant of subsurface fluid chemistry and reservoir pressure. All shale formations examined in this study have generated thermogenic hydrocarbons in the geologic past, and hydrocarbon pressure persists today in many areas. Modern reservoir temperatures range greatly depending on depth and geothermal gradient, and deep, warm reservoirs can have vastly different reservoir properties than shallow, cool reservoirs.

Petrology and geochemistry are important for characterizing reservoir quality. All shale formations studied contain a broad suite of detrital and authigenic minerals. Rock fabric was influenced by sedimentation, diagenesis, and hydrocarbon generation, and the degree of alignment of platy clay minerals appears to reflect structure and basin hydrodynamics. Detrital and authigenic minerals, moreover, affect shale geomechanics and the applicability of hydraulic fracturing technologies. Most prospective shale reservoirs can be classified as type III or IV source rocks that are sufficiently mature to have exhausted most hydrocarbon generative potential. However, analysis of gas storage and mobility indicates that the shale units have favorable reservoir properties. Shale is a dual-porosity reservoir in which some gas is stored in a free state, and some is adsorbed on organic matter.

OGIP in the Alabama shale formations is estimated to be about 826 Tcf. Technically recoverable resources in areas with significant development potential are estimated to be between 70 and 139 Tcf. Hence, the prospective shale formations contain enough natural gas to have a major impact on domestic gas reserves. Important technical hurdles that must be overcome to bring these resources to market include the development of completion technologies for giant, tectonically deformed shale masses, as well as development strategies for thin shale formations.

**SIGNATURE AND DATE STAMP**

A handwritten signature in black ink, appearing to read "J. P. Ri".

---

August 15, 2011

Head, Energy Investigations Program  
Geological Survey of Alabama

Geological Survey of Alabama  
Berry H. (Nick) Tew, Jr.  
State Geologist

ENERGY INVESTIGATIONS PROGRAM

**Geological Foundation for Production of Natural Gas  
from Diverse Shale Formations**

**FINAL REPORT**

Reporting Period: August 19, 2008-July 30, 2011

**Geological Survey of Alabama Open-File Report 1110**

by

Jack C. Pashin, David C. Kopaska-Merkel,  
Ann C. Arnold, and Marcella R. McIntyre

Geological Survey of Alabama  
P.O. Box 869999, Tuscaloosa, AL 35486-6999

Prepared by the Geological Survey of Alabama  
in partial fulfillment of an agreement with the Research Partnership to Secure Energy for  
America (RPSEA) under Subcontract 07122-17

Tuscaloosa, Alabama  
August 2011

## EXECUTIVE SUMMARY

Shale gas reservoirs in the Black Warrior basin and Appalachian thrust belt are diverse, occurring in Cambrian, Silurian, Devonian, and Mississippian strata. Development in this area has been affected by uncertainty about best practices for reservoir evaluation, exploration, and completion. Indeed, an integrated, multidisciplinary approach is required to evaluate shale and is the focus of this study. Key geologic variables to be considered when exploring shale reservoirs, are stratigraphy, sedimentation, structure, hydrodynamics, geothermics, petrology, geochemistry, gas storage, and permeability.

Many characteristics of shale gas reservoirs are determined in the original depositional environment, thus stratigraphy and sedimentation are critical variables. Shale gas reservoirs in Alabama were deposited on the North American craton as organic-rich mud in euxinic sedimentary basins. These basins formed in extensional and compressional tectonic settings contemporaneously with Iapetan rifting and Appalachian-Ouachita foreland basin development. Processes within the euxinic basins were varied and were influenced by the development of coeval carbonate ramps and siliciclastic coastal plains and shelves. In all formations studied, black shale deposition was highly dynamic, reflecting changing redox conditions, variable sediment and nutrient flux, and reworking by storms. The result of these processes was a complex stratigraphic architecture that gave rise to heterogeneous facies and reservoir quality.

Geologic structure affects the geometry, continuity, and permeability of shale gas reservoirs. Extensional faults are common in the Black Warrior basin and reflect a multiphase tectonic development that spanned Paleozoic time. The faults are developed above multiple detachments, including a thick-skinned, mid-crustal detachment and thin-skinned detachments at the top of the Cambrian shale section and within the Carboniferous synorogenic clastic wedge. These faults

pose significant risk for leakoff of stimulation fluid during well completion, so careful mapping is required to define coherent structural panels favorable for shale gas development. Thrust belt structures in Alabama include giant antiformal stacks in Cambrian Conasauga shale and ramp-flat structure in younger strata. Structural deformation in the antiformal stack has resulted in shale accumulations thicker than 12,000 feet but poses challenges for drilling and completion. Fold hinges in ramp-flat structures may be associated with productivity sweet spots, but can also be sources of co-produced water that must be managed responsibly. Fracture networks, including joints and shear zones, are common in the shale gas reservoirs and appear to form important hydraulic conduits in shallow shale reservoirs. Fractures in deep reservoirs are cemented, and petrologic analysis indicates that the fractures have hosted fluids that have alternated between alkaline and acidic and included carbonate scavenged by dissolution of older sediment and rock. Major shear zones can be associated with significant gas shows, but caution should be applied because of the potential for leakoff of stimulation fluid.

Hydrodynamics and geothermics are strong determinants of shale reservoir characteristics. Fluid chemistry and reservoir pressure are influenced strongly by recharge along the Appalachian frontal structures. Significant gas pressure, by contrast, exists in the deep parts of the Black Warrior basin and the Appalachian thrust belt and resulted in a blowout in the Conasauga shale. Modern reservoir temperatures are related to the depth of target formations, and geothermal gradients in the region are generally between 9 and 15°F per thousand feet. Shallow shale reservoirs in the frontal Appalachians can be classified as shallow, cool reservoirs, whereas those in the deep subsurface are substantially warmer and thus have different gas reservoir properties. Petrologic evidence indicates that the shale reservoirs were substantially warmer in the geologic past than they are today, and burial history modeling indicates that major

thermogenic gas generation was associated with synorogenic tectonic subsidence during Carboniferous and Permian time.

Petrology and geochemistry are critical determinants of reservoir quality. Detrital minerals are dominated by clay, quartz, and carbonate. Authigenic minerals include pyrite, calcite, dolomite, silica, and illite. SEM analysis was used to evaluate shale fabric, which represents a network of detrital minerals, authigenic minerals, organic matter, and porosity. As such, the rock fabric is the product of sedimentation, compaction, diagenesis, and hydrocarbon generation. Weak alignment of platy clay minerals in Cambrian shale appears to reflect overpressuring related to formation of the giant antiformal stacks. Devonian shale is distinctive because it contains biogenic silica formed by radiolarians and sponges that may help contribute to the brittleness of the shale and may thus facilitate effective hydraulic fracture treatments. Organic matter in the shale gas reservoirs is dominated by matrix bituminite and includes minor amounts of vitrinite, liptinite, and inertinite. Most of the prospective reservoirs can be classified as type III to type IV source rocks. Geochemical evidence points toward an evolution from sapropelic source material toward thermally mature kerogen that has exhausted most if not all of its generative potential. Although the generative potential is largely exhausted, the shale is capable of storing large volumes of natural gas.

Shale is a dual-porosity reservoir in which some gas is stored in a free state, and some is adsorbed on organic matter and minerals with high surface area. Effective porosity in Alabama gas shale is between 1.2 and 7.7 percent, and about 68 percent of the pore volume is capable of free gas storage. Pressure-decay permeability averages 0.191 microdarcies and is locally as high as 0.393 microdarcies. Adsorption isotherms indicate that Langmuir volume is as high as 128 standard cubic feet per ton, and adsorption capacity correlates directly with total organic carbon

content. Langmuir pressure in the Paleozoic shale units is between 526 and 1,012 pounds per square inch (absolute), which indicates significant sorbed gas mobility at elevated initial reservoir pressure. Free gas is mobile across a spectrum of pressure-temperature conditions. Sorbed gas, by contrast, has greatest mobility at low reservoir pressure, where the isotherm is steep. In addition, the adsorption capacity of organic matter decreases as reservoir temperature increases. Therefore, the adsorbed gas fraction is most mobile in shallow, cool geologic settings, which are common in the frontal Appalachians. Original gas-in-place in the Alabama shale formations is estimated to be about 826 trillion cubic feet (Tcf). Technically recoverable resources in areas with significant development potential are estimated to be between 70 and 139 Tcf. Hence, the prospective shale formations contain enough natural gas to have a major impact on domestic gas reserves. Important technical hurdles that must be overcome to bring these resources to market include the development of completion technologies for giant, tectonically deformed shale masses, as well as development strategies for thin shale formations.

## CONTENTS

Executive summary .....	ii
Contents .....	vi
Abstract .....	1
Introduction .....	3
Geologic setting .....	6
Stratigraphic setting .....	6
Tectonic setting .....	10
Analytical methods .....	14
Stratigraphy and sedimentation .....	19
Conasauga shale .....	19
Devonian shale .....	33
Neal (Floyd) shale .....	44
Structural geology .....	52
Extensional faults in the Black Warrior basin .....	52
Compressional structures in Conasauga shale .....	56
Compressional structures in Devonian shale .....	64
Fracture networks .....	68
Hydrodynamics and geothermics .....	75
Porosity and permeability .....	66
Water chemistry .....	79
Reservoir pressure and geothermics .....	81
Petrology and geochemistry .....	88
Detrital composition .....	89
Authigenesis .....	99
Vein fills .....	104
Organic petrology .....	107
Microfabric .....	111
Gas storage and permeability .....	123
Porosity and permeability .....	124
Adsorption .....	130
Shale Gas Resources and Reserves .....	135
Summary and conclusions .....	144
Acknowledgments .....	148
References cited .....	149

## Illustrations

Figure 1.—Generalized map showing location of shale-gas development areas in Alabama .....	4
Figure 2.—Conceptual model of shale gas producibility based on key geologic variables .....	5
Figure 3.—Balanced structural cross sections of the southern Appalachian thrust belt in Alabama .....	8
Figure 4.—Regional cross section showing the relationship of the Chattanooga Shale and correlative black shale formations to the Acadian clastic wedge .....	9
Figure 5.—Regional cross section showing facies relationships in Devonian-Mississippian strata of the Black Warrior basin .....	10
Figure 6.—Structural contour map of the top of the Tuscumbea Limestone in the Black Warrior basin of Alabama.....	12
Figure 7.—Geologic map of the frontal Appalachian structures showing areas of shale gas development .....	13
Figure 8.—Generalized depositional model of the Conasauga Formation in Alabama .....	21
Figure 9.—Photographs of Conasauga shale in core from the Dawson 33-09 #2A well, Big Canoe Creek Field.....	22
Figure 10.—Laminated shale and interbedded micrite in Conasauga shale, Pinedale Lake Spillway, St. Clair County, Alabama.....	23
Figure 11.—Subparallel and ripple cross-laminae in Conasauga shale from the Dawson 33-09 #2A well, Big Canoe Creek Field, 7554.6 ft .....	23
Figure 12.—Trace and body fossils in the Dawson 34-03-01 exploratory core, Big Canoe Creek Field.....	25
Figure 13.—Pinstripe-laminated shale and limestone in the Conasauga Formation .....	26
Figure 14.—Nodular- and wavy-bedded limestone and shale in the Dawson 34-03-01 core .....	27
Figure 15.—Conglomeratic limestone in the Dawson 34-03-01 core .....	28
Figure 16.—Conglomeratic limestone and shale in the Dawson 34-03-01 core containing convolute bedding .....	29
Figure 17.—Limestone and shale in upper part of the Dawson 34-03-01 core .....	31
Figure 18.—Outcrop of Chattanooga Shale at Big Ridge, Etowah County, Alabama .....	33
Figure 19.—Measured section of the Chattanooga Shale at Big Ridge, Etowah County, Alabama .....	35
Figure 20.—Isopach map of the Chattanooga Shale in the Black Warrior basin and unnamed Devonian shale in the Greene-Hale synclinorium of Alabama.....	36
Figure 21.—Geophysical well log and mud log showing relationship of gas shows to the Ordovician-Mississippian section in the Bayne-Etheridge 36-9 #1 well.....	37

Figure 22.—Core photographs of Devonian shale in the Black Warrior basin and the Appalachian thrust belt of Greene County, Alabama .....	39
Figure 23.—Black shale with ripple cross-strata, erosional discontinuities, and pyrite nodules .....	40
Figure 24.—Photomicrograph showing radiolarians and detrital quartz in the Chattanooga Shale .....	41
Figure 25.—Depositional model showing sedimentary processes in Devonian black shale and related strata in the Appalachian region .....	42
Figure 26.—Depositional model for Devonian shale in the Black Warrior basin and the Greene-Hale synclinorium .....	43
Figure 27.—Photos of Neal shale in the Exum Trust 16-6 #1 well, Pickens County, Alabama .....	47
Figure 28.—Depositional model of an idealized 3 <sup>rd</sup> -order parasequence in Upper Mississippian strata of the Black Warrior basin .....	48
Figure 29.—Isopach map of the Neal shale in the Black Warrior basin of Alabama.....	49
Figure 30.—Isopach map of the Pride Mountain Formation, Hartselle Sandstone, and equivalent strata in the Neal shale in the Black Warrior basin of Alabama .....	50
Figure 31.—Isopach map of the Bangor Limestone and equivalent strata in the Neal shale of the Black Warrior basin in Alabama .....	51
Figure 32.—Isopach map of the lower Parkwood Formation and equivalent strata in the Neal shale of the Black Warrior basin in Alabama.....	51
Figure 33.—Structural trace map of the Black Warrior basin showing relationships among frontal Appalachian structures and normal faults in the Black Warrior basin.....	54
Figure 34.—Structural cross section showing multiple levels of normal faulting in the Black Warrior basin .....	55
Figure 35.—Structural cross section showing growth faults cutting basement in the Black Warrior basin .....	55
Figure 36.—Isopach map of deformed Conasauga shale constituting the Gadsden, Palmerdale, and Bessemer MUSHWADs.....	58
Figure 37.—Closely jointed Conasauga shale, Pinedale Lake Spillway, St. Clair County, Alabama .....	60
Figure 38.—Bed-parallel carbonate vein in Conasauga shale, Pinedale Lake Spillway, St. Clair County, Alabama .....	60
Figure 39.—En echelon veins, Conasauga shale, Pinedale Lake Spillway, St. Clair County, Alabama .....	61
Figure 40.—Mylonitic fault gouge, Conasauga shale, Pinedale Lake Spillway, St. Clair County, Alabama .....	61

Figure 41.—Chevron folds in Conasauga shale at Springville rest area, Interstate 59, St. Clair County, Alabama .....	62
Figure 42.—Tectonic deformation structures in the Dawson 34-03-01 core .....	63
Figure 43.—Structural interpretation based on seismic profile of the Wills Valley anticline and associated structures above a listric thrust fault .....	67
Figure 44.—Structural interpretation based on seismic profile of the Wills Valley anticline and associated structures above a thrust fault with multiple dip bends .....	67
Figure 45.—Structural interpretation based on seismic profile of ramp-flat thrust belt structure below the Gulf of Mexico coastal plain .....	68
Figure 46.—Outcrop in the backlimb of the Sequatchie anticline showing jointed Chattanooga Shale disconformably overlying the Silurian-age Red Mountain Formation .....	69
Figure 47.—Planar systematic joints in the Chattanooga Shale at Big Ridge, Etowah County, Alabama .....	69
Figure 48.—Conceptual model showing relationship of reservoir-scale deformation in shale to thrust belt structure .....	71
Figure 49.—Inclined shear fractures in the Chattanooga Shale at Big Ridge, Etowah County, Alabama .....	71
Figure 50.—Formation micro-imager and dipmeter logs showing complex deformation associated with gas shows in the Bayne-Etheridge 36-9 #1 well .....	73
Figure 51.—Strata-bound fractures filled with silica and calcite in Chattanooga Shale .....	75
Figure 52.—Mineralized fracture cutting across rock fabric, including radiolarians in Chattanooga Shale .....	76
Figure 53.—Mineralized fractures showing cement stratigraphy in Chattanooga Shale .....	77
Figure 54.—Idealized paragenetic sequence showing precipitation and dissolution events identified in the Chattanooga shale of the Black Warrior basin .....	77
Figure 55.—Corroded boundary between calcite and quartz in Neal shale.....	78
Figure 56.—Hydrodynamic model of shale gas reservoirs in the Appalachian thrust belt of Alabama .....	80
Figure 57.—Plot of vitrinite reflectance versus depth in the Conasauga shale of Big Canoe Creek Field, St. Clair County, Alabama .....	85
Figure 58.—Cross-plot of stable isotope data showing thermogenic origin of natural gas produced from the Conasauga Formation in Big Canoe Creek Field .....	86
Figure 59.—Plot of vitrinite reflectance versus depth in the Ralph W. Holliman 13-6 well, Pickens County, Black Warrior basin, Alabama .....	87
Figure 60.—Lopatin model of burial history and hydrocarbon generation, Robinson et al. well, Pickens County, Black Warrior basin, Alabama.....	88

Figure 61.—Photomicrograph showing detrital organic matter in dolomitic Conasauga shale .....	90
Figure 62.—Photomicrograph showing siliceous ovoids in Conasauga carbonate .....	93
Figure 63.—Photomicrograph showing detrital quartz and siliceous and calcareous fossil fragments.....	96
Figure 64.—Photomicrograph of organic-rich Neal shale.....	96
Figure 65.—Photomicrograph of limestone with pyrite-dented peloids in Neal shale.....	101
Figure 66.—SEM image of pyrite framboid, Chattanooga Shale.....	101
Figure 67.—SEM image of a sample from core of the Bayne Etheridge 36-9 #1 well, Greene County, Alabama (8,317 ft) showing illite forms in Devonian black shale.....	103
Figure 68.—Intensely recrystallized dolostone in Conasauga shale .....	103
Figure 69.—Cross-plot comparing the stable isotopic characteristics of vein fills in shale gas reservoirs in Alabama to those in coalbed methane reservoirs of the Black Warrior basin .....	105
Figure 70.—Relationship of isotopic composition of calcite veins to depth in the Conasauga Formation .....	106
Figure 71.—Results of kerogen analysis in the Conasauga shale of Big Canoe Creek Field, St. Clair County, Alabama .....	108
Figure 72.—Results of kerogen analysis in Devonian shale of the Black Warrior basin and the Greene-Hale synclinorium .....	110
Figure 73.—Results of kerogen analysis in the Neal shale of the Black Warrior basin, Alabama .....	112
Figure 74.—Map of calculated vitrinite reflectance in the Neal shale of the Black Warrior basin of Alabama .....	113
Figure 75.—Map of Tmax in the Neal shale of the Black Warrior basin of Alabama.....	114
Figure 76.—SEM image showing weakly aligned clay fabric of Conasauga shale .....	116
Figure 77.—SEM image showing aligned clay fabric of Chattanooga Shale, Lamb 1-3 #1 well, Greene County, Alabama.....	117
Figure 78.—Platy illite and calcite rhomb in Neal Shale .....	117
Figure 79.—Calcite with pock marks suggesting dissolution, Devonian shale.....	118
Figure 80.—Diverse pyrite forms in Chattanooga Shale.....	118
Figure 81.—Pyrite fracture fill in Chattanooga Shale .....	119
Figure 82.—Pyrite framboid with rounded and pitted crystals and clay overgrowth.....	119
Figure 83.—Row of pyrite framboids with clay overgrowth in Neal shale.....	120
Figure 84.—Pyrite crystals lining peloid in Neal shale .....	121

Figure 85.—Porosity and pore-filling clay in pyrite framboid .....	121
Figure 86.—Organic particle in Neal shale .....	122
Figure 87.—Sub-micrometer scale illite bridges demonstrating open porosity within the clay matrix of shale .....	124
Figure 88.—Generalized diagram showing gas storage mechanisms and their effect on the mobility of gas in shale .....	125
Figure 89.—Absolute methane adsorption isotherms from Devonian shale in the Bayne-Etheridge 36-9 #1 well, Greene County, Alabama .....	131
Figure 90.—Correlation between Langmuir volume and TOC content in Alabama gas shale .....	134
Figure 91.—Effect of temperature on methane adsorption in activated carbon .....	135
Figure 92.—Map of estimated original gas-in-place within the deformed Conasauga shale masses of the southern Appalachian thrust belt .....	138
Figure 93.—Map of estimated original gas-in-place in the Chattanooga shale of the Black Warrior basin and the unnamed Silurian-Devonian shale of the Greene-Hale synclinorium .....	139
Figure 94.—Map of estimated original gas-in-place in the Neal shale of the Black Warrior basin .....	141

### Tables

Table 1. Permeability and porosity of sandstone in the Black Warrior basin based on 989 conventional core analyses .....	80
Table 2. Results of geochemical analysis of natural gas produced from the Conasauga Formation in Big Canoe Creek Field .....	84
Table 3. Particle classes employed in this study .....	90
Table 4. Non-clay mineralogy of Conasauga shale .....	91
Table 5. Clay mineralogy of Conasauga shale.....	92
Table 6. Non-clay mineralogy of Devonian shale .....	93
Table 7. Clay mineralogy of Devonian shale.....	94
Table 8. Non-clay mineralogy of Neal shale .....	97
Table 9. Clay mineralogy of Neal shale.....	99
Table 10. Basic reservoir properties of Conasauga shale as determined by core analysis .....	126
Table 11. Basic reservoir properties of Devonian shale in the Greene-Hale synclinorium as determined by core analysis .....	127
Table 12. Basic reservoir properties of Chattanooga shale as determined by core analysis .....	128

Table 13. Basic reservoir properties of Neal shale as determined by core analysis .....	130
Table 14. Summary results of adsorption isotherm analysis in the Conasauga Formation .....	132
Table 15. Summary results of adsorption isotherm analysis in Devonian shale of the Greene-Hale synclinorium .....	132
Table 16. Summary results of adsorption isotherm analysis in Chattanooga shale .....	133
Table 17. Summary results of adsorption isotherm analysis in Neal shale .....	133
Table 18. Estimates of original gas in place and reserve potential based on deterministic volumetric analysis of prospective Alabama shale formations.....	137

### Plates

Plate 1.—Graphic log of Conasauga Formation, Big Canoe Creek Field .....	pocket
Plate 2.—Stratigraphic cross section of Devonian-Mississippian strata in the Black Warrior basin .....	pocket
Plate 3.—Stratigraphic cross sections of Ordovician-Mississippian strata in the Black Warrior basin and Appalachian thrust belt .....	pocket

## ABSTRACT

Shale gas development is taking place in multiple Paleozoic formations in the Black Warrior basin and the Appalachian thrust belt of Alabama. The diversity of these formations, which range in age from Cambrian to Mississippian, provides an excellent opportunity to examine shale formations with a wide range of reservoir properties in varied geologic settings. To facilitate the development of shale gas reservoirs in the region, this study employs a systematic, multidisciplinary approach to the evaluation of shale reservoirs. Key geologic variables addressed are stratigraphy, sedimentation, structure, hydrodynamics, geothermics, petrology, geochemistry, gas storage, and permeability.

Stratigraphy and sedimentation are important because many of the fundamental characteristics of shale are determined in the original depositional environment. Alabama shale reservoirs were deposited in euxinic sedimentary basins that were influenced by the development of cratonic carbonate ramps and orogenic foreland basins. Numerous sedimentary processes were active in these basins, and secular variation of physical, geochemical, and biological processes resulted in complex stratigraphic architecture and heterogeneous reservoir quality, which are important considerations for shale gas development. Folding and faulting affect the geometry and continuity of reservoirs, and fracturing affects subsurface flow and the applicability of completion technology to shale formations. The Black Warrior basin and Appalachian thrust belt contain a spectrum of extensional and compressional tectonic structures, and these structures are expressed differently in each target shale formation.

Hydrodynamics and geothermics in the study area are influenced by recharge along the frontal Appalachian structures, as well as gas pressure in the interiors of deep geologic structures. Heterogeneous permeability in stacked geologic formations is a key determinant of

subsurface fluid chemistry and reservoir pressure. All shale formations examined in this study have generated thermogenic hydrocarbons in the geologic past, and hydrocarbon pressure persists today in many areas. Modern reservoir temperatures range greatly depending on depth and geothermal gradient, and deep, warm reservoirs can have vastly different reservoir properties than shallow, cool reservoirs.

Petrology and geochemistry are important for characterizing reservoir quality. All shale formations studied contain a broad suite of detrital and authigenic minerals. Rock fabric was influenced by sedimentation, diagenesis, and hydrocarbon generation, and the degree of alignment of platy clay minerals appears to reflect structure and basin hydrodynamics. Detrital and authigenic minerals, moreover, affect shale geomechanics and the applicability of hydraulic fracturing technologies. Most prospective shale reservoirs can be classified as type III or IV source rocks that are sufficiently mature to have exhausted most hydrocarbon generative potential. However, analysis of gas storage and mobility indicates that the shale units have favorable reservoir properties. Shale is a dual-porosity reservoir in which some gas is stored in a free state, and some is adsorbed on organic matter.

Original gas-in-place in the Alabama shale formations is estimated to be about 826 trillion cubic feet (Tcf). Technically recoverable resources in areas with significant development potential are estimated to be between 70 and 139 Tcf. Hence, the prospective shale formations contain enough natural gas to have a major impact on domestic gas reserves. Important technical hurdles that must be overcome to bring these resources to market include the development of completion technologies for giant, tectonically deformed shale masses, as well as development strategies for thin shale formations.

## INTRODUCTION

The Black Warrior basin and Appalachian thrust belt of Alabama contain a diversity of emerging shale gas plays in Cambrian, Silurian-Devonian, and Mississippian strata (fig. 1). Development of these reservoirs has been slowed by uncertainty about best practices for exploration, drilling, and well completion. A large part of this uncertainty stems from limited knowledge of the basic geologic framework of the targeted shale formations. This uncertainty is compounded by major differences of composition, thickness, geometry, and fracture architecture that exist between the emerging shale reservoirs of the Black Warrior basin and Appalachian thrust belt and the established shale reservoirs in other regions.

Unconventional gas plays require an integrated, multidisciplinary approach to exploration and development, yet broadly applicable geologic models of resource distribution and producibility analogous to those for coalbed methane reservoirs (e.g., Pashin and others, 1991; Ayers and Kaiser, 1994; Pashin, 1998, 2007; Pashin and Groshong, 1998; Scott, 2002) are just beginning to be developed for shale gas reservoirs (e.g., Hill and Jarvie, 2007; Ross and Bustin, 2008). Shale formations in Alabama pose a broad range of technical challenges, and many of these challenges relate to insufficient characterization of the regional geologic framework, as well as an inadequate understanding of the fundamental geologic controls governing the producibility of shale gas. Therefore, a need exists to develop integrated geologic models for the emerging shale plays of the Black Warrior basin and Appalachian thrust belt that take into account the broad range of reservoir types and reservoir conditions (fig. 2). This type of approach has been applied to coalbed methane reservoirs of the Black Warrior basin, where an industry that was initially limited by technological and economic impediments now ranks third

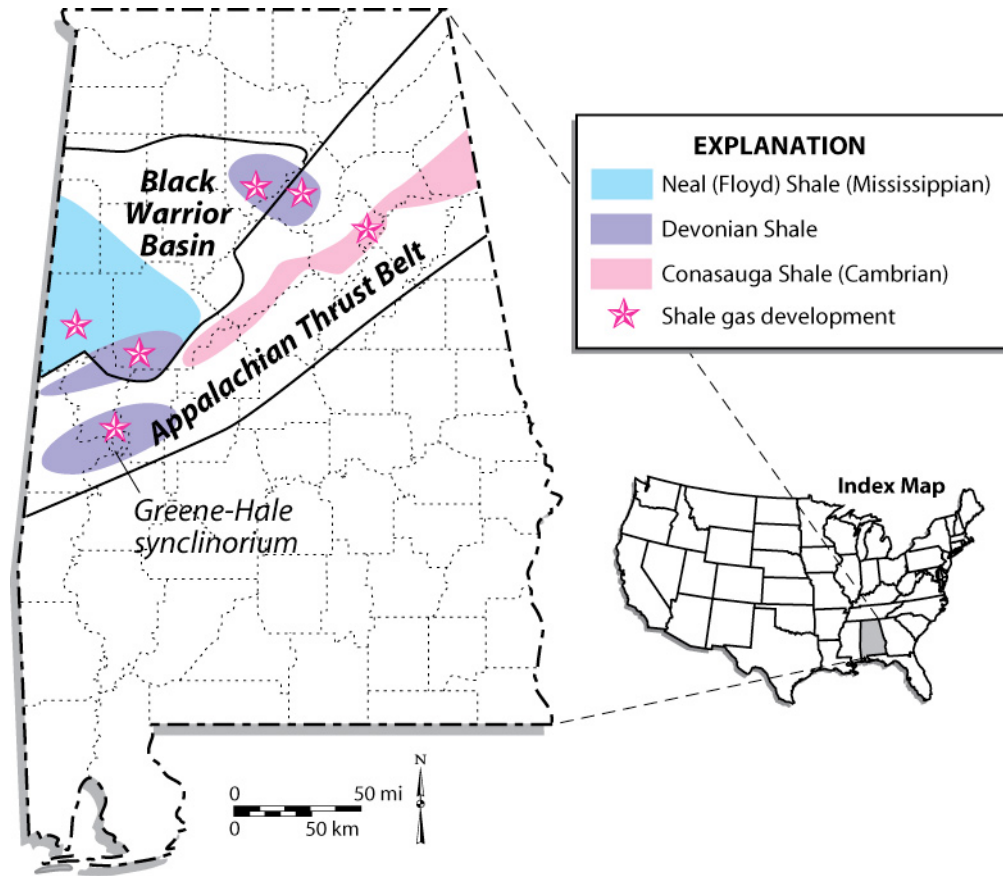


Figure 1.—Generalized map showing location of shale-gas development areas in Alabama.

globally in cumulative coalbed gas production (Pashin and others, 1991; Pashin and Hinkle, 1997; Pashin, 2010a). Applying a similar multidisciplinary approach to gas shale reservoirs is assisting the natural gas industry by providing new insights on the distribution of and producibility of shale gas resources (Pashin, 2008, 2009; Pashin, Carroll, and others, 2010; Pashin, Grace, and Kopaska-Merkel, 2010) (fig. 2). This type of approach affords flexibility that can be applied to a spectrum of emerging and frontier gas shale plays, thereby increasing the efficiency of exploration and development programs.

To assist in the development of emerging gas shale plays in Alabama, the Geological Survey of Alabama has completed a three-year study that provides a geologic foundation for exploration

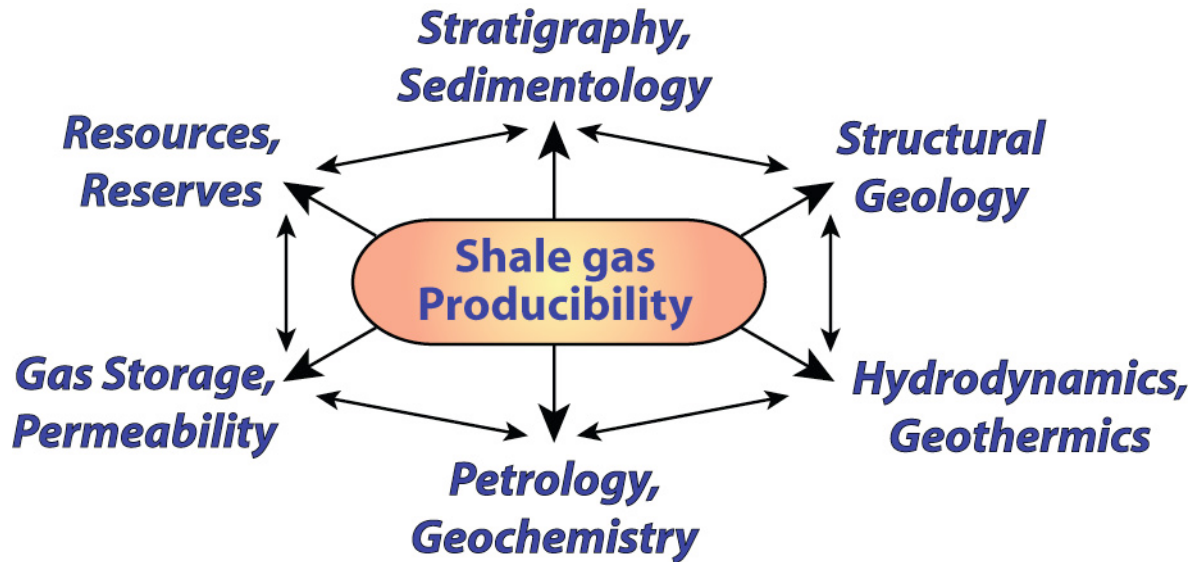


Figure 2.—Conceptual model of shale gas producibility based on key geologic variables.

and development. This study employed an integrated approach that draws on a spectrum of geologic disciplines (fig. 2). The general approach of this study is to systematically evaluate reservoir potential by characterizing the stratigraphy, sedimentology, geologic structure, hydrodynamics, geothermics, petrology, geochemistry, gas storage, and permeability of the shale formations. This characterization can then be used to define the resource and reserve base.

This report summarizes the results of work performed during this study, which was completed in July 2011. The report begins with an overview of the regional geologic setting of the shale gas plays and the analytical methods employed in this study. The discussion continues with a systematic evaluation of the stratigraphy, sedimentology, structural geology, hydrodynamics, geothermics, petrology, geochemistry, gas storage, and permeability. The results of this evaluation was used to develop a baseline determination of natural gas resources and reserves. This evaluation lays the foundation for determining the reservoir potential of each

prospective shale formation and further provides a framework that will help guide exploration and development.

## **GEOLOGIC SETTING**

Shale gas development focuses on fine-grained sedimentary rocks that are rich in organic matter. These rocks, commonly referred to as black shale, have long been recognized as important petroleum source rocks and reservoir seals. Natural gas has been produced commercially from organic-rich shale of the Appalachian region for well over a century, with the first recorded production in New York in 1821 (Martin, 2009) and in Kentucky between 1863 and 1865 (Nuttall and others, 2009). Recent developments in hydraulic fracturing technology have facilitated high gas production rates from shale and have had a strong impact on U.S. gas supply and markets (Hill and Jarvie, 2007).

Black shale can form in settings ranging from ocean basins to lakes. The basic requirements for deposition of black shale are the low-energy conditions associated with the accumulation of fine-grained sediment and the reducing conditions required for the preservation of organic matter. Although these requirements are fairly specific, the environments in which organic-rich shale accumulates are highly dynamic and host a diversity of sedimentary processes (e.g., Schieber and others, 1998), and this is true of the shale formations being developed in Alabama (Pashin, 2008, 2009; Pashin, Grace, and Kopaska-Merkel, 2010).

### **Stratigraphic Setting**

Shale plays in the Black Warrior basin and the Appalachian thrust belt are in the Middle-Upper Cambrian Conasauga Formation, Silurian-Devonian shale units that include the Devonian

Chattanooga Shale, and the Upper Mississippian Neal (Floyd) shale. The Conasauga Formation is composed of shale, limestone and dolostone and was deposited on a carbonate ramp (Astini and others, 2000; Thomas and others, 2000). The productive shale facies is in black shale with abundant nodules and thin beds of limestone and was deposited in outer ramp environments (Pashin, 2008). This shale facies was deposited in a graben that formed during late Precambrian-Early Cambrian Iapetan rifting and was deformed into giant shale masses during late Paleozoic Appalachian thrusting (Thomas, 2001; Thomas and Bayona, 2005) (fig. 3). The discovery of gas in the Conasauga Formation by Dominion Exploration and Production, Incorporated, was a landmark event. This discovery resulted in the first commercial gas production from shale in Alabama and the establishment of Big Canoe Creek Field, which is Alabama's first shale gas field. The Conasauga further has the distinction of being geologically the oldest and most structurally complex shale from which production of natural gas has been established.

Devonian shale is widespread in the Black Warrior basin and Appalachian thrust belt of Alabama, and development is active in multiple areas (fig. 1). The Chattanooga Shale is of Middle to Late Devonian age and is the most widespread black shale unit in Alabama. The shale is equivalent stratigraphically to the Ohio Shale of the Appalachian basin, the Antrim Shale of the Michigan basin, and the Woodford Shale of the southern Midcontinent region, which have produced gas for many years. The Chattanooga Shale has been interpreted as an euxinic basin facies that was deposited in a cratonic extension of the Acadian foreland basin (Pashin, Grace, and Kopaska-Merkel, 2010) (fig. 4). The Chattanooga is being developed in the Black Warrior basin along the frontal structures of the Appalachian thrust belt (Pashin, 2008, 2009; Pashin, Grace, and Kopaska-Merkel, 2010; Haynes and others, 2010). In the interior of the thrust belt below the Gulf Coastal Plain, potential has been recognized in a thick section of organic-rich

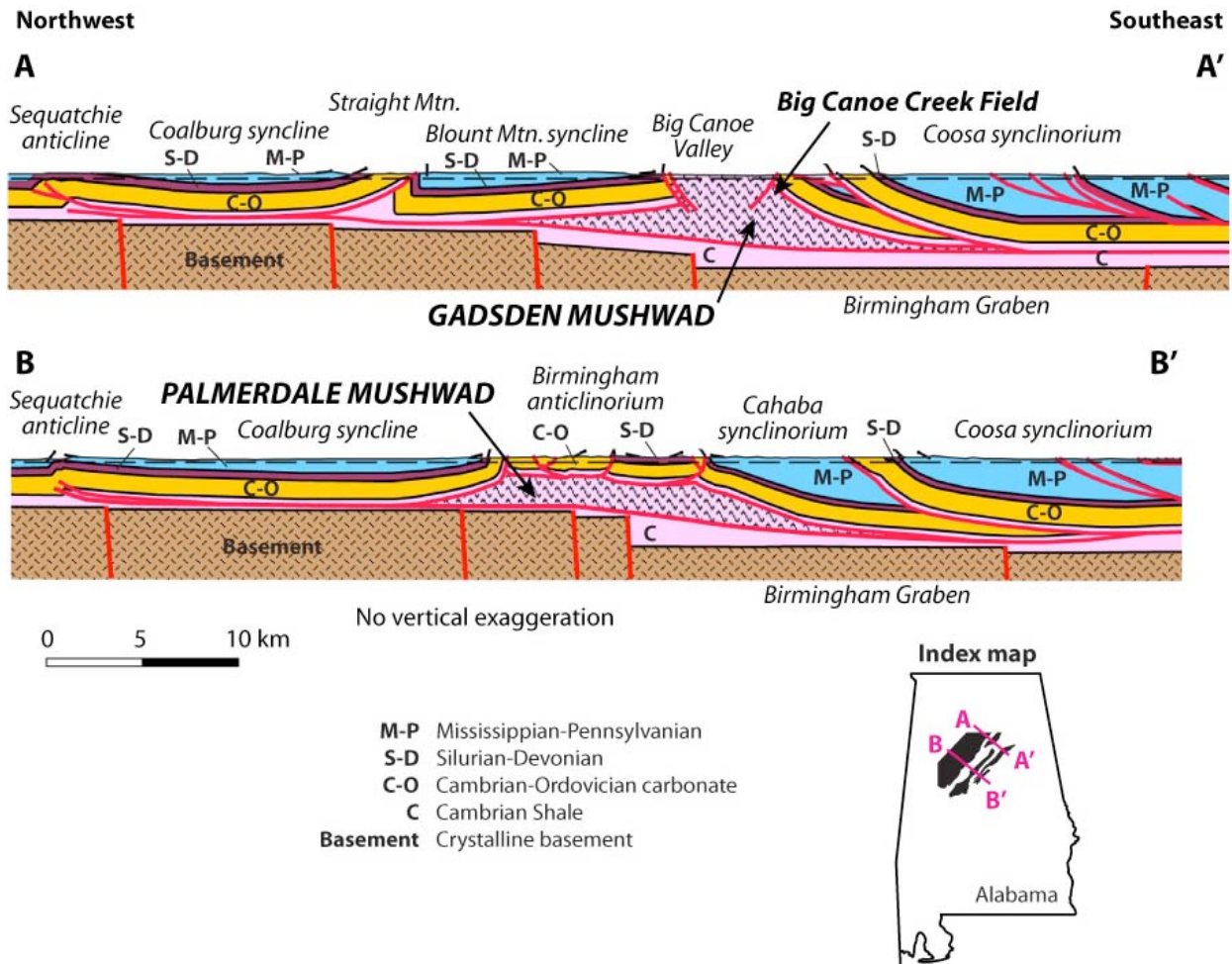


Figure 3.—Balanced structural cross sections of the southern Appalachian thrust belt in Alabama (modified from Thomas and Bayona, 2005).

shale that is interpreted to be of Silurian-Devonian age and includes Chattanooga equivalents (Pashin, Carroll and others, 2010; Pashin, Grace, and Kopaska-Merkel, 2010).

The Mississippian-age Neal (Floyd) shale (fig. 5) has been the subject of significant exploration activity in the Black Warrior basin and is a stratigraphic equivalent of the established gas shale reservoirs of the Barnett Shale of the Fort Worth basin and the Fayetteville Shale of the Arkoma basin. The Floyd has long been recognized as containing the principal source beds for conventional hydrocarbons in the Black Warrior Basin (e.g., Carroll and others,

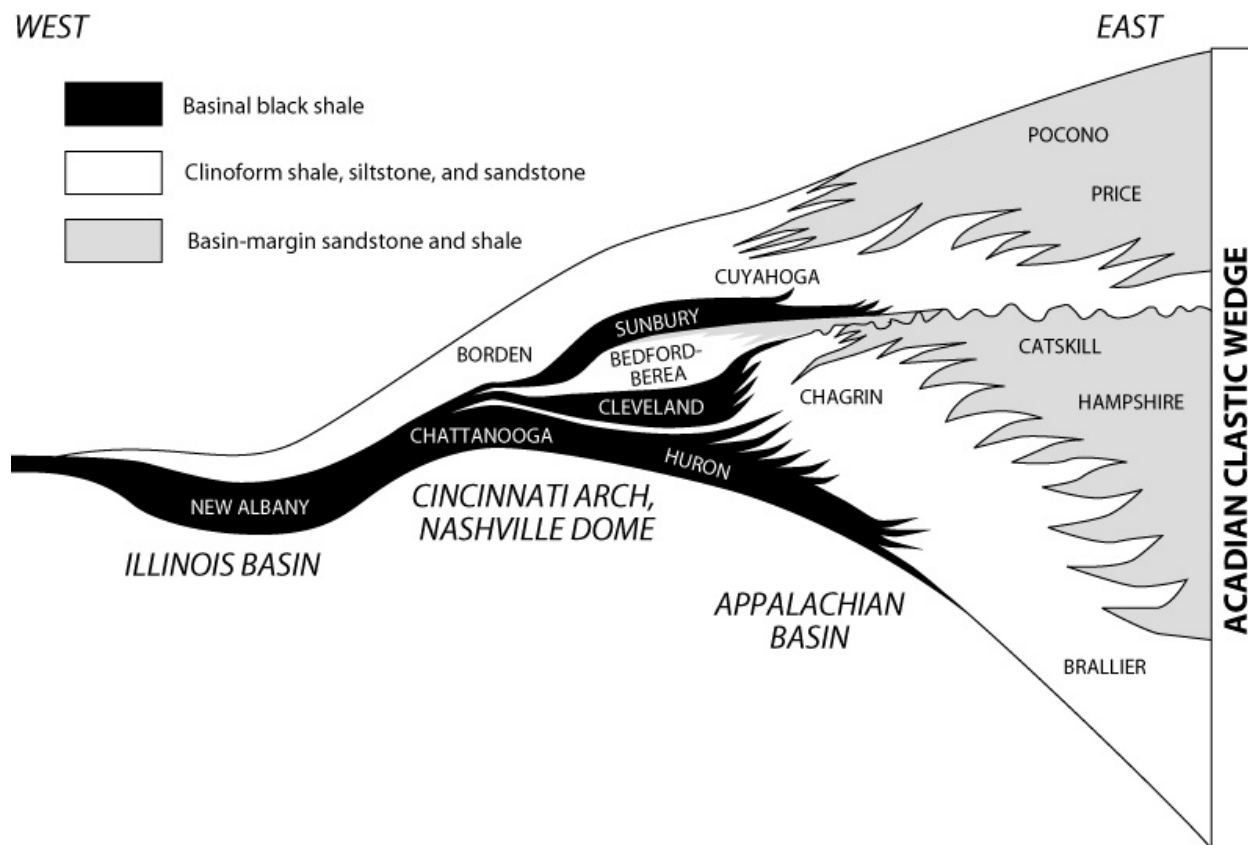


Figure 4.—Regional cross section showing the relationship of the Chattanooga Shale and correlative black shale formations to the Acadian clastic wedge (modified from Pashin and Ettensohn, 1995).

1995). However, the Floyd Shale is in complex facies relationship with a large number of siliciclastic and carbonate units and contains a varied suite of rock types that has caused some confusion in exploration and development. The Floyd constitutes organic-lean gray shale and limestone in most of the basin, whereas organic-rich black shale (called the Neal shale by drillers) is restricted to the southwestern part of the basin, where the shale was deposited in slope and basin-floor environments (e.g., Cleaves and Broussard, 1980; Pashin, 1993, 1994a). The greatest gas potential is in the Neal shale, which has been the subject of most exploration activity, but some wells have been drilled in search of gas in organic-lean facies of the Floyd.

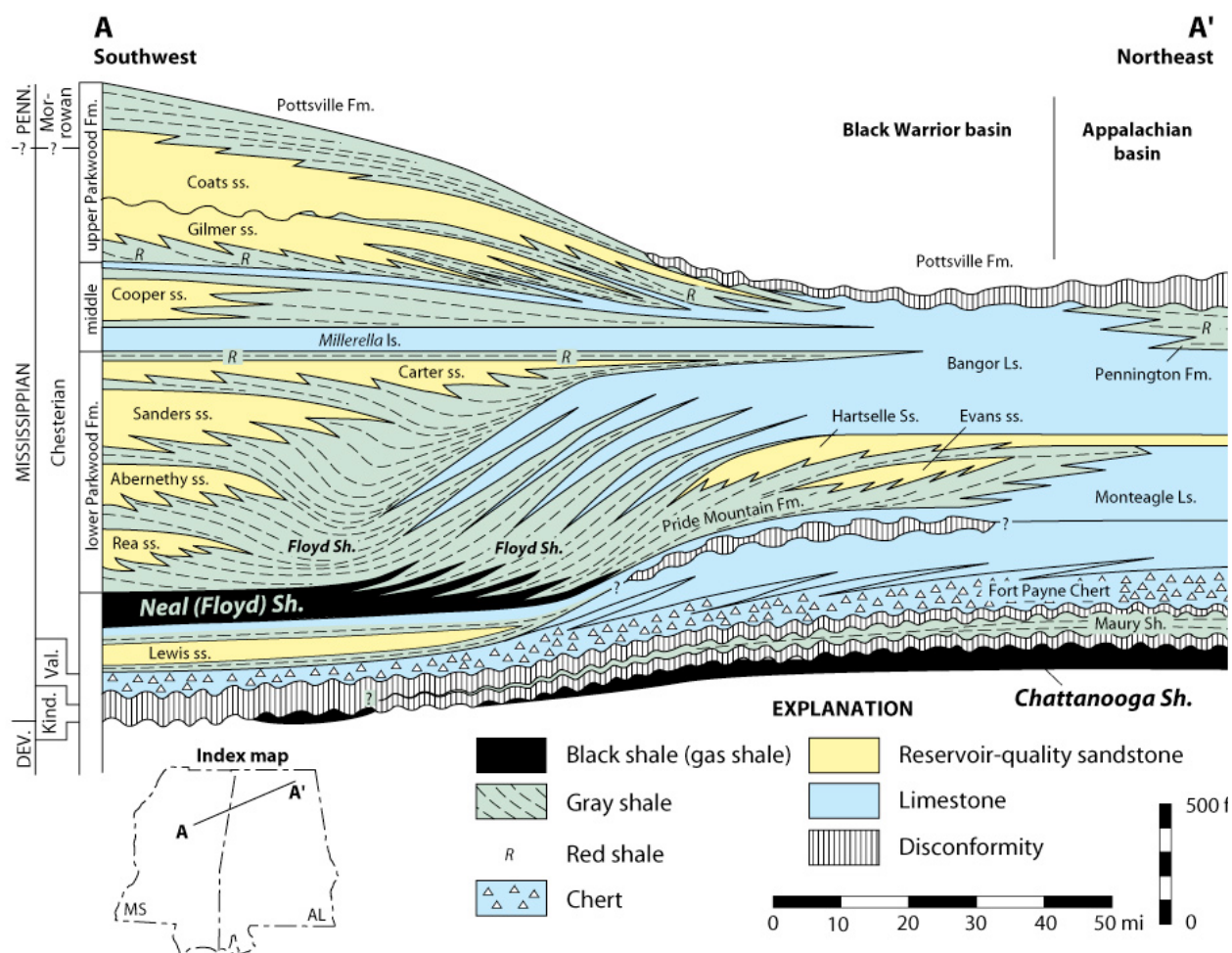


Figure 5.—Regional cross section showing facies relationships in Devonian-Mississippian strata of the Black Warrior basin (modified from Pashin, 1994a).

### Tectonic Setting

Folding, faulting, and fracturing are basic controls on the geometry, continuity, and permeability of shale formations, and shale gas reservoirs in Alabama are being developed in diverse and contrasting tectonic settings. In the Black Warrior basin, for example, development is focused on an extensional tectonic setting in which strata are subhorizontal and are weakly deformed. In the Appalachian thrust belt, by comparison, shale gas is being developed in a compressional tectonic setting in which strata are folded and faulted. Paleozoic strata of the Black Warrior basin and the Appalachian thrust belt are exposed in the northeastern part of the

study area. In the southwestern part, however, these strata are concealed below Cretaceous strata of the Gulf of Mexico basin, which dip gently southwestward, lack significant folds and faults, and overlie the Paleozoic section with angular unconformity.

The Black Warrior basin is a late Paleozoic foreland basin that formed adjacent to the juncture of the Appalachian and Ouachita orogenic belts (Thomas, 1977, 1988). The basin is developed on the Alabama Promontory, which is a protuberance of the Laurentian continental platform that formed during late Precambrian-Cambrian Iapetan rifting. The basin is a structural homocline that dips southwest toward the Ouachita orogen and is broken by numerous extensional faults (e.g., Thomas, 1988; Pashin and Groshong, 1998; Groshong and others, 2010) (fig. 6). These faults strike northwest; some have traces that extend for tens of miles and have displacement exceeding 1,000 feet. Appalachian folds and thrust faults strike northeast and are superimposed along the southeast margin of the homocline. Ouachita orogenesis was initiated along the southwest margin of the promontory during Mississippian time (Thomas, 1977). The Black Warrior can be considered to be mainly an Ouachita foreland basin, and major Appalachian thrust and sediment loads did not impinge on the southeastern part of the basin until Early Pennsylvanian time (Pashin, 2004). However, evidence exists for a Devonian subsidence event along the southeastern margin of the promontory that is coeval with the Acadian Orogeny (Pashin, Grace, and Kopaska-Merkel, 2010).

The Appalachian thrust belt separates the gently dipping strata of the Black Warrior basin from the igneous-metamorphic internides of the Appalachian orogen. The thrust belt is composed of deformed pre-orogenic carbonates of Cambrian through Mississippian age and synorogenic siliciclastic rocks of Late Mississippian and Early Pennsylvanian age (e.g., Thomas, 1985; Thomas and Bayona, 2005) (figs. 3, 7). The frontal part of the thrust belt, where

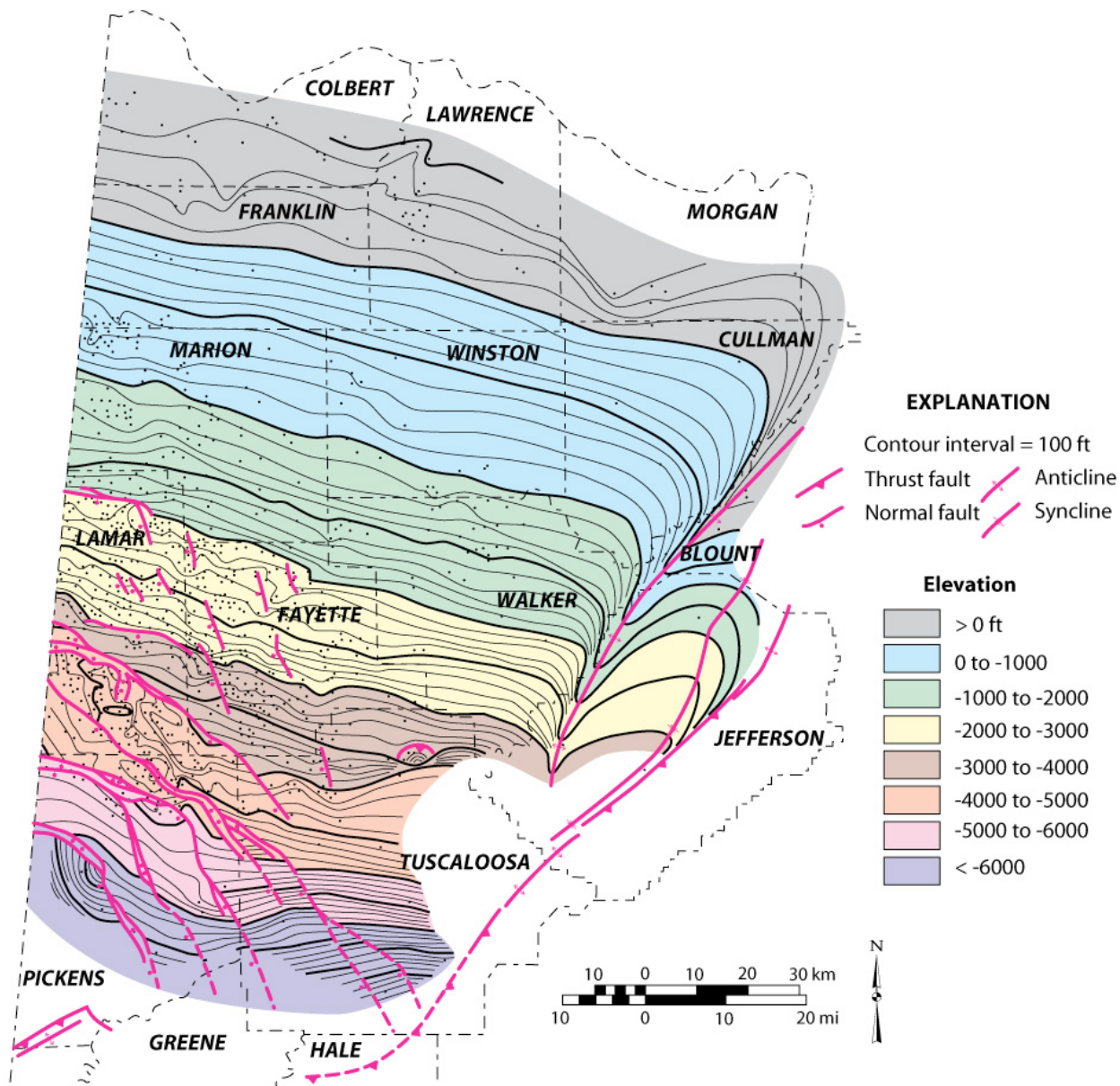


Figure 6.—Structural contour map of the top of the Tuscumbia Limestone in the Black Warrior basin of Alabama (modified from Pashin, 1993).

shale gas exploration has been concentrated, is dominated by thin-skinned deformation in which Paleozoic strata have been translated northwestward above a basal detachment in Cambrian shale (Rodgers, 1950; Thomas, 1985). The Cambrian shale, which includes the Conasauga Formation, forms a geomechanically weak lithotectonic unit that not only hosts the basal detachment but is, in places, duplicated into giant antiformal stacks that are locally thicker than 12,000 feet

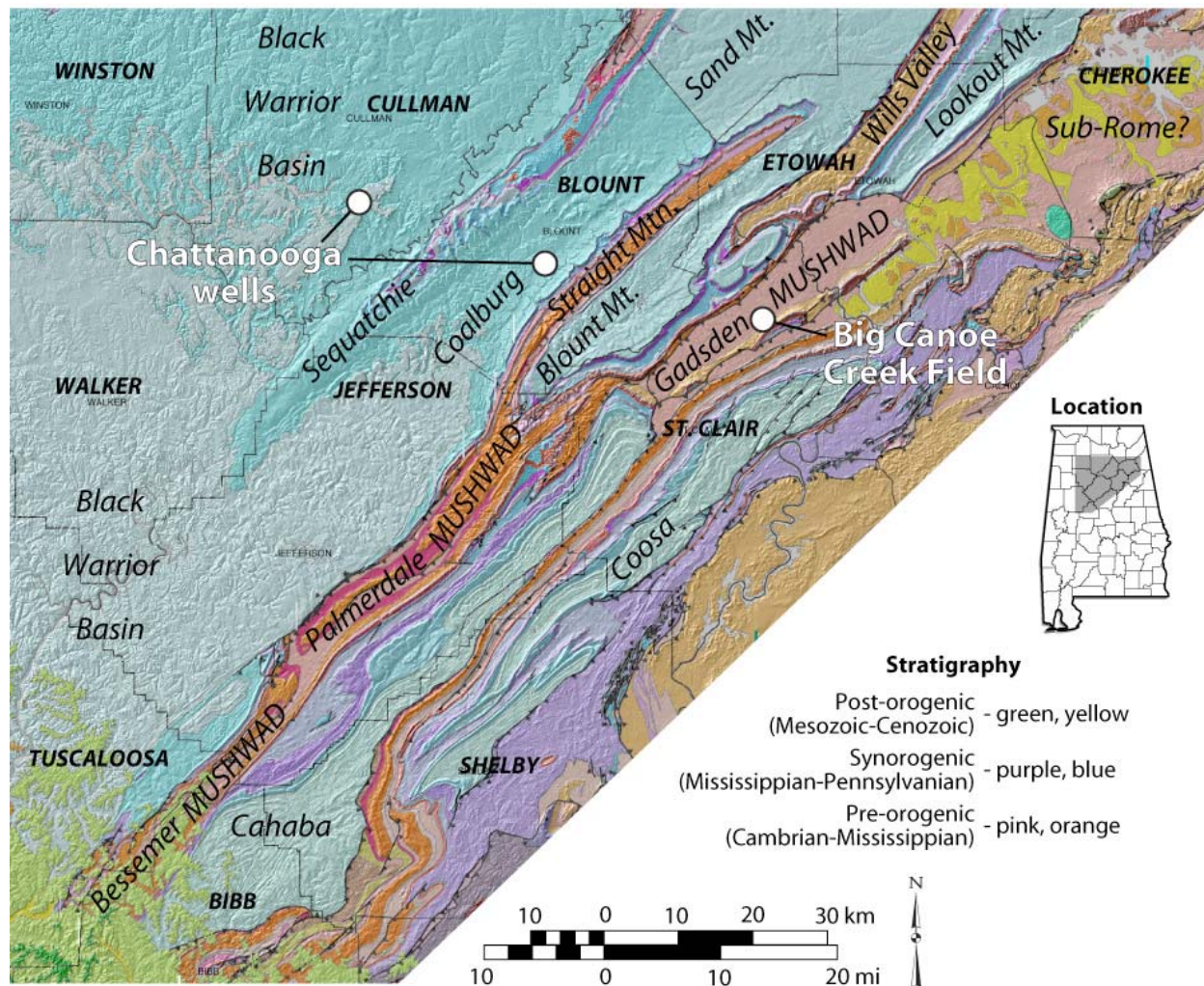


Figure 7.—Geologic map of the frontal Appalachian structures showing areas of shale gas development (modified from Pashin, 2008, 2009).

(Thomas, 2001). The pre-orogenic carbonate section, by contrast, is a stiff mechanical layer that hosts frontal and lateral thrust ramps that dictate structural geometry above the basal detachment, and secondary detachments are developed locally in the Silurian-Devonian section (Thomas and Bayona, 2005). The synorogenic siliciclastic section constitutes a weak geomechanical unit that was transported cratonward along with the pre-orogenic carbonates and locally hosts upper-level and secondary detachments (Thomas, 1985; Pashin and Groshong, 1998; Thomas and Bayona, 2005). This mechanical stratigraphy has resulted in a distinctive suite of faults, folds, and

fracture systems that should be taken into consideration when formulating shale gas development strategies.

## **ANALYTICAL METHODS**

The multidisciplinary approach of this study (fig. 2) necessitates that a great range of analytical methods be applied to characterize shale gas formations. This section provides an overview of the basic materials and methods used in this study. The basic materials employed in this research include outcrops, cores, well logs, and seismic profiles. Methods include standard stratigraphic, sedimentologic, and structural procedures for rock description, correlation, mapping, cross-section construction, and interpretation. Hydrodynamic and geothermic analysis relied mainly on well records, as well as application of fundamental hydrogeologic principles to the regional geological framework. In addition, a battery of petrologic procedures, including tight-rock analysis and isotherm analysis, were employed to characterize petrology, geochemistry, gas storage, and permeability. A deterministic approach to reservoir volumetrics was used to estimate gas resources and reserves.

To determine the stratigraphic, sedimentologic, and structural architecture of the shale gas reservoirs, geophysical well logs from throughout the Black Warrior basin and Appalachian thrust belt of Alabama were correlated. A series of stratigraphic cross sections depicting geophysical well logs were constructed to analyze stratal markers and geometry in prospective black shale units, as well as the associated carbonate and siliciclastic strata. Faults were also identified as wells were correlated. Normal faults were identified on the basis of missing section, whereas thrust faults were identified on the basis of repeated section. To facilitate subsurface mapping, stratigraphic, structural, and well-location data from 1,089 wells were assembled into a

database using Petra software. Structural data include bed elevation and fault-cut information. The elevation of each stratigraphic marker was computed by subtracting depth from the appropriate structural datum, which is typically the elevation of the kelly bushing. The depth, elevation, and vertical separation were determined and recorded for each fault cut identified. Maps of shale thickness and geologic structure were made using Petra software and were gridded and contoured in Petra using a minimum curvature algorithm.

Cores and outcrops of the studied shale units were described using standard procedures. Cores are stored at the Geological Survey of Alabama and are accessible to the public. Cores and outcrops were measured with a tape, and rock types, grain size, color, and sedimentary structures were described. Occurrences of trace fossils and body fossils were recorded. Faults and fractures were identified and described. The data were compiled into measured sections that include graphic logs. In outcrop major structural attributes were recorded, such as the attitude and geometry of bedding, faults, fractures, and folds. Seismic profiles donated to the Department of Geological Sciences at the University of Alabama by Shell Western and Vastar Resources were used to analyze large-scale structural geometry and refine balanced structural cross sections of the Black Warrior basin and the Appalachian thrust belt.

Hydrologic and geothermic information were obtained from geophysical well logs and file reports made available by the State Oil and Gas Board of Alabama. Water chemistry information is available locally for the Chattanooga Shale. Information on reservoir pressure is scarce, but driller's reports and mud logs were used to identify significant zones of gas pressure. Geothermic information was determined from bottom-hole temperatures recorded in the headers of well logs. The geothermal gradient for each well was calculated by dividing the difference between average near-surface ground temperature (62°F) and bottom-hole temperature by total well depth.

Extreme care was taken to eliminate anomalously low bottom-hole temperature readings on the bases of insufficient circulation time (less than 6 hours) and unrealistically low geothermal gradient. The geothermal gradient was then used to estimate the reservoir temperature at the depth of each shale unit.

Gas samples were collected from five wells producing from Conasauga shale using an isotube system. The samples were sent to Weatherford Laboratories and analyzed for bulk gas composition. In addition, isotopic analysis was performed to determine  $\delta^{13}\text{C}$  and  $\delta\text{D}$  values for methane. The values were then cross-plotted using the method of Whiticar (1994) to determine the origin of the gas.

Preliminary petrologic observations were made from slabbed cores as they were described, and billets of representative samples were cut to make thin sections so that rock fabric and mineralogy could be analyzed. However, intensely fissile or fractured shale could not be sampled in this way, and so the thin section collection is biased toward competent shale samples. Thin sections were prepared to standard 30 micrometer ( $\mu\text{m}$ ) thickness, stained with Alizarin red S for calcite and sodium cobaltinitrite for potassium feldspar, and examined with a petrographic microscope. Typical and diagnostic features were identified and documented using digital microphotography.

Stable isotopic analysis was performed to determine  $\delta^{13}\text{C}$  and  $\delta^{18}\text{O}$  values for vein-filling calcite cement, which can provide insight into thermal and geochemical conditions during burial and hydrocarbon generation (e.g., Friedman and O'Neil, 1977). Isotopic compositions were measured with a GasBench-IRMS system in the Department of Geological Sciences at the University of Alabama using methods similar to those described by Debajyoti and Skrzypek (2007). Powdered carbonate samples (50-100 micrograms) were reacted with anhydrous  $\text{H}_3\text{PO}_4$

for a minimum of 24 hours to assure complete reaction of robust carbonate species such as dolomite. Isotope values are expressed in per mil (‰) relative to the Vienna Pee Dee Belemnite (VPDB) scale by use of the NBS-19 standard. Standard corrections to all measured carbonate  $^{18}\text{O}$  compositions were made to account for reaction temperature (50 °C). Reproducibility for both  $\delta^{13}\text{C}$  and  $\delta^{18}\text{O}$  was calculated to be  $\pm 0.1$  ‰ based on NBS-19 and sample repeats. Analysis of 46 samples derived from 18 veins helped constrain isotopic variability among calcite crystals. Results of this analysis indicate that variability of isotopic ratios within veins averages 0.55 ‰ for C and 0.42 ‰ for O.

Selected samples were broken from cores, and rough surfaces were examined with a JEOL 7000 field emission scanning electron microscope (SEM). Samples were viewed at operating voltages of 15 or 20 kiloelectronvolts (keV) at a working distance of 10  $\mu\text{m}$ . One of the goals of the SEM study was to use digital photography and energy dispersive x-ray analysis to investigate and document the size, shape, fabric, and chemical composition of gas shale and its constituent particles. In many samples, laminae much thinner than 1 millimeter were observed.

Core samples of shale were sent to Terra Tek (Schlumberger) and Weatherford Laboratories for total organic carbon content (TOC), rock-eval pyrolysis, x-ray diffraction, tight-rock analysis (TRA), and methane adsorption isotherm analysis. TOC and rock-eval pyrolysis provide information on organic content, kerogen type and quality, residual hydrocarbon content, and thermal maturity. TOC and rock-eval pyrolysis analyses were performed on 331 shale samples from the prospective shale formations, and 565 legacy analyses from numerous laboratories were compiled from the files of the Geological Survey of Alabama and the State Oil and Gas Board of Alabama. The mineralogy of 62 shale samples was determined by x-ray diffraction. TRA provides information on the grain density, porosity, fluid saturation, and permeability of gas

shale and is important for estimating free gas storage. Permeability was determined parallel to bedding by the pressure-decay method. Adsorption isotherm measurements were used to determine how adsorbed gas storage capacity varies with pressure at reservoir temperature. TRA analysis was performed on 77 samples of Cambrian, Devonian, and Mississippian shale from the Black Warrior basin and the Appalachian thrust belt, and adsorption isotherm analysis has been performed on 35 samples.

Gas resources and reserves were estimated using a deterministic approach to reservoir volumetrics. Isopach maps made in Petra provided primary control on reservoir volume. Key variables, such as formation thickness and thermal maturity, were used to define regions of interest for volumetric evaluation. Isotherm and porosity data were used to estimate the volume of sorbed and free gas in each target shale formation. Reservoir pressure in the target formations is sufficiently high that the amount of sorbed gas could be estimated at Langmuir volume. Accordingly, the sorbed gas estimate can be considered as an upper limit. Free gas volume, by contrast, was estimated on the bases of porosity, reservoir pressure, and reservoir temperature. Reservoir pressure was assumed to be normal hydrostatic for the calculation, and so the free gas estimate can be considered conservative. Sorbed and free gas volumes were gridded and contoured in Petra. The grids were then added together and contoured to develop maps of original gas-in-place (OGIP). In addition, estimates of reservoir area, sorbed, free, and total OGIP were derived for each formation and region of interest using the basic volumetric functions in Petra.

According to the Energy Information Administration of the U.S. Department of Energy, significant shale gas reserves have yet to be proven in Alabama. Estimates of the long-term recoverability of shale gas vary greatly, and uncertainty exists regarding the types of production

decline curves that should be used for reserve estimation (Seidle and O'Connor, 2011; SPEE, in press) . Since few data are available to bracket the long-term performance of Alabama shale prospects, simple estimates of 10 to 20 percent of OGIP were made to provide baseline information on the volumes of gas that may be technically recoverable from the target shale formations.

## **STRATIGRAPHY AND SEDIMENTATION**

Many key characteristics of shale, such as bulk composition, thickness patterns, and continuity, are determined largely in the original depositional environment, and so stratigraphy and sedimentology are critical components of exploration and development strategies. As mentioned in the section on stratigraphic setting, black shale accumulates in a range of environments, and depositional processes in those environments can be highly dynamic. In Alabama, Cambrian-Mississippian gas shale was deposited in marine environments and is in facies relationship with a variety of carbonate and siliciclastic deposits. In the following sections, the stratigraphic and sedimentologic characteristics of each formation are discussed to highlight regional correlation, diagnostic rock types, and sedimentary structures, as well as the types of sedimentary processes that were active during deposition.

### **Conasauga Shale**

The Conasauga Formation constitutes a thick succession of shale, limestone, and dolostone containing a diverse suite of depositional facies (Butts, 1910, 1926; Astini and others, 2000; Thomas and others, 2000) (plate 1; fig. 8). The Conasauga gradationally overlies the Lower Cambrian Rome Formation, which contains interbedded shale, siltstone, sandstone, and

limestone and includes redbeds, which are helpful for distinguishing Rome shale from Conasauga shale. The Conasauga is a Middle to Upper Cambrian formation with stratigraphic thickness ranging from 1,500 to 3,000 feet in Alabama, although tectonic deformation has resulted in the development of shale masses with thickness locally exceeding 12,000 feet (Thomas and Bayona, 2005) (fig. 3). The Conasauga is overlain conformably by Upper Cambrian chert and dolostone of the Copper Ridge Dolomite, which forms the base of the Knox Group.

The Conasauga is characterized by complex internal stratigraphy and facies relationships (Butts, 1910, 1926, 1927; Osborne and others, 2000). In general, shale predominates in the lower part of the formation, and limestone and dolostone predominate in the upper part. Thus, in a grand sense, the Conasauga represents a giant shoaling-upward succession in which subtidal shale passes into ramp carbonate deposits (Astini and others, 2000) (plate 1).

Shale gas development is restricted to strata composed of interbedded shale and limestone (figs. 9, 10; plate 1). Big Canoe Creek Field is at the edge of the Gadsden MUSHWAD (see Thomas, 2001) (figs. 3, 7), which is a giant tectonic structure where the productive shale facies is exposed at the surface. Cores and outcrops from this structure provide insight into Conasauga shale sedimentation. Core from the Dawson 33-09 #2A well provides a glimpse of Conasauga shale at depths greater than 7,500 feet (fig. 9.) The shale is dark gray to very dark gray, is calcareous and dolomitic, and forms laminae to thick beds. It is brittle in dry samples, but will swell and retain water when wet. Internally, the shale is laminated (fig. 9A), and the laminae are defined by variations in the proportions of clay, organic matter, carbonate, and quartz silt. Locally, ripple cross-laminae with low relief have been identified (fig. 11). Sand- to granule-size pyrite nodules occur locally. No bioturbation has been observed within the shale in this core.

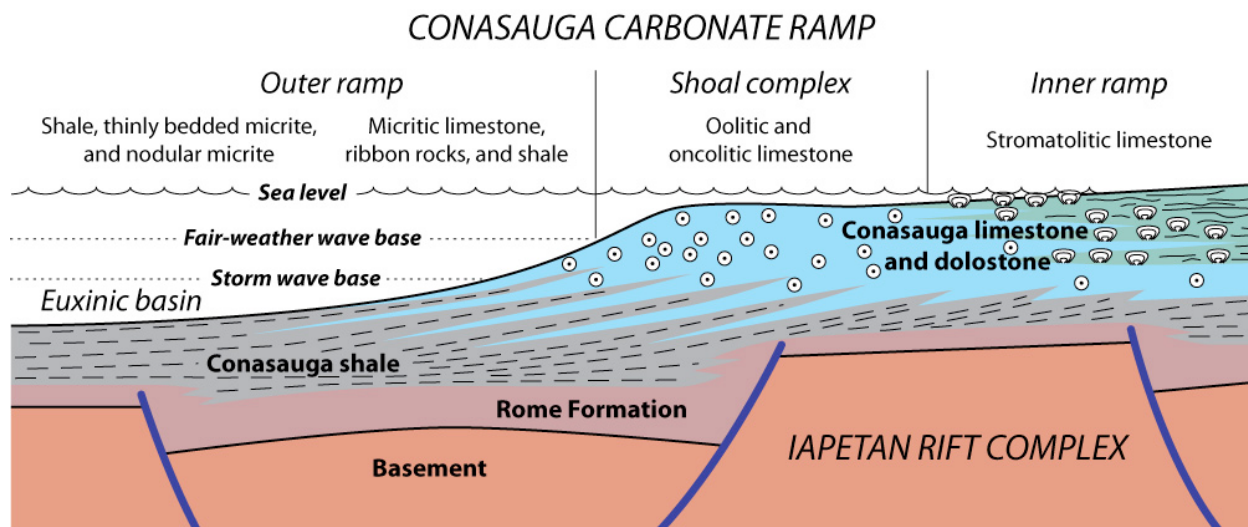


Figure 8.—Generalized depositional model of the Conasauga Formation in Alabama (modified from Markello and Read, 1982; Astini and others, 2000).

Laminae, thin beds, and nodules of fine-grained limestone are common throughout the Conasauga shale (figs. 9, 10). The limestone is typically medium gray to light gray and brittle. The limestone is dominantly peloidal micrite, and thin sections indicate that most of the carbonate has been recrystallized. Many limestone nodules appear to correlate with pale laminae in the shale, whereas other laminae diverge around the nodules (fig. 9B). The thickest limestone beds are argillaceous and can have sharp bases with flame structures and gradational tops (fig. 9C). Internal structures within the limestone beds include faint burrows and ripple cross-laminae. Although most limestone beds and nodules appear to be in facies relationship with adjacent strata, some nodules have been rotated, and layers of imbricate micrite pebbles have been preserved locally (fig. 9D).

The Dawson 34-03-01 exploratory core provides an exceptional record of the upper part of the Conasauga shale mass in Big Canoe Creek Field (plate 1). This core displays a broad range

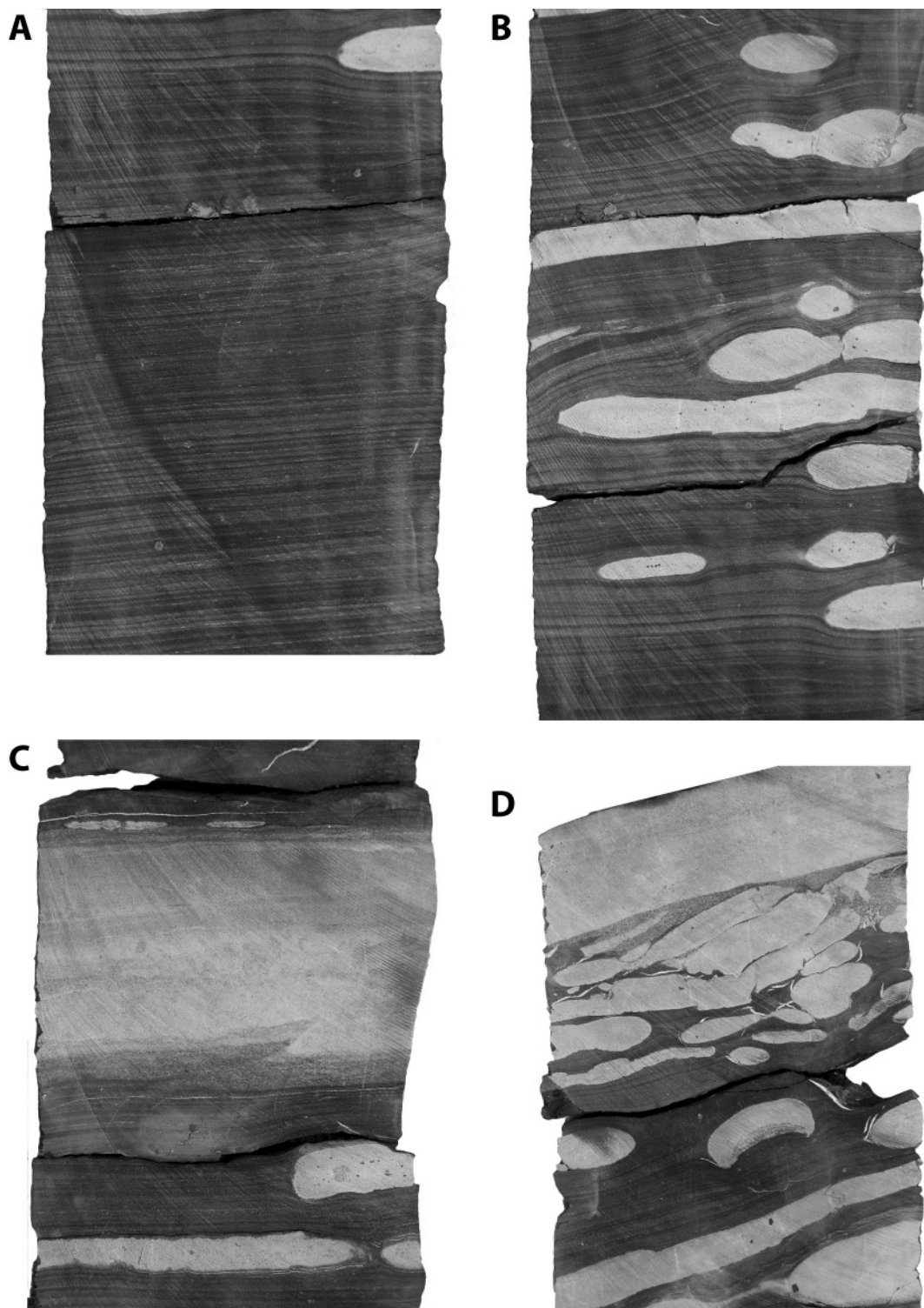
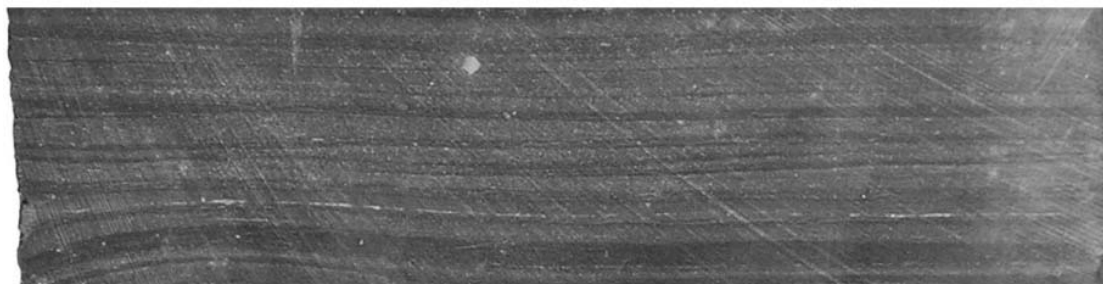


Figure 9.—Photographs of Conasauga shale in core from the Dawson 33-09 #2A well, Big Canoe Creek Field. (A) Laminated shale, 7,553.2 ft. (B) Laminated shale with micrite nodules, 7,552.8 ft. (C) Micrite bed with flame structure, internal grading, and burrows, 7,555.8 ft. (D) Imbricate micrite clasts in shale, 7,544 ft. Core diameter = 4 inches.



Figure 10.—Laminated shale and interbedded micrite in Conasauga shale, Pinedale Lake Spillway, St. Clair County, Alabama.

**Uninterpreted photograph**



**Photograph with tracing**

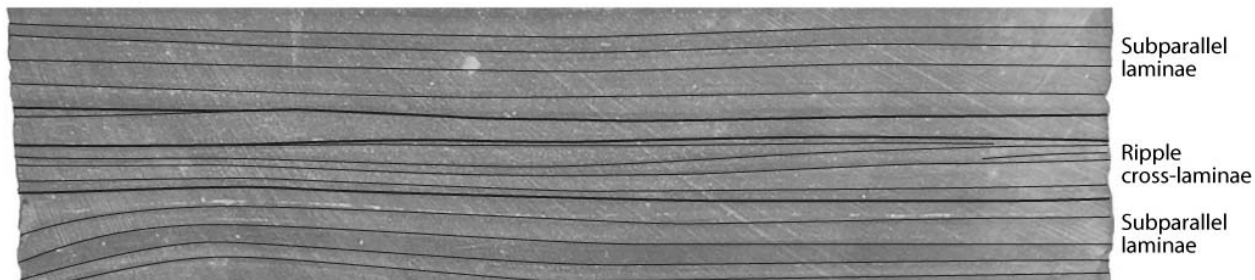


Figure 11.—Subparallel and ripple cross-laminae in Conasauga shale from the Dawson 33-09 #2A well, Big Canoe Creek Field, 7554.6 ft. Core diameter = 4 inches.

of sedimentary structures and bedding styles that provide insight into Conasauga depositional dynamics. The core is dominated by interbedded limestone and shale, and the proportion of limestone tends to increase upward in section. Micritic carbonate rocks are most common in the lower 500 feet of the core. Higher in section, the carbonates are mainly calcarenite with abundant peloids and coated grains. Scattered through the section, moreover, are conglomeratic carbonate rocks (i.e., calcirudite).

Shale in the exploratory core is dark gray to very dark gray and tends to be fissile. However, laminae are not as clearly defined as in the deeper core. In contrast to the other Conasauga core, the shale in the shallow exploratory core does not appear to retain water or swell when wet. Biogenic structures are common in medium to thick shale beds and include horizontal burrows (*Planolites*), trilobite trails (*Cruziana*), lingulid brachiopods, and a variety of agnostid and ptychoparioid trilobites (fig. 12). Physical sedimentary structures in shale include mud ripples, and pinstripe bedding formed by interlamination of shale and limestone is common in parts of the core (fig. 13). Interestingly, the carbonate pinstripes are commonly paired. In some sections of the core carbonate laminae occur in bundles of 10 or more pairs.

Thin to medium beds of wavy, lenticular, and nodular limestone are interbedded with shale throughout the core (fig. 14). Indeed, thinly interbedded shale and limestone can be considered the signature Conasauga lithology. The limestone has a variety of sedimentary structures and textures, including ripple cross-laminae (fig. 14A), fenestral fabric (fig. 14C), chert nodules, and sphaerulitic cracks (fig. 14D). Thick beds of calcirudite are preserved between depths of 880 and 1,000 feet and include clast-supported and matrix-supported fabrics (fig. 15). Some of the calcirudite, moreover, contains abundant soft-sediment deformation structures (fig. 16).

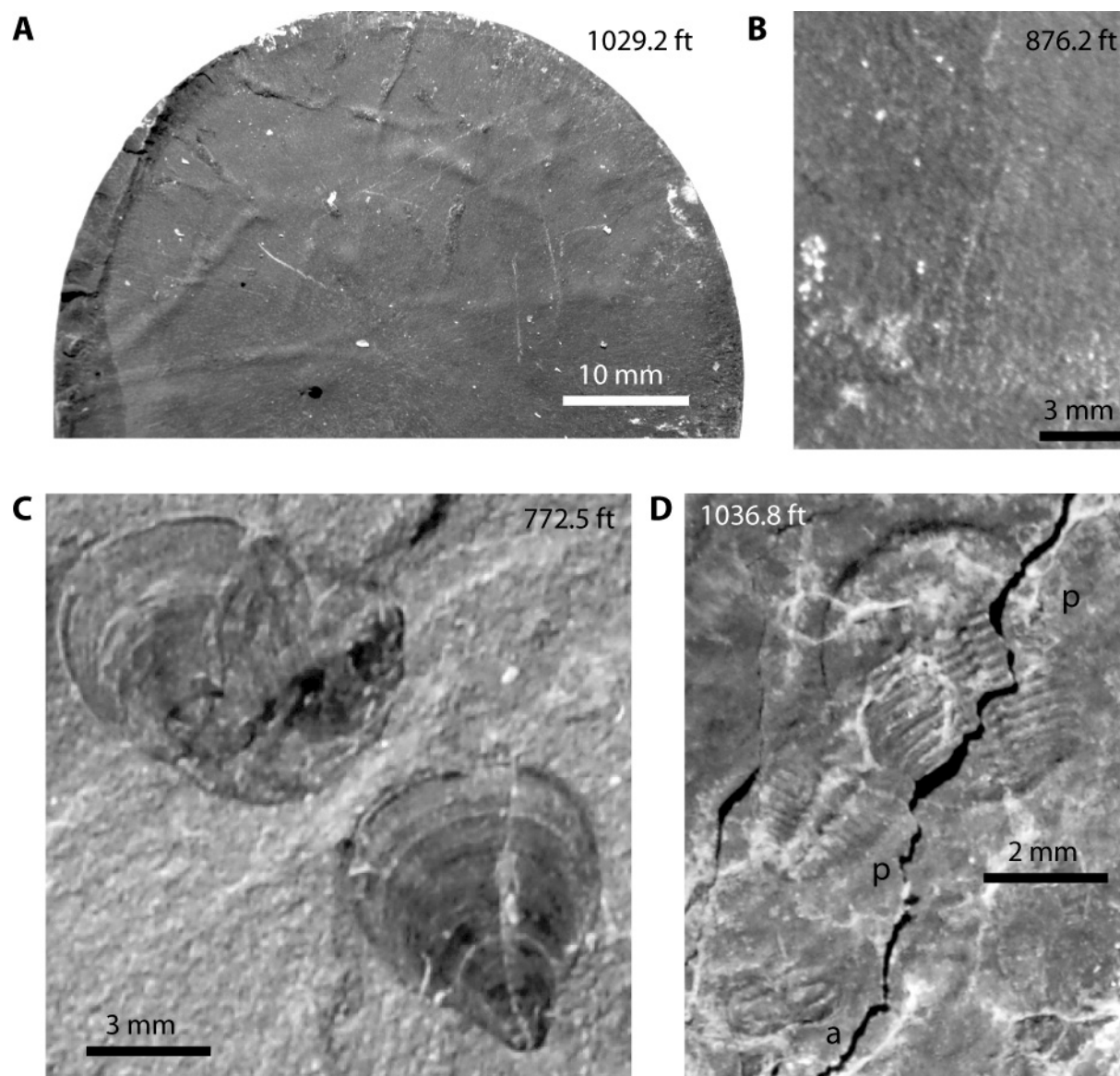


Figure 12.—Trace and body fossils in the Dawson 34-03-01 exploratory core, Big Canoe Creek Field. (A) *Planolites* burrows, (B) *Cruziana* trail, (C) lingulid brachiopods, (D) ptychoparioid (p) and agnostid (a) trilobites.

Strata in the upper 400 feet of the core display different rock types and sedimentary structures than those deeper in the Conasauga Formation (fig. 16). Interbedded limestone and shale includes ribbon rock, and stylonodular fabrics and fitted fabrics are common (fig. 16B). Oncoidal limestone is also present and includes irregular dolostone laminae, which weather to orange color (fig. 16A). An interval of cross-bedded oolitic calcarenite with echinoderm

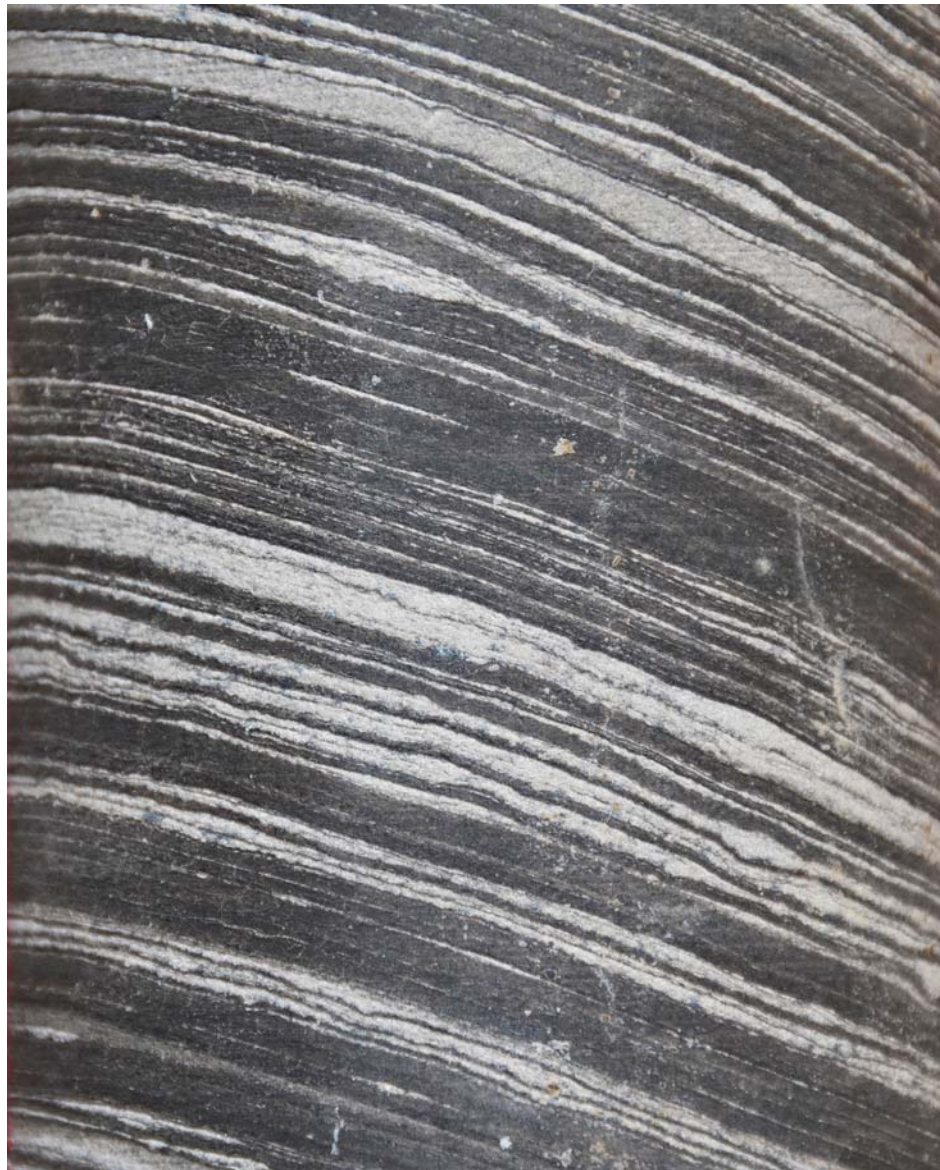


Figure 13.—Pinstripe-laminated shale and limestone in the Conasauga Formation (Dawson 34-03-01 core, depth =1,037 ft). Note frequent pairing of pale limestone laminae.

ossicles was identified at a depth of about 250 feet. Near the top of the core, some of the limestone contains thrombolitic structures, as well as spar-cemented shelter voids (plate 1).

Following the lead of Markello and Read (1981, 1982), Astini and others (2000) applied carbonate ramp models to the Conasauga Formation of Alabama (fig. 8). The shale facies of the Conasauga was recognized by Astini and others as an outer ramp deposit that accumulated on what they referred to as an oxygen-deficient intrabasin shelf. The predominance of laminated

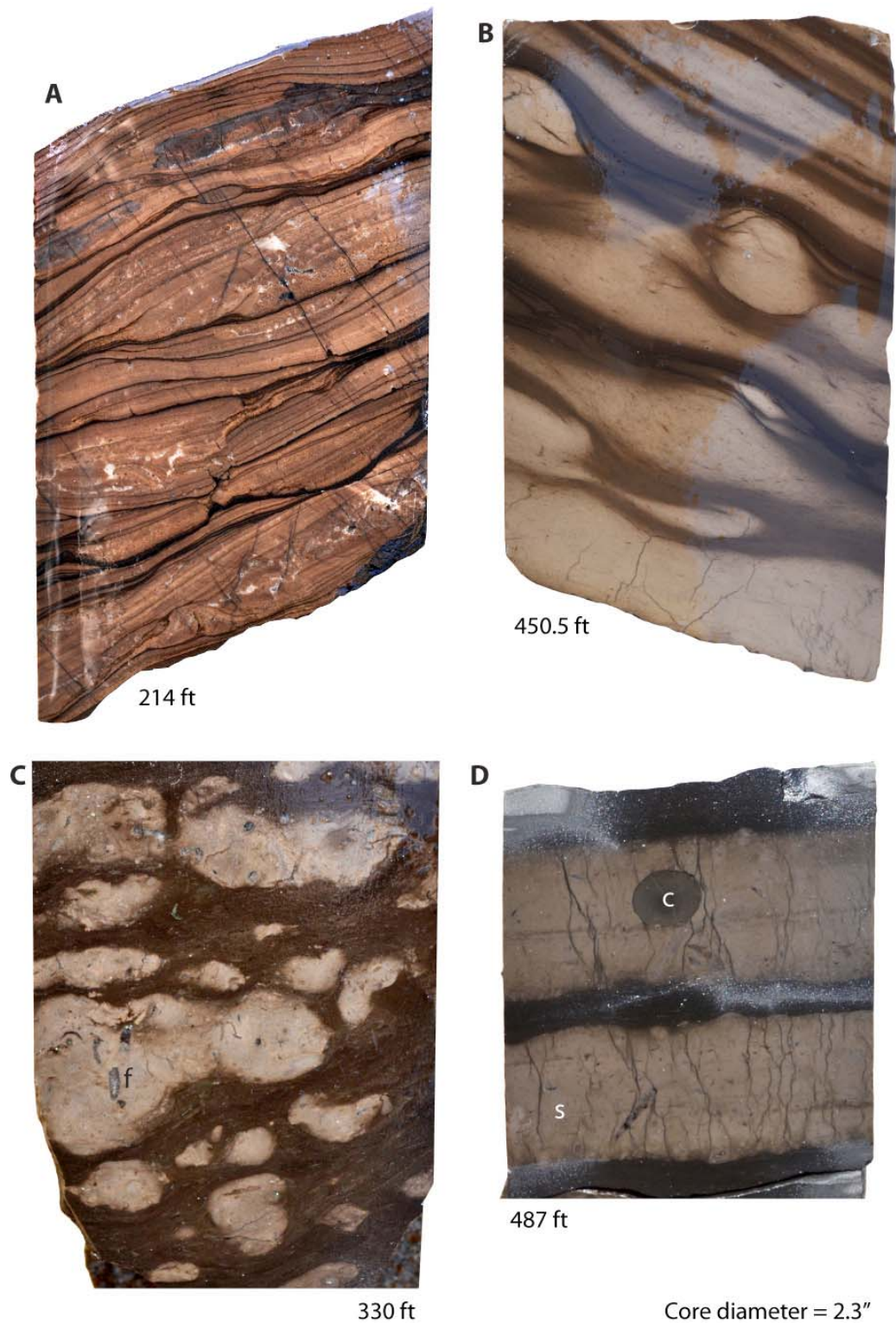


Figure 14.—Nodular- and wavy-bedded limestone and shale in the Dawson 34-03-01 core. (A) Wavy-bedded limestone with ripple cross-laminae and fenestrae. (B) wavy-bedded limestone with nodules and possible relict ripples. (C) nodular limestone with spar-filled fenestrae (f). (D) limestone with abundant synaeresis cracks (s) and a chert nodule (c).

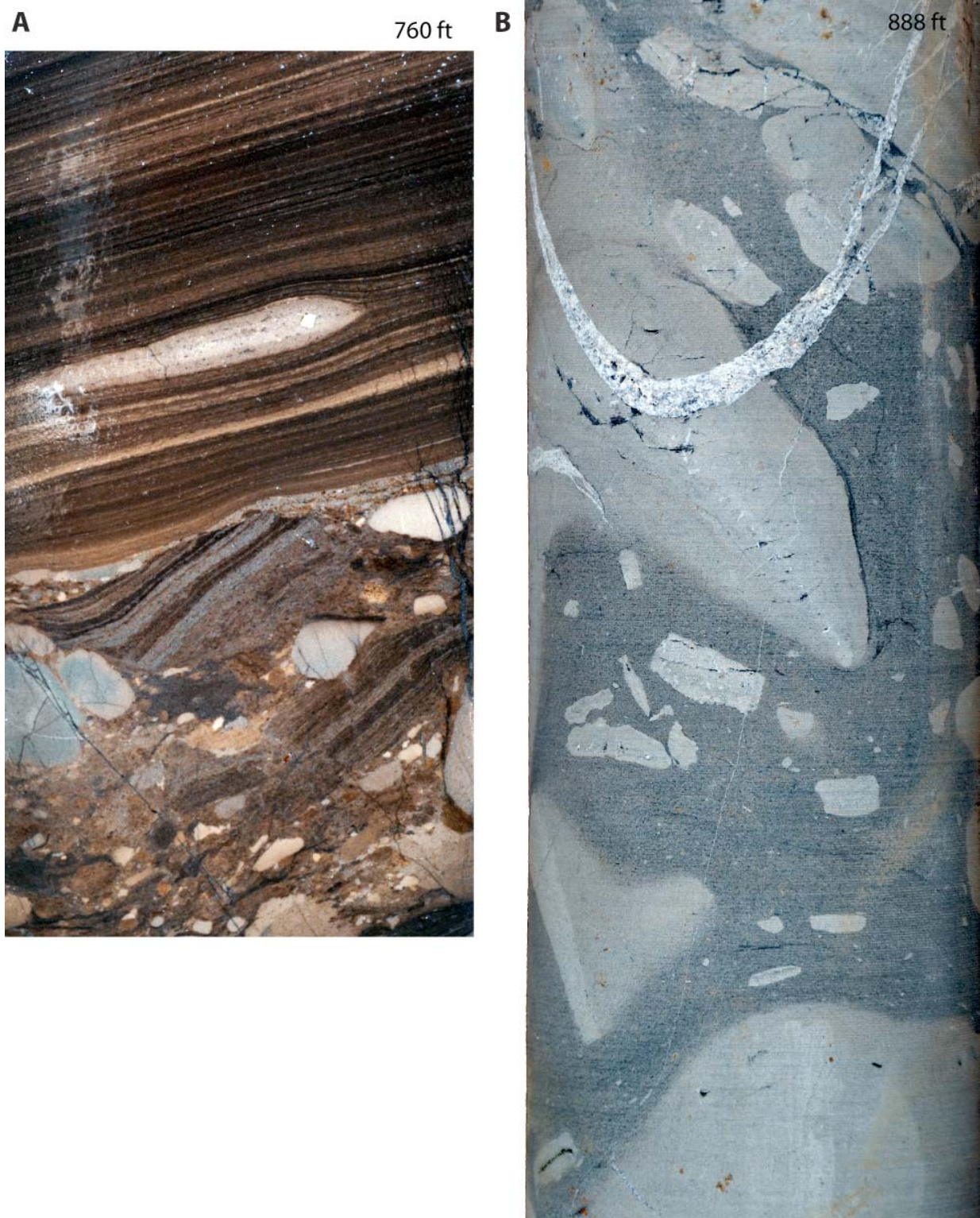


Figure 15.—Conglomeratic limestone (calcirudite) in the Dawson 34-03-01 core. (A) Clast-supported conglomerate underlying laminated shale. (B) Poorly sorted clasts floating in argillaceous matrix.

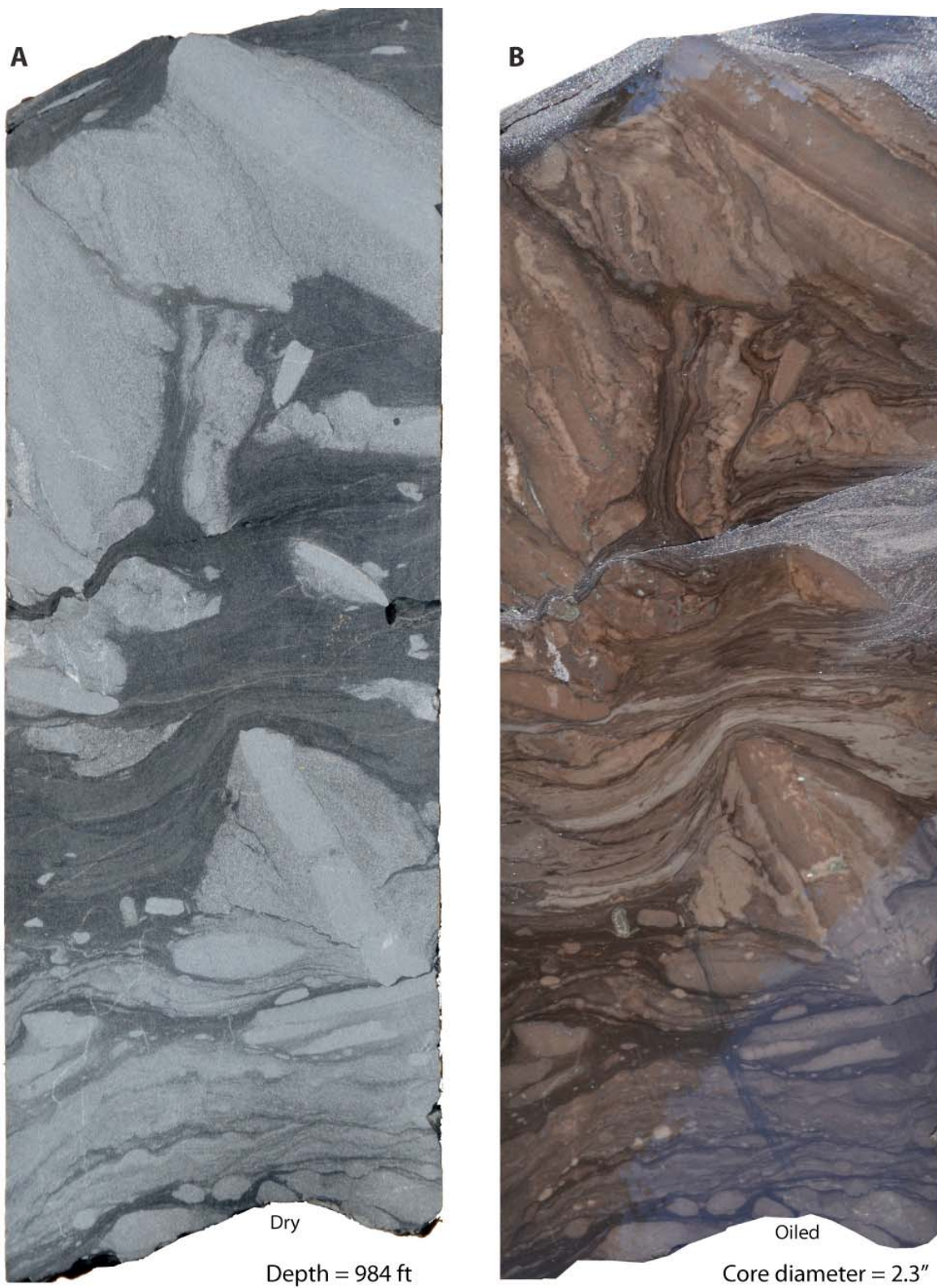


Figure 16.—Conglomeratic limestone and shale in the Dawson 34-03-01 core containing convolute bedding. (A) Dry slab showing differentiation between limestone (pale) and shale (dark). (B) Oiled slab showing intensely deformed laminae.

shale and a lack of bioturbation in the Dawson 33-09 #2A core (fig. 9A) supports the interpretation of sedimentation in an euxinic basin. Ripples in the shale and micrite provide evidence for episodic currents that swept the sea floor. Graded micrite beds (fig. 9C) are suggestive of distal storm deposits (e.g., Aigner, 1985), although it seems that most shale sedimentation took place below storm wave base. Bioturbation within the micrite beds indicates that the water in which the carbonate mud was transported was at times sufficiently oxygenated to support infauna. Divergence of laminae around micrite nodules (fig. 9B) and angular micrite clasts (fig. 9D) indicate early lithification of the carbonate. The presence of imbricate limestone clasts, moreover, indicates that currents were episodically strong enough to rip up, transport, and resediment the micrite layers.

The Dawson 34-03-01 exploratory core contains evidence for sedimentation in shallower water and is important for characterizing depositional processes on the Conasauga carbonate ramp. Bioturbation and body fossils suggest more consistent oxygenation of the water column (fig. 12). Agnostid trilobites are considered by many to have been pelagic organisms (Muller and Walossek, 1987; Fortey and Theron, 1994). However, ptychoparioid trilobites were benthic forms, and preservation of *Cruziana* trails indicates that trilobites did indeed inhabit Conasauga mud substrates. Pairing of pinstripe laminae (fig. 13) suggests paired sedimentation events, such as flood and ebb tide or semidiurnal tides. Indeed, bundling of paired laminae into groups of 10 or more is suggestive of spring-neap tidal bundles, such as those described by Kvale and Archer (1989). Some of the wavy, lenticular, and nodular limestone beds (fig. 14) also may have formed in response to tidal action, although most may be storm deposits similar to those identified in the deep core. Clast-supported calcirudite (fig. 15A) may have been deposited as ravinement and channel lags. Matrix-supported conglomerate (fig. 15B, 16), by contrast, indicates sedimentation

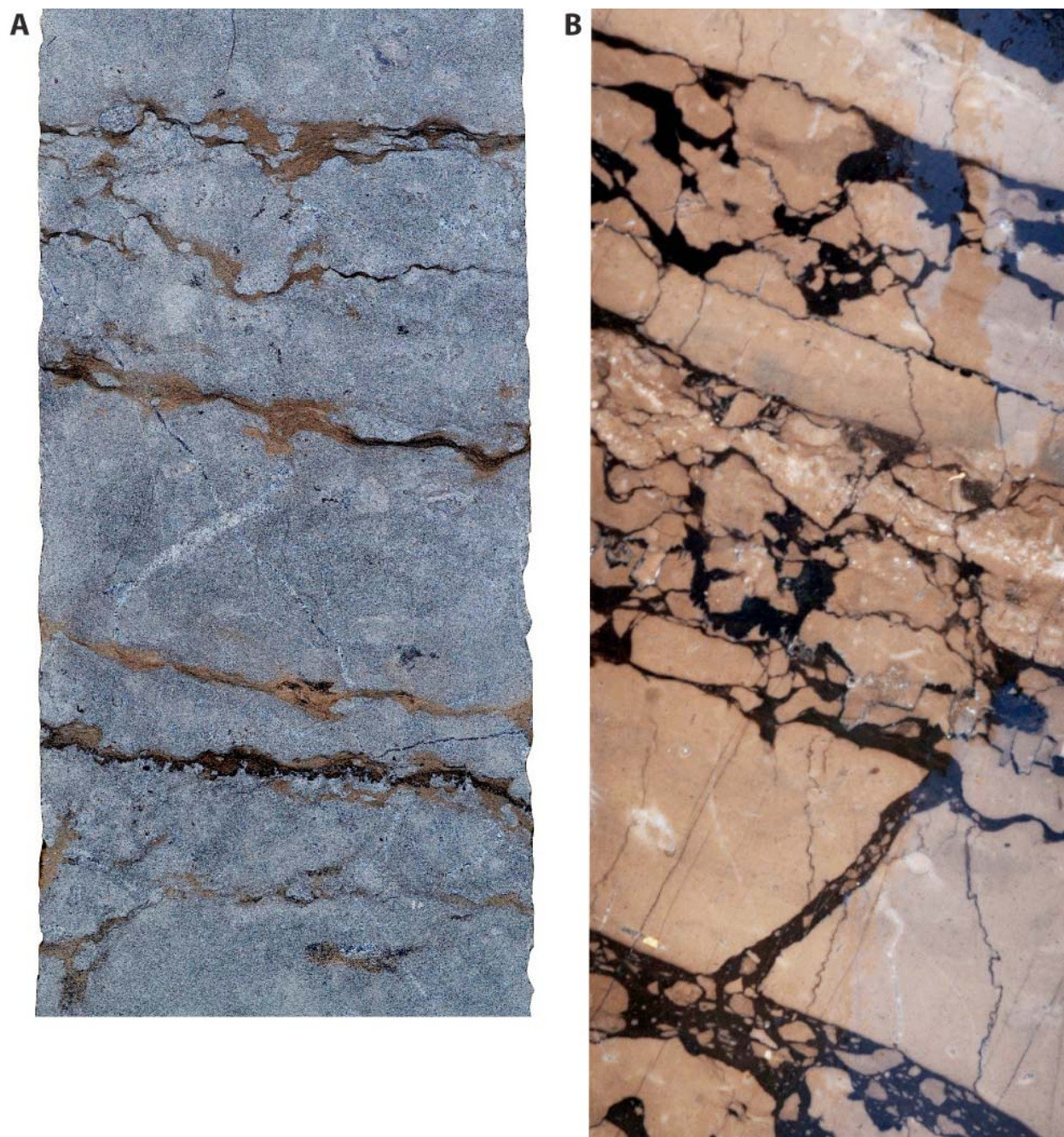


Figure 17.—Limestone and shale in upper part of the Dawson 34-03-01 core. (A) Oncoidal limestone with irregular dolostone laminae. (B) Limestone and shale with cracks, fitted fabric, injectite, and stylonodular texture.

in debris flows, which may have been generated by slope and channel-bank failures. Strata in the upper part of the core were apparently deposited in inner ramp environments (fig. 17; plate 1). Cross-bedded calcarenite indicates shoal development, and ribbon rocks with fitted fabrics

suggest exposure (e.g., Markello and Read, 1982). Oncoidal limestone is suggestive of lagoonal environments, and dolostone laminae indicate supratidal conditions. Thrombolitic strata with shelter voids may further represent the development of lagoonal algal mats within the inner ramp.

At a regional scale, uncertainty exists regarding the distribution of the black shale facies of the Conasauga Formation. This is because few wells penetrate the shale, and nearly all outcrops and cores of the shale are in the Gadsden MUSHWAD. One possibility is that the black shale facies is extremely widespread, which would indicate shale gas potential over a large part of northern Alabama. Alternatively, black shale may have been deposited only in the Birmingham graben, which is a major Iapetan basement graben that houses a large part of the Appalachian thrust belt in Alabama (e.g., Thomas, 1985; Thomas and Bayona, 2005).

### **Devonian Shale**

Devonian strata in Alabama contain carbonate and siliciclastic rocks, including an organic-rich shale facies that is characteristically black, fissile, and brittle (fig. 18). Although the shale can at first glance appear lithologically homogeneous, parts of the shale are argillaceous, whereas other parts are siliceous or calcareous. These strata disconformably overlie strata of Silurian age, and the characteristics of the Devonian section vary considerably depending on location. In the Appalachian thrust belt, sandstone and limestone assigned to the Frog Mountain Sandstone form the lower part of the Devonian section and are largely of Early to Middle Devonian age. Equivalent strata in the Black Warrior basin are dominated by a northeast-thinning wedge of limestone and chert and have not been assigned to any formal stratigraphic unit (Kidd, 1975; Thomas, 1988) (plate 2).



Figure 18.—Outcrop of Chattanooga Shale at Big Ridge, Etowah County, Alabama. Note sheared and folded zone in lower part of shale and orthogonal joints in upper part.

This carbonate-dominated section is overlain disconformably by the organic-rich black shale of the Chattanooga Shale (plate 2), which is of Middle to Late Devonian age. The shale onlaps the disconformity and directly overlies Silurian strata northeast of the pinchout of the Devonian limestone-chert section (Conant and Swanson, 1961; Kidd, 1975; Rheams and Neathery, 1988) (fig. 19). The Chattanooga is overlain sharply by the Lower Mississippian Maury Shale, which is commonly thinner than 2 feet, and the Maury is in turn overlain by the Fort Payne Chert.

The Chattanooga Shale is characterized by elevated radioactivity and is thus readily identified in gamma ray logs (plate 2). An isopach map of the Chattanooga Shale in the Black Warrior basin demonstrates that shale thickness varies regionally (fig. 20). The shale is thinner than 10 feet and is locally absent in much of Lamar, Fayette, and Pickens Counties, which is the principal area of conventional oil and gas production in the Black Warrior basin. The shale is thicker than 25 feet in a belt that extends northwestward from Blount County into Franklin and Colbert Counties. GeoMet, Incorporated, is producing shale gas from vertical and directional wells near the southeast end of the belt in Blount and Cullman Counties, where the shale is locally thicker than 70 feet (Haynes and others, 2010). A prominent depocenter is developed along the southwestern basin margin in Tuscaloosa and Greene Counties. Here, the shale is consistently thicker than 25 feet and is locally thicker than 90 feet. Energen Resources Corporation and Chesapeake Energy Corporation have been exploring this depocenter, and activities have included the drilling and testing of directional wells.

An exceptionally thick section of organic-rich shale with significant gas shows is preserved deep in the interior of the Appalachian thrust belt below the Gulf Coastal Plain in Greene and Hale Counties (figs. 1, 21, 22; plate 2). Accordingly, the structure containing these strata is called the Greene-Hale synclinorium (Pashin, Grace, and Kopaska-Merkel, 2010). Three wells

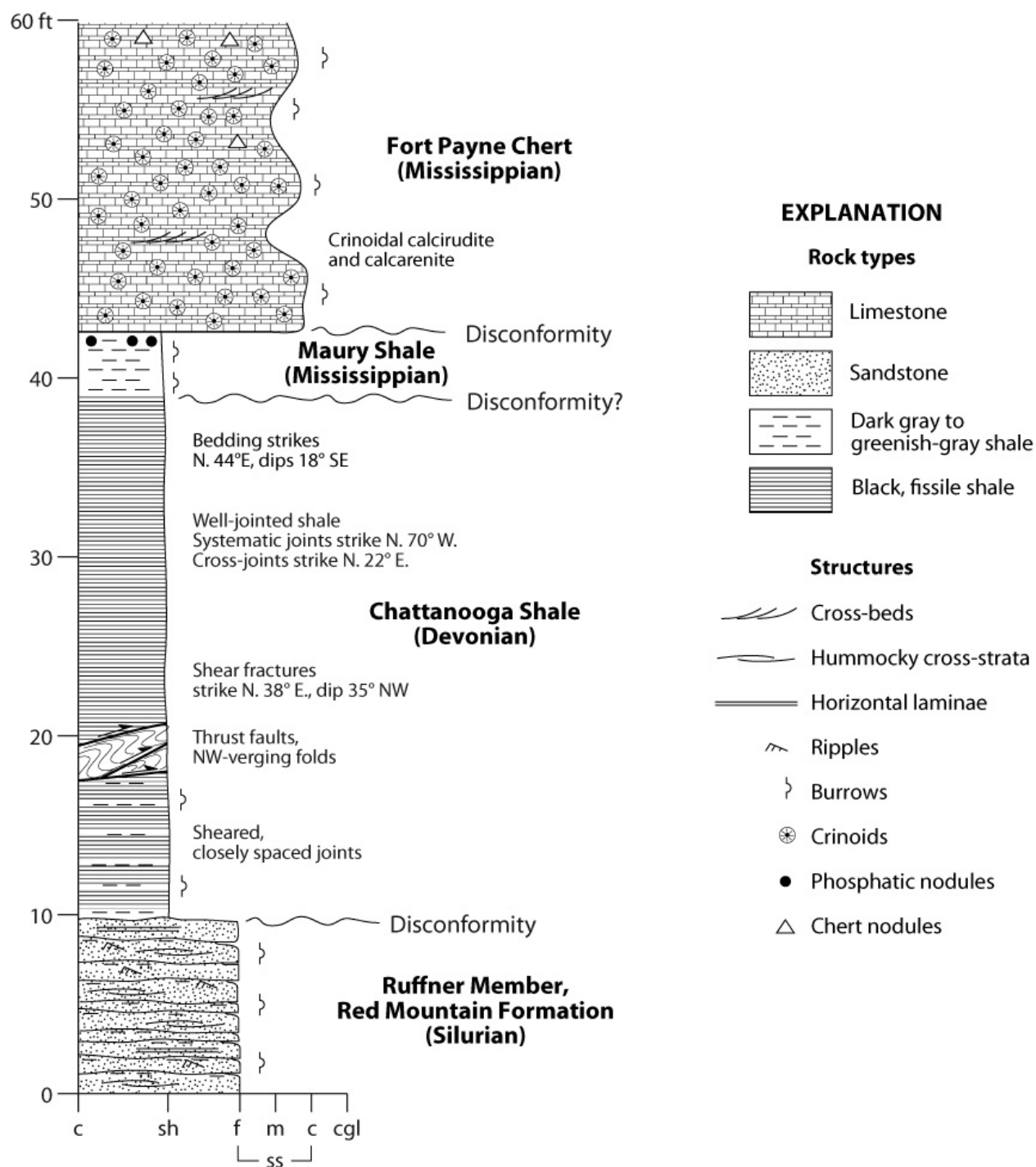


Figure 19.—Measured section of the Chattanooga Shale at Big Ridge, Etowah County, Alabama (modified from Pashin, Carroll and others, 2010).

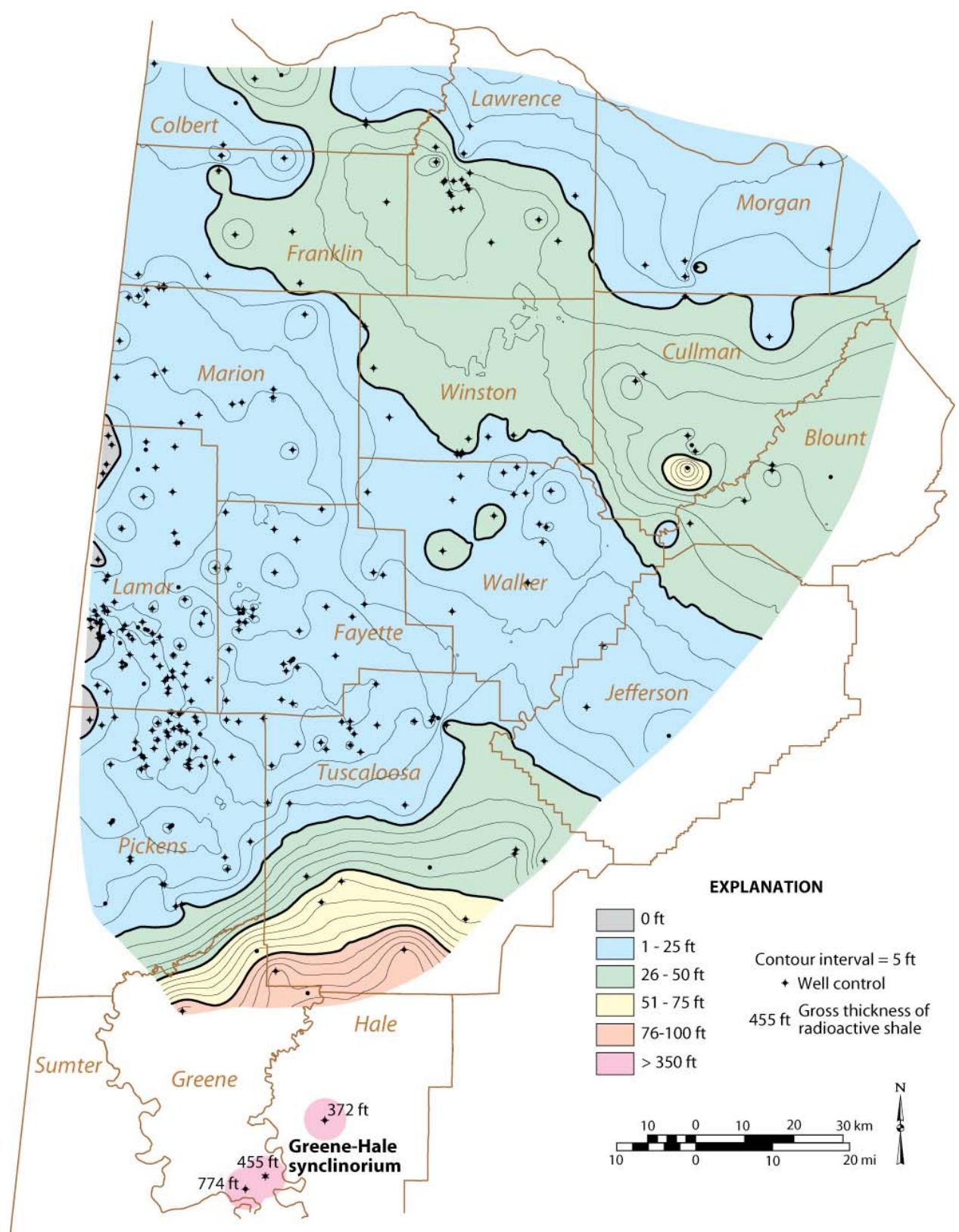


Figure 20.—Isopach map of the Chattanooga Shale in the Black Warrior basin and unnamed Devonian shale in the Greene-Hale synclinorium of Alabama.

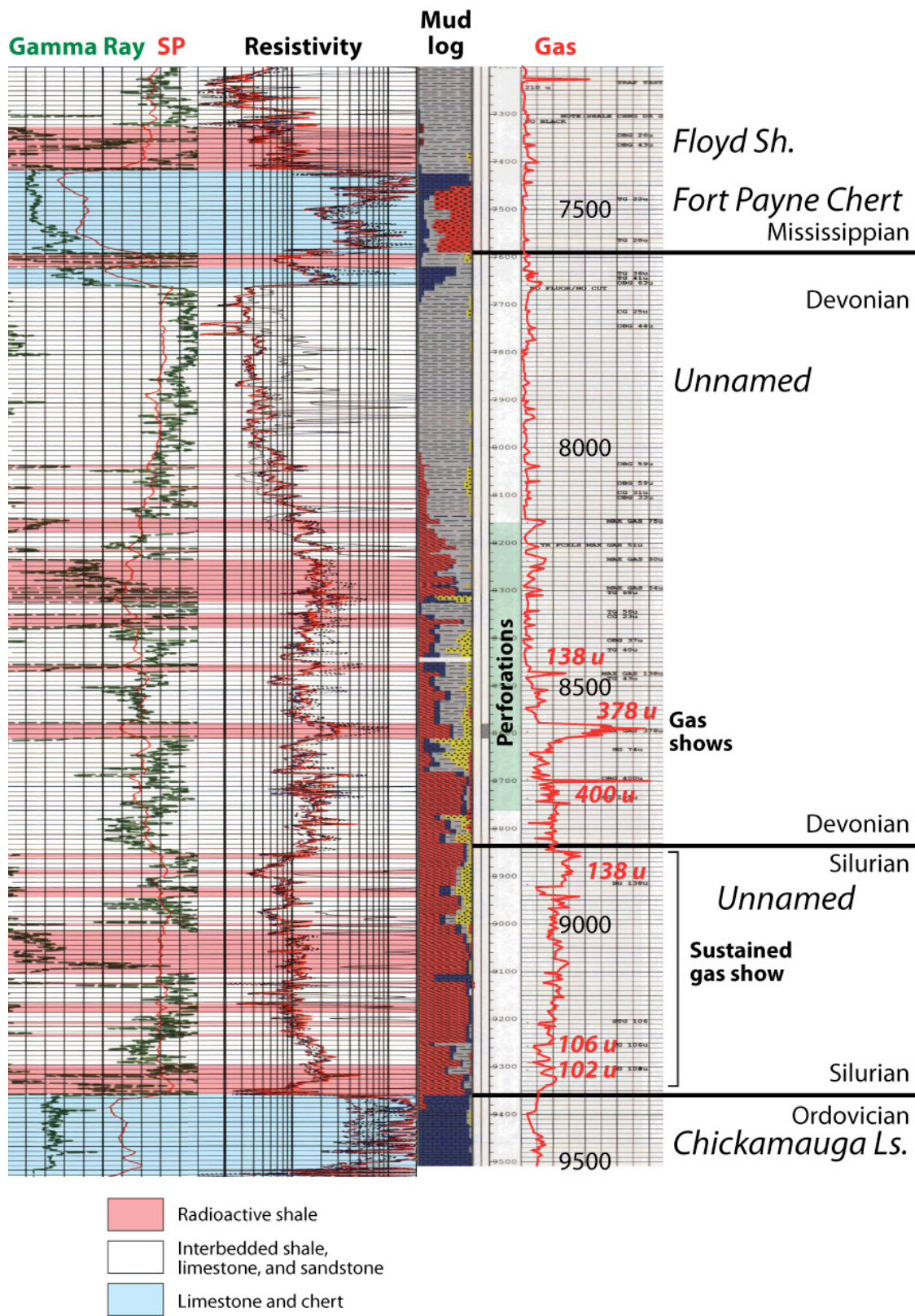


Figure 21.—Geophysical well log and mud log showing relationship of gas shows to the Ordovician-Mississippian section in the Bayne-Etheridge 36-9 #1 well.

penetrating the Silurian-Devonian section logged more than 1,750 feet of section dominated by organic-rich shale with numerous radioactive zones (plate 2). The Silurian-Devonian boundary is placed provisionally at the base of a zone with low radioactivity and elevated resistivity that appears to correlate with the Devonian carbonate-chert section in the Black Warrior basin. Core from this resistive zone in the Burke 29-7 #1 well in Hale County contains principally dark gray micrite and shale with horizontal laminae and soft-sediment deformation structures and thus contrasts sharply with the chert-bearing carbonates of the Black Warrior basin. Core of the Devonian section includes black shale interstratified with gray shale, siltstone, and crinoidal limestone (Bayne-Etheridge 36-9 #1 well).

Black, fissile shale is the signature rock type of the Devonian shale section in the Appalachian region, and close examination reveals a variety of physical and biogenic sedimentary structures (fig. 22). Much of the shale is horizontally laminated (fig. 22A), and low-amplitude ripple cross-strata and erosional discontinuities can be discerned in places (fig. 23). In some cores, thin beds of structureless mudstone occur within thinly laminated shale (fig. 22B). Much of the black shale is bioturbated (fig. 22C), and examination of bedding planes reveals that much of the laminated shale contains horizontal burrows (fig. 22D). Body fossils are not common in the shale, although some siliceous layers are rich in radiolarians (fig. 24) or monaxon-type spicules. Soft-sediment deformation is common in the Devonian shale of Alabama, particularly in the Greene-Hale synclinorium (Bayne-Etheridge 36-9 #1 well). Small-scale overturned and recumbent folds have been observed in the gray shale, siltstone, and limestone that separates the black shale units. Within the black shale, a tilted block that is overlapped by younger strata was also observed (fig. 22E).

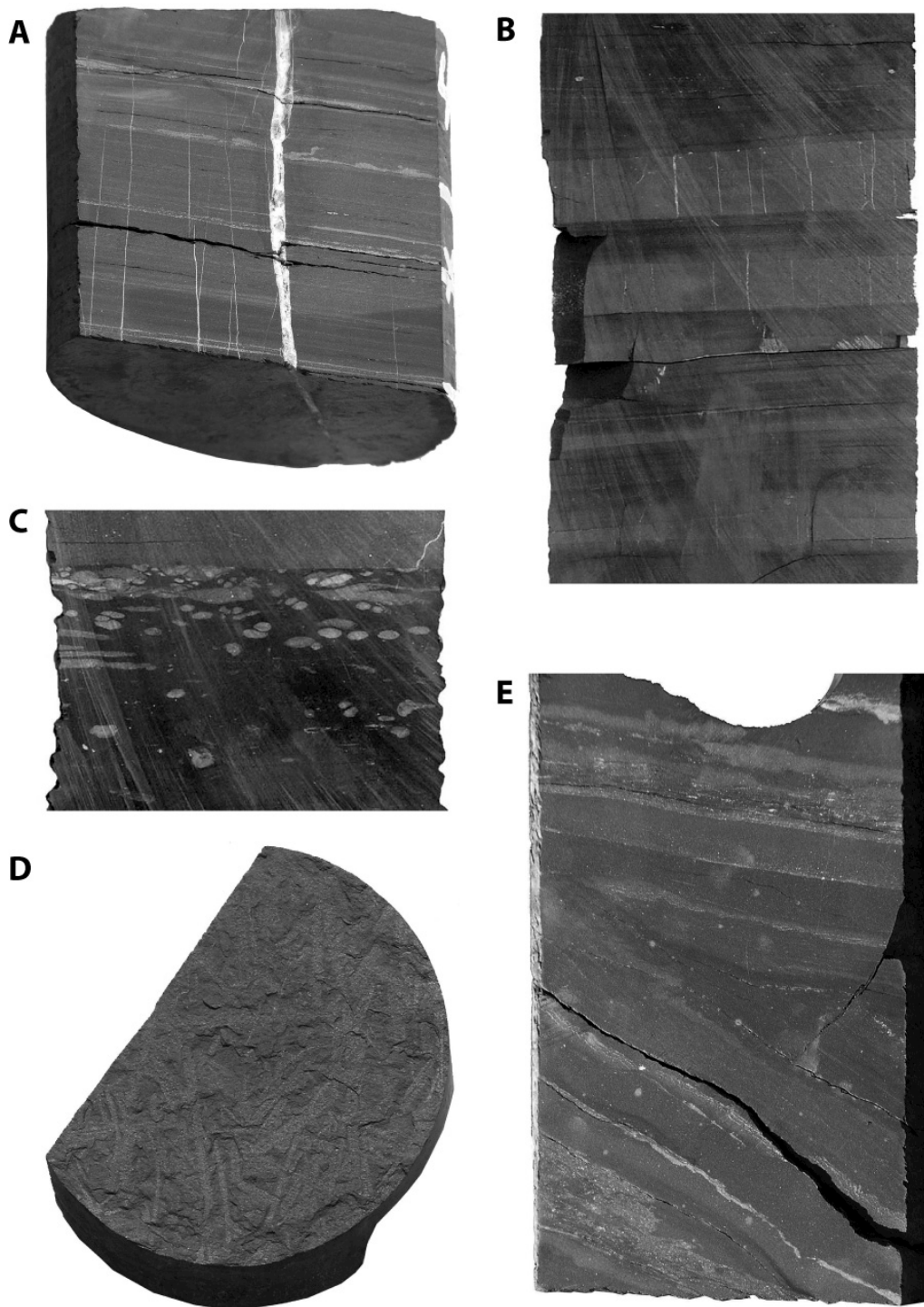


Figure 22.—Core photographs of Devonian shale in the Black Warrior basin and the Appalachian thrust belt of Greene County, Alabama. (A) Laminated shale with mineralized joints, Bayne-Etheridge 36-9 #1 well, 8,444 ft. (B) Laminated shale with jointed structureless mudstone, Lamb 1-3 #1 well, 9,168 ft. (C) Black shale with siltstone-filled burrows, Lamb 1-3 #1 well, 9,174 ft. (D) Bedding-plane view of horizontal burrows, Bayne-Etheridge 36-9 #1 well, 8,441 ft. (E) Dipping strata onlapped by subhorizontal bedding, Bayne-Etheridge 36-9 #1 well, 8,446 ft. Core diameter = 4 inches.

**Uninterpreted photograph**



**Photograph with tracing**

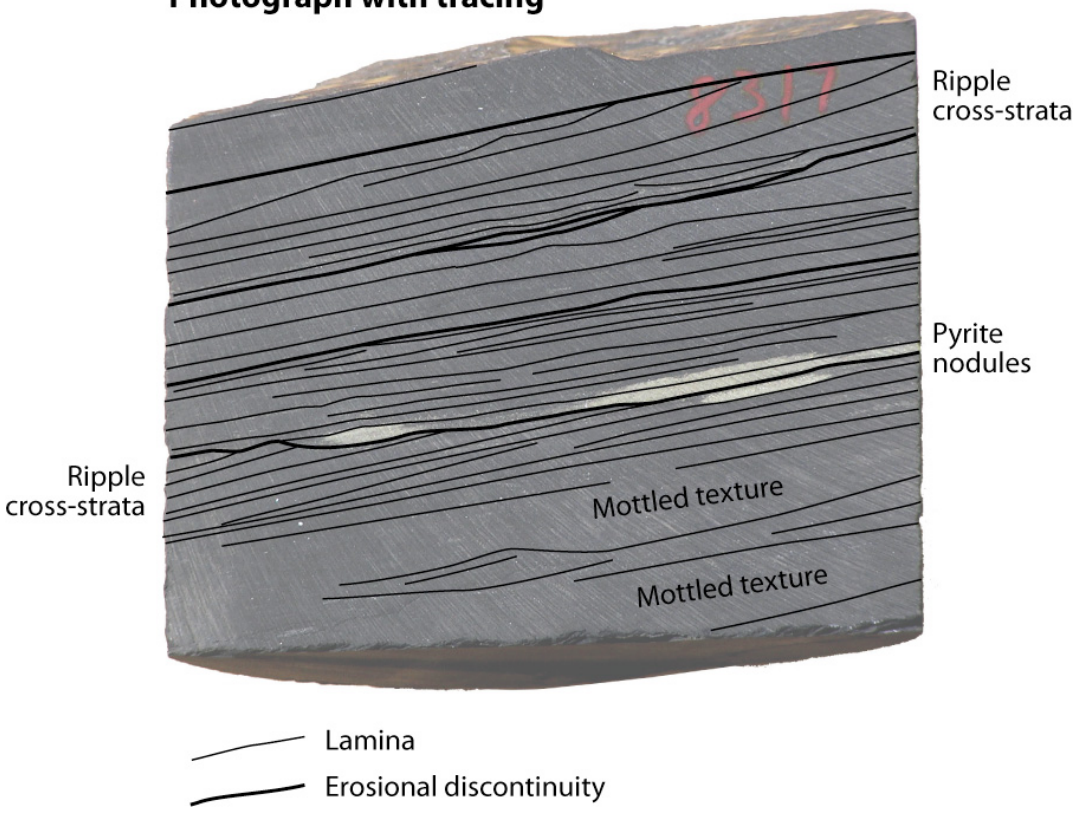


Figure 23.—Black shale with ripple cross-strata, erosional discontinuities, and pyrite nodules, Bayne-Etheridge 36-9 #1 well, 8,317 ft.

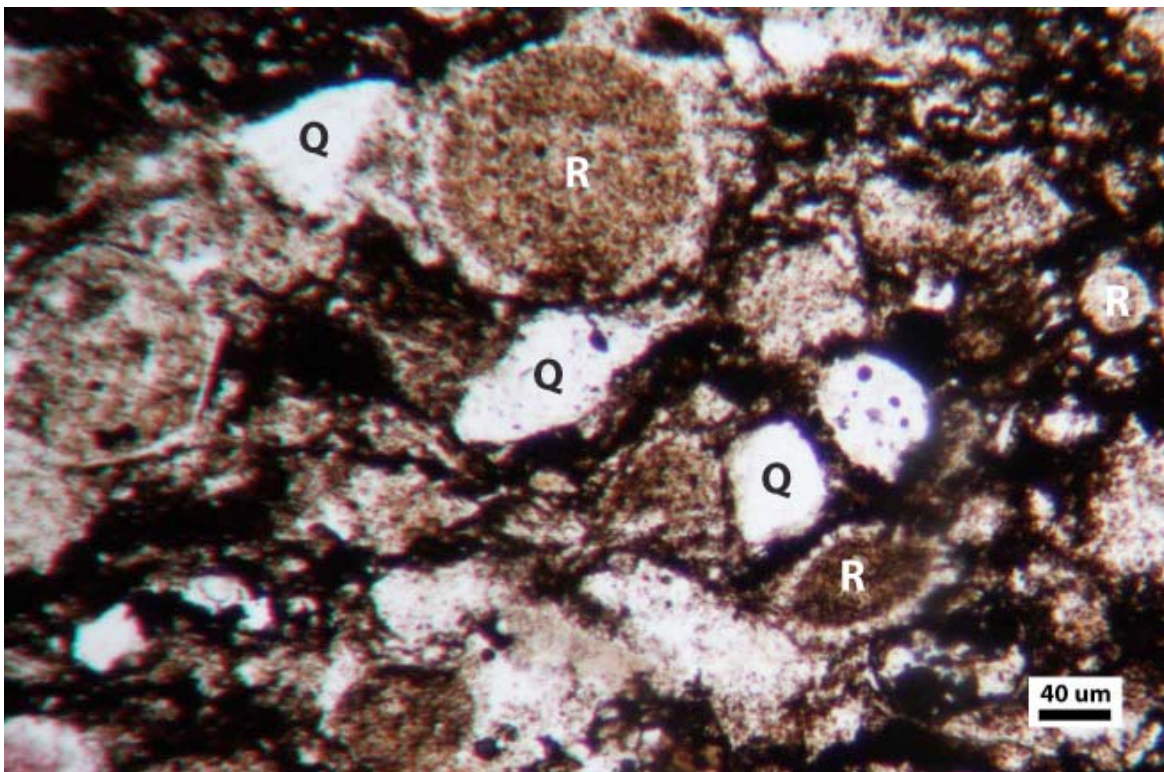


Figure 24.—Photomicrograph showing radiolarians (R) and detrital quartz (Q) in the Chattanooga Shale (Weyerhaeuser 2-43-2402 well, 8,204 ft, Greene County, Alabama).

The depositional environment of Devonian black shale has long been a subject of debate. Conant and Swanson (1961) favored a shallow-water origin in which organic-rich mud accumulated in what could be considered a cratonic lagoon. More recent workers recognized that the black shale facies is linked to the Acadian foreland basin in the central Appalachians and developed euxinic basin models in which the shale accumulated below storm wave base in water depths ranging from less than 100 to more than 700 feet (e.g., Ettensohn, 1985; Ettensohn and others, 1988) (fig. 25). Indeed, depositional processes in the black shale basin were complex, and evidence for in-situ marine faunas and high-energy structures indicates that some of the shale accumulated in dysoxic environments and was episodically reworked above storm wave base in the cratonic reaches of the basin (e.g., Pashin and Ettensohn, 1992, 1995; Schieber, 1994).

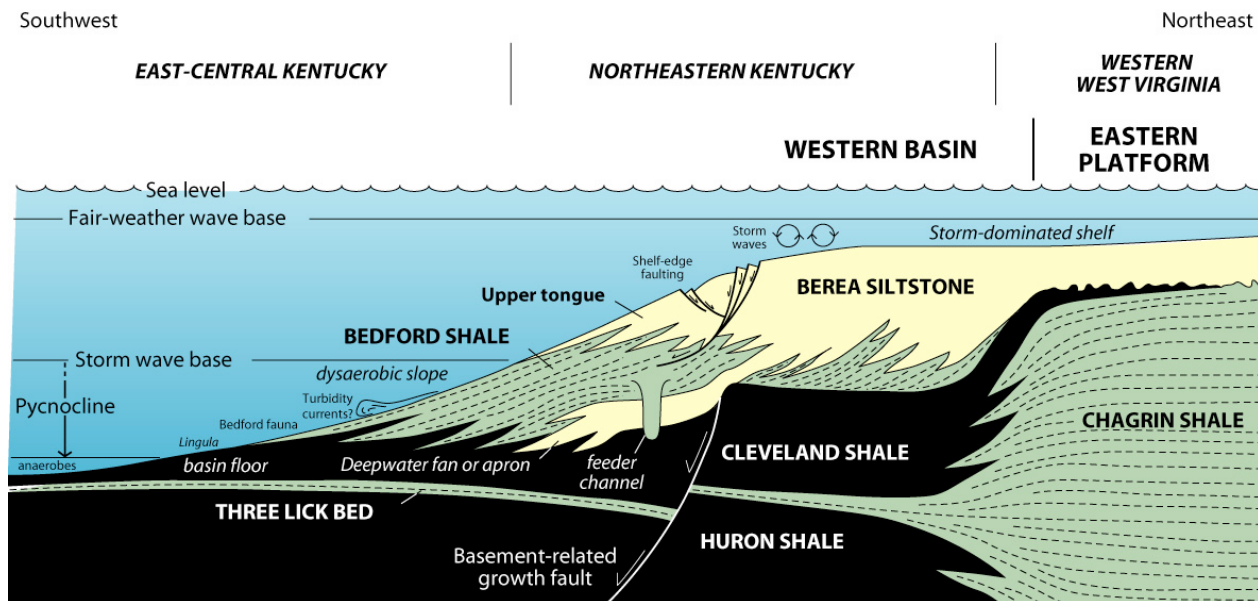


Figure 25.—Depositional model showing sedimentary processes in Devonian black shale and related strata in the Appalachian region (modified from Pashin and Etensohn, 1995).

Layers rich in radiolarians (fig. 24), moreover, suggest that upwelling of nutrient-laden water supported plankton blooms in the Chattanooga basin. Upwelling currents could have entered the basin from the southwest via the Ouachita embayment. Alternatively, episodic stirring of the organic-rich mud bottom by storm waves may have fed the blooms (fig. 26).

Evidence from cores in the Black Warrior basin and the Greene-Hale synclinorium (figs. 22, 23) reveals that black shale sedimentation in Alabama was dynamic (fig. 26). Bioturbation indicates that bottom water was at times oxygenated enough to support some infauna, and ripple cross-strata demonstrate that some sedimentation was associated with currents. Regional facies relationships and soft-sediment deformation further suggest that Devonian shale sedimentation in the Greene-Hale synclinorium occurred on a slope that was in many places unstable. The lateral transition from chert-bearing ramp carbonates to laminated, organic-rich shale and micrite (plate 2) is suggestive of a carbonate bank margin. Small-scale recumbent and overturned folds, moreover, are characteristic of submarine slumps and slides with significant lateral transport

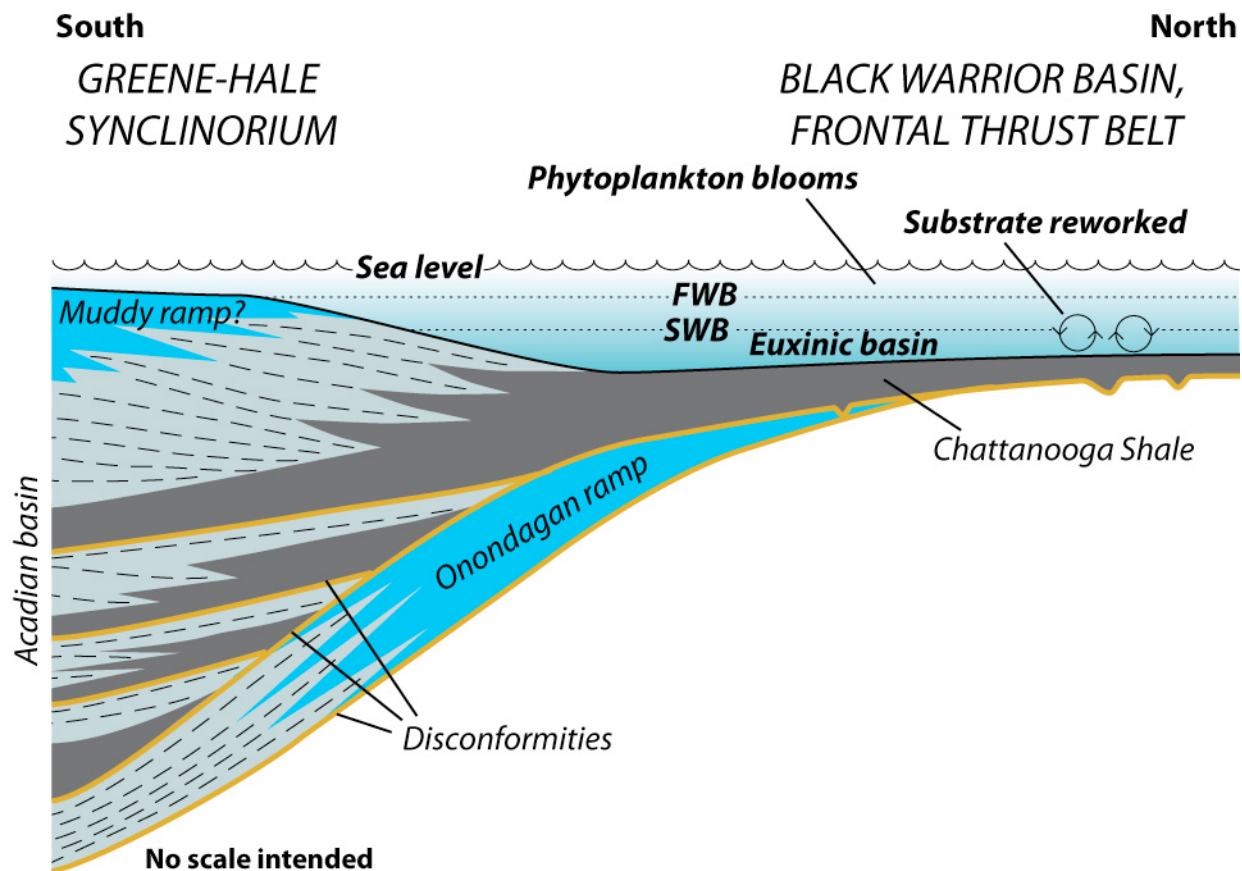


Figure 26.—Depositional model for Devonian shale in the Black Warrior basin and the Greene-Hale synclinorium.

(Farrell and Eaton, 1987), and the tilted shale that is onlapped by younger sediment may be part of a slump structure (fig. 22E). Indeed, the structureless shale layers within the laminated shale (fig. 22B) may represent the distal parts of mudflows that were generated by slope failure.

At a regional scale, Devonian tectonics and sedimentation in Alabama appear more complex than previously realized. The thin, widespread Chattanooga Shale of the Black Warrior basin and Appalachian thrust belt appears to have been deposited in a cratonic shelf setting that was, for the most part, tectonically stable. Thickening of the shale in the depocenter of southern Tuscaloosa, northern Greene, and northern Hale Counties (fig. 20) corresponds with a younger depocenter that persisted during Early Pennsylvanian time and has been interpreted as the

product of Appalachian thrust and sediment loading (Pashin, 1994b; 2004). Thus, the Devonian depocenter appears to foreshadow later foreland basin deformation. Indeed, the exceptionally thick Devonian shale section in the Greene-Hale synclinorium may be a remnant of an Acadian foreland basin.

### **Neal (Floyd) Shale**

The Upper Mississippian Floyd Shale is an equivalent of the prolific Barnett Shale of the Fort Worth basin and the Fayetteville Shale of the Arkoma basin. Thus, the Floyd has been the subject of intense interest for shale gas exploration. The Floyd is a broadly defined formation that is dominated by shale and limestone and extends from the Appalachian thrust belt of Georgia through the Black Warrior basin of Alabama and Mississippi (Thomas, 1972). Usage of the term “Floyd” can be confusing. The type Floyd Shale of Georgia includes strata equivalent to the Tuscumbia Limestone. In Alabama and Mississippi, complex facies relationships place the Floyd above the Tuscumbia Limestone, Pride Mountain Formation, or Hartselle Sandstone and below the first sandstone in the Parkwood Formation (fig. 5; plate 3).

Importantly, not all Floyd facies are prospective as gas reservoirs. Drillers have long recognized a resistive, organic-rich shale interval in the lower part of the Floyd Shale that is called informally the Neal shale (Cleaves and Broussard, 1980; Pashin, 1994a). The Neal is substantially less radioactive than Devonian black shale, and the parts of the Neal with radioactivity higher than 200 API units are highlighted in plate 3. In addition to being the probable source rock for conventional oil and gas (Telle and others, 1987; Carroll and others, 1995), the Neal has the greatest potential as a shale-gas reservoir in the Mississippian section of

Alabama and Mississippi. Accordingly, usage of the term, Neal, helps specify the facies of the Floyd that contains prospective hydrocarbon source rocks and shale-gas reservoirs.

The Neal shale is developed mainly in the southwestern part of the Black Warrior basin and is in facies relationship with strata of the Pride Mountain Formation, Hartselle Sandstone, the Bangor Limestone, and the Parkwood Formation (fig. 5; plate 3). The Pride Mountain-Bangor interval in the northeastern part of the basin constitutes a progradational sequence set or, alternatively, a progradational parasequence set in which numerous stratigraphic markers can be traced southwestward into the Neal shale (Pashin, 1993). Marine flooding surfaces within the upper Mississippian section can be defined with greater confidence than depositional sequence boundaries, thus parasequences are given priority for convenience. Individual parasequences tend to thin southwestward and define a clinoform stratal geometry in which nearshore facies of the Pride Mountain-Bangor interval pass into condensed deposits of the Neal shale. Conveniently, the Neal maintains the resistivity pattern of the Pride Mountain-Bangor interval, which facilitates regional correlation and assessment of reservoir quality at the parasequence level.

In the central part of the regional cross section (plate 3), where the Neal intertongues with the Bangor Limestone, Neal strata have a clinoform geometry. Farther south, where the Neal underlies a thick wedge of lower Parkwood strata, stratigraphic markers in the resistive shale are subparallel, defining a clinoform stratal geometry (see Rich, 1951). At the south end of the regional cross section, the upper part of the Neal includes beds that are equivalent to the lower Parkwood Formation and the basal strata of the *Millerella* limestone. These strata are preserved above the lower Parkwood stratigraphic wedge in northern Pickens County and merge southward with the main Neal shale mass.

In cores, the Neal is a black shale unit that superficially resembles the Chattanooga Shale. The shale is silty and is commonly calcareous, and internal laminae are more difficult to distinguish than in the Chattanooga. The Neal is laminated to thick-bedded and contains thin interbeds of limestone and siltstone, which tend to be wavy and lenticular and contain ripple cross-laminae (fig. 27). These interbeds are abundant in the clinofoliated shale that is transitional with the Bangor Limestone and are less common farther south where the shale exhibits a conformable stratal geometry. The high-resistivity shale that is so distinctive in well logs (plate 3) is difficult to distinguish from low resistivity intervals within the Neal by color alone. However, low-resistivity shale tends to be less fissile and more distinctly bioturbated; it contains a more diverse fauna that includes brachiopods, mollusks, and echinoderms. Well logs demonstrate that as shale resistivity increases, radioactivity also increases. Conversely, bulk density and density porosity decrease as resistivity increases. In addition, high-resistivity intervals are less prone to caving during drilling than are low-resistivity intervals.

Pashin (1993, 1994a) interpreted the Neal as an oxygen-deficient basin deposit (fig. 28) that formed during the early stages of the Ouachita orogeny. Correlation of the Neal with equivalent strata indicates a close relationship between the internal stratigraphy of the shale and that of equivalent shale, sandstone, and limestone units that were deposited to the northeast in nearshore environments (fig. 28; plate 3). The parasequences in the Neal shale and equivalent strata are apparently third-order depositional cycles that record a complex sea level history. Progradational gray shale-sandstone packages were deposited during highstand, whereas the Hartselle Sandstone and many of the carbonate intervals were deposited during marine transgressions. Correlation of these deposits with black shale suggests that most of the low-resistivity shale was

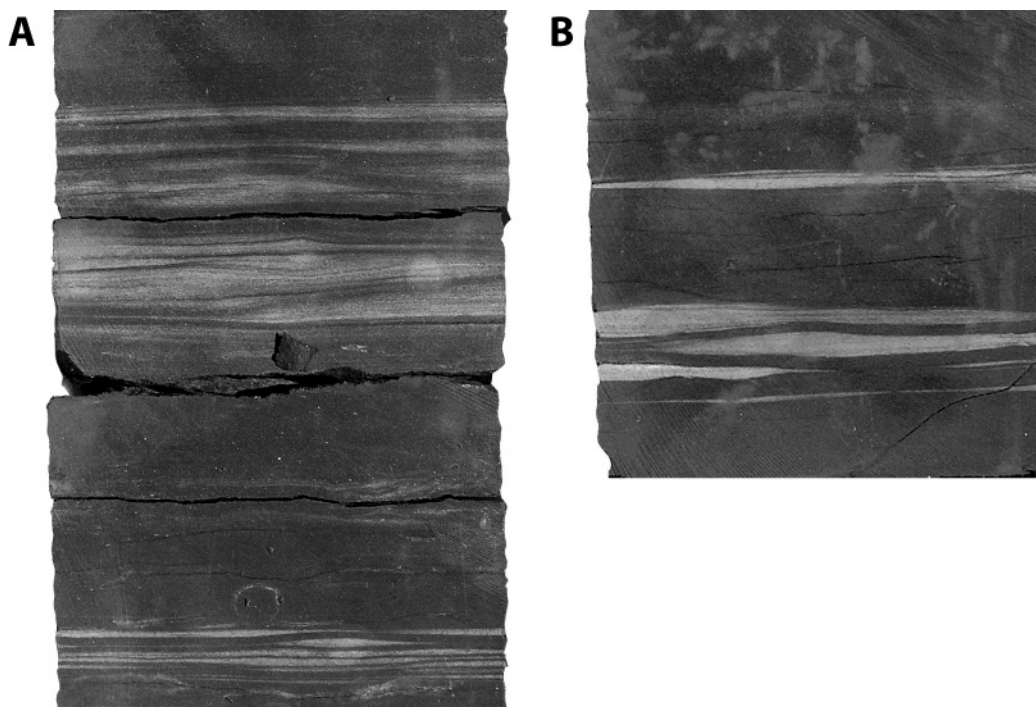


Figure 27.—Photos of Neal shale in the Exum Trust 16-6 #1 well, Pickens County, Alabama. (A) Shale with wavy- and lenticular-bedded siltstone, 6,565.7 ft. (B) wavy-bedded limestone in shale, 6,569.6 ft.

deposited during highstand events and that the resistive shale includes highstand and transgressive deposits.

The Neal shale has a gross thickness of 200 to 350 feet in a belt extending from west-central Lamar County to southwestern Fayette County (fig. 29). This thick shale corresponds with the clinof orm shale facies that was deposited on the distal slope of the Bangor carbonate ramp. The shale thins northeastward to less than 50 feet as it intertongues with the Bangor Limestone. Southwest of this belt, where the shale has a fondof orm geometry, gross thickness is typically between 100 and 250 feet.

The Neal shale and equivalent strata can be subdivided into three major intervals, and isopach maps of these intervals define the depositional framework and illustrate the stratigraphic evolution of the Black Warrior basin in Alabama (Pashin, 1993, 2008). The first interval includes

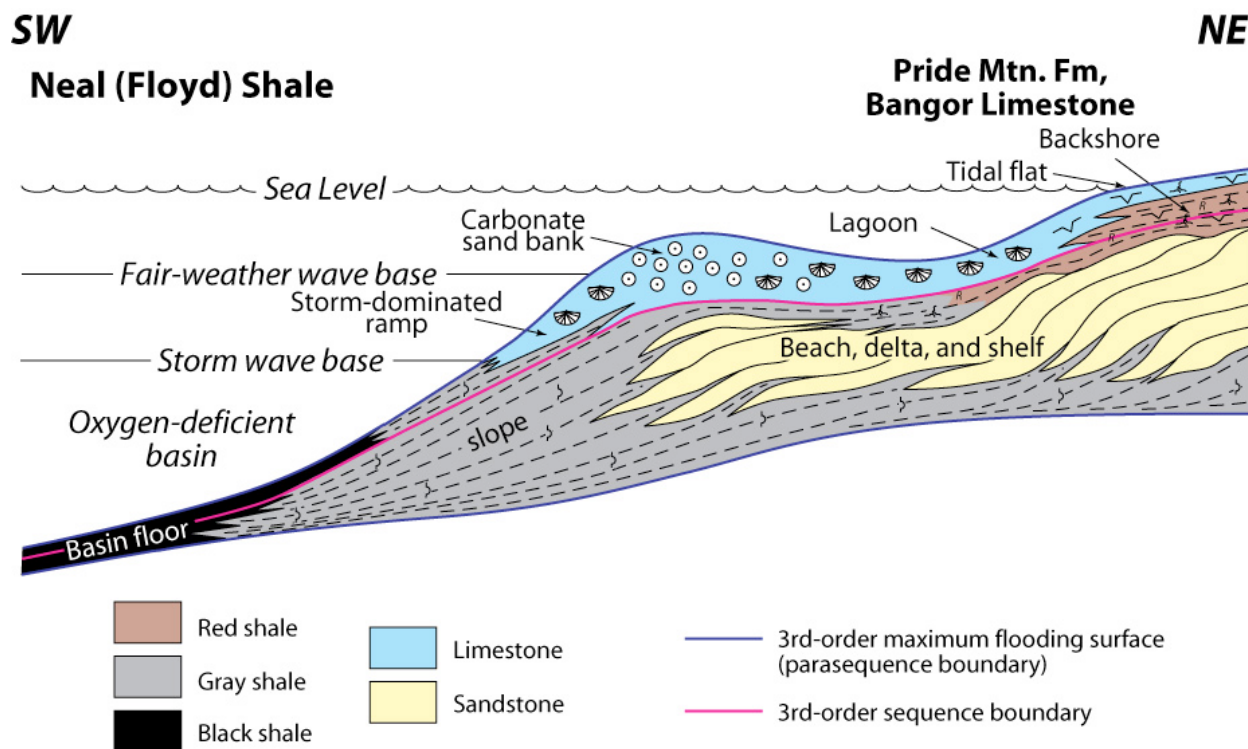


Figure 28.—Depositional model of an idealized 3<sup>rd</sup>-order parasequence in Upper Mississippian strata of the Black Warrior basin (modified from Pashin, 1994a).

strata equivalent to the Pride Mountain Formation and the Hartselle Sandstone and thus shows the early configuration of the Neal basin (fig. 30). The Pride Mountain-Hartselle interval is thought to contain barrier-strandplain deposits (Cleaves and Broussard, 1980; Thomas and Mack, 1982). Isopach contours define the area of the barrier-strandplain system in the northeastern part of the basin, and closely spaced contours where the interval is between 25 and 225 feet thick define a southwestward slope that turns sharply and faces southeastward in western Marion County. The black shale facies of the Neal is in the southwestern part of the map area and is thinner than 25 feet.

The second interval includes strata equivalent to the main part of the Bangor Limestone (fig. 31). A generalized area of inner ramp carbonate sedimentation is defined in the northeastern part

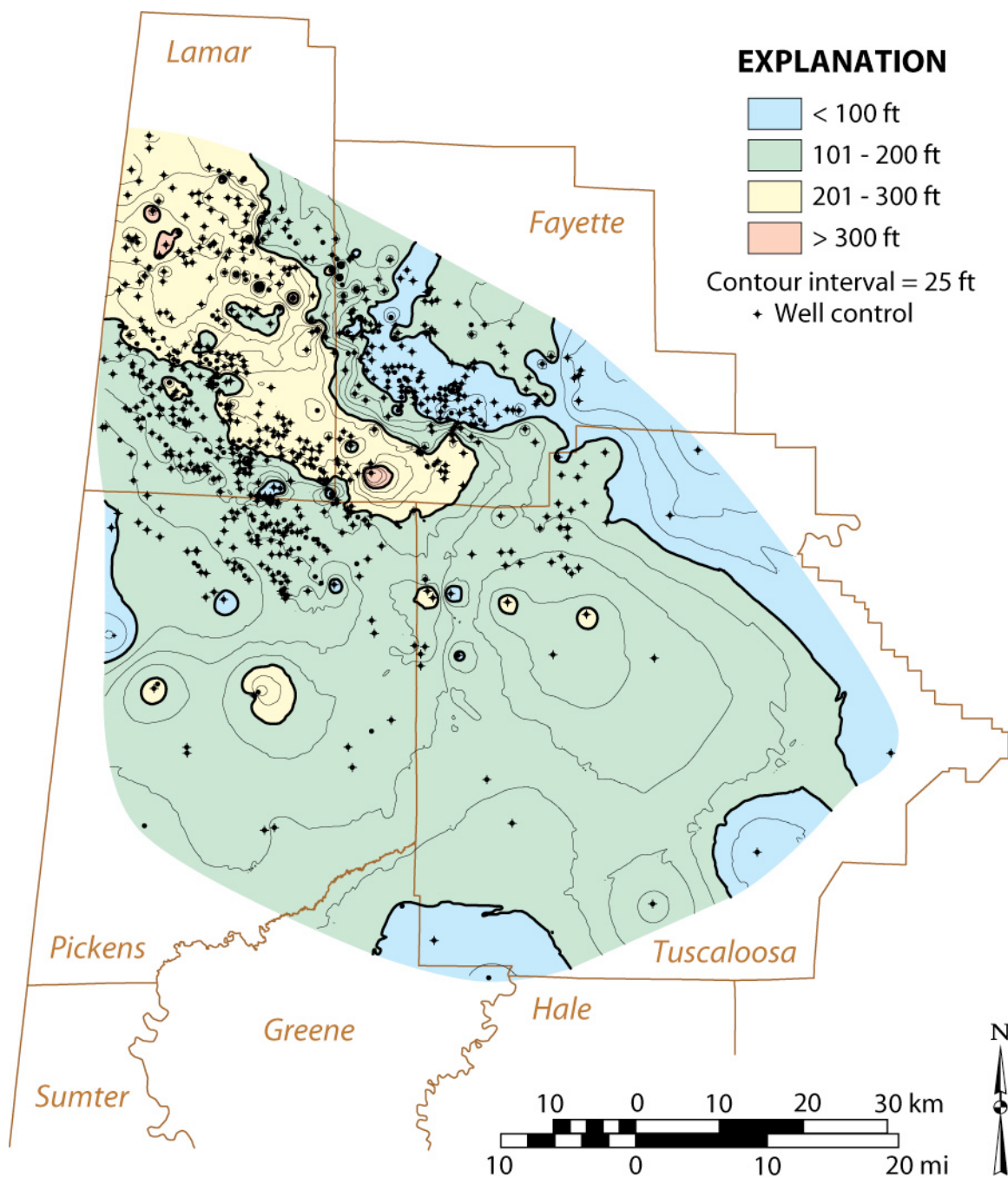


Figure 29.—Isopach map of the Neal (Floyd) shale in the Black Warrior basin of Alabama.

of the map area where the interval is thicker than 300 feet. Muddy, outer-ramp facies are concentrated where this interval thins from 300 to 150 feet and includes clinoform strata of the Neal shale. A basinal region, where the shale has a fondoform geometry, is marked by widely

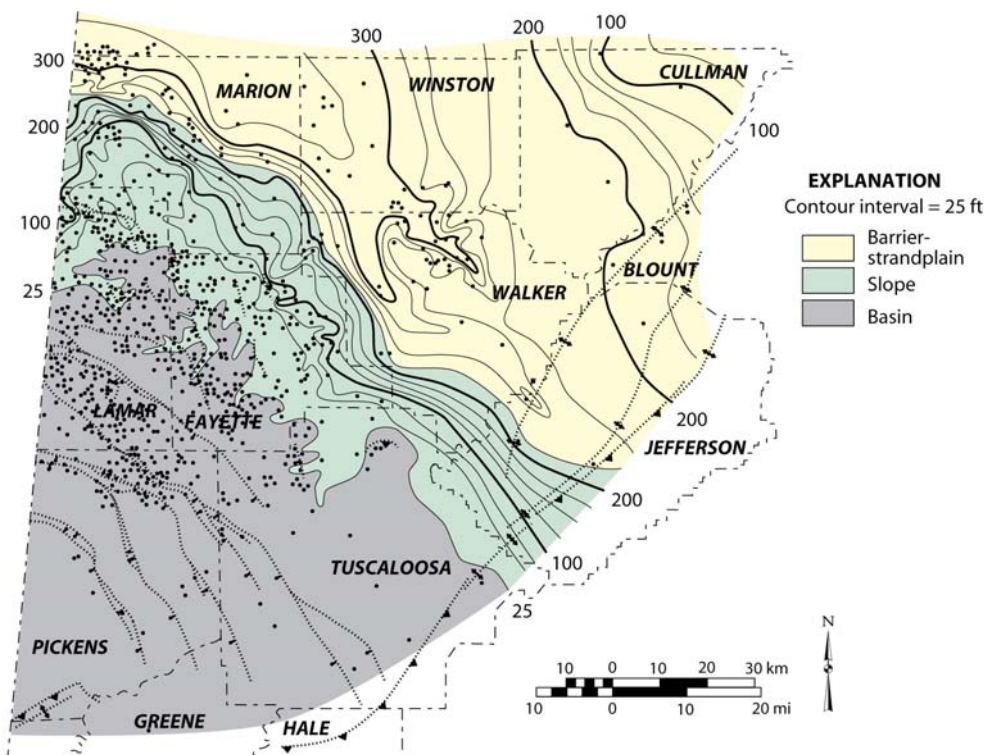


Figure 30.—Isopach map of the Pride Mountain Formation, Hartselle Sandstone, and equivalent strata in the Neal shale in the Black Warrior basin of Alabama (modified from Pashin, 1993).

spaced contours where the shale is thinner than 200 feet. Importantly, this interval contains the vast majority of the prospective Neal reservoir facies, and the isopach pattern indicates that the slope prograded more than 25 miles southwestward during Bangor deposition.

The final interval includes strata equivalent to the lower Parkwood Formation and the basal part of the *Millerella* limestone (fig. 32). The lower Parkwood separates the Neal shale and the main part of the Bangor Limestone from carbonate-dominated strata of the middle Parkwood Formation (plate 3). The lower Parkwood is a succession of siliciclastic deltaic sediment that prograded onto the Bangor ramp in the northeastern part of the study area and into the Neal basin in the southern part. This section contains the most productive conventional reservoirs in the Black Warrior basin (Cleaves, 1983; Pashin and Kugler, 1992; Mars and Thomas, 1999). The lower Parkwood is thinner than 25 feet above the inner Bangor ramp and includes a variegated

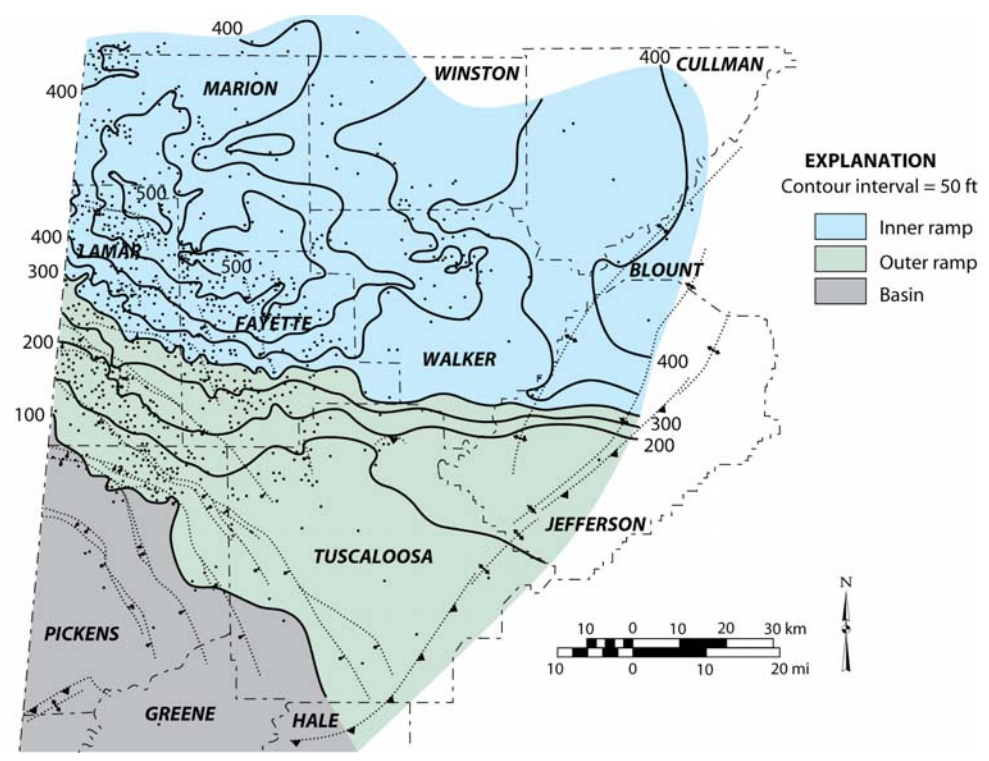


Figure 31.—Isopach map of the Bangor Limestone and equivalent strata in the Neal shale of the Black Warrior basin in Alabama (modified from Pashin, 1993).

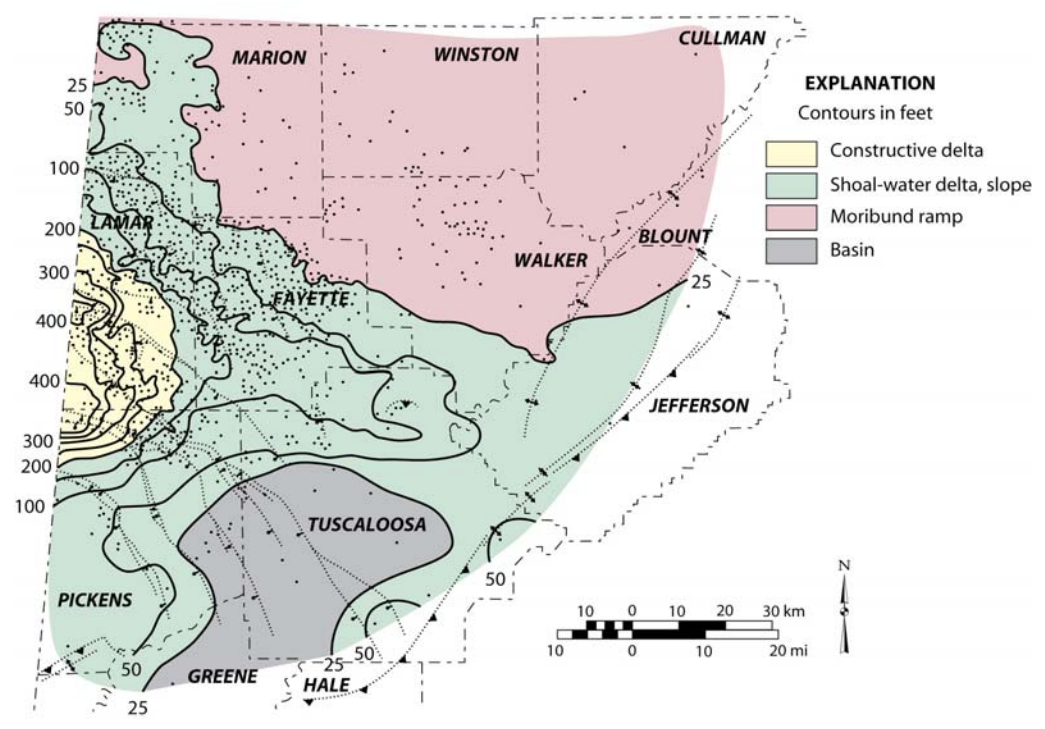


Figure 32.—Isopach map of the lower Parkwood Formation and equivalent strata in the Neal shale of the Black Warrior basin in Alabama (after Pashin, 1993).

shale interval containing abundant slickensides and calcareous nodules, which indicate exposure and vertic soil formation. The area of deltaic sedimentation is where the lower Parkwood is thicker than 50 feet and includes constructive deltaic facies in the Neal basin and destructive, shoal-water deltaic facies along the margin of the Bangor ramp. In the southern part of the study area, the 50-foot contour defines a remnant of the Neal basin that persisted through lower Parkwood deposition. It is in this area that Neal strata equivalent to the middle Parkwood merge with the main black shale body (plate 2), and it is where most gas exploration has taken place in the Neal shale.

## **STRUCTURAL GEOLOGY**

Following sedimentation and burial, strata in the Black Warrior basin and the Appalachian thrust belt were folded, faulted, and fractured. This deformation can have a strong influence on the basic reservoir properties of the Paleozoic black shale units, and the contrasting extensional and compressional structural styles in the region necessitate diversified exploration strategies. This section begins with a discussion of folding and faulting in the Black Warrior basin and Appalachian thrust belt and concludes with a discussion of the fracture networks that were observed in the shale gas reservoirs.

### **Extensional Faults in the Black Warrior Basin**

Experience from the Barnett Shale in the Fort Worth basin indicates that extensional faulting can have a detrimental influence on shale reservoir performance. Bowker (2007), for example, suggested that even fault zones that have been sealed naturally can reopen when pressured and thus facilitate leak-off of stimulation fluid, which would limit the effectiveness of hydrofracture

treatments. Accordingly, production from the Barnett has been most successful in large structural panels lacking faults.

Northwest-striking normal faults are abundant in the Black Warrior basin and define a regionally extensive horst-and-graben system in which the majority of the faults are downthrown toward the southwest (e.g., Thomas, 1988; Groshong and others, 2009, 2010) (figs. 6, 33-35). The geometry of the fault systems is quite complex. In the northeastern part of the basin, deformation has been interpreted to be dominated by thin-skinned faulting in which faults are developed above a detachment within the synorogenic Pennsylvanian section (Pashin and Groshong, 1998; Groshong and others, 2009). These faults have nearly linear traces that are generally shorter than 10 miles and typically have vertical displacement of less than 250 feet. In the backlimb of the Sequatchie anticline, which is the frontal structure of the Appalachian thrust belt, the faults have an echelon map patterns that indicate an origin related to left-lateral transtension and a kinematic linkage between regional extension and Appalachian structure (fig. 33).

Deformation steps down to deeper structural levels toward the southwest, where multiple fault sets are developed (figs. 33-35). One set of planar faults offsets the top of basement and dies out near the top of the Rome-Conasauga section (fig. 34). Accordingly, these faults were apparently contemporaneous with Rome-Conasauga sedimentation and thus reflect deformation associated with late-stage Iapetan rifting. Another set of planar faults offsets basement and dies out near the top of the Cambrian-Ordovician carbonate section, and yet another set penetrates the complete Paleozoic section (fig. 35). Many of these faults exhibit major thickening of Paleozoic strata in the hanging walls and are thus interpreted as synsedimentary growth structures that were active during long spans of geologic time. Whereas most faults are planar and cut basement,

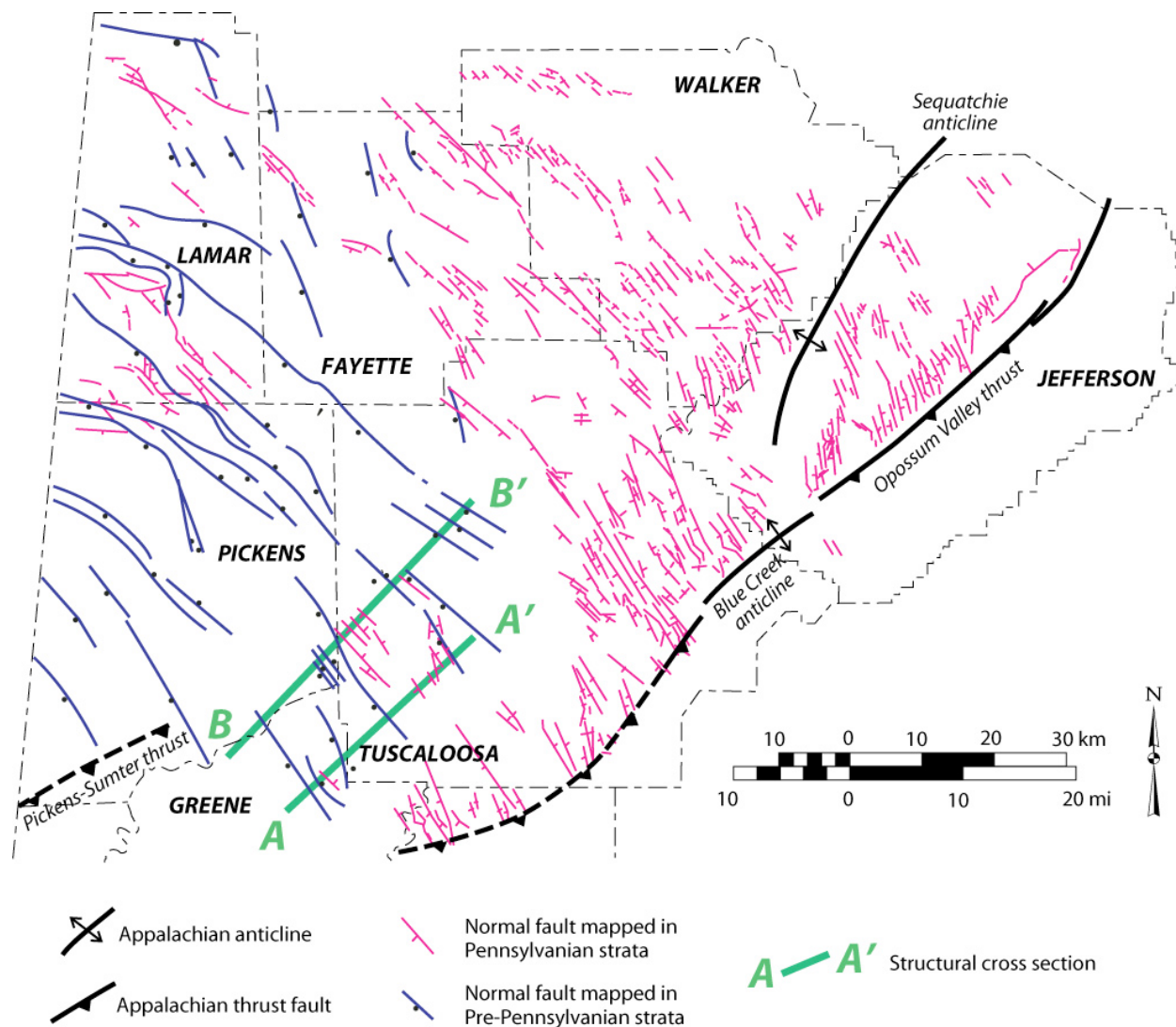


Figure 33.—Structural trace map of the Black Warrior basin showing relationships among frontal Appalachian structures and normal faults in the Black Warrior basin (modified from Pashin and others, 1991).

some of the faults are listric and are interpreted to flatten at the top of the mechanically weak Rome-Conasauga shale section. Interestingly, these faults show no evidence of syndepositional growth and may thus be the youngest faults offsetting the pre-orogenic stratigraphy. Although many faults extend upward to the sub-Cretaceous unconformity, none of the extensional faults in the Black Warrior basin offset the Cretaceous section (Thomas, 1988; Groshong and others, 2010). Because displacement of the faults increases southwestward toward the Ouachita orogenic

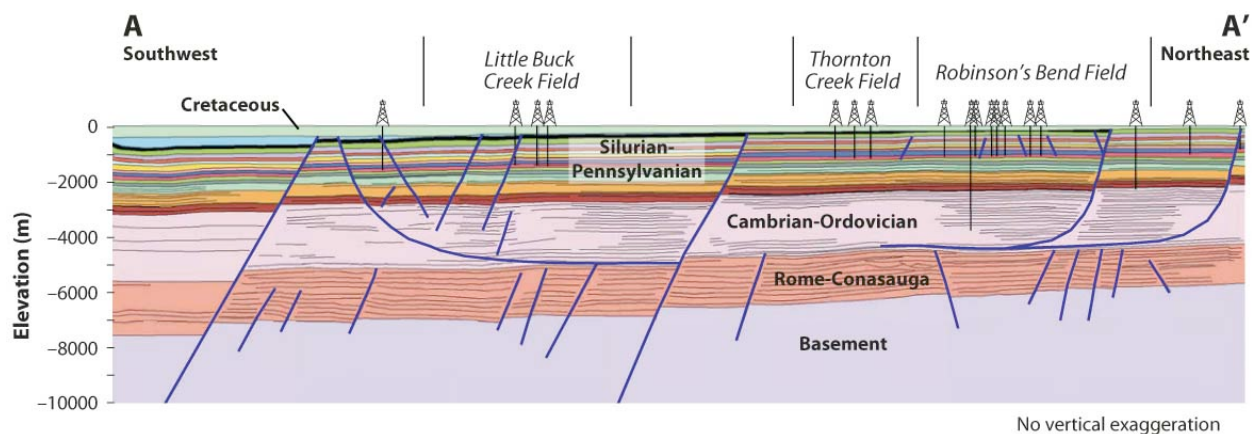


Figure 34.—Structural cross section showing multiple levels of normal faulting in the Black Warrior basin (modified from Groshong and others, 2010). See Figure 26 for location.

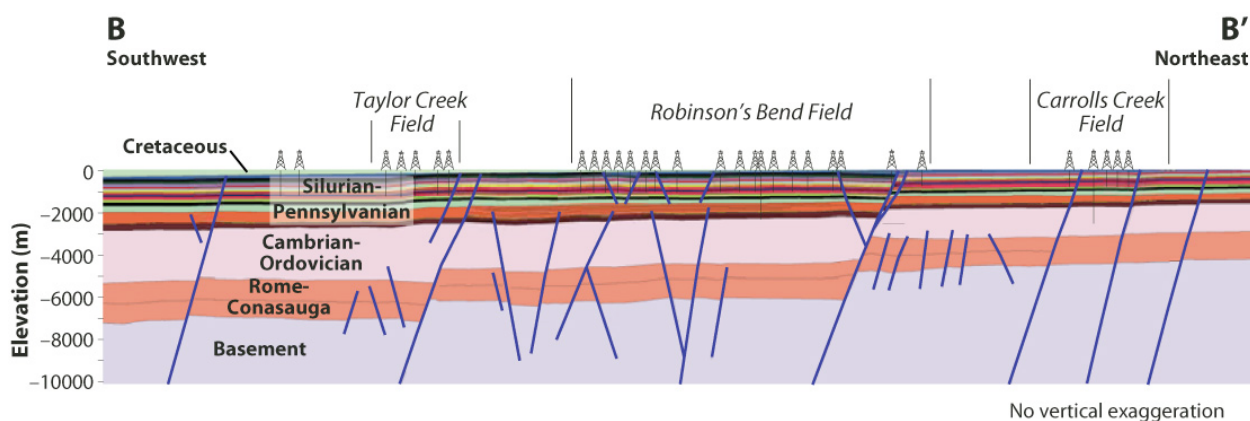


Figure 35.—Structural cross section showing growth faults cutting basement in the Black Warrior basin (modified from Groshong and others, 2010). See Figure 26 for location.

belt, one possibility is that Pennsylvanian-Permian fault movement was related to foreland flexural extension driven by crustal accommodation of Ouachita thrust and sediment loads (Cates and Groshong, 1999).

In plan view, the normal faults that have been mapped below the Pennsylvanian section have planar, arcuate, or weakly sinuous structural traces that can extend for tens of miles (figs. 6, 33). Vertical displacement of the faults is generally greater than 300 feet, and one fault in southwestern Lamar County has displacement that locally exceeds 2,400 feet. Fault-related

folding associated with the large-displacement faults is difficult to discern in cross section, reflecting development above a deep detachment, which may be in the middle crust (Groshong and others, 2010). However, structural contour maps reveal that large three-way fault closures are developed in the hanging wall blocks of many faults, and these closures have been the focus of conventional hydrocarbon exploration. The origin of these closures is a matter for debate and may in part represent rollover folds that were tilted southwestward during subsidence of the Gulf of Mexico basin.

The abundance of normal faults in the Black Warrior basin indicates that care should be taken when exploring for shale gas. Well and seismic data indicate that large structural panels can be identified where structural conditions are favorable for shale gas development. Mapping these panels appears crucial for minimizing the risk of stimulation fluid leaking into fault zones, which can limit the effectiveness of hydrofracturing. Furthermore, faulting may be an important consideration for siting and orienting directional wells to maximize the effectiveness of stimulation treatments.

### **Compressional Structures in Conasauga Shale**

Compressional folds and faults in the Appalachian thrust belt have fundamentally different geometric and mechanical properties than the extensional structures in the Black Warrior basin, thus posing a different set of variables to be considered in shale gas development. Indeed, the structural style of the southern Appalachian thrust belt is influenced strongly by the geomechanical properties of the stratigraphic section (Rodgers, 1950; Thomas, 1985, 2001). As mentioned previously, the basal detachment of the thrust belt is developed within a weak Cambrian shale section that overlies crystalline basement (fig. 3).

The Cambrian shale of the Conasauga Formation hosts giant antiformal stacks of intensely deformed shale that are locally more than 12,000 feet thick and have been a focus of shale gas development in Alabama (figs. 3, 36). These antiformal stacks were referred to as MUSHWADs (i.e., Malleable, Unctuous SHale, Weak-layer Accretion in a ductile Duplex) by Thomas (2001) to emphasize the extremely complex deformation within widespread structural duplexes that were preserved below a more gently deformed carbonate roof. Below the shale masses, the basal detachment ramps upward above the edge of the Birmingham graben, which is a late Precambrian-Early Cambrian Iapetan rift structure. Structural inversion of the Birmingham graben is thought to have begun during the Taconic orogeny (Butts, 1926; Thomas, 2001; Thomas and Bayona, 2005), which may have helped make the shale prone to deformation and overthickening during the Pennsylvanian-Permian Alleghanian orogeny.

Surface mapping and seismic exploration reveal that at least three Conasauga MUSHWADs are preserved in the Alabama Appalachians (fig. 7). Exploration has focused primarily on the southeastern portion of the Gadsden MUSHWAD, which is in St. Clair and Etowah Counties. The Palmerdale and Bessemer MUSHWADs constitute the core of the Birmingham anticlinorium. The Palmerdale and Bessemer MUSHWADs are overlain by a thin roof of brittle Cambrian-Ordovician carbonate rocks, and Conasauga shale is exposed locally. The Palmerdale structure is in the heart of the Birmingham metropolitan area and thus may be difficult to develop, whereas the southwestern part of the Bessemer structure includes rural areas and may be a more attractive exploration target. Additional thick shale bodies may be concealed below the shallow Rome thrust sheet in Cherokee and northeastern Etowah Counties (Maher, 2002) and perhaps in adjacent parts of Georgia (Mittenthal and Harry, 2004; Cook and Thomas, 2010).

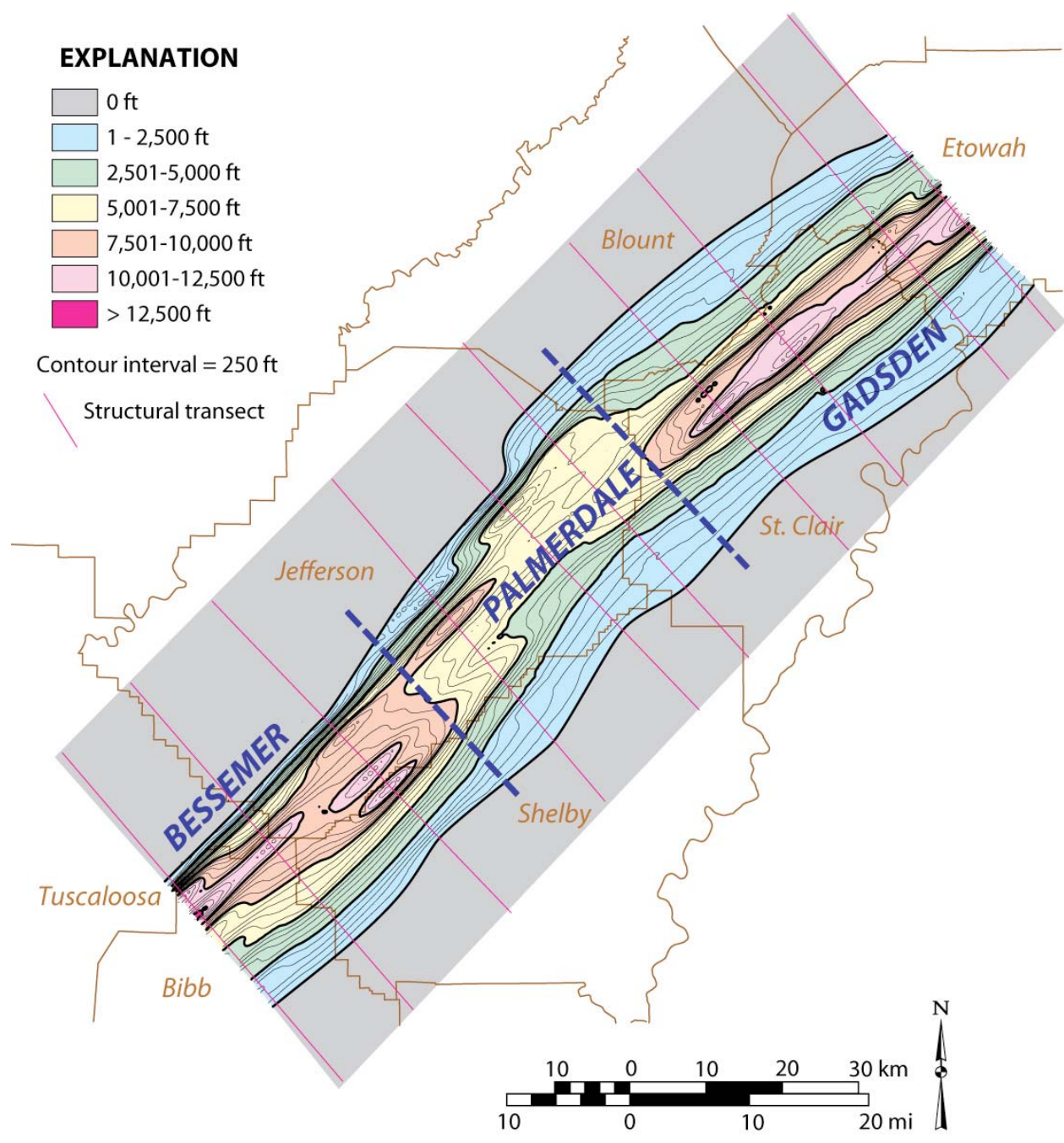


Figure 36.—Isopach map of deformed Conasauga shale constituting the Gadsden, Palmerdale, and Bessemer MUSHWADs. Structural control from balanced cross sections of Thomas and Bayona (2005).

An isopach map of the deformed Conasauga shale was made using the balanced cross sections of Thomas and Bayona (2005) to control thickness (fig. 36). The resulting map suggests that the deformed shale mass constitutes a giant antiformal ridge that strikes about N. 45° E., and in which the three MUSHWADs mark significant along-strike structural variations. The Gadsden MUSHWAD is locally thicker than 12,000 feet and is nearly symmetrical, with the northwestern flank underlying the Blount Mountain syncline and the southeastern flank underlying the Coosa synclinorium (figs. 3, 36). A large part of the shale mass is exposed at the surface (fig. 7), and so the original shale mass must have been much thicker (Thomas, 2001). The Palmerdale MUSHWAD contains a structural saddle in the roof, and most of the shale mass is thinner than 7,500 feet (fig. 36). Farther southwest, the Bessemer MUSHWAD is much thicker, and maximum shale thickness exceeds 12,500 feet at the southwestern end of the mapped shale mass. The Palmerdale and Bessemer MUSHWADS are strongly asymmetrical, with the southeast flanks thinning gently below the Cahaba synclinorium and the northeast flanks buttressing the steeply dipping strata that form the southeast margin of the Black Warrior basin (figs. 3, 36).

Thomas (2001) recognized that the Conasauga MUSHWADs are composed internally of regionally dipping thrust horses separated by zones of intense deformation. Exposures within the Gadsden MUSHWAD, where a large shale mass is exposed at the surface, provide the best views of internal deformation (Pashin, Carroll and others, 2010). The regionally dipping horses contain weakly deformed strata (fig. 10) with minor folds, abundant joints (fig. 37), and carbonate-filled veins (figs. 38, 39). Regionally, the horses tend to strike N. 55° E. and dip about 10° SE, although dip locally exceeds 30°. Intensely deformed strata between the structurally coherent horses range from mylonitic fault gouge (fig. 40) to chaotic deformation zones with abundant folds and faults (fig. 41). Fold types within the chaotic zones include similar folds, chevron



Figure 37.—Closely jointed Conasauga shale, Pinedale Lake Spillway, St. Clair County, Alabama.



Figure 38.—Bed-parallel carbonate vein in Conasauga shale, Pinedale Lake Spillway, St. Clair County, Alabama.



Figure 39.—En echelon veins, Conasauga shale, Pinedale Lake Spillway, St. Clair County, Alabama.



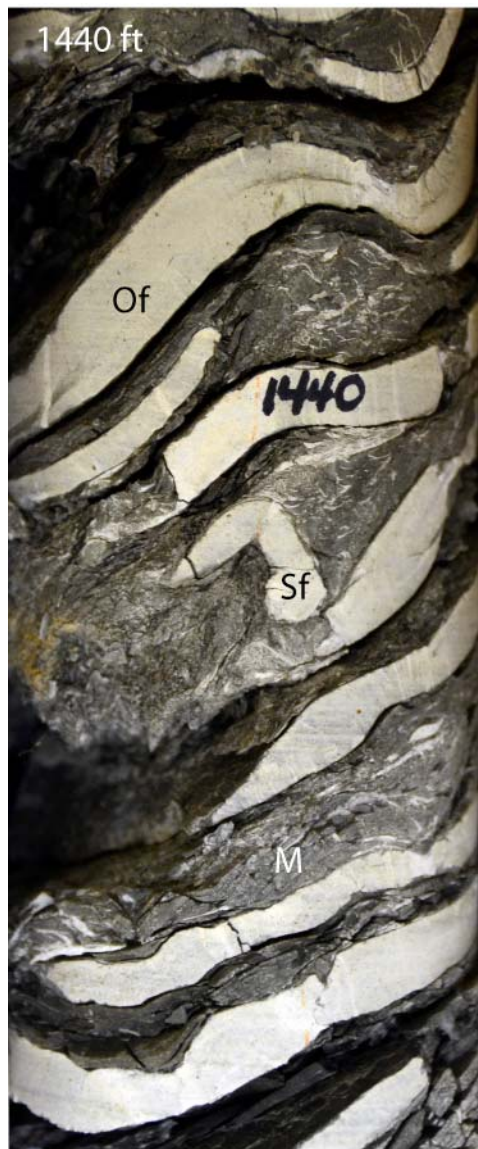
Figure 40.—Mylonitic fault gouge, Conasauga shale, Pinedale Lake Spillway, St. Clair County, Alabama.



Figure 41.—Chevron folds in Conasauga shale at Springville rest area, Interstate 59, St. Clair County, Alabama (photograph courtesy of Dan Irvin).

folds, and isoclinal folds, and the axial planes of the folds can be near vertical. One possibility is that these intensely deformed strata are accommodation zones that help fill space along the margins of the regionally dipping thrust horses.

Similar deformation structures are abundant in the Dawson 34-03-01 exploratory core (fig. 42). Most of the core exhibits bedding dip between 10 and 30° and appears, for the most part, to preserve original stratigraphic order. Numerous faults and shear fractures are distributed through the core; many such structures have millimeter- to centimeter-scale displacement, whereas others have displacement exceeding core diameter. Shear fractures include conjugate fractures and tension gashes, which are filled with calcite spar. Locally, oil is present in voids within the calcite fill. Stylolites are also important deformation structures in the core. Most are bed-parallel,



Core diameter = 2.3"

Of - Open fold  
 Sf - Sheared fold  
 If - Isoclinal fold  
 Mf - Microfault  
 M - Mylonite



Figure 42.—Tectonic deformation structures in the Dawson 34-03-01 core.

whereas others are subvertical. Some stylolites truncate bedding, indicating that they may have formed along faults or that a significant amount of carbonate has been dissolved. Deformation is especially intense in the basal 100 feet of the core, which appears to constitute a major shear zone. Here, numerous open folds (fig. 42A), sheared isoclines (fig. 42B), and microfaults (fig. 42B) are preserved. Much of the shale has a mylonitic texture in which a multitude of shear fractures have been cemented with calcite (fig. 42).

Big Canoe Creek has been established in the Gadsden MUSHWAD as Alabama's first shale gas field. Within the field, 18 wells were drilled by Dominion Exploration and Production, Incorporated, 13 are of which active. Structural deformation within the field has presented several challenges for drilling. Wells are deviated substantially toward the northwest, which reflects the predominant southeastern dip of the Conasauga Formation along the southeast margin of the Gadsden structure. Small-scale deformation contributes to the difficulty of drilling, as does the sensitivity of the interbedded shale and micrite to water. The Palmerdale MUSHWAD underlies the Birmingham metropolitan area, which may make development difficult. Two wells have been drilled near the southwestern end of the Bessemer MUSHWAD by Energen Resources, Incorporated. Both wells are listed as active and have yet to be completed.

### **Compressional Structures in Devonian Shale**

Above the Cambrian shale is a stiff carbonate succession of Cambrian-Ordovician age, which is geomechanically the strongest stratigraphic unit in the thrust belt and thus dictates shallow structural geometry (Thomas, 1985; Thomas and Bayona, 2005). Within the Cambrian-Ordovician section, deformation is dominated by frontal and lateral ramps. Silurian through Pennsylvanian strata constitute a large volume of interbedded shale, sandstone, and limestone

that is substantially weaker than the Cambrian-Ordovician carbonate. Even so, frontal ramps commonly rise upward through the complete Cambrian-Pennsylvanian section in the footwalls of the major thrusts, and strata above the Conasauga were in many areas transported cratonward in unison (fig. 3).

In the hanging walls of the major thrusts, the pre-orogenic Cambrian-Ordovician section crops out in a series of ramp anticlines and major fold limbs, whereas the synorogenic Pennsylvanian section is preserved in broad, flat-bottomed synclines (figs. 3, 7). Locally, however, upper-level thrust flats and secondary detachments are developed at the top of the Cambrian-Ordovician carbonate section and within weak shale units in the Ordovician-Pennsylvanian section (e.g., Thomas, 1985; Pashin and Groshong, 1998; Thomas and Bayona, 2005). Indeed, many second-order folds within the Late Paleozoic section are developed above these secondary detachments in the frontal thrust sheets, and complexly deformed carbonate duplexes are preserved in the interior of the thrust belt adjacent to the metamorphic front.

The salient type of structure in the southern Appalachian thrust belt is a ramp anticline with a steep or vertical forelimb and a gently dipping backlimb (fig. 3). Fold and thrust geometry are intimately related, and recent structural interpretations indicate that significant variations of geometry that may affect reservoir performance occur within and among the major Appalachian structures (e.g., Maher, 2002; Groshong, 2006; Gates, 2006). Thrust faults in the southern Appalachians have been interpreted to include listric thrust faults and ramp-flat structures. The Sequatchie and Wills Valley anticlines, for example, have been interpreted to be at least partly developed above listric thrust faults (Maher, 2002; Groshong, 2005, 2006).

Seismic data have been used to constrain along-strike variation in the Wills Valley anticline, and balanced cross sections document the consequences of changing fault geometry on fold

geometry. Deformation above a listric thrust near the southwest terminus of the Wills Valley anticline is associated with a broadly folded backlimb structure lacking distinct fold hinges in the Lookout Mountain syncline (Maher, 2002) (fig. 43). Farther northeast, this same thrust fault, while maintaining an overall listric geometry, is interpreted to contain multiple dip bends that localize distinct fold hinges in the backlimb of the anticline (fig. 44). Importantly, southern Appalachian fold hinges are zones of enhanced natural fracturing associated with productivity sweet spots in coalbed methane reservoirs (Pashin and Groshong, 1998; Pashin, 2005; Groshong and others, 2009), and similar hinge effects may influence the performance of shale reservoirs.

Bailey (2007) interpreted a seismic profile that shows the geometry of the Greene-Hale synclinorium in Greene County (fig. 45). This profile shows that thrust-belt structure below the Gulf of Mexico coastal plain is dominated by a ramp-flat geometry that differs significantly from the exposed frontal structures farther northeast. A large frontal ramp defines the boundary between the Appalachian thrust belt and the Black Warrior basin, and repetition of the Cambrian-Ordovician carbonate section in the hanging wall defines an imbricate pair of thrust panels with large displacement. Devonian and younger strata of the Greene-Hale synclinorium are preserved in the hanging wall of the imbricate thrust panels and are thickest at the southeastern end of the profile. A large ramp anticline is developed within the synclinorium and has been the subject of exploration activity. The Ethel M. Koch 10-6 #1 well penetrates the crest of the anticline as well as a thrust fault that places Cambrian Conasauga limestone on top of the Cambrian-Ordovician Knox Group. The Bayne-Etheridge 36-9 #1 well was drilled in the backlimb of the anticline, and the dipmeter log confirms that dip is about 20° SE. A new well (Tate 9-4 #1) has been drilled in the forelimb of the anticline southwest of the Koch well and penetrated a near-vertical structural panel in the Devonian section.

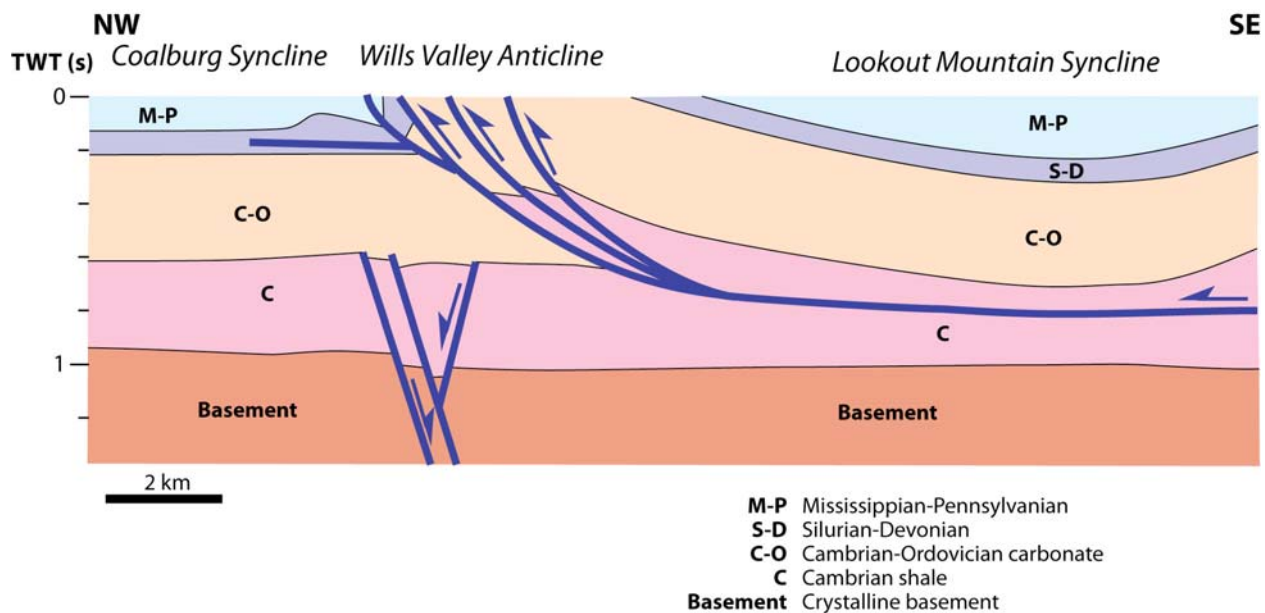


Figure 43.—Structural interpretation based on seismic profile of the Wills Valley anticline and associated structures above a listric thrust fault (modified from Maher, 2002).

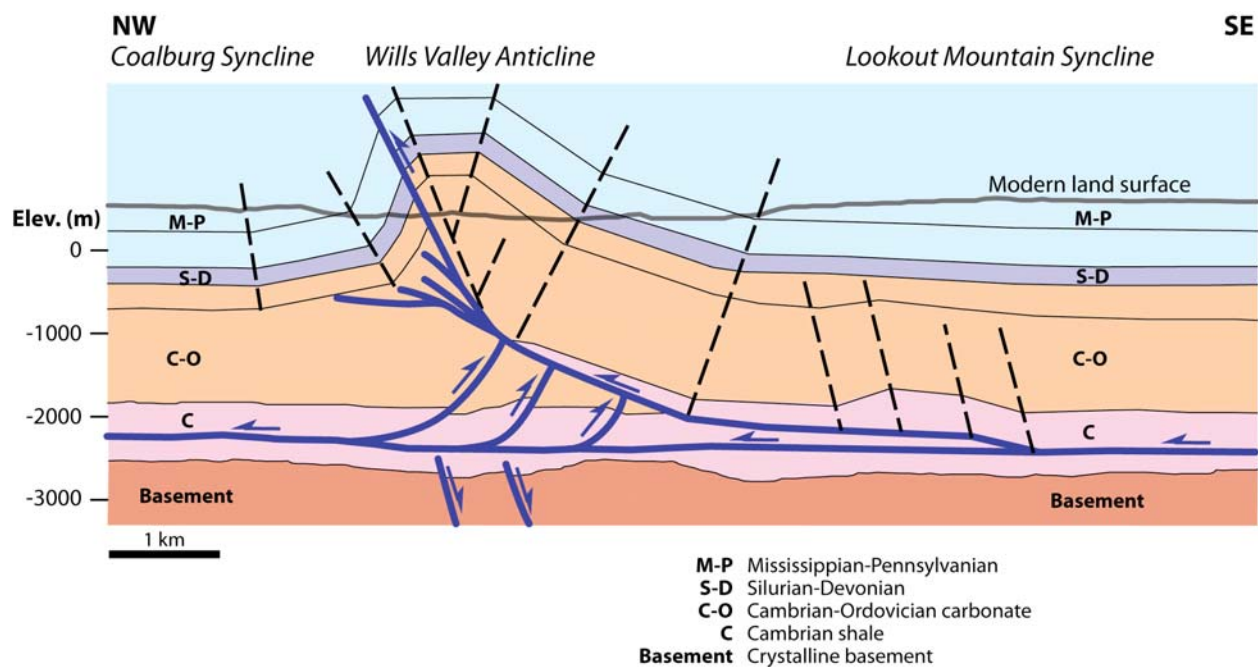


Figure 44.—Structural interpretation based on seismic profile of the Wills Valley anticline and associated structures above a thrust fault with multiple dip bends (modified from Gates, 2006).

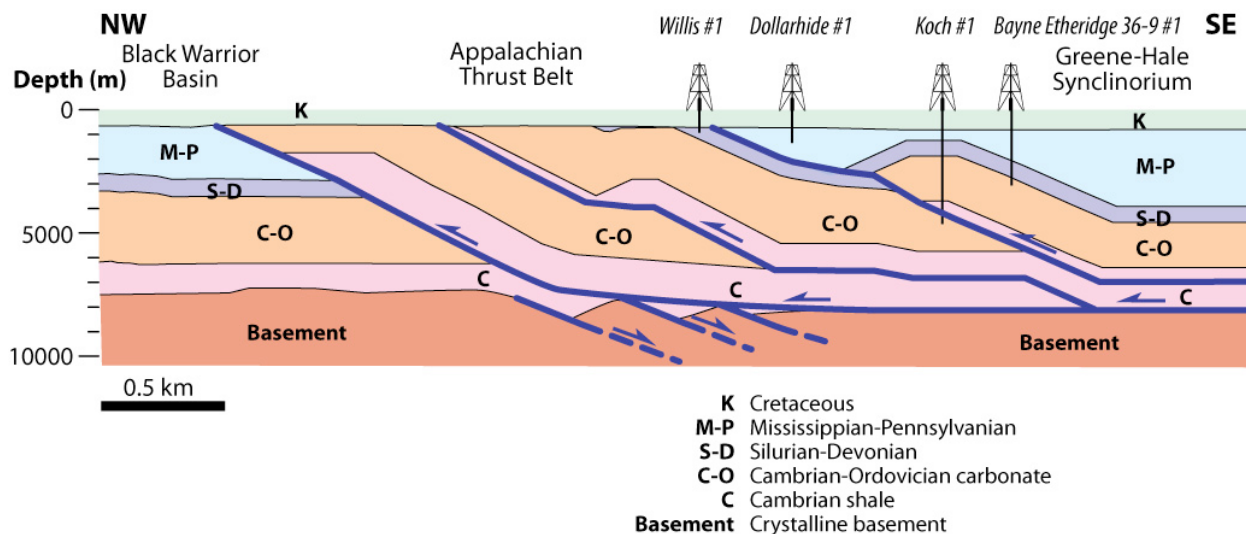


Figure 45.—Structural interpretation based on seismic profile of ramp-flat thrust belt structure below the Gulf of Mexico coastal plain (modified from Bailey, 2007).

### Fracture Networks

Natural fracture networks are important recorders of the stress history of sedimentary basins and can have a strong influence on the reservoir properties of shale (e.g., Gale and others, 2007; Engelder and others, 2009). Fractures in Alabama's shale gas reservoirs include orthogonal joint networks and shear fracture networks. In this section, we discuss the properties of joints and shear fractures and their relevance for shale gas exploration.

Joints are common in all the gas shale formations considered in this study (figs. 18, 46, 47). These fractures are characteristically perpendicular to bedding and form orthogonal networks consisting of systematic joints and cross joints. Systematic joints tend to be planar fractures that extend laterally for great distances, whereas cross joints tend to have rougher surfaces and can be more sinuous (fig. 47). Cross joints typically strike perpendicular to systematic joints and tend to terminate at intersections with systematic joints. Organic-rich strata, such as coal and gas shale, typically contain closely spaced orthogonal fractures, and the close fracture spacing is thought to be a product of stresses generated by tectonic forces as well as stresses generated by

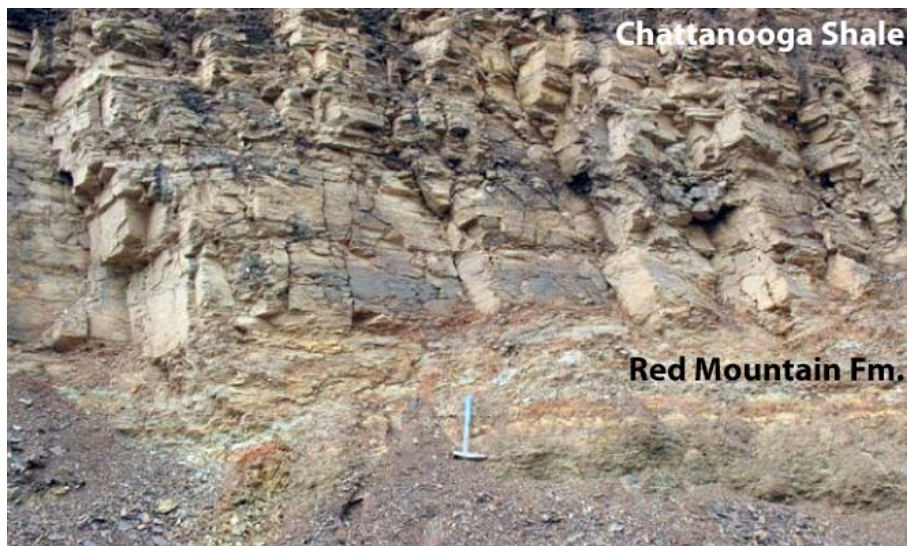


Figure 46—Outcrop in the backlimb of the Sequatchie anticline showing jointed Chattanooga Shale disconformably overlying the Silurian-age Red Mountain Formation (photograph courtesy of Dan Irvin).

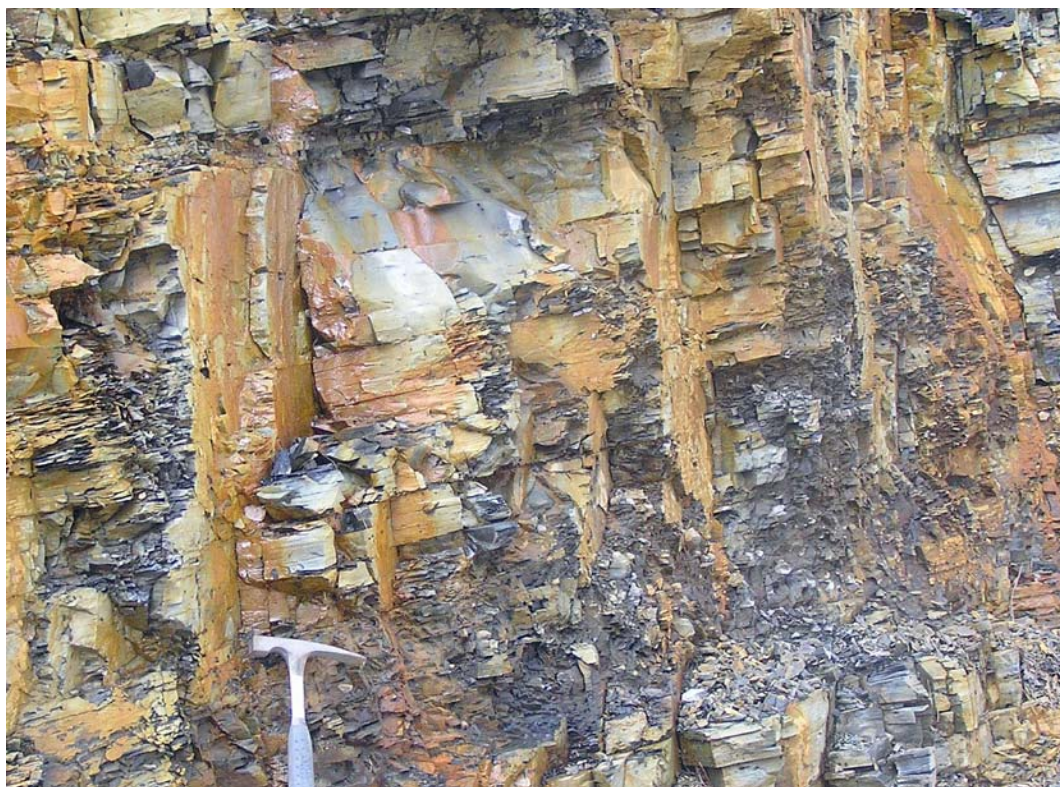


Figure 47.—Planar systematic joints in the Chattanooga Shale at Big Ridge, Etowah County, Alabama.

devolatilization and hydrocarbon generation during burial thermal maturation (e.g., Laubach and others, 1998; Engelder and others, 2009).

In Conasauga shale, joints are best developed within the coherent structural panels in outcrop (fig. 48). Systematic joints tend to strike N. 45° E., which is near regional strike, and cross joints are poorly developed. Joint spacing is in places about an inch and thus rivals the cleat systems in many coalbed methane reservoirs. Although joints are abundant in outcrop, they have not been observed in core and may thus be of limited significance for hydrocarbon exploration.

In the Chattanooga Shale, some joints extend through the full thickness of the shale (figs. 46, 47), whereas others are strata-bound; that is, restricted to individual beds and laminae (fig. 22B). Joints are readily observed in cores of black shale and are typically filled with calcite, dolomite, pyrite, silica, and clay (fig. 22A). Systematic joints typically strike east-northeast in outcrop (azimuths between 60 and 100°), and cross joints are in places abundant (figs. 46, 47). The joints are perpendicular to bedding, even in dipping fold limbs, thus the joint systems are interpreted to predate regional folding (Pashin, 2008, 2009) (fig. 48). Joint networks in the Appalachian region with similar orientation have been interpreted as the product of a continent-wide stress field associated with the early assembly of the Pangaeon supercontinent (Engelder and Whitaker, 2006).

Shear fractures include a variety of bed-parallel and dipping fractures that are associated with folds and faults (fig. 49). Mineralized bed-parallel fractures, or veins, are abundant in shale of the Conasauga Formation (fig. 38). These veins contain fibrous carbonate that grew perpendicular to the vein walls. The carbonate fibers typically terminate at a keel line in the interior of the veins. Some of the veins, by contrast, cut across bedding, and many fill tension gashes, forming an en echelon geometry (fig. 39). These types of structures have been observed

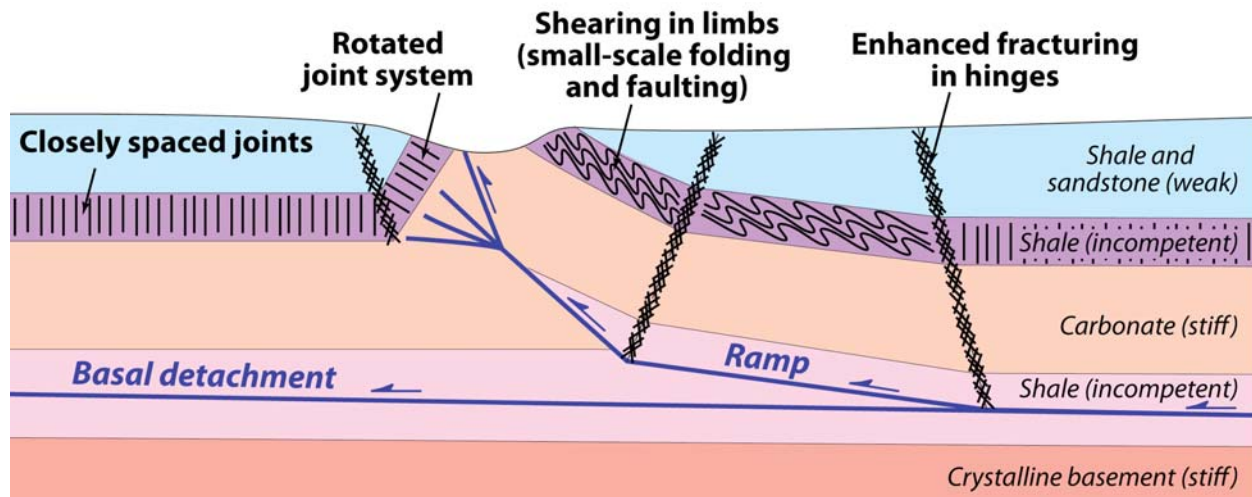


Figure 48.—Conceptual model showing relationship of reservoir-scale deformation in shale to thrust belt structure.



Figure 49.—Inclined shear fractures in the Chattanooga Shale at Big Ridge, Etowah County, Alabama.

in core from Big Canoe Creek Field and are thus of significance in shale gas exploration. This fibrous cement is typical of synkinematic crack-seal textures (Laubach and others, 2004); thus vein filling is considered to be contemporaneous with MUSHWAD formation.

Outcrops demonstrate that the Chattanooga Shale is in itself a weak lithotectonic unit that is bounded above and below by stiff carbonate and sandstone units (figs. 18, 19). Parts of the shale are well-jointed, whereas other parts can contain shear zones with overturned folds. Similar deformation is apparent in the Devonian shale of the Greene-Hale synclinorium. Dipmeter and formation micro-imager logs from the Bayne-Etheridge 36-9 #1 well indicate that, although regional dip is about 20°, the shale interval is complexly deformed (fig. 50). Analysis of these logs indicates that dip varies between 10 and 40°, and some significant dip discordances correspond with zones of deformation that are interpreted as shear zones (Pashin, 2009). Hence, the Devonian section contains parasitic folds and faults that are superimposed on regionally dipping structural panels and are interpreted to have formed by flexural slip (fig. 48).

Importantly, two of the most prominent gas shows in the Bayne-Etheridge well correspond with shear zones (figs. 21, 50). Similar shear structures are developed in the vertical fold limb penetrated by the Tate 9-4 #1 well, and abundant gas shows are distributed through more than 1,500 feet of section. Mineral cements in fractures can be sensitive recorders of the opening history of fractures, as well as the geochemical processes that were active within the fracture networks (Laubach and others, 2004; Gale and others, 2007; Olson and others, 2009). The most common mineral cements are, in order of abundance, calcite, dolomite, silica, and pyrite. In the Cambrian Conasauga Formation, calcite commonly has a fibrous habit. Locally, botryoidal silica fills veins. As mentioned previously, the fibrous calcite is characteristic of synkinematic fracture filling associated with Alleghanian deformation.

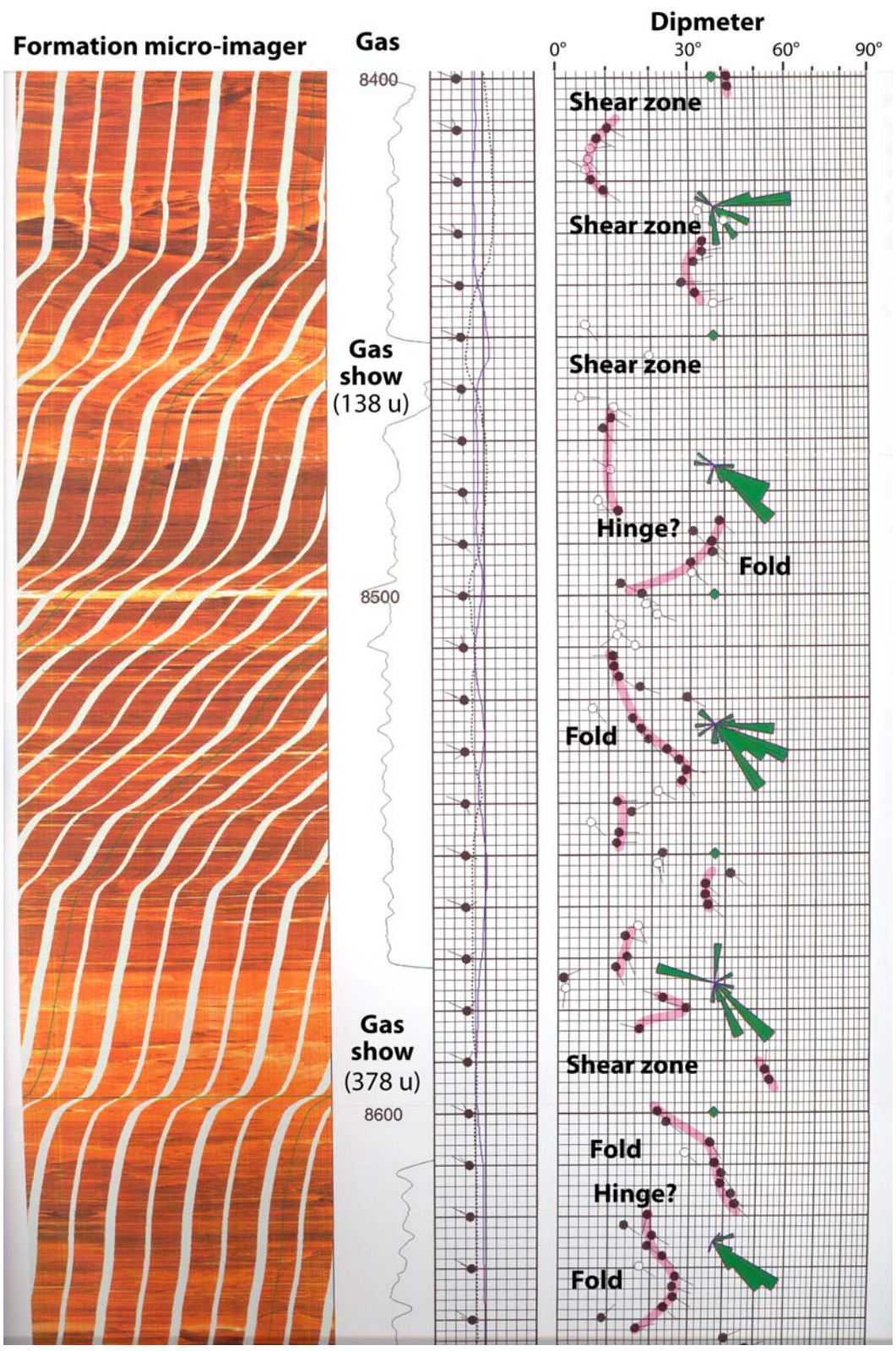


Figure 50.—Formation micro-imager and dipmeter logs showing complex deformation associated with gas shows in the Bayne-Etheridge 36-9 #1 well.

In the Chattanooga Shale of the Weyerhaeuser 2-43-2402 well, some short, subvertical fractures are restricted to a single lamina (fig. 51), whereas others cut directly across the rock fabric (fig. 52). Virtually all fractures examined from this well exhibit multi-stage cementation (figs. 52, 53). Dolomite, which coats the outer surfaces of the fractures, was the first mineral to precipitate, whereas calcite (red stain) is preserved in the interior of the fractures and was thus precipitated later. Floating particles of rock matrix within the veins indicate that cementation was contemporaneous with opening of the fracture. Detailed analysis indicates that mineralization within these fractures was complex and includes multiple episodes of cementation with dolomite, silica, calcite, and pyrite (fig. 54). Corroded mineral boundaries further indicate that dissolution events occurred. In the Neal shale, for example, early silica cement was precipitated, corroded, and then buried by calcite cement (fig. 55). The basic sequence of precipitation and dissolution events (fig. 54) holds true in most or all fractures in this core regardless of size or orientation (figs. 51-53, 55), and similar paragenetic sequences have been observed in other cores of Devonian shale in the Black Warrior basin and the Greene-Hale synclinorium.

Cement stratigraphy in the Weyerhaeuser well records a succession of chemically disparate water masses. Dolomite and calcite precipitate from alkaline water and dissolve in acidic water. Silica does the opposite. Thus, at a minimum, alkaline fluids were replaced by acidic fluids, which were in turn replaced by alkaline fluids, all after the rocks were fractured. Each time fluid chemistry changed, moreover, the new fluid remained in the pores long enough and moved through the pores with sufficient volume to precipitate substantial amounts of cement. Indeed, the diagenetic history of the Devonian shale provides evidence for a complex hydrodynamic and geothermic history, which should be taken into account when evaluating shale gas reservoirs.

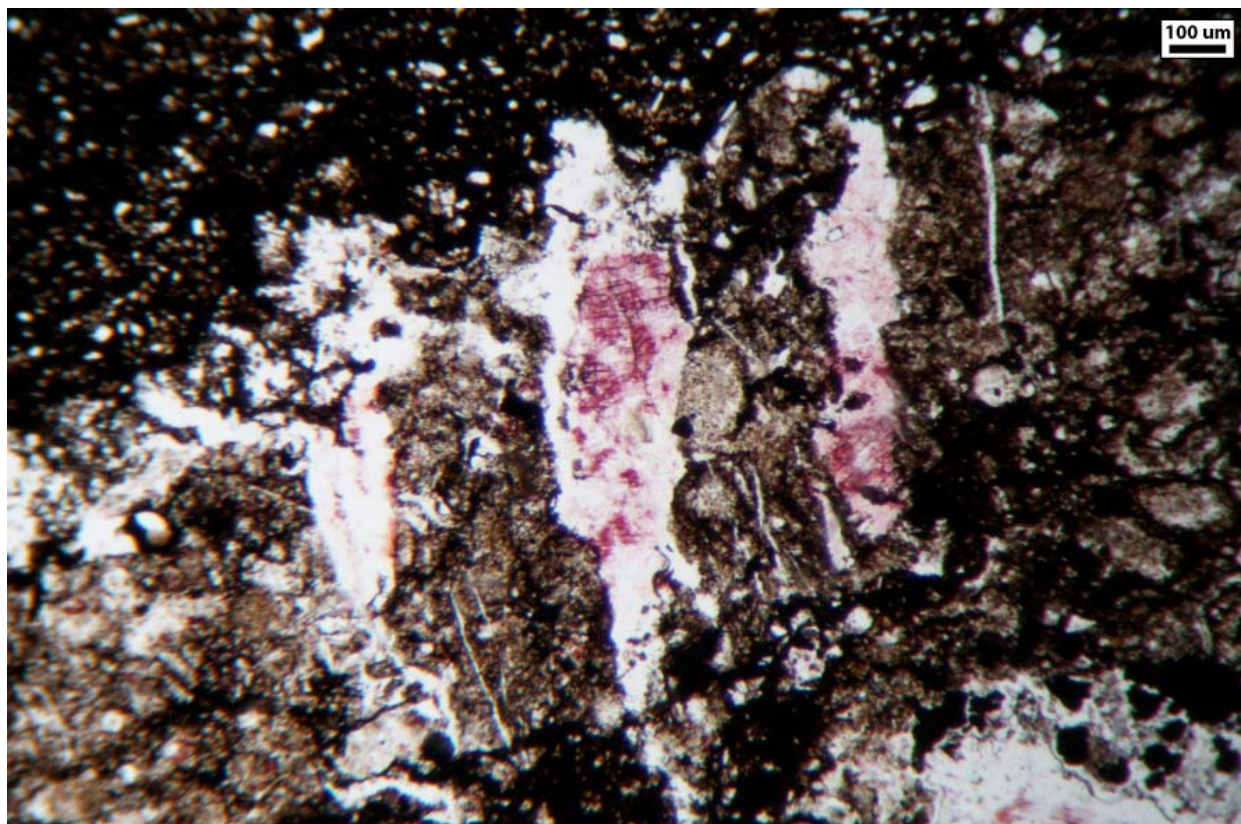


Figure 51.—Strata-bound fractures filled with silica (white) and calcite (red stain) in Chattanooga Shale, Weyerhaeuser 2-43-2402 well, Greene County, Alabama, 8,204.4 ft.

### **HYDRODYNAMICS AND GEOTHERMICS**

The stratigraphic and structural framework of a sedimentary basin provide the basic container in which hydrodynamic and geothermic processes operate. These processes are vital considerations for evaluating shale gas reservoirs because they have a strong influence on the generation, composition, storage, and mobility of reservoir fluid. The principal elements used to characterize basin hydrodynamics and geothermics are porosity, permeability, fluid chemistry, reservoir pressure, and reservoir temperature, which are discussed in the following paragraphs.

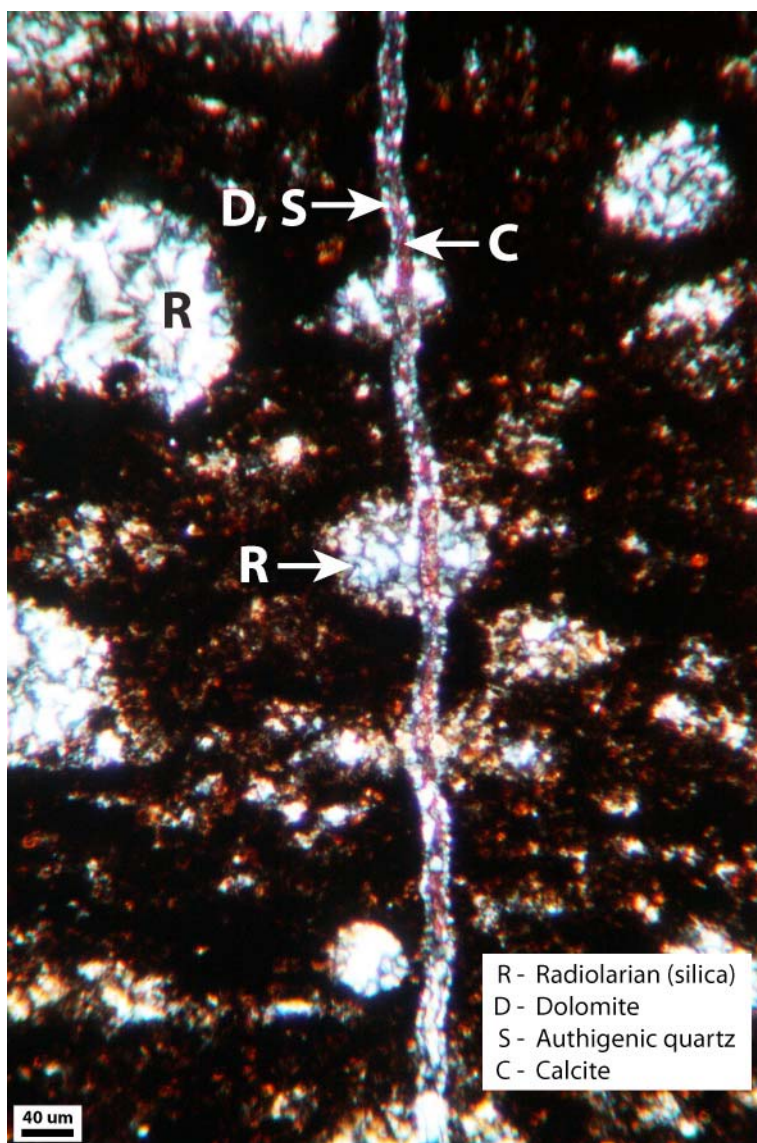


Figure 52.—Mineralized fracture cutting across rock fabric, including radiolarians in Chattanooga Shale (Weyerhaeuser 2-43-2402 well, Greene County, Alabama, 8,215.1 ft).

### Porosity and Permeability

The Black Warrior basin and Appalachian thrust belt contain numerous shale, sandstone, and carbonate units that have a broad range of reservoir properties. Shale characteristically has matrix permeability on the order of 0.1 microdarcy ( $\mu\text{D}$ ) (e.g., Soeder, 1988) and is thus typically considered a reservoir seal, although natural fractures in shale may transmit significant

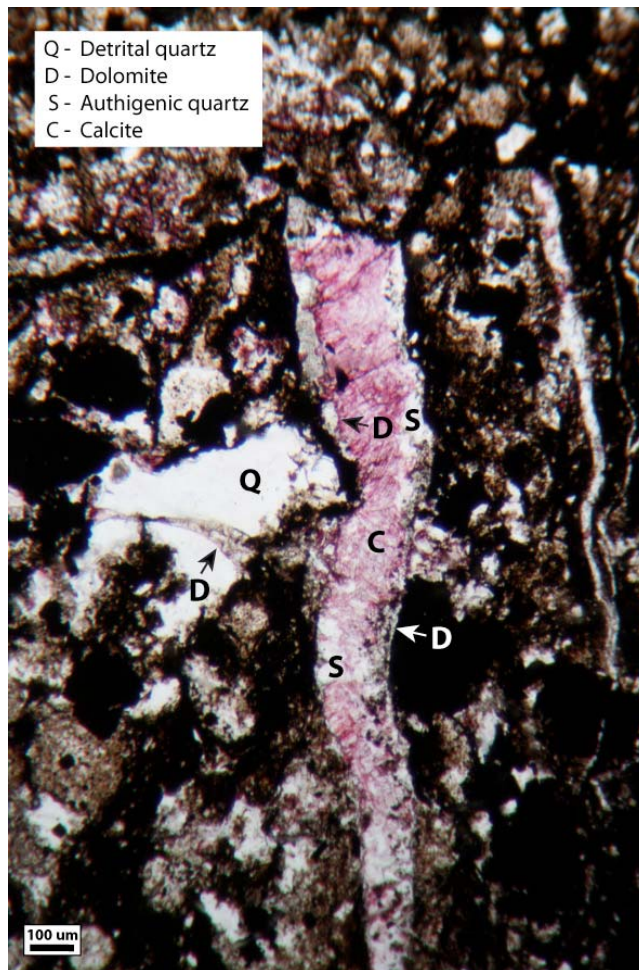


Figure 53.—Mineralized fractures showing cement stratigraphy in Chattanooga Shale (Weyerhaeuser 2-43-2402 well, Greene County, Alabama, 8,204.4 ft).

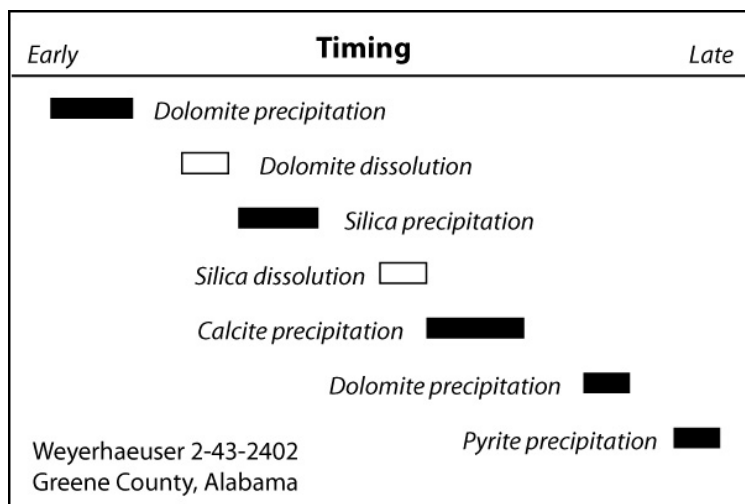


Figure 54.—Idealized paragenetic sequence showing precipitation and dissolution events identified in the Chattanooga Shale of the Black Warrior basin.

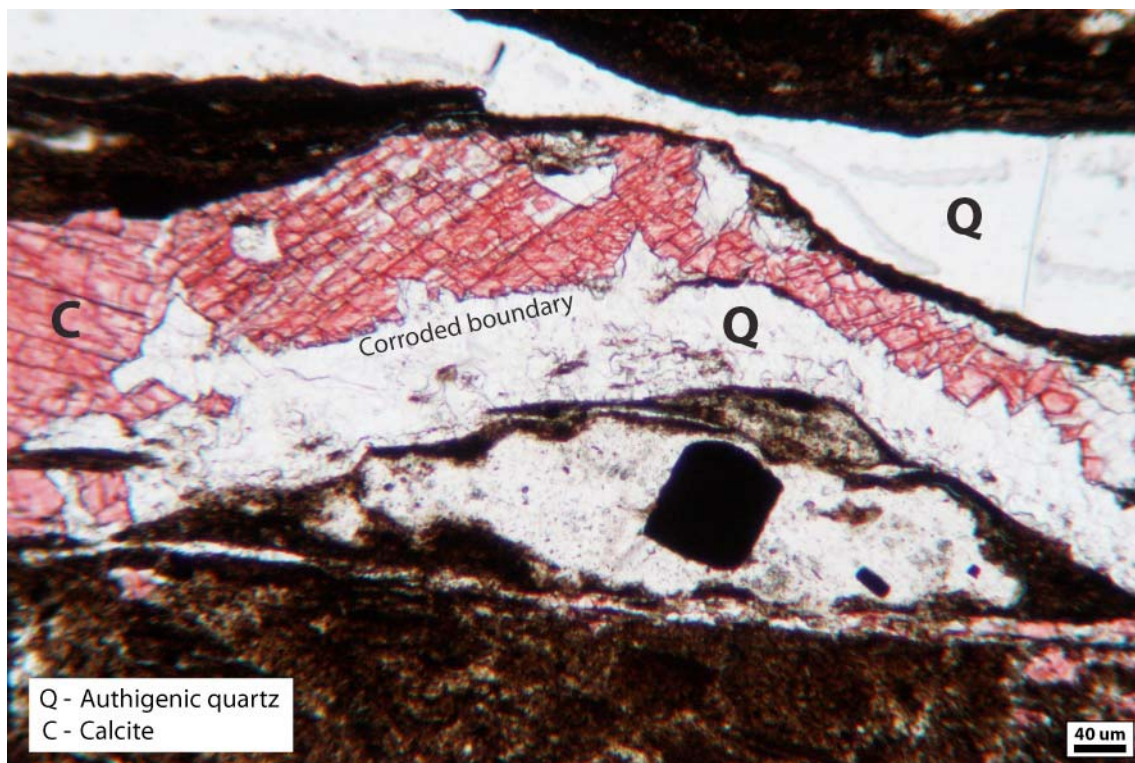


Figure 55.—Corroded boundary between calcite and quartz in Neal shale (Weyerhaeuser 2-43-2402 well, Greene County, Alabama, 7,998.4 ft).

volumes of fluid. Detailed information on the permeability of shale in the Black Warrior basin and Appalachian thrust belt is discussed in a later section on gas storage and permeability.

Limestone and dolostone are abundant in Cambrian through Mississippian rocks and have varied hydrologic properties (Ortiz and others, 1993). Porosity varies from negligible to more than 20 percent, and permeability ranges from the  $\mu\text{D}$  scale to hundreds of millidarcies (mD). Accordingly, some carbonate units have high sealing capacity, whereas others serve as important aquifers. Few hydrocarbons have been produced from the carbonate formations, but permeable layers in the Cambrian-Ordovician Knox Group and in the Lower-Middle Devonian section (plate 2) have been used for subsurface disposal of produced water. Sandstone is common in Silurian, Devonian, Mississippian and Pennsylvanian deposits, and reservoir properties are best developed in quartz-rich Mississippian-Pennsylvanian sandstone, where aquifers are developed

in the shallow subsurface and conventional hydrocarbon reservoirs are developed below 2,000 feet. Abundant core analysis data are available from Mississippian-Pennsylvanian sandstone of the Black Warrior basin, where porosity ranges from 3 to 19 percent, and permeability is typically 26 to 89 mD and is locally higher than 400 mD (table 1).

### **Water Chemistry**

Water chemistry data indicate that a complex interplay exists between near-surface hydrologic processes and deep subsurface processes in the Black Warrior basin and the Appalachian thrust belt (Pashin and others, 1991; Pashin, 2007, 2009). Subsurface chemistry ranges from fresh, sodium bicarbonate water with less than 300 milligrams per liter (mg/L) total dissolved solids (TDS) to saline, sodium chloride brine with TDS content exceeding 108,000 mg/L (National Energy Technology Laboratory, 2002; Pashin and Payton, 2005). Where the Appalachian thrust belt is exposed at the surface, meteoric recharge in thrust belt structures, which bring reservoir strata to the surface, facilitates the development of fresh-water plumes at reservoir depth (Pashin, 2007, 2009) (fig. 56). Where the Black Warrior basin and Appalachian thrust belt plunge below the Cretaceous sedimentary cover of the Gulf of Mexico basin, by contrast, Paleozoic strata are sheltered from surface-driven processes.

In the Chattanooga Shale of Blount and Cullman Counties (fig. 7), a significant amount of water is co-produced with shale gas, typically about 1 barrel per thousand cubic feet (Pashin, 2009; Haynes and others, 2010). Considering the low matrix permeability of shale, water is probably being produced from natural fracture systems, including joint networks and shear zones. The wells are sited in fold hinges, which can be zones of enhanced fracturing that may

Table 1. Permeability and porosity of sandstone in the Black Warrior basin based on 989 conventional core analyses.

Interval	Porosity			Permeability		
	Maximum %	Minimum %	Mean %	Maximum mD	Minimum mD	Mean mD
All data	28.3	3.0	9.9	663.00	0.01	29.15
Mississippian-age Lewis, Carter, Gilmer, and Chandler sandstone	27.7	3.0	9.6	663.00	0.01	26.24
Pennsylvanian-age Pottsville Formation sandstone	28.3	10.2	19.2	471.00	1.20	89.45

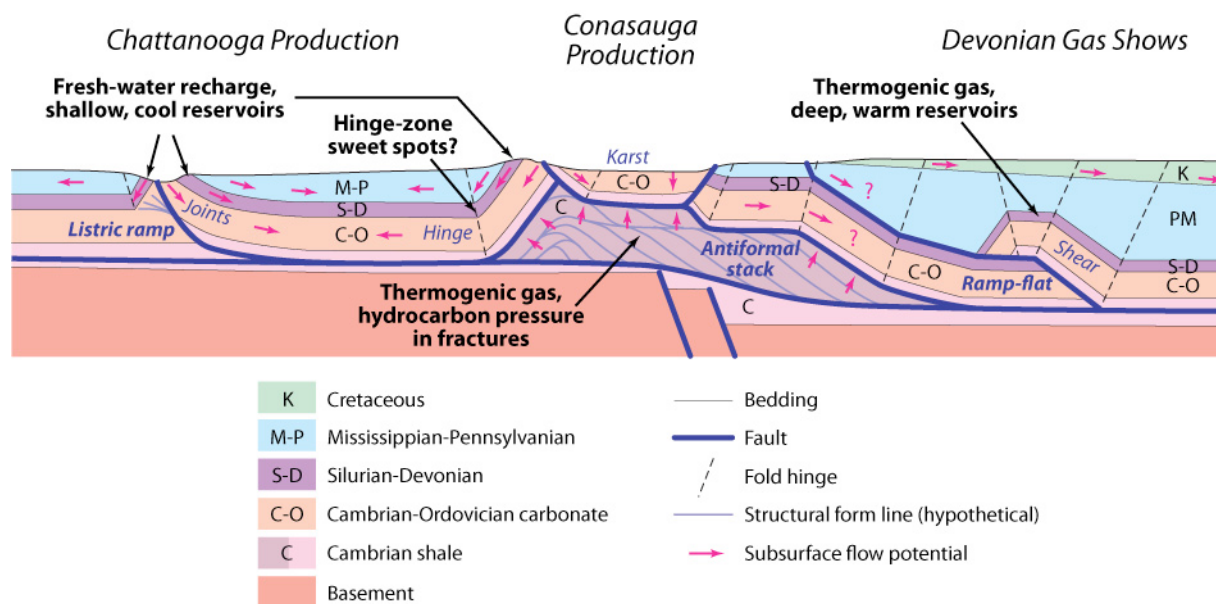


Figure 56.—Hydrodynamic model of shale gas reservoirs in the Appalachian thrust belt of Alabama (modified from Pashin, 2009).

contribute to water volume (fig. 48). The produced water is rich in chlorides and has TDS content between 20,000 and 40,000 mg/L, and thus needs to be disposed of in the subsurface.

In an effort to dispose of the water, Geomet drilled a deep well in the backlimb of the Sequatchie anticline and encountered abundant fresh water with about 400 mg/L TDS at depths

between 4,600 and 5,300 feet in the Copper Ridge Dolomite, which forms the lower part of the Cambrian-Ordovician Knox Group. This fresh water was apparently sourced from the southeast by recharge in the hanging wall of the Straight Mountain structure, where lower Knox strata are at the surface (figs. 3, 7). This example further underscores the influence of Appalachian structure on regional hydrodynamics and the development of complexly interstratified formation waters.

Below Cretaceous cover in the Chattanooga depocenter of the Black Warrior basin and in the Greene-Hale synclorium (figs. 20, 56), Paleozoic carbonate rocks contain brine with elevated salinity and so meteoric recharge of these strata is ineffective (e.g., Ortiz and others, 1993). Prominent gas shows in the Devonian shale in this area have been interpreted as the product of high gas pressure in the Silurian-Devonian shale formations (Pashin, 2008; Pashin, Grace, and Kopaska-Merkel, 2010). Hydrodynamic sheltering is also possible within the exposed Appalachian thrust belt. For example, no water is produced from the deformed and fractured Conasauga shale of the Gadsden MUSHWAD, but elevated gas pressure in the shale led to blowout of the Andrews 27-14 well in Big Canoe Creek Field (Williams, 2007).

### **Reservoir Pressure and Geothermics**

Reservoir pressure data are abundant in coalbed methane reservoirs of the Black Warrior basin, and these data indicate that fresh-water supports near-normal reservoir pressure gradients near structurally influenced recharge areas and that underpressure related to hydrodynamic gas sweep is common in the basin interior (Pashin and McIntyre, 2003; Pashin, 2007). Few reservoir pressure data are available from shale gas reservoirs in Alabama, but some important clues can be derived from drilling records and regional geology.

The Chattanooga reservoirs of Blount and Cullman Counties are shallow gas reservoirs along the frontal structures of the Appalachian thrust belt and thus have much in common with the coalbed methane reservoirs of the Black Warrior basin in terms of their gas and water production characteristics (Haynes and others, 2010). No indications of major gas pressure have been reported from the area, and so the shallow Chattanooga reservoirs in this area may be normally pressured to underpressured. By contrast, several wells penetrating Cambrian Conasauga shale in the Gadsden MUSHWAD and Devonian shale in the Greene-Hale synclinorium have reported significant gas shows, which demonstrate that gas pressure exceeded fluid pressure during drilling. Since many of these wells were drilled with mud, it follows that the shale contains significant gas pressure. The aforementioned blowout of the Andrews 27-14 well in Big Canoe Creek Field, moreover, indicates that gas pressure can give rise to major overpressure in some areas.

Reservoir temperature varies depending on reservoir depth and geothermal gradient and has a strong influence on gas generation and storage. Sparse data from the Conasauga Formation indicate that maximum reservoir temperatures are on the order of 130°F at a depth of 7,500 feet. Based on these data, geothermal gradient in the Conasauga is only 9°F per 1,000 feet and thus appears lower than in the other shale formations. The shallow Chattanooga reservoirs of Blount and Cullman Counties have reservoir temperatures lower than 86°F, and modern geothermal gradients are generally lower than 13°F per 1,000 feet. By contrast, the deeper Devonian and Neal shale reservoirs in the southern Black Warrior basin and Greene-Hale synclinorium have reservoir temperatures between 130°F and 196°F at depths ranging from 6,400 to 9,105 feet. Geothermal gradients in these wells are generally between 11 and 15°F per 1,000 feet. Based on

the available temperature data, all shale gas reservoirs today sit below the temperature associated with active thermogenic gas generation (260°F; Hunt, 1979).

Gases preserved in shale can be of thermogenic or late-stage biogenic origin. Fresh-water recharge can facilitate the generation of late-stage biogenic gases in shale (Martini and others, 1998, 2008), and late-stage biogenic gas related to recharge along the Appalachian frontal structures has been identified in coalbed methane reservoirs of the Black Warrior basin (Pashin and others, 1991; Pashin, 2007). A similar hydrodynamic setup appears to exist in Blount and Cullman Counties, although the elevated salinity of the produced water in the Chattanooga Shale may inhibit bacterial methanogenesis. Isotopic data are required to definitively identify late-stage bacterial gases, and the project team hopes to obtain gas samples for analysis later in this project.

Although gas shale formations in Alabama are not warm enough to generate thermogenic hydrocarbons today, vitrinite reflectance data indicate that these formations have been heated sufficiently in the geologic past to have generated large volumes of natural gas (Telle and others, 1987; Carroll and others, 1995; Pashin, Carroll and others, 2010). The woody plant material most commonly associated with vitrinite did not exist during Cambrian time. Instead, herbaceous vitreous kerogen can be used as a surrogate for true vitrinite reflectance in Cambrian strata (Burchard and Lewan, 1990). Reflectance of the Conasauga ranges from 1.1 percent and increases with depth to 1.9 percent, indicating that the full thickness of the shale is in the thermogenic gas window (fig. 57). Beyond a depth of 3,500 feet, the shale lies in the main gas generation window. The geochemistry of produced gas from the Conasauga further supports a thermogenic origin (table 2). Plotting  $\delta^{13}\text{C}_1$  and  $\delta\text{D}_{\text{CH}_4}$  isotopic ratios supports thermogenesis (fig. 58), and a dryness index ( $100 \cdot \text{C}_1/\text{C}_{1.5}$ ) of 95 to 97 suggests derivation from a sapropelic source. The ratio of  $\text{C}_2$  to  $\text{C}_3$  hydrocarbons is between 7 and 10, and the difference between  $\delta^{13}\text{C}_2$  and

Table 2. Results of geochemical analysis of natural gas produced from the Conasauga Formation in Big Canoe Creek Field (analyses courtesy of Weatherford Laboratories).

Well	Gas Composition (%)							Isotopic data (‰)							
	CH <sub>4</sub>	C <sub>2</sub> H <sub>6</sub>	C <sub>3</sub> H <sub>8</sub>	C <sub>4</sub> H <sub>10</sub>	C <sub>5</sub> H <sub>12</sub>	C <sub>6</sub> H <sub>14</sub>	CO <sub>2</sub>	δ <sup>13</sup> C <sub>1</sub>	δ <sup>13</sup> C <sub>2</sub>	δ <sup>13</sup> C <sub>3</sub>	δ <sup>13</sup> C <sub>4</sub>	δ <sup>13</sup> C <sub>5</sub>	δ <sup>13</sup> C <sub>6</sub>	δ <sup>13</sup> C <sub>CO<sub>2</sub></sub>	δD <sub>CH<sub>4</sub></sub>
Beason E33-06-14	94.94	3.36	0.40	0.03	0.01	0.00	0.01	1.22	-39	-36	-31	-23	-30	-11	-130
Dawson 33-09 #2A	96.56	3.05	0.30	0.02	0.00	0.01	0.04	0.04	-39	-37	-33				-129
Dawson 34-03-01	96.06	3.39	0.43	0.03	0.01	0.00	0.05	0.05	-40	-36	-32				-130
Bearden E26-11-29	96.27	3.23	0.38	0.03	0.00	0.00	0.06	0.06	-39	-35	-31				-130
Oakes E23-11-26	94.24	4.13	0.54	0.02	0.00	0.00	1.03	1.03	-38	-39	-39	-35	-12		-136

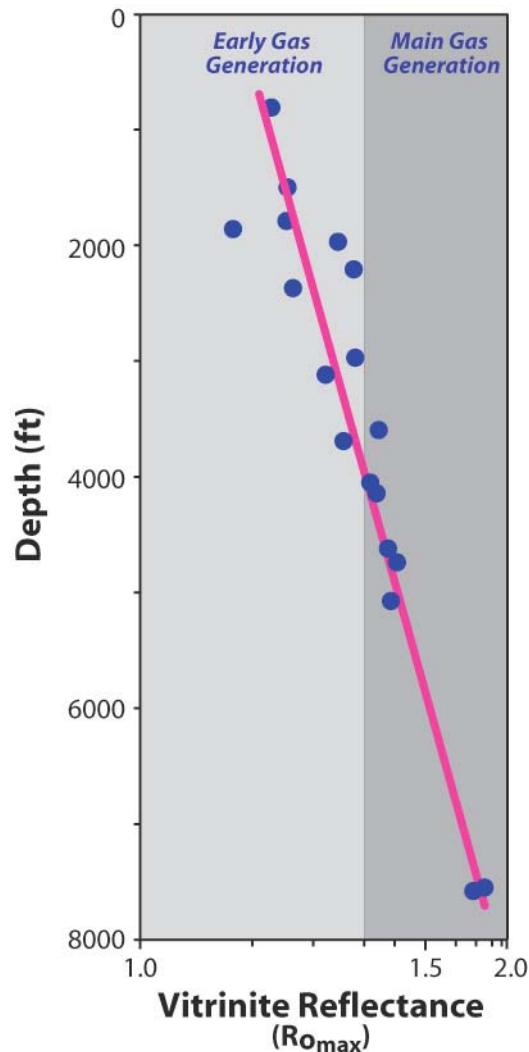


Figure 57.—Plot of vitrinite reflectance versus depth in the Conasauga shale of Big Canoe Creek Field, St. Clair County, Alabama.

$\delta^{13}\text{C}_3$  between -5 and 0, which is consistent with an origin by secondary cracking of oil and gas (see Lorant and others, 1998). The increase of reflectance with depth is log-linear and fairly uniform. This suggests that there are no major anomalies of thermal maturity that correspond with folding and thrust repetition within the Gadsden MUSHWAD, indicating that thermal maturation and gas generation was effectively post-kinematic. Therefore, it appears that the MUSHWAD was emplaced relatively early in the Alleghanian orogeny and that major thermal maturation occurred during subsequent burial.

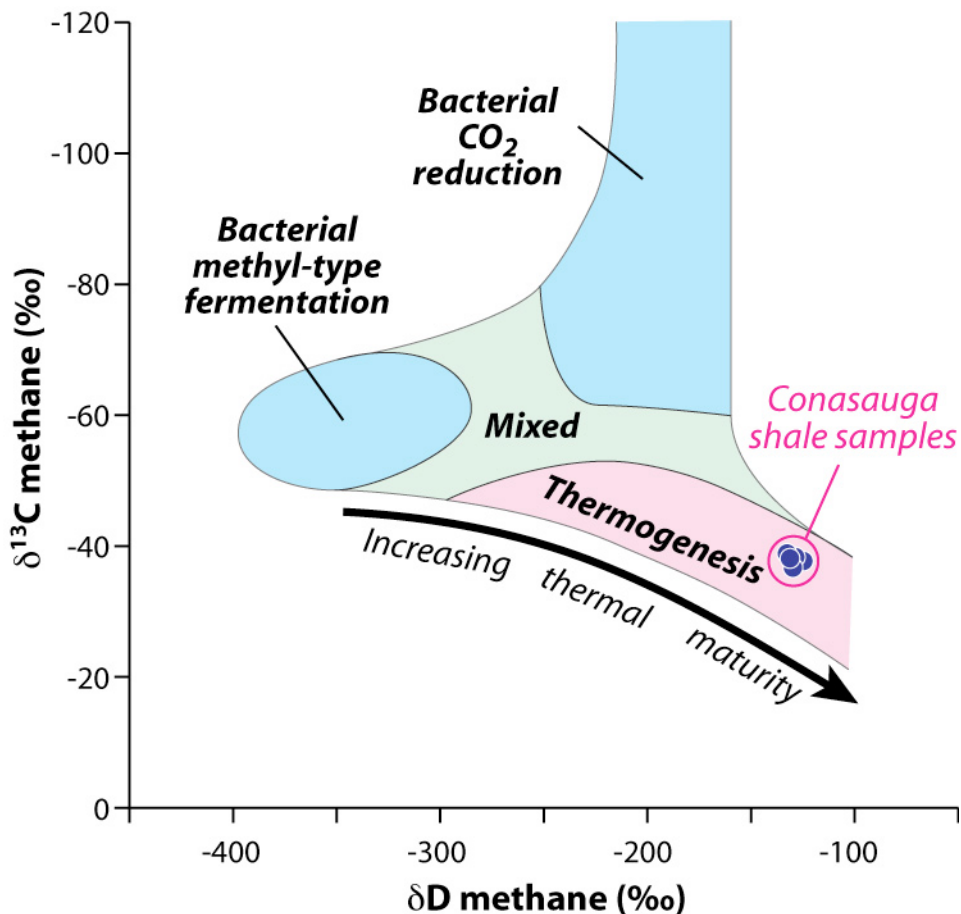


Figure 58.—Cross-plot of stable isotope data showing thermogenic origin of natural gas produced from the Conasauga Formation in Big Canoe Creek Field (analyses courtesy of Weatherford Laboratories, Incorporated).

A similar log-linear relationship between vitrinite reflectance and depth has been identified in the parts of the Black Warrior basin where shale gas exploration is active (Carroll and others, 1995). Although the Neal-Chattanooga section is in the oil window in parts of Lamar and Fayette Counties, the shale lies in the thermogenic gas window in deeper parts of the basin (Telle and others, 1987; Carroll and others, 1995). A reflectance-depth plot from the Ralph W. Holliman 13-6 well in Pickens County indicates that the Neal-Chattanooga section sits in the main gas generation window (fig. 59). Burial history modeling in the nearby Robinson et al. well, which reaches total depth in the Knox Group, indicates that the Cambrian-Ordovician

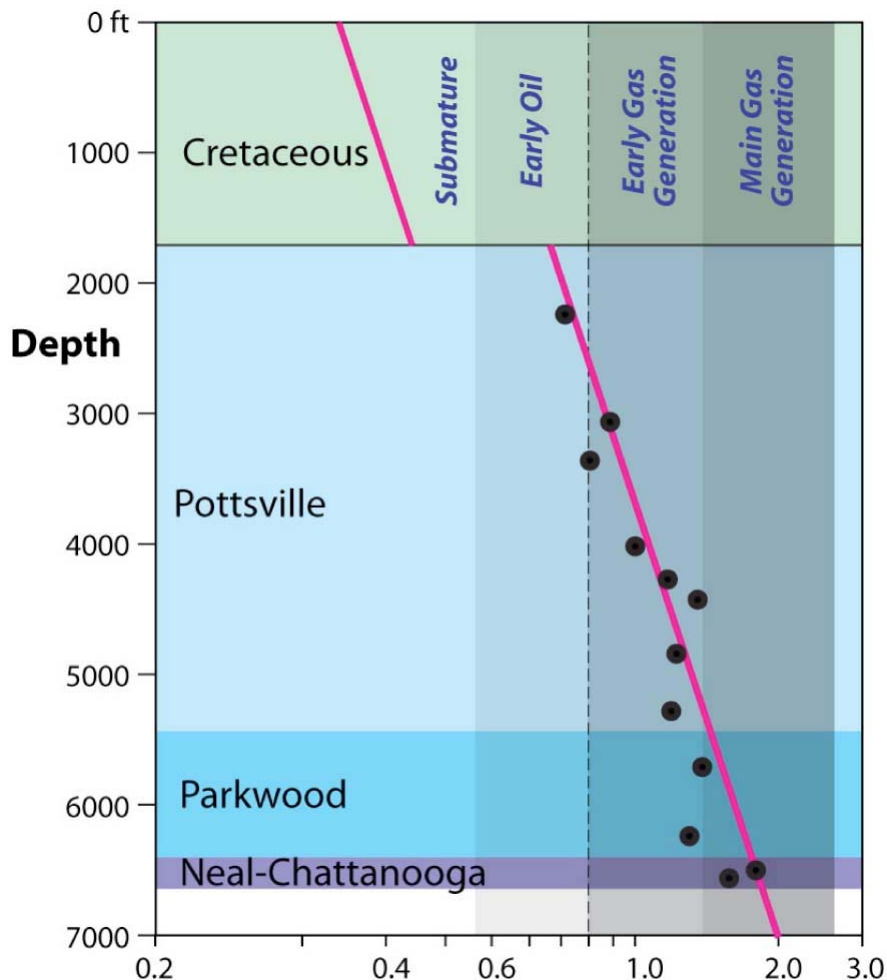


Figure 59.—Plot of vitrinite reflectance versus depth in the Ralph W. Holliman 13-6 well, Pickens County, Black Warrior basin, Alabama.

carbonate section reached thermal maturity with respect to oil generation shortly after burial (fig. 60). Major thermal maturation corresponds with accelerating burial rate during Appalachian-Ouachita orogenesis during the Pennsylvanian and Permian, and Silurian-Devonian strata entered the main gas generation window by Permian time. A prolonged episode of post-orogenic unroofing took place from Permian to Late Cretaceous time, and some minor upgrading of thermal maturity was apparently associated with this event. Renewed subsidence was concomitant with Late Cretaceous sedimentation in the Gulf of Mexico basin, but this event

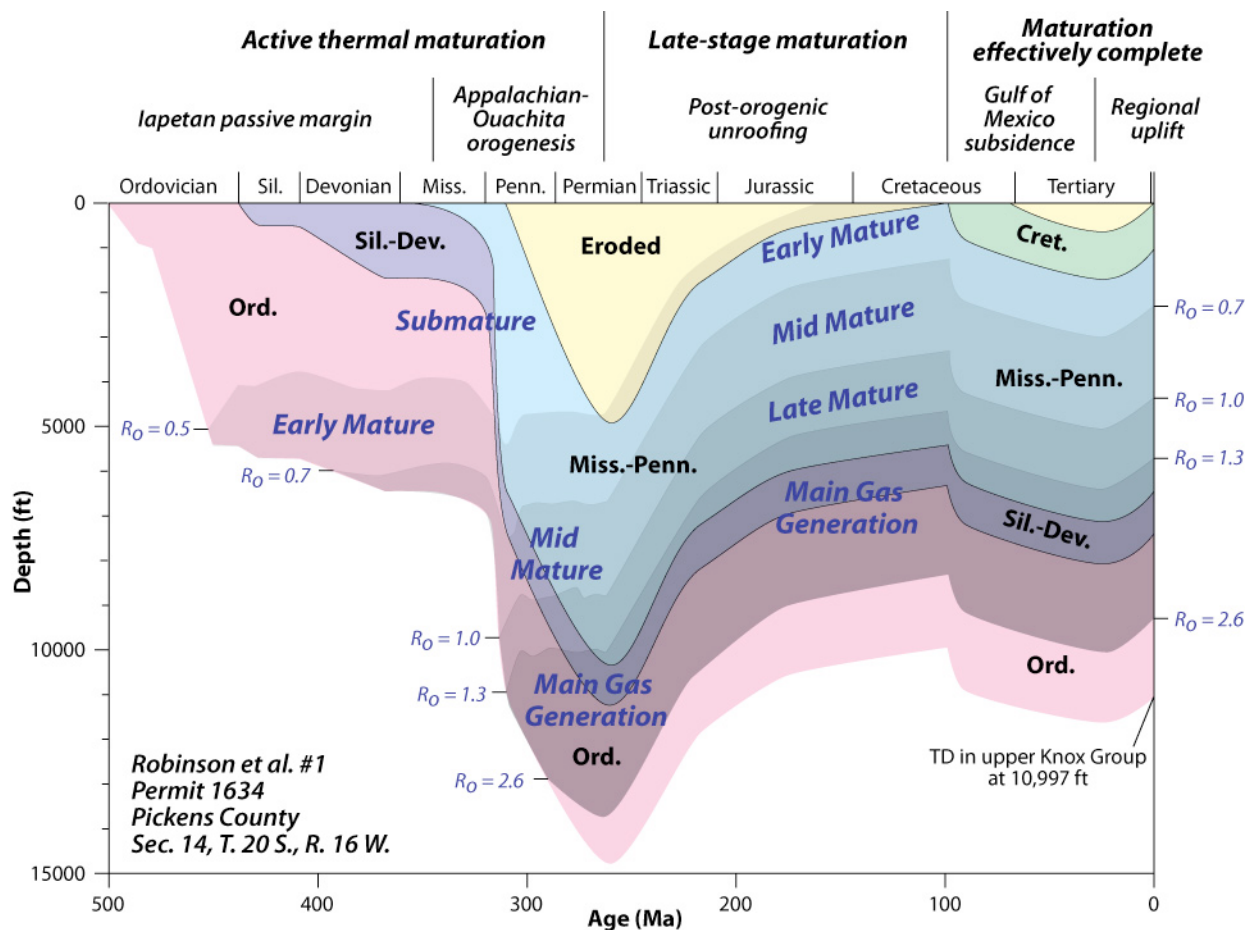


Figure 60.—Lopatin model of burial history and hydrocarbon generation, Robinson et al. well, Pickens County, Black Warrior basin, Alabama.

apparently had no effect on the thermal maturity of Paleozoic shale formations in the Black Warrior basin.

## PETROLOGY AND GEOCHEMISTRY

Shale can appear compositionally simple to the naked eye, but it is quite complex and heterogeneous in terms of mineralogic composition, organic composition, and geochemistry.

This section begins with a discussion of the detrital composition of gas shale in the Black

Warrior basin and the Appalachian thrust belt of Alabama and continues with a discussion of authigenesis, which constitutes the formation of secondary minerals by geochemical alteration of the shale. The discussion then shifts to organic petrology and geochemistry, which are important for characterizing hydrocarbon potential and reservoir quality. This section concludes with an analysis of shale microfabric that is based on SEM microscopy.

### **Detrital Composition**

Shale constitutes a mixture of clay minerals, silica, carbonate, pyrite, and organic matter, and the proportions of these constituents vary greatly. Whereas some samples can be classified petrographically as clay shale, many can be classified as siltstone, and some can even be classified as limestone. Whereas much of the material in the shale can be classified as clay and silt, detrital and biogenic particles can be as large as coarse sand (see table 3 for particle size classification used in this study). Examination of shale in thin section always risks sampling bias because the most friable rock types cannot be sampled this way. This was a particular problem in the Conasauga Formation, where friability and fluid sensitivity made thin section preparation very difficult. This section of the report describes similarities and differences among the shale units of different ages based on x-ray diffraction results and petrographic examination of the rock types that could be thin sectioned.

Conasauga shale differs significantly from the other shale units examined in this study given that it contains an abundance of carbonate (fig. 61). However, x-ray diffraction reveals that a diverse mineral suite is present (tables 4, 5). Non-clay minerals are dominated by calcite, dolomite, and quartz. Calcite content is highly variable, ranging from 8 to 49 percent. Dolomite content increases with depth and is as high as 25 percent, Quartz content is remarkably

Table 3. Particle size classes employed in this study.

Class	Size ( $\mu\text{m}$ )
Coarse sand	500-1000
Medium sand	250-500
Fine sand	125-250
Very fine sand	62-125
Silt	4-62
Clay	< 4

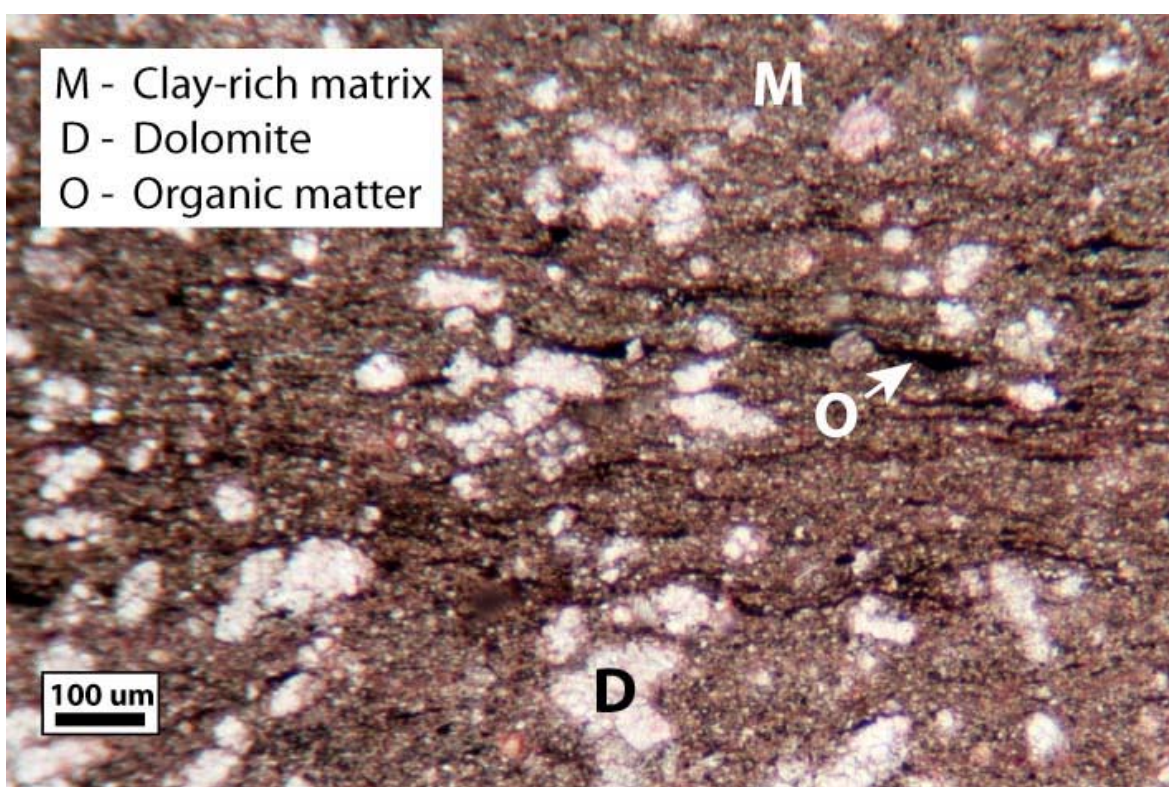


Figure 61.—Photomicrograph showing detrital organic matter in dolomitic Conasauga shale, Dawson 33-09 #2A well, Big Canoe Creek Field, 7,573.8 ft.

consistent, typically being between 12 and 20 percent. Most quartz appears biogenic or authigenic. Feldspar constitutes up to 19 percent of some shale and appears to be associated with the clay fraction. Clay minerals account for 12 to 50 percent by weight of the samples analyzed

Table 4. Non-clay mineralogy of Conasauga shale. Numbers in weight percent unless otherwise indicated.

Well	Depth (ft)	Quartz	K-Feldspar	Plagioclase	Calcite	Ankerite, Ferroan Dolomite	Dolomite	Pyrite	Fluorapatite	Barite	Total Non- Clay
Dawson 34-3-1	578	7	5	3	40	5	4	1	0	0	66
Dawson 34-3-1	844	19	8	7	13	7	0	1	0	0	54
Dawson 34-3-1	853	20	8	7	11	3	0	1	0	0	50
Dawson 34-3-1	873	21	6	8	12	3	0	1	1	0	52
Dawson 34-3-1	904	22	13	6	8	2	1	1	0	2	54
Dawson 34-3-1	910	17	2	6	55	1	0	0	0	0	81
Dawson 34-3-1	947	14	1	1	41	6	25	0	1	0	88
Dawson 34-3-1	950	13	6	5	49	1	1	1	0	0	75
Dawson 34-3-1	1178	16	2	6	20	6	23	1	0	0	74
Dawson 34-3-1	1204	17	1	6	30	7	11	1	0	0	72
Dawson 34-3-1	1220	17	1	5	17	10	17	1	0	0	67
Dawson 34-3-1	1307	15	0	3	43	6	20	1	1	0	88
<b>Statistics</b>											
n		12	12	12	12	12	12	12	12	12	12
Mean		16	4	5	28	5	8	1	0	0	68
Minimum		7	0	1	8	1	0	0	0	0	50
Maximum		22	13	8	55	10	25	1	1	2	88
Std. deviation		4	4	2	16	3	10	0	0	0	13

and are dominated by illite, smectite, and mica. Chlorite composes up to 14 percent of some samples, whereas kaolinite is a minor rock constituent.

Determining the original detrital composition of Conasauga shale is difficult because of extensive recrystallization of carbonate minerals. Aside from clay, carbonate, and organic matter, the principal detrital components are fossil fragments and siliceous ovoids (fig. 62). The siliceous ovoids are of enigmatic origin; some are filled with polycrystalline quartz, and some are hollow, which suggests a biogenic origin. Some of these ovoids are the altered remains of radiolarians, although many may represent replacement of peloids and coated grains by chert. Further research is required before a definitive interpretation can be made.

Table 5. Clay mineralogy of Conasauga shale. Numbers in weight percent unless otherwise indicated.

Well	Depth (ft)	Smectite	Illite-Smectite	Illite, Mica	Kaolinite	Chlorite	Total Clay
Dawson 34-3-1	578	12	5	15	0	1	34
Dawson 34-3-1	844	1	17	15	1	13	46
Dawson 34-3-1	853	2	26	9	0	14	50
Dawson 34-3-1	873	0	20	14	0	14	48
Dawson 34-3-1	904	1	15	15	2	14	47
Dawson 34-3-1	910	0	0	15	0	4	19
Dawson 34-3-1	947	0	0	11	0	2	12
Dawson 34-3-1	950	0	7	12	0	7	25
Dawson 34-3-1	1178	1	10	12	1	3	26
Dawson 34-3-1	1204	1	7	15	1	4	28
Dawson 34-3-1	1220	1	11	13	1	7	32
Dawson 34-3-1	1307	0	0	9	1	2	12
<b>Statistics</b>							
n		12	12	12	12	12	12
Mean		1	10	13	1	7	31
Minimum		0	0	9	0	1	12
Maximum		12	26	15	2	14	50
Standard deviation		3	8	2	1	5	13

The detrital petrology of Devonian Shale differs greatly from that of the Conasauga Formation, and the black shale can be classified as clay shale or siltstone. The principal minerals in the shale are quartz and illite (tables 6, 7). Quartz composes 34 to 52 percent by weight of the samples analyzed and is the dominant non-clay mineral. Feldspar constitutes 6 to 18 percent of the shale. Carbonate minerals include calcite, dolomite, ferroan dolomite-ankerite, and siderite. Calcite content is as high as 14 percent, although some samples contain no calcite. Clay minerals form 27 to 42 percent by weight of the shale specimens analyzed. Illite, illite-smectite, and mica are the dominant clay minerals, whereas only minor quantities of chlorite and kaolinite are present.

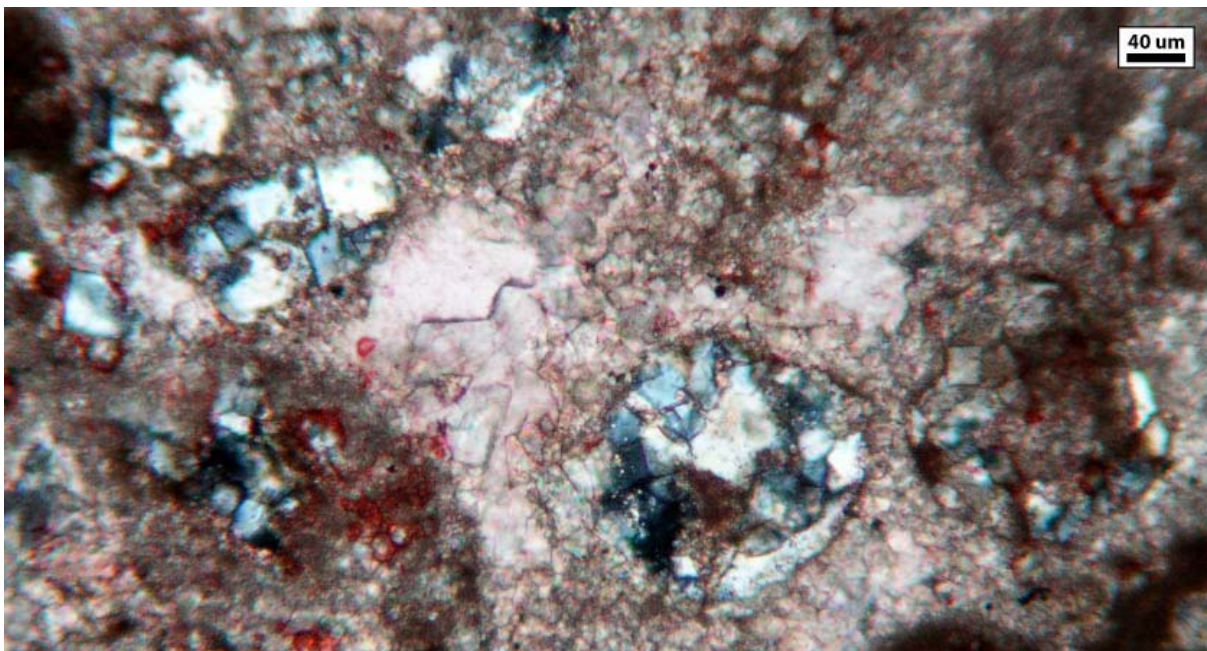


Figure 62.—Photomicrograph showing siliceous ovoids in Conasauga carbonate, Dawson 33-09 #2A well, Big Canoe Creek Field, 7,555.7 ft.

Table 6. Non-clay mineralogy of Devonian shale. Numbers in weight percent unless otherwise indicated.

Well	Formation	Depth (ft)	Quartz	K-Feldspar	Plagioclase	Calcite	Siderite	Ankerite, Ferroan Dolomite	Dolomite	Pyrite	Fluorapatite	Barite	Total Non-clay
Bayne-Etheridge 36-9 #1	Unnamed	8318	52	2	5	1	0	3	0	5	0	0	69
Bayne-Etheridge 36-9 #1	Unnamed	8328	52	1	5	3	0	2	3	4	0	0	70
Bayne-Etheridge 36-9 #1	Unnamed	8341	44	2	6	14	1	4	0	3	0	0	72
Bayne-Etheridge 36-9 #1	Unnamed	8429	45	2	7	4	3	4	0	1	1	0	66
Bayne-Etheridge 36-9 #1	Unnamed	8438	44	1	7	9	3	2	0	0	1	0	67
Bayne-Etheridge 36-9 #1	Unnamed	8451	43	2	5	3	0	5	2	4	1	1	64
Bayne-Etheridge 36-9 #1	Unnamed	8461	45	3	8	1	3	4	0	1	1	0	65
Bayne-Etheridge 36-9 #1	Unnamed	8471	46	0	7	11	3	3	2	1	1	0	73
Lamb 1-3 #1	Chattanooga	9135	35	12	8	0		0	2	12	0	0	68
Lamb 1-3 #1	Chattanooga	9137	41	7	5	0		2	0	6	0	4	65
Lamb 1-3 #1	Chattanooga	9141	34	15	3	0		0	3	4	0	0	58
<b>Statistics</b>													
n			11	11	11	11	8	11	11	11	11	11	11
Mean			44	4	6	4	1	2	1	4	0	1	67
Minimum			34	0	3	0	0	0	0	0	0	0	58
Maximum			52	15	8	14	3	5	3	12	1	4	73
Standard deviation			5	5	1	4	1	1	1	3	0	1	4

Table 7. Clay mineralogy of Devonian shale. Numbers in weight percent unless otherwise indicated.

Well	Formation	Depth (ft)	Illite-Smectite	Illite, Mica	Kaolinite	Chlorite	Total Clay
Bayne-Etheridge 36-9 #1	Unnamed	8318	10	22	0	0	32
Bayne-Etheridge 36-9 #1	Unnamed	8328	11	19	0	0	30
Bayne-Etheridge 36-9 #1	Unnamed	8341	7	20	0	1	28
Bayne-Etheridge 36-9 #1	Unnamed	8429	11	21	0	3	35
Bayne-Etheridge 36-9 #1	Unnamed	8438	12	18	1	2	33
Bayne-Etheridge 36-9 #1	Unnamed	8451	10	22	1	3	36
Bayne-Etheridge 36-9 #1	Unnamed	8461	14	19	0	3	35
Bayne-Etheridge 36-9 #1	Unnamed	8471	8	17	0	2	27
Lamb 1-3 #1	Chattanooga	9135	7	25	0	0	32
Lamb 1-3 #1	Chattanooga	9137	0	35	0	0	35
Lamb 1-3 #1	Chattanooga	9141	10	32	0	0	42
<b>Statistics</b>							
n			11	11	11	11	11
Mean			9	23	0	1	33
Minimum			0	17	0	0	27
Maximum			14	35	1	3	42
Standard deviation			3	6	0	1	4

The Chattanooga Shale in the Weyerhaeuser 2-43-2402 well of northern Greene County was studied extensively. In this well, the Chattanooga contains distinctive thin laminae (thickness = 1-3 mm) of argillaceous, very fine sand. Many of the sand-size particles are the skeletons of radiolarians, which exhibit various degrees of alteration (figs. 24, 52). In the Weyerhaeuser well, all radiolarians appear to belong to a single unidentified species, whose shells are densely perforate spiny spheres. Radiolarian laminae are embedded in very silty dark gray and black clay shale containing silt and very fine sand particles composed chiefly of monocrystalline quartz. Minor polycrystalline quartz, potassium feldspar, plagioclase feldspar, sand-size clasts of very silty brown to red shale, and siliceous sponge spicules also occur in the shale. The shale also contains traces of muscovite; calcitic fossil fragments; and some detrital organic matter, including vitrodetrinite and inertodetrinite. Radiolarian layers provide evidence for episodic

plankton blooms in the Chattanooga basin, and it is unclear whether these blooms were driven by upwelling along the Ouachita continental margin (e.g., Heckel and Witzke, 1979) or enrichment of the water column by storm events that reworked organic-rich sediment (e.g., Schieber, 1994).

In the Bayne Etheridge 36-9 #1 well of the Greene-Hale synclinorium, the Devonian black shale facies looks much like that in the Weyerhaeuser well. However, interstratified with the black shale is gray mudstone that is silty and sandy. Silt and sand particles primarily consist of monocrystalline quartz with lesser amounts of plagioclase feldspar, chert, muscovite, and bioclastic debris. This bioclastic debris is diverse and includes globular, fenestrate, and ramose bryozoans; brachiopod debris; echinoderm ossicles; ostracodes; fragments of benthic foraminifera; siliceous sponge spicules; fragments of microbial crust; and plant fragments (fig. 63). Particles range from silt to coarser than sand; relatively coarse particles are very well-rounded. Thin sandstone layers are poorly sorted and contain the same particle types found in the mudstone. Significantly, bioclasts are scattered in the silty shale, but also occur as thin, structureless, sandy grainstone laminae. Abundant and diverse fossil debris generated by shallow-water organisms, and especially the occurrence of bioclastic grainstone, indicates transport of sediment into the black shale basin from a nearby shelf or platform. Hand samples of the sandy and calcareous beds are graded to massive and in places matrix-supported, indicating mass-flow deposition related to storms and perhaps gravity- or seismic-induced failure on a depositional slope.

The resistive Neal shale lacks biogenic silica and ranges compositionally from clay shale to siltstone (fig. 64). The Neal tends to be richer in clay than the other formations studied herein (tables 8, 9). Quartz content is typically between 25 and 47 weight percent of the samples analyzed. Feldspar content averages 11 percent. Carbonate content is significantly lower in the

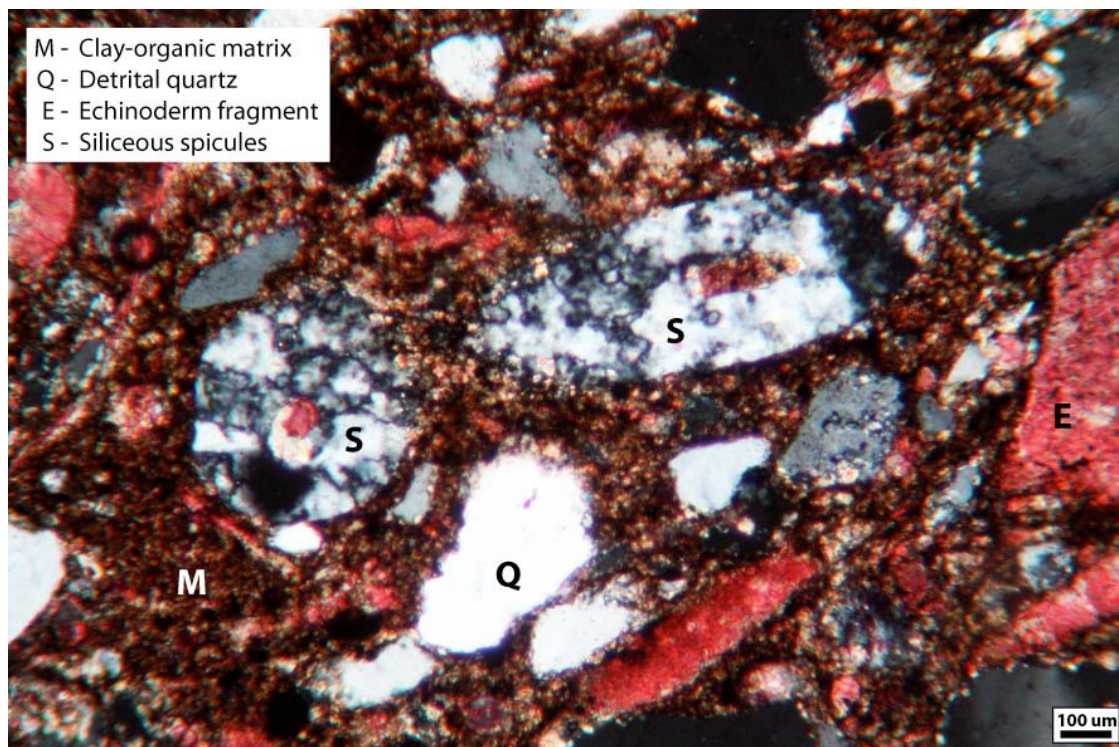


Figure 63.—Photomicrograph showing detrital quartz and siliceous and calcareous fossil fragments, Bayne Etheridge 36-9 #1 well, Greene County, Alabama, 8,312.4 ft.

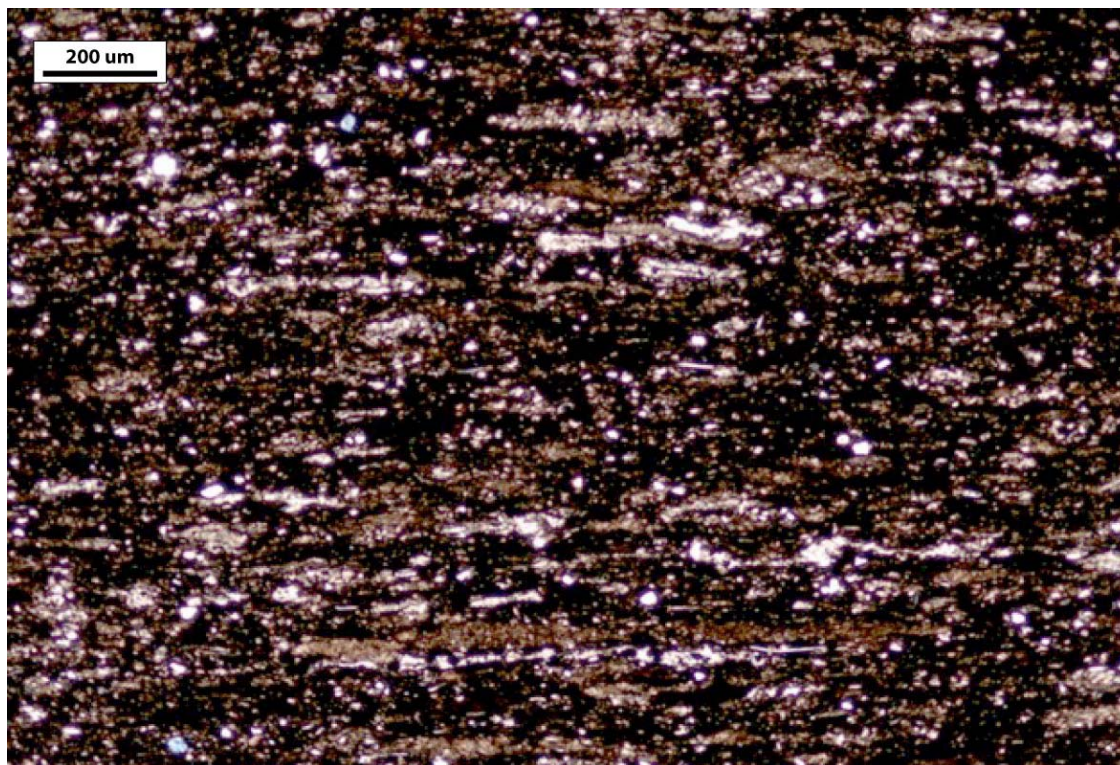


Figure 64.—Photomicrograph of organic-rich Neal shale in the Exum Trust 16-6 #1 well, Pickens County, Alabama, 6,549.5 ft.

Table 8. Non-clay mineralogy of Neal shale. Numbers in weight percent unless otherwise indicated. Table continued next page.

Well	Depth (ft)	Quartz	K-Feldspar	Plagioclase	Calcite	Siderite	Ankerite, Ferroan Dolomite	Dolomite	Pyrite	Fluorapatite	Barite	Total Non-clay
Lamb 1-3 #1	9013	28	8	1	0		0	4	4	0	0	44
Lamb 1-3 #1	9017	36	16	3	0		1	2	4	0	1	62
Lamb 1-3 #1	9021	31	15	0	2		0	3	4	0	0	54
Lamb 1-3 #1	9023	43	12	1	1		0	4	4	1	0	65
Lamb 1-3 #1	9024	37	3	6	0		1	2	6	0	0	55
O'Bryant 6-15 #1	6989	35	3	6	1	0	3	0	3	0	1	52
O'Bryant 6-15 #1	7022	25	6	3	1	0	1	0	4	0		40
O'Bryant 6-15 #1	7041	19	7	4	1		2	0	4	0	0	37
O'Bryant 6-15 #1	7075	31	5	9		1	3	0	3	1	0	53
O'Bryant 6-15 #1	7105	33	10	4	0		0	4	3		0	54
O'Bryant 6-15 #1	7124	35	9	5	2		1	2	5	0	0	59
Parker 3-16 #1	8352	38	7	4	2	0	1	0	4	0	0	57
Parker 3-16 #1	8362	46	4	7	2	1	3	0	3	0	0	65
Parker 3-16 #1	8373	24	8	4	2	0	3	7	4	2	0	55
Parker 3-16 #1	8413	23	7	6	2	1	0	3	3	0	1	45
Parker 3-16 #1	8433	26	9	4	2	1	3	2	6	1	1	54
Parker 3-16 #1	8447	28	9	5	2	1	2	2	4	0	0	52
Parker 3-16 #1	8468	30	8	6	1	0	1	2	3	0	0	52
Parker 3-16 #1	8479	36	4	8	1	0	1	3	4	0	0	57
Parker 3-16 #1	8632	61	4	6	0	0	0	1	7	0	0	79

Neal than in Conasauga and Devonian shale. Calcite is commonly absent and has a maximum value of 10 percent. Dolomite content reaches a maximum of 14 percent but averages only 2 percent. Pyrite content averages 4 percent of the mineral fraction and is notably higher in the Neal than in the other shale formations. Clay typically constitutes 33 to 55 percent by weight of the Neal shale samples. Illitic clay predominates, and chlorite content averages 5 percent. However, chlorite content is locally as high as 22 percent.

In thin section, the shale appears laminated, and lenses of clay-rich material, which may include microburrows, can be abundant. Carbonate layers in Neal shale typically do not show the degree of recrystallization that is apparent in Conasauga shale (fig. 56). Carbonate layers in the Neal reflect proximity to the Bangor carbonate ramp. Depending on location in the basin and

Table 8 (continued). Non-clay mineralogy of Neal shale. Numbers in weight percent unless otherwise indicated.

Well	Depth (ft)	Quartz	K-Feldspar	Plagioclase	Calcite	Siderite	Ankerite, Ferroan Dolomite	Dolomite	Pyrite	Fluorapatite	Barite	Total Non-clay
Smith 18-12 #1	6375	35	6	6	1	0	3	1	4	2		57
Smith 18-12 #1	6404	27	9	3	8	1	0	2	2	0		51
Smith 18-12 #1	6466	32	9	3	1	1	3	2	3	0		53
Smith 18-12 #1	6480	35	6	7	1	1	3	1	2	0		55
Smith 18-12 #1	6497	35	8	4	0	0	3	1	3	0		55
Smith 18-12 #1	6523	33	8	6	0	0	2	0	4	0		55
Smith 18-12 #1	6561	84	2	3	0	0	1	0	0	0		90
Smith 18-12 #1	6575	36	10	2	0	2	1	1	3	1		55
Smith 18-12 #1	6614	39	10	4	1	0	0	1	5	0		60
Exum Trust 6-16 #1	6424	52	0	7	0	0	0		4	0		64
Exum Trust 6-16 #2	6439	35	1	9	10	2	6		6	2		71
Exum Trust 6-16 #3	6460	30	1	6	1	1	14		6	1		60
Exum Trust 6-16 #4	6491	35	1	2	0	0	0		1	1		40
Exum Trust 6-16 #5	6510	36	1	9	0	0	0		10	0		56
Exum Trust 6-16 #6	6521	21	1	2	0	0	5		4	1		35
Exum Trust 6-16 #7	6534	44	1	10	0	0	1		3	1		60
Exum Trust 6-16 #8	6550	32	1	6	0	0	0		4	1		44
Exum Trust 6-16 #9	6591	47	0	7	16	0	3		3	0		76
<b>Statistics</b>												
n		38	38	38	37	30	38	29	38	37	19	38
Mean		36	6	5	2	0	2	2	4	0	0	56
Minimum		19	0	0	0	0	0	0	0	0	0	35
Maximum		84	16	10	16	2	14	7	10	2	1	90
Standard deviation		11	4	2	3	1	2	2	2	1	0	11

stratigraphic position, the carbonate layers range from peloid and fossil wackestone to grainstone. Fossils include fenestrate, globular, and ramose bryozoans; benthic foraminifera; brachiopods; ostracodes; echinoderms; mollusks; and apparent fecal pellets. Some peloids, however, have a relict concentric fabric and thus appear to be altered ooids (fig. 65). The broad range of fossil assemblages in the shale and carbonate layers indicate significant fluctuation of redox conditions in the Neal basin, as well as extremely variable degrees of sediment transport.

Table 9. Clay mineralogy of Neal shale. Numbers in weight percent unless otherwise indicated.  
Table continued next page.

Well	Depth (ft)	Illite-Smectite	Illite, Mica	Kaolinite	Chlorite	Total Clay
Lamb 1-3 #1	9013	24	32	0	0	56
Lamb 1-3 #1	9017	13	23	0	2	38
Lamb 1-3 #1	9021	22	23	0	0	46
Lamb 1-3 #1	9023	11	23	0	0	34
Lamb 1-3 #1	9024	18	27	0	0	45
O'Bryant 6-15 #1	6989	16	26	2	4	48
O'Bryant 6-15 #1	7022	24	28	6	2	60
O'Bryant 6-15 #1	7041	29	28	2	4	63
O'Bryant 6-15 #1	7075	10	31	1	5	47
O'Bryant 6-15 #1	7105	23	20	1	2	46
O'Bryant 6-15 #1	7124	15	25		1	41
Parker 3-16 #1	8352	12	25	1	5	43
Parker 3-16 #1	8362	7	21	1	5	35
Parker 3-16 #1	8373	18	24	1	3	45
Parker 3-16 #1	8413	29	12	6	8	55
Parker 3-16 #1	8433	11	23	3	8	46
Parker 3-16 #1	8447	12	28	2	6	48
Parker 3-16 #1	8468	14	27	2	5	48
Parker 3-16 #1	8479	11	28	1	4	43
Parker 3-16 #1	8632	8	13	0	0	21

### Authigenesis

The diagenetic history of gas shale in Alabama is complex and varied. This section focuses specifically on the growth of new minerals within the water column. Authigenesis in these shale units can be broken down to three major sets of processes: precipitation and settling of minerals in the water column, cementation in voids, and replacement of preexisting minerals. Cementation in voids invariably destroys porosity and reduces permeability, whereas replacement can result in reduction of mineral volume and therefore an increase in both porosity and permeability.

Much of the pyrite in shale consists of framboids, which are tiny spheres composed of nearly identical crystals (fig. 66). Framboids are common in all shale units studied herein and are particularly abundant in Devonian shale and Neal shale. In these units, pyrite framboids range in

Table 9 (continued). Clay mineralogy of Neal shale. Numbers in weight percent unless otherwise indicated.

Well	Depth (ft)	Illite-Smectite	Illite, Mica	Kaolinite	Chlorite	Total Clay
Smith 18-12 #1	6375	16	21	2	4	43
Smith 18-12 #1	6404	18	19	8	4	49
Smith 18-12 #1	6466	14	28	2	4	47
Smith 18-12 #1	6480	11	26	2	6	45
Smith 18-12 #1	6497	11	27	1	6	45
Smith 18-12 #1	6523	14	28	1	3	45
Smith 18-12 #1	6561	4	6	1	0	10
Smith 18-12 #1	6575	22	18	3	3	45
Smith 18-12 #1	6614	19	22	0	0	40
Exum Trust 6-16 #1	6424	2	22	3	9	36
Exum Trust 6-16 #2	6439	5	17	2	6	29
Exum Trust 6-16 #3	6460	6	24	3	7	40
Exum Trust 6-16 #4	6491	4	25	9	22	60
Exum Trust 6-16 #5	6510	4	26	2	12	44
Exum Trust 6-16 #6	6521	5	51	3	7	65
Exum Trust 6-16 #7	6534	3	26	1	10	40
Exum Trust 6-16 #8	6550	3	39	3	11	56
Exum Trust 6-16 #9	6591	3	15	2	4	24
<b>Statistics</b>						
n		38	38	37	38	38
Mean		13	24	2	5	44
Minimum		2	6	0	0	10
Maximum		29	51	9	22	65
Standard deviation		7	7	2	4	11
Standard deviation		7	7	2	4	11

diameter from about 3 to 10  $\mu\text{m}$ . Framboids form early, commonly in unlithified sediment or in the water column (Sawlowicz, 1993; Wilkin and Barnes, 1997). Framboids that form in the water column vary in size according to the amount of oxygen that is available (Wignall and Newton, 1998). Framboids smaller than about 5  $\mu\text{m}$  in diameter form in sulfidic water completely devoid of oxygen. Because most samples contain framboids up to about 10  $\mu\text{m}$  in size, the bottom water in Alabama's black shale basins probably contained at least traces of oxygen and thus can be classified as exaerobic or dysaerobic. For framboids that formed within the sediment, the

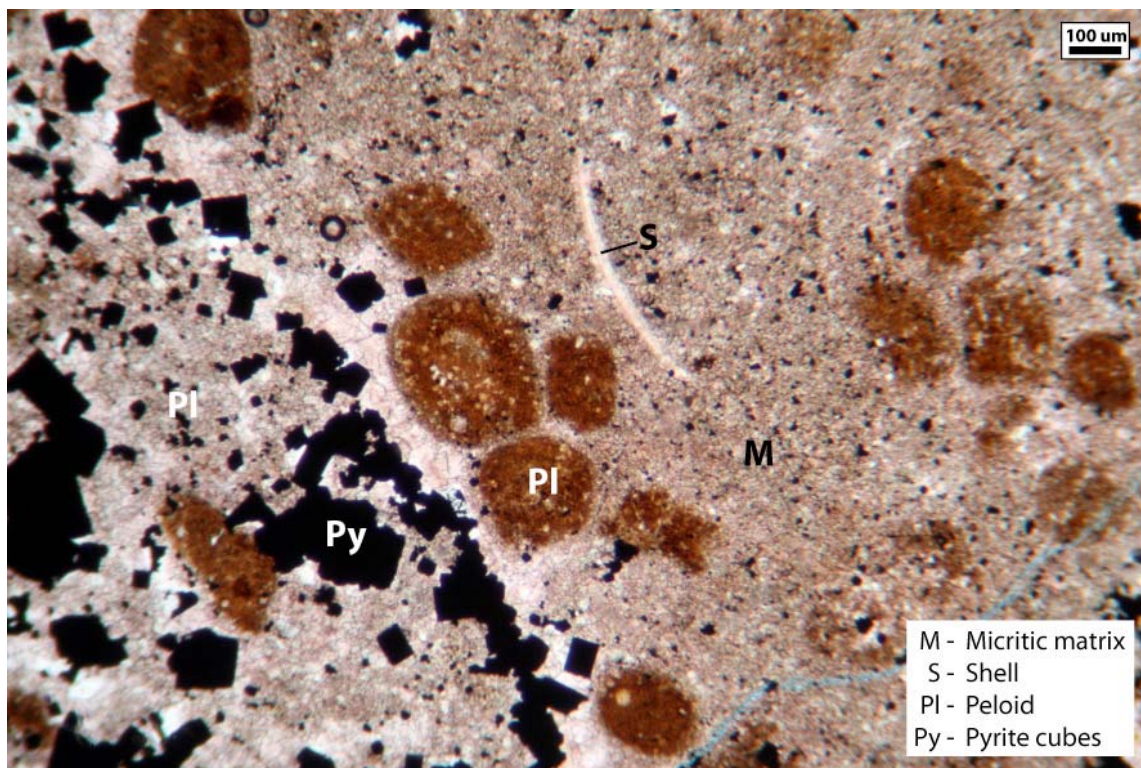


Figure 65.—Photomicrograph of limestone with pyrite-dented peloids in Neal shale, O'Bryant 6-15 #1 well, Pickens County, Alabama, 6,995.8 ft.

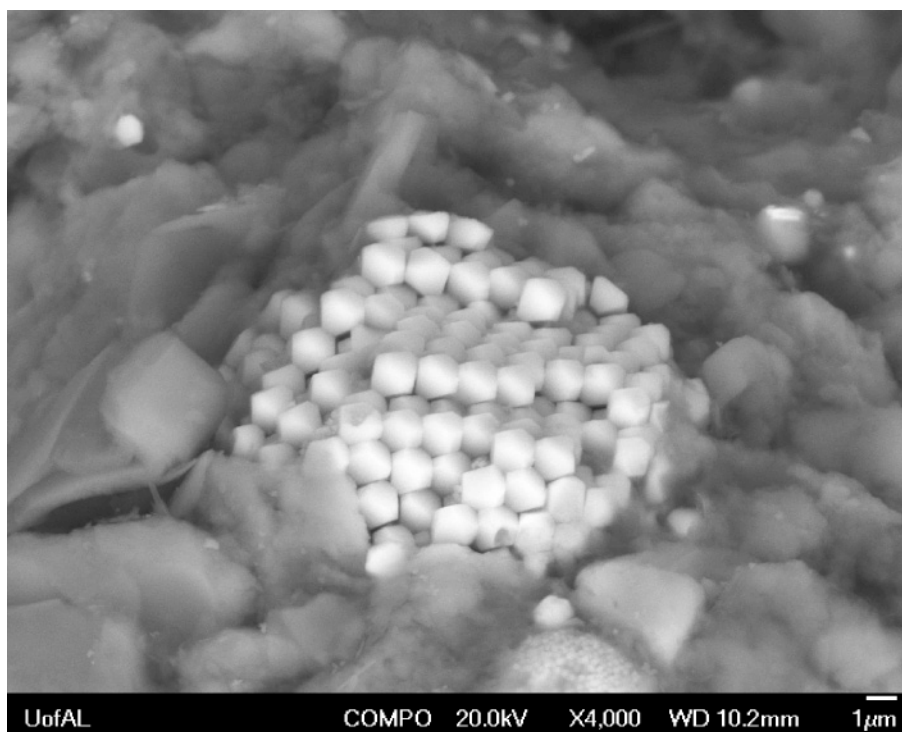


Figure 66.—SEM image of pyrite framboid, Chattanooga Shale, Weyerhaeuser 2-43-2402 well, Greene County, Alabama, 8,211.9 ft.

relationship between framboid size and oxygen level in the pore water probably still holds. Pyrite crystallization and its implications are described further in the section on microfabric.

The most important cement minerals in the black shale units are clay, calcite, dolomite, silica, and pyrite. Pyrite nodules can appear similar to framboids in texture but are much larger and have irregular shapes (fig. 67). This type of pyrite almost certainly grew below the sediment-water interface. Calcite and dolomite form under alkaline conditions, whereas silica forms under acidic conditions. Therefore, although carbonate and silica often occur together, they cannot have formed at the same time in the same place and thus indicate secular variation of water chemistry. Illite is the dominant authigenic clay mineral and is distinguished from platy detrital clay as euhedral laths that extend into open pores within the shale (fig. 67). Interstitial pore space within the shale matrix is minimal, and so it is difficult to determine the paragenetic sequence based on cement stratigraphy. However, much of the authigenesis in the gas shale units occurred in natural fractures, and as discussed earlier, cement stratigraphy in these fractures records a complex history of authigenesis (figs. 52-56).

The chemical environment in the subsurface changes over time, as do pressure-temperature conditions. All of these factors can facilitate the replacement of existing crystals by new crystals of the same or different minerals. Because calcite and dolomite are far more soluble than clay minerals or quartz, most replacement activity involves carbonate. Recrystallization of calcite and dolomite and replacement of calcite by dolomite are widespread in the subsurface. These processes were evidently most intense in the Conasauga shale facies, particularly in the limestone interbeds (fig. 68).

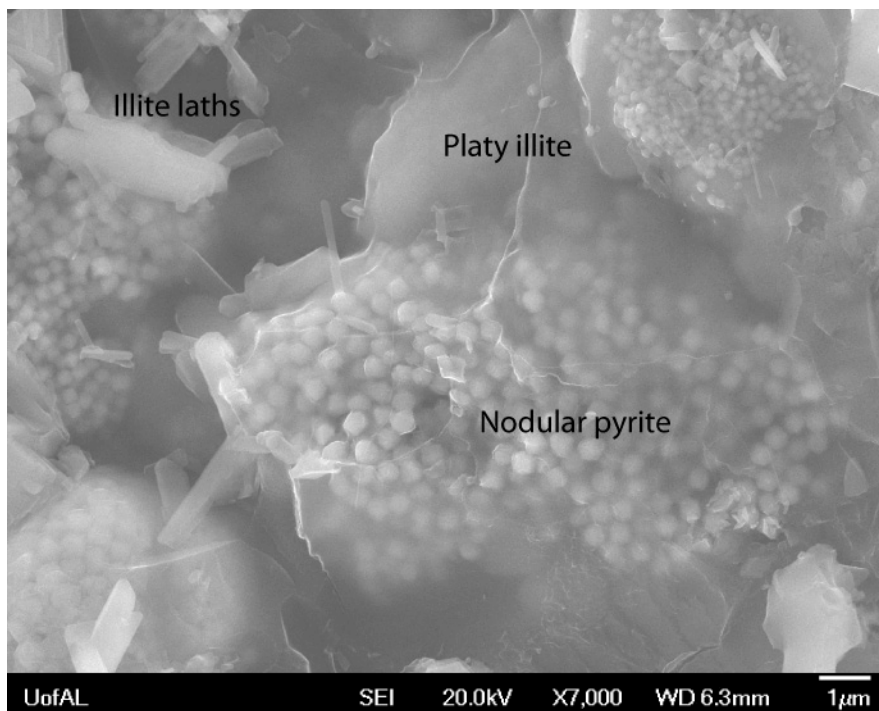


Figure 67.—SEM image of a sample from core of the Bayne Etheridge 36-9 #1 well, Greene County, Alabama (8,317 ft) showing illite forms in Devonian black shale.

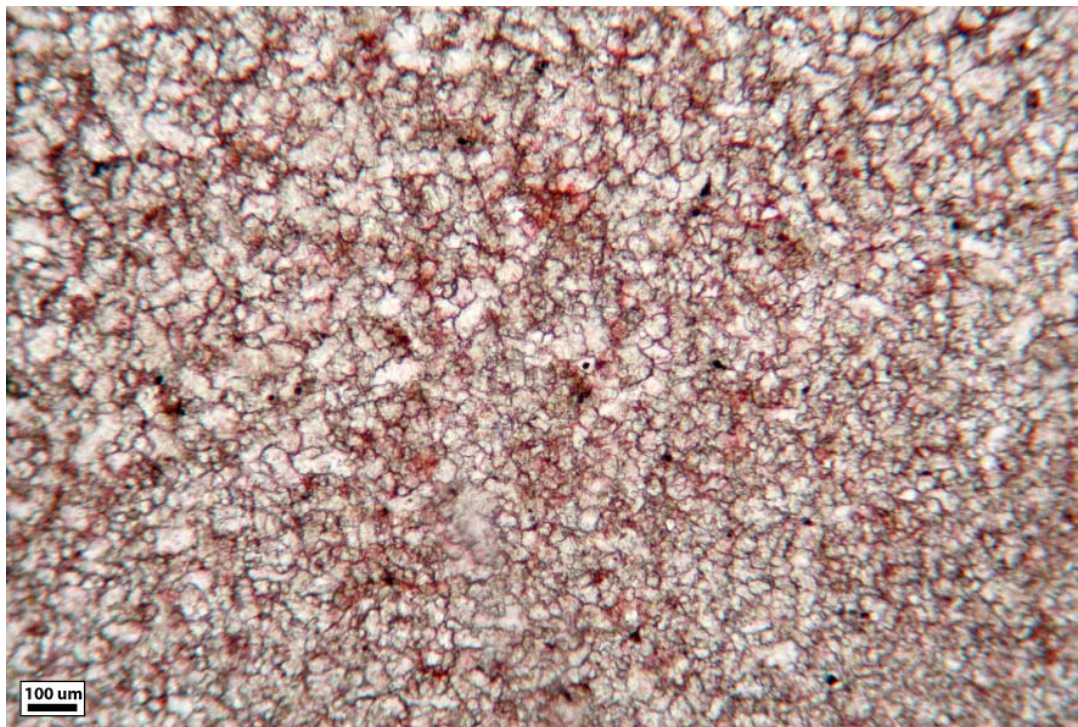


Figure 68.—Intensely recrystallized dolostone in Conasauga shale, Dawson 33-09 #2A well, Big Canoe Creek Field, 7,573.8 ft.

### Vein Fills

As mentioned in the section on structural geology, mineral cements in fractures can be sensitive recorders of geochemical processes (Laubach and others, 2004; Olson and others, 2009). Carbon and oxygen isotopes are valuable for determining the relationships of vein-filling calcite cement to burial and hydrocarbon generation. In coalbed methane reservoirs of the Black Warrior basin, for example,  $\delta^{13}\text{C}$  values have been used to distinguish cementation in brine from that associated with late-stage bacterial methanogenesis, and  $\delta^{18}\text{O}$  values have been used to constrain the temperature of mineralization (Pitman and others, 2003) (fig. 69).

Plotting values from vein-filling calcite in Cambrian, Devonian, and Mississippian shale with those from the coalbed methane reservoirs reveals a strong contrast (fig. 69). Whereas the coalbed methane data have a large range of  $\delta^{13}\text{C}$  values, the shale data cluster between -5 and +6 ‰, indicating precipitation in water with near-normal marine salinity. Furthermore, the  $\delta^{18}\text{O}$  values range from -3 to -11 ‰, indicating precipitation at low temperatures comparable to those recorded in the coalbed methane data (<120°F). This result is surprising, considering that most of the coalbed methane data come from strata shallower than 3,000 feet and much of the shale data come from strata deeper than 7,000 feet, where reservoir temperature can approach 200°F and can support the precipitation of mineral cements with depleted  $\delta^{18}\text{O}$  values below -20 ‰ (Friedman and O'Neil, 1977). In addition, many veins cut across stylolites, are faulted, and contain synkinematic cement, indicating that fracturing and cementation occurred at substantial burial depth.

Most of the shale data come from a limited depth range and are thus of limited value for examining the vertical variation of stable isotopic values. Data from the Conasauga Formation, by contrast, span more than 7,500 feet of section and provide some insight into vein filling

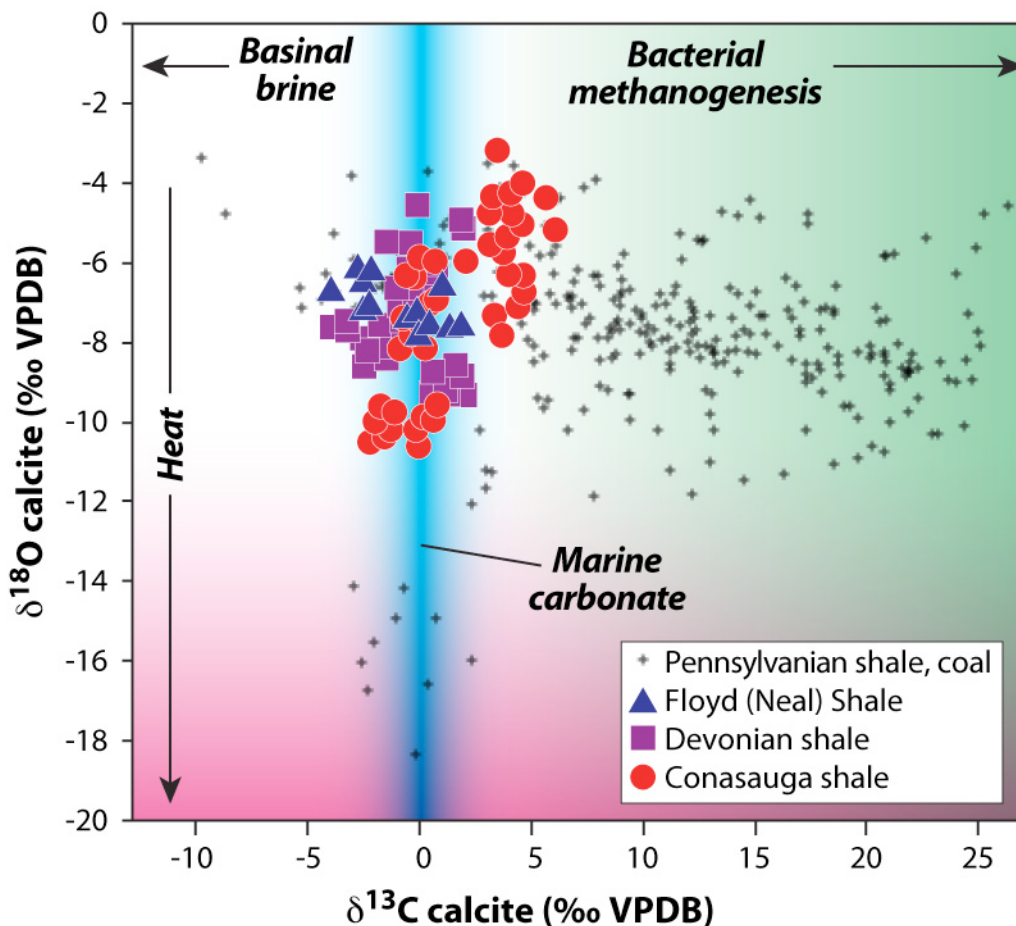


Figure 69.—Cross-plot comparing the stable isotopic characteristics of vein fills in shale gas reservoirs in Alabama to those in coalbed methane reservoirs of the Black Warrior basin.

processes (fig. 70). Calcite from the shallow Dawson 34-03-01 core is enriched in  $^{13}\text{C}$  and  $^{18}\text{O}$  near the surface and becomes depleted with depth. Positive  $\delta^{13}\text{C}$  values are suggestive of near-surface bacterial activity, which may include the digestion of light hydrocarbons, and the values trend downward toward those of normal marine carbonate ( $\sim 0$  ‰). Values of  $\delta^{18}\text{O}$  as low as  $-2$  ‰ indicate precipitation at or near surface temperature, and decreasing values with depth are consistent with modern burial temperature. Values from the deep Dawson 33-09 #2A core are not appreciably more depleted in  $^{13}\text{C}$  and  $^{18}\text{O}$  than those from the shallow core and are consistent with those observed from the other shale formations (fig. 69).

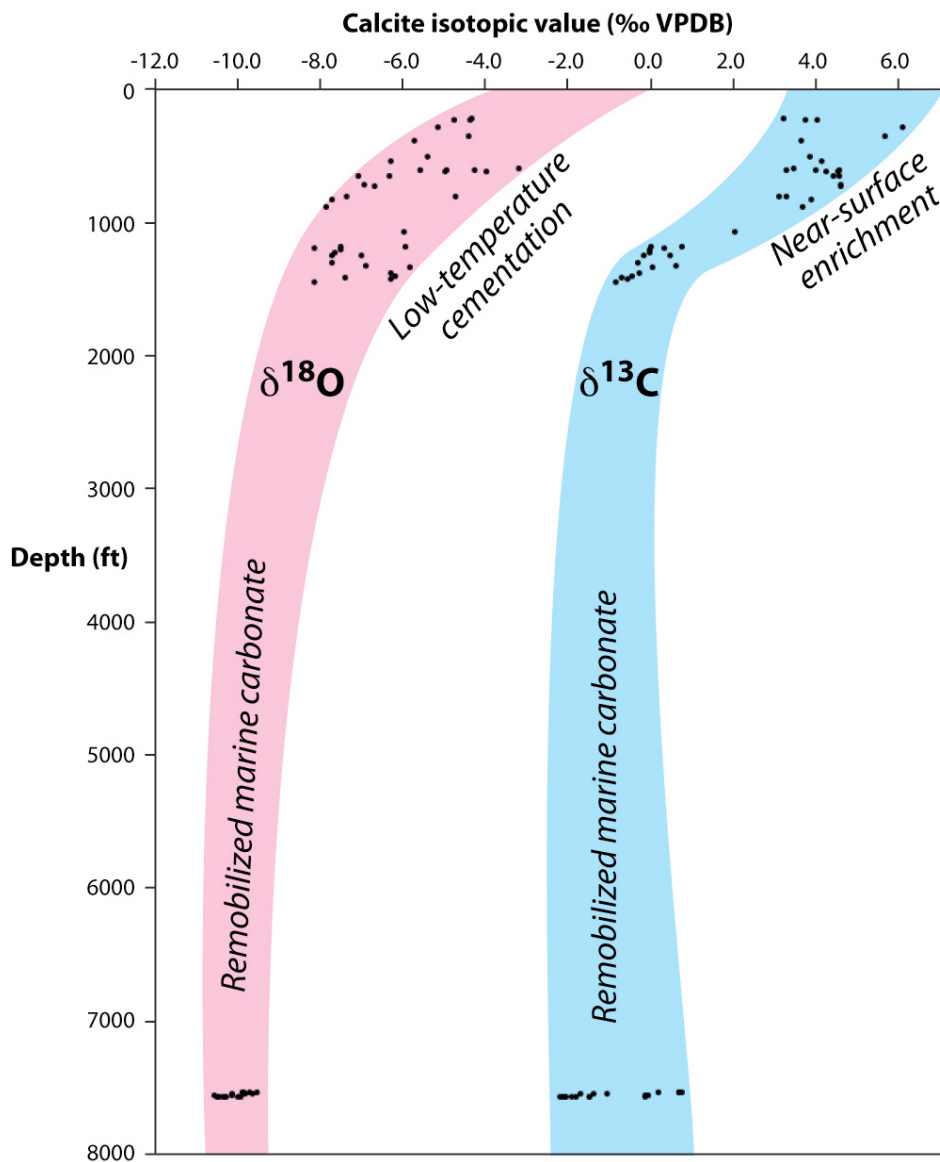


Figure 70.—Relationship of isotopic composition of calcite veins to depth in the Conasauga Formation.

So, the question remains, why are carbon and oxygen isotopic data from the calcite veins more consistent with shallow marine carbonate than deep burial cement? The answer is probably related to the abundance of marine limestone beds within and adjacent to the prospective shale gas formations. Much of the carbon and oxygen in the vein fills probably was derived from dissolution of the limestone by basal fluids during burial, and stylolites provide the clearest

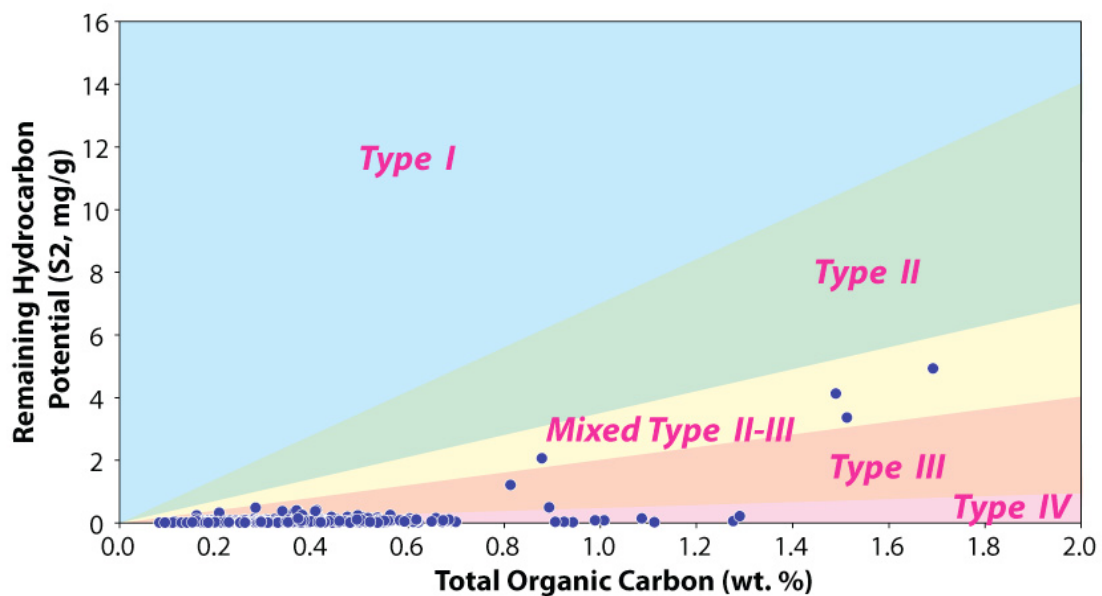
evidence for this dissolution. The scavenged carbonate apparently retained the isotopic signature of the parent carbonate, thereby enriching the basinal fluids in  $^{13}\text{C}$  and  $^{18}\text{O}$ .

### **Organic Petrology**

The organic petrology of Alabama's shale gas reservoirs is as complex as the mineral petrology described above and reflects the preservation and geochemical alteration of a broad range of biologically derived organic materials. The Cambrian-age Conasauga Formation predates the earliest land plants, which are of Silurian age, and so the types of kerogen preserved differ from those in the Devonian-Mississippian black shale units. In the Conasauga, identifiable organic particles include types II through IV kerogen types. Type II kerogen is oil-prone and includes palynomorphs, or sporinite, which during the Cambrian consisted primarily of acritarchs. As mentioned in the section on geothermics, true vitrinite, which is derived from wood and constitutes gas-prone type III kerogen, did not exist in the Cambrian. However, herbaceous kerogen that resembles vitrinite is present in Cambrian strata and can be used for reflectance analysis (fig. 57). In addition, small amounts of inertinite are present, which is type IV kerogen that principally represents oxidized and fungal organic matter. Type IV kerogen lacks significant potential for hydrocarbon generation. The dominant type of organic matter in Conasauga shale is matrix bituminite. Matrix bituminite is amorphous kerogen that is dispersed throughout the argillaceous rock matrix and gives the shale its dark color. Matrix bituminite can be oil-prone, gas-prone, or inert and is generally considered type II kerogen.

Geochemical analysis of Conasauga shale indicates that TOC content averages 0.4 percent but can be higher than 1.7 percent (fig. 71A). Rock-eval pyrolysis reveals that the shale plots geochemically as a type IV source rock on the pseudo-Van Krevelen diagram, indicating that

### A. KEROGEN QUALITY



### B. KEROGEN TYPE

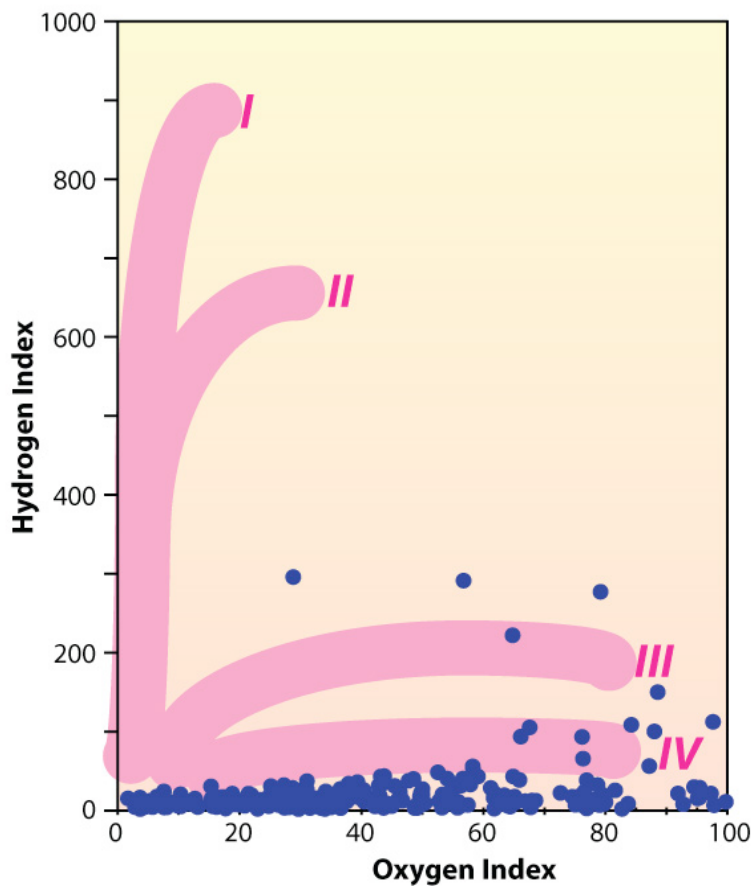


Figure 71.—Results of kerogen analysis in the Conasauga shale of Big Canoe Creek Field, St. Clair County, Alabama.

much of its hydrocarbon generation and expulsion potential has been exhausted (fig. 60B). Some of the most organic-rich shale plots as a mixed type II-III source rock, which stands in stark contrast to the bulk of the shale. One possibility is that layers rich in acritarchs or herbaceous kerogen (fig. 61) help elevate the organic and hydrogen content.

Diverse types of kerogen have been identified in the Chattanooga Shale of Alabama. Near the outcrop along the northern margin of the Black Warrior basin, where the Chattanooga contains oil shale, the shale has low thermal maturity and contains the oil-prone alga, *Tasmanites*, which is a form of type I kerogen (Rheams and Neathery, 1988). Matrix bituminite, which forms a fluorescent groundmass in the shale, is the most abundant type of kerogen. Other kerogen types include minor amounts of vitrinite and inertinite (Carroll and others, 1995). The TOC content of the shale is highly variable. Rheams and Neathery (1988) reported TOC content as high as 19 percent along the northern rim of the Black Warrior basin and characterized the shale as an oil-prone type I to type II source rock. Indeed, the subsurface data from this current study indicate a type II to III geochemistry in the northern Black Warrior basin, where the shale is shallower than 4,000 feet (fig. 72). In the thermally mature shale of the southeastern Black Warrior basin and the Greene-Hale synclinorium, TOC content is generally lower than 6 percent, although some samples contain more than 9 percent. *Tasmanites* is absent in the thermally mature shale and probably dispersed into the matrix bituminite during burial and maturation. Kerogen in thermally mature Devonian shale typically has low S<sub>2</sub> values and low hydrogen indices and thus plots as a type IV source rock with exhausted generative potential.

Organic matter in the Neal shale is dominated by matrix bituminite with minor amounts of vitrinite and inertinite (Carroll and others, 1995). No algal kerogen analogous to *Tasmanites* in the Chattanooga has been identified in the Neal, which may simply be a reflection of thermal

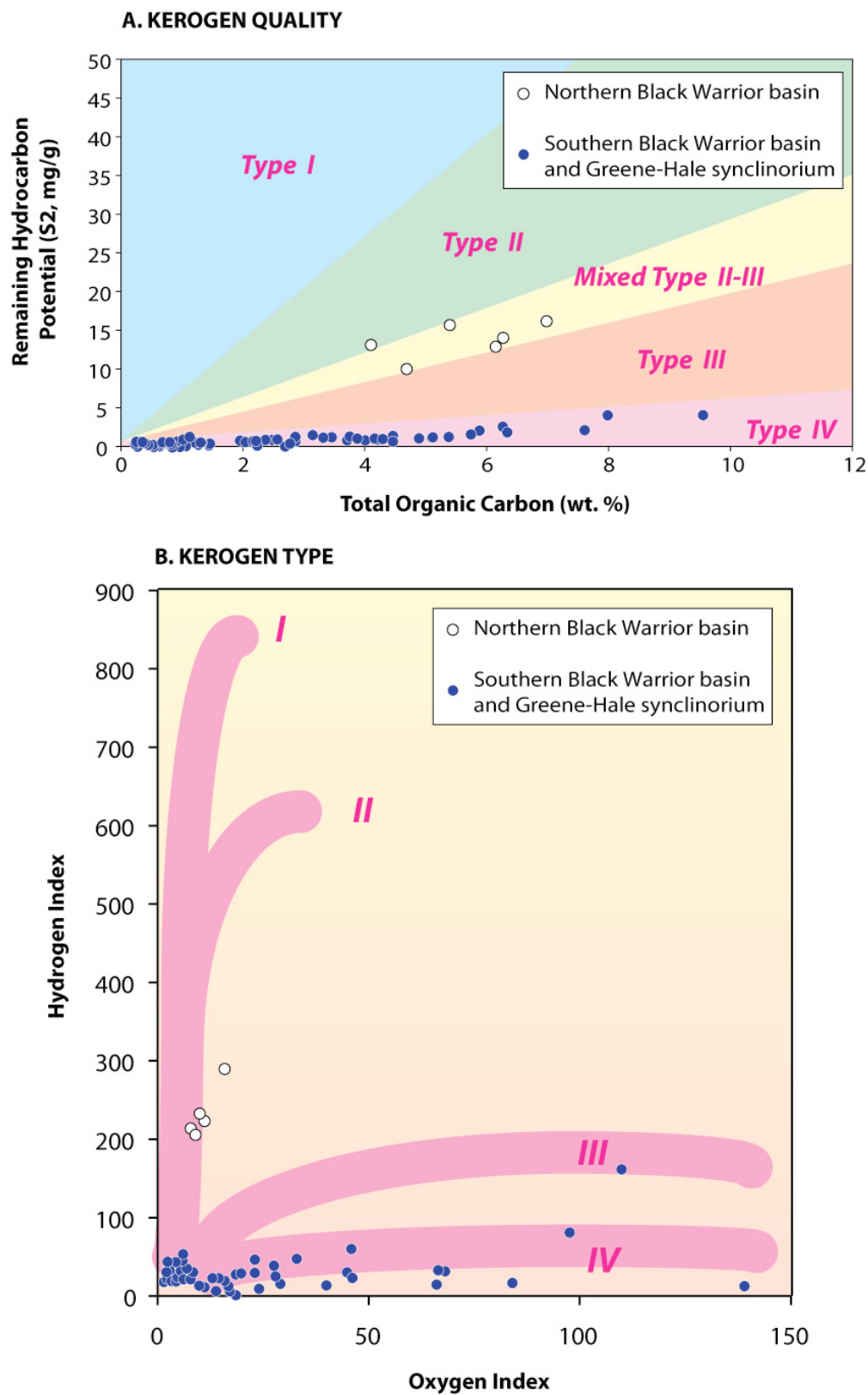


Figure 72.—Results of kerogen analysis in Devonian shale of the Black Warrior basin and the Greene-Hale synclinorium.

maturity. A kerogen quality plot of the Neal shale indicates that it can be classified as a type III to type IV source rock (fig. 73A). However, many of the shale samples have hydrogen index values between 200 and 400, and the bulk of the samples plot on a trajectory from type II to type IV kerogen (fig. 73B). This variability of hydrogen index reflects changing thermal maturity in the Neal basin. Indeed, calculated vitrinite reflectance based on rock-eval pyrolysis results demonstrates that thermal maturity increases substantially toward the south (fig. 74). The calculated reflectance values are substantially lower than measured values, but the map does confirm southward passage of the shale deep into the thermogenic gas generation window (reflectance = 0.8-2.6 percent) (figs. 50, 63). Tmax is another indicator of thermal maturity and measures the temperature of pyrolysis at which a peak quantity of hydrocarbons is generated (Espitalié and others, 1977). In the Neal shale, Tmax values range from 439 to 500°C, indicating that the shale is thermally mature. Mapping Tmax yields a result similar to mapping calculated vitrinite reflectance in the Neal shale (fig. 75).

### **Microfabric**

Not only is gas shale complex in terms of mineralogic and organic composition, but it is also complex in terms of rock fabric. Shale fabric represents a network of detrital minerals, authigenic minerals, organic matter, and porosity. As such, the rock fabric is ultimately the product of sedimentation, compaction, diagenesis, and hydrocarbon generation. SEM microscopy is an excellent way to explore rock fabric, and this section summarizes the results of SEM analysis of Alabama gas shale.

Platy clay minerals are a fundamental part of the petrologic framework of shale and are perhaps the most conspicuous elements of rock fabric. Each shale unit examined in this study

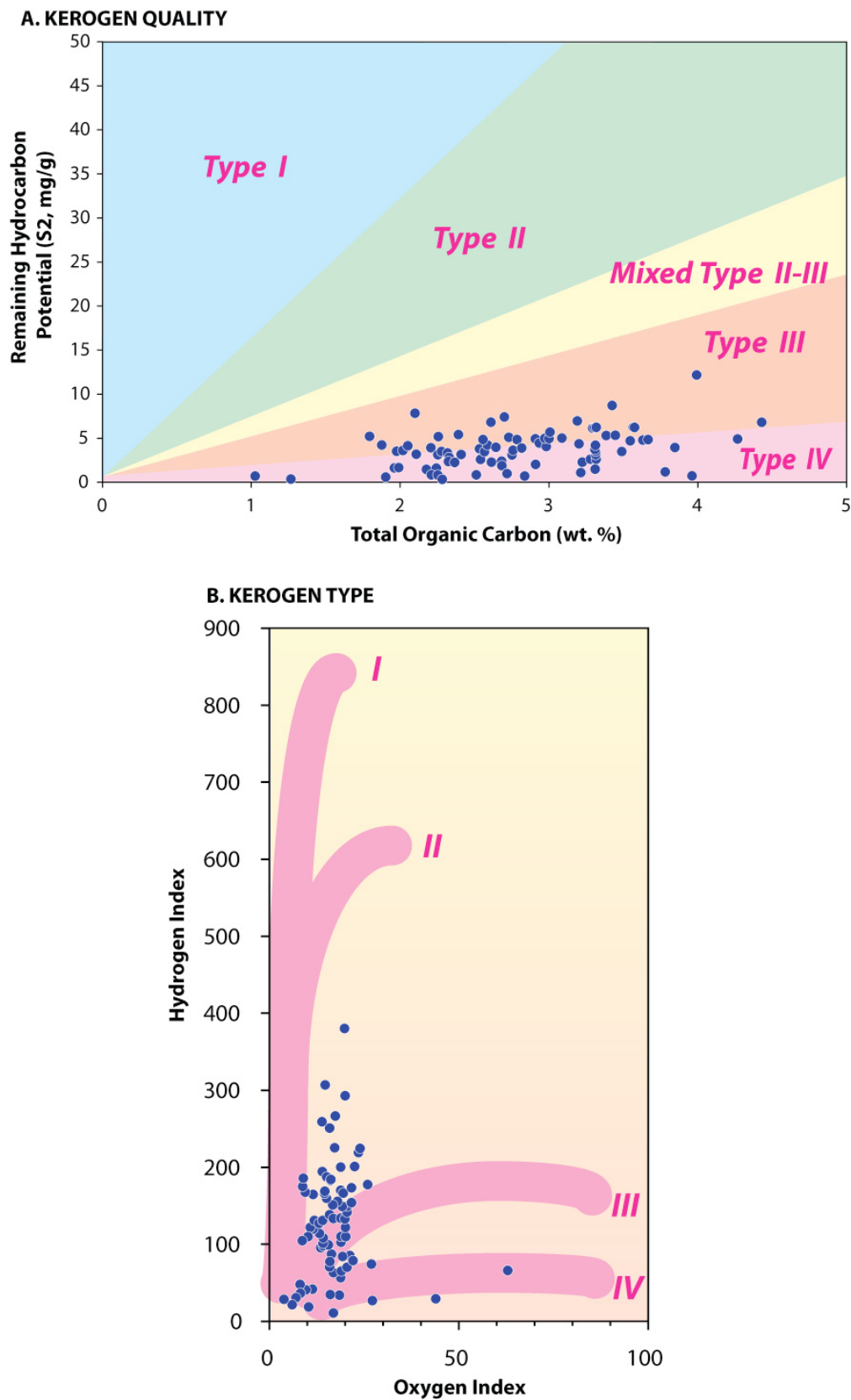


Figure 73.—Results of kerogen analysis in the Neal shale of the Black Warrior basin, Alabama.

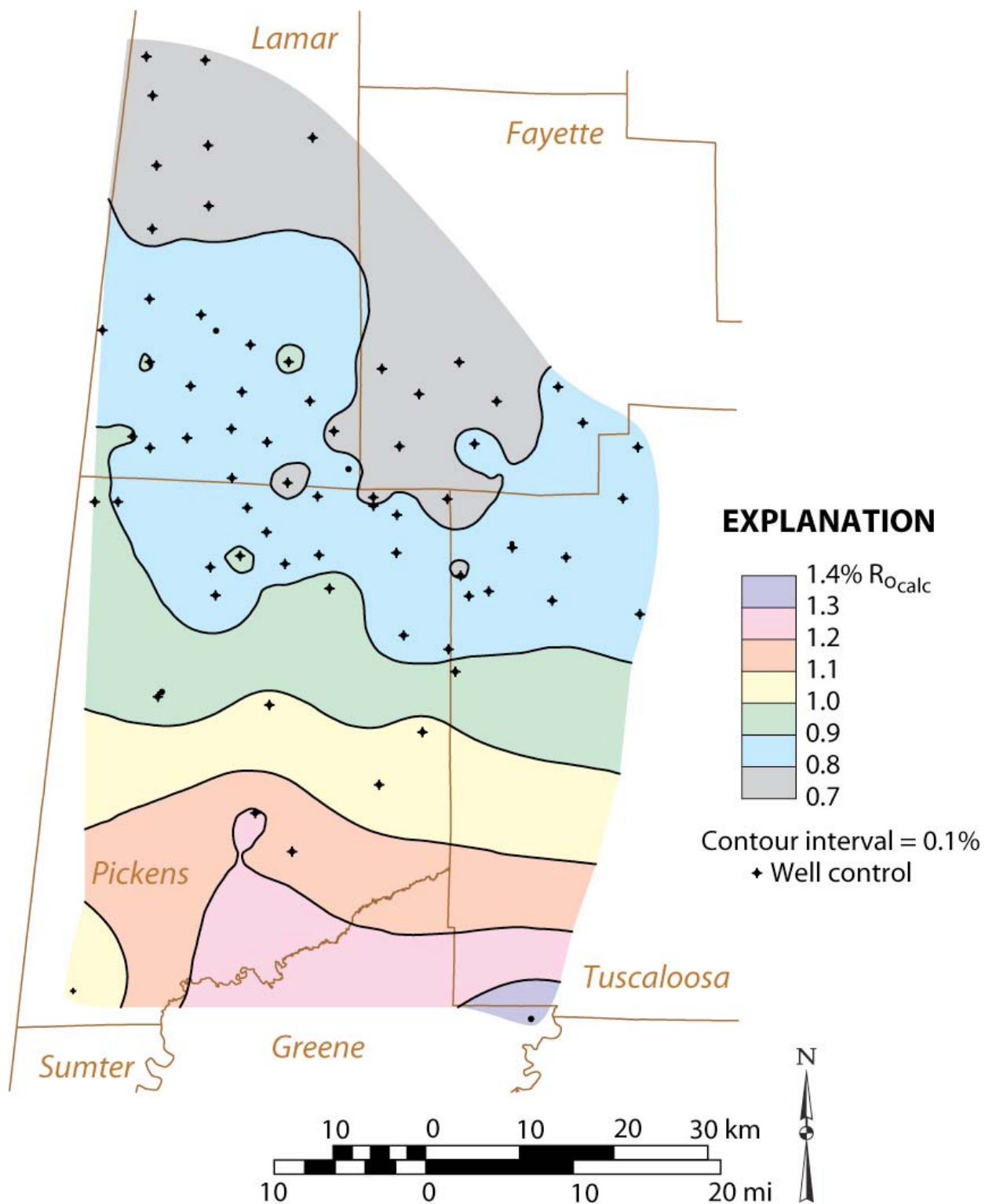


Figure 74.—Map of calculated vitrinite reflectance in the Neal shale of the Black Warrior basin of Alabama.

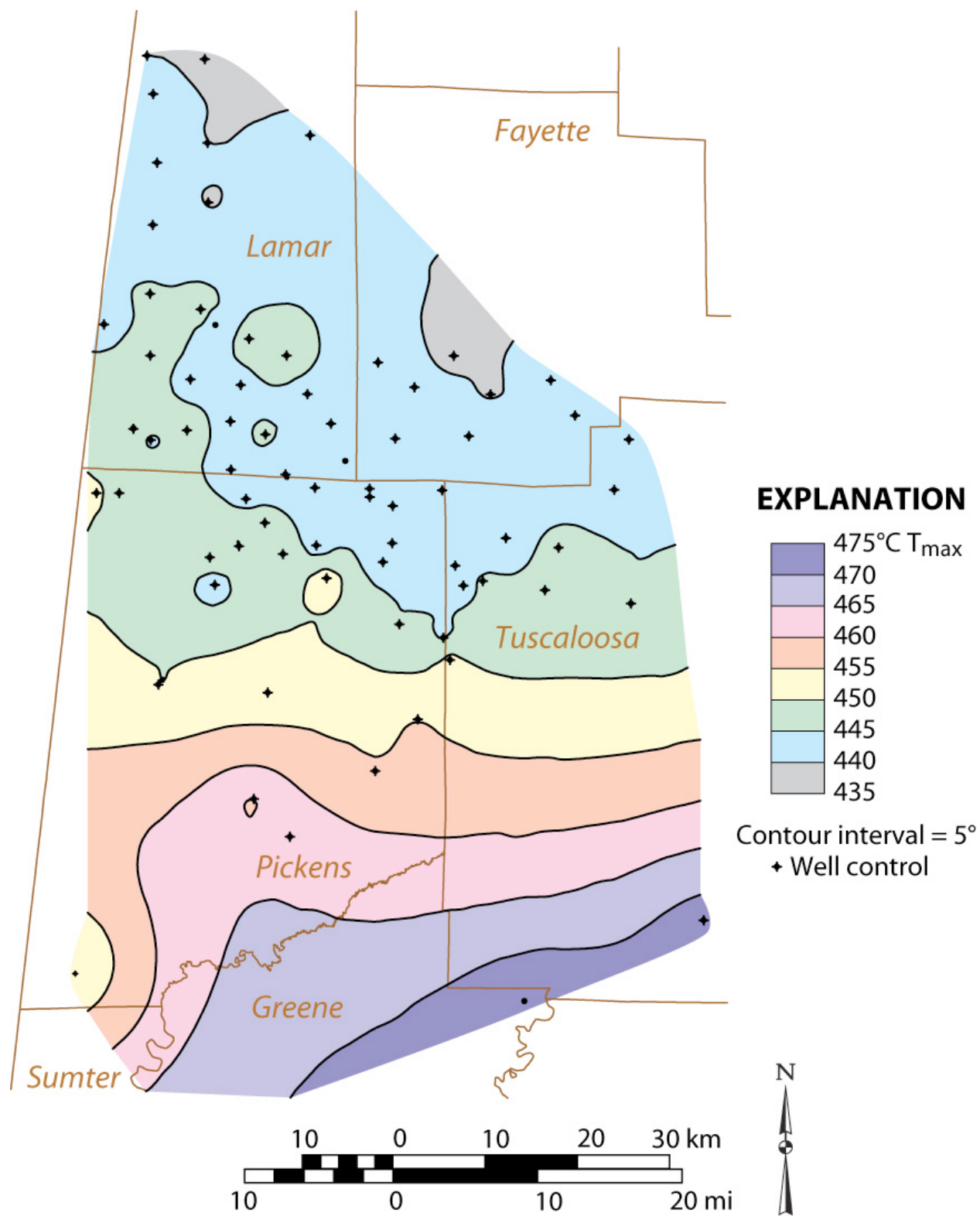


Figure 75.—Map of  $T_{max}$  in the Neal shale of the Black Warrior basin of Alabama.

displays a range of platy clay fabric. In Conasauga shale, illite plates commonly exhibit weaker alignment than the illite plates in Chattanooga and the illite and chlorite plates in Neal shale (figs. 76-78). Where aligned, platy clay tends to be folded around quartz and carbonate particles (fig. 78), and this combination of alignment and folding is interpreted to be a product of compaction. The weak alignment of clay plates in the Conasauga, however, may reflect undercompaction associated with high fluid pressure in the Gadsden MUSHWAD.

Euhedral illite laths and fibers (fig. 67) demonstrate that clay can be diagenetic as well as depositional. Laths and fibers require open space in which to grow, and thus provide the best evidence for open porosity in the shale gas reservoirs. The laths are not folded or broken, which indicates formation after major compaction. Indeed, the high degree of illite crystallinity in all the shale units studied reflects deep burial and high thermal maturity.

Quartz, feldspar, and carbonate minerals are dispersed through the matrix of all the shale units studied. Quartz and feldspar grains typically appear as rounded bodies but can be difficult to record because they have similar backscatter properties to clay and carbonate. Carbonate minerals occur as distinct rhombs and are thus readily identified (figs. 76, 78). In the Shell Burke 27-9 #1 well of the Greene-Hale synclinorium, calcite particles commonly exhibit irregular surfaces with pock marks, which are suggestive of dissolution (fig. 79).

Pyrite is the densest mineral in the studied shale samples and thus appears bright in backscatter SEM images (fig. 80). Pyrite occurs in many forms ranging from framboids and nodules to isolated crystals of varying size. Common crystal habits include cubes, bipyramids, and pyritohedra. Framboidal pyrite is abundant in all the shale units, but the Chattanooga contains the greatest variety of crystal forms, many of which can be displayed in a fraction of a millimeter (fig. 80). This range of form indicates repeated changes in pore fluid chemistry early

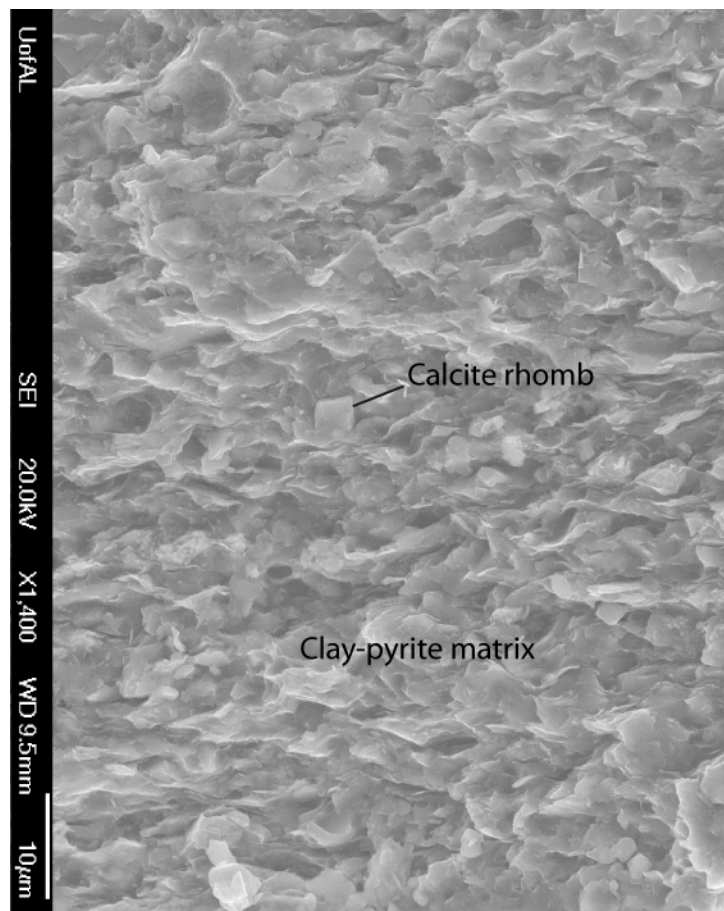


Figure 76.—SEM image showing weakly aligned clay fabric of Conasauga shale, Dawson 33-09 #2A well, Big Canoe Creek Field, 7,558.8 ft.

in the depositional and diagenetic history. Most pyrite was deposited directly from the water column or formed within pre-existing sediment or rock (e.g., Wignall and Newton, 1998), although some grew within open fractures (fig. 81).

The sheer variety of framboid forms in the gas shale units is remarkable (figs. 66, 80, 82, 83). Many framboids in Neal shale contain crystals with rounded edges and pitted centers (fig. 82), indicating dissolution by corrosive fluid. Many of these framboids are coated with diagenetic clay (figs. 82, 83). Schieber (2011) suggested that pyrite is corroded during short-lived periods of oxygenation in pore water, which is consistent with the observations of bioturbation and storm deposition reported in the discussion of stratigraphy and sedimentation. Pyrite clusters also occur

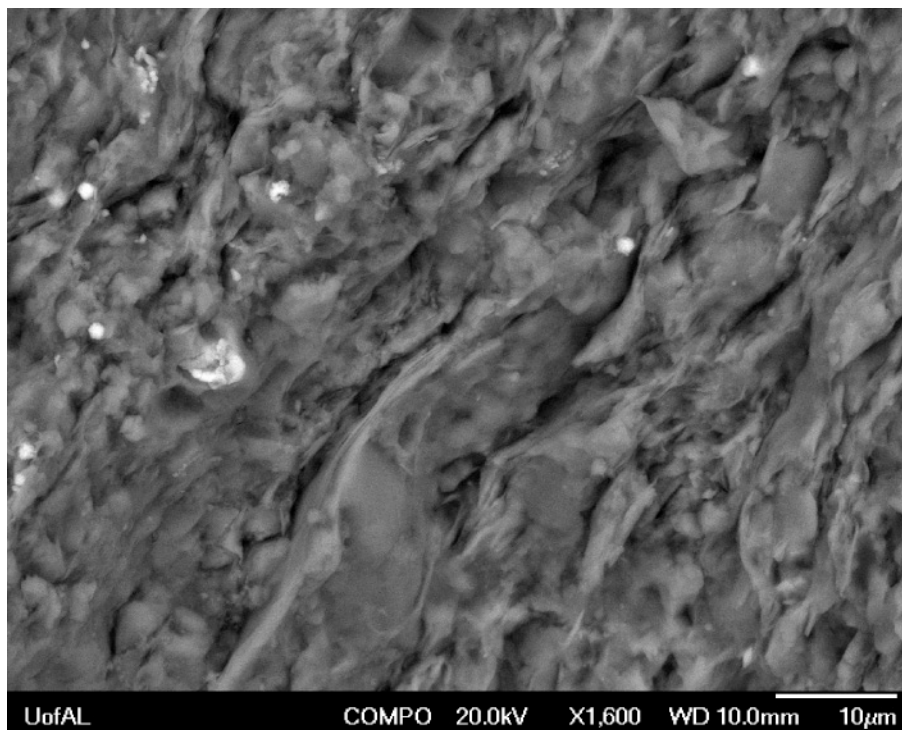


Figure 77.—SEM image showing aligned clay fabric of Chattanooga Shale, Lamb 1-3 #1 well, Greene County, Alabama, 9,022.3 ft.

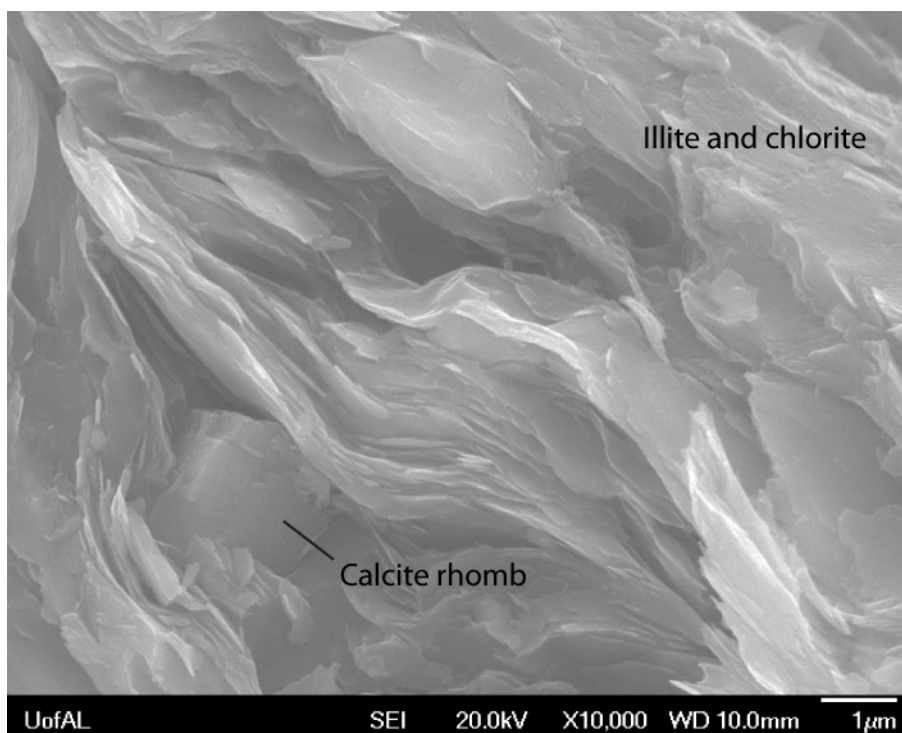


Figure 78.—Platy illite and calcite rhomb in Neal shale, Weyerhaeuser 2-43-2402 well, Greene County, Alabama, 8,011.4 ft.

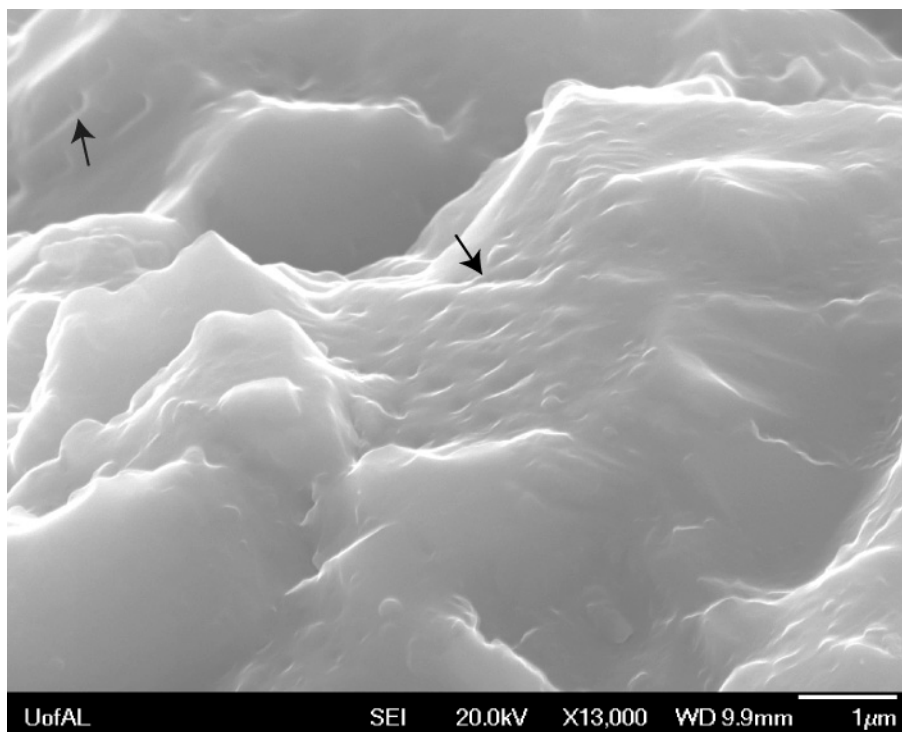


Figure 79.—Calcite with pock marks suggesting dissolution, Devonian shale, Shell Burke 27-9 #1 well, Hale County, Alabama, 10,354.9 ft.

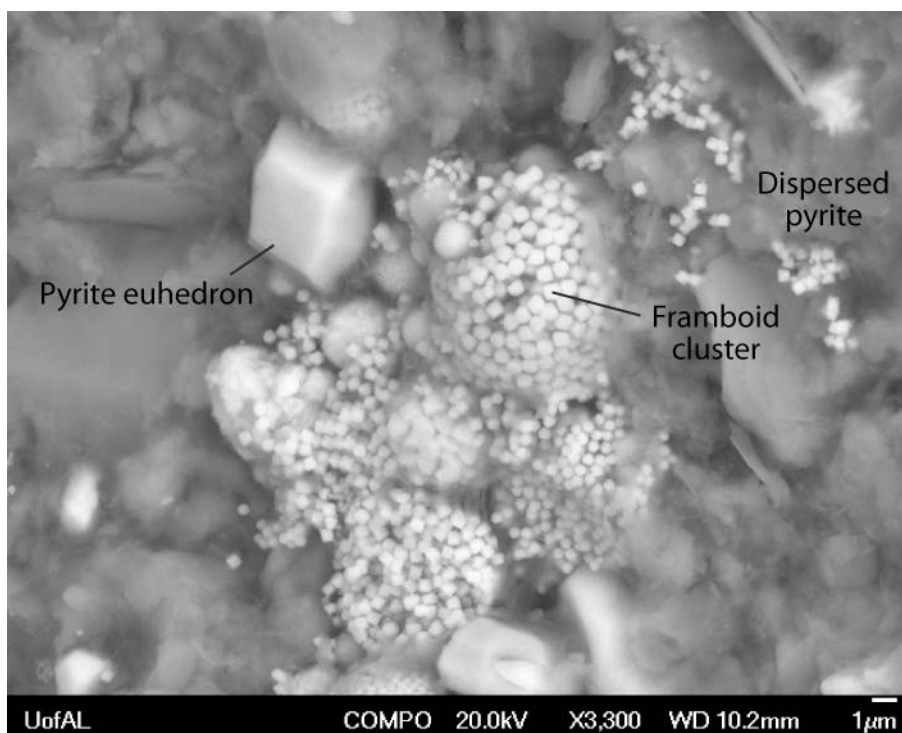


Figure 80.—Diverse pyrite forms in Chattanooga Shale, Weyerhaeuser 2-43-2402 well, Greene County, Alabama, 8,211.9 ft.

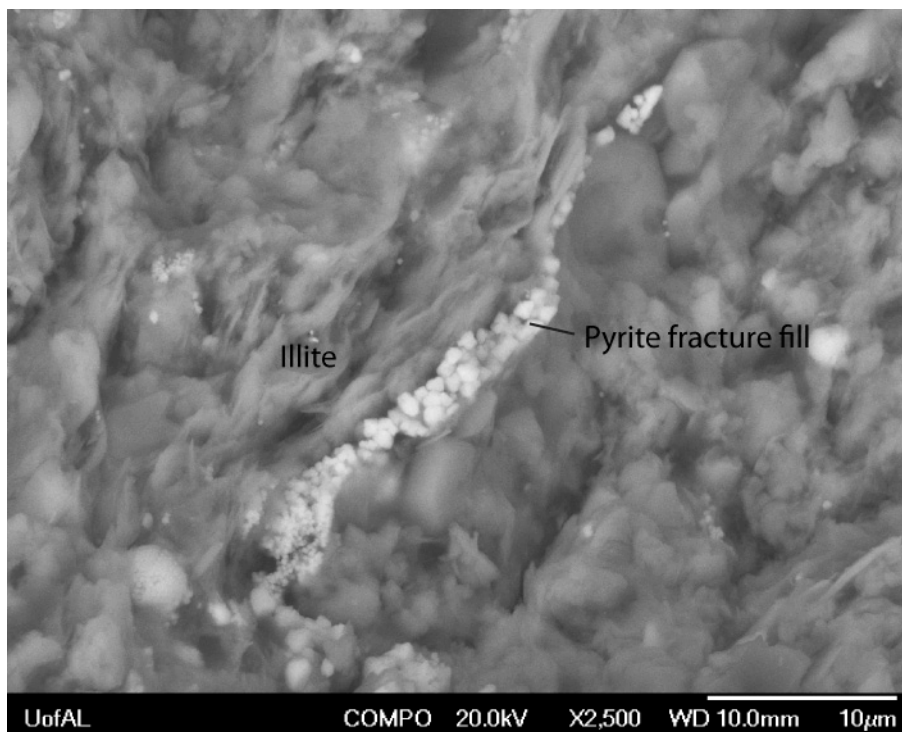


Figure 81.—Pyrite fracture fill in Chattanooga Shale, Weyerhaeuser 2-43-2402 well, Greene County, Alabama, 8,211.9 ft.



Figure 82.—Pyrite framboid with rounded and pitted crystals and clay overgrowth, Neal shale, Weyerhaeuser 2-43-2402 well, Greene County, Alabama, 8,011.4 ft.

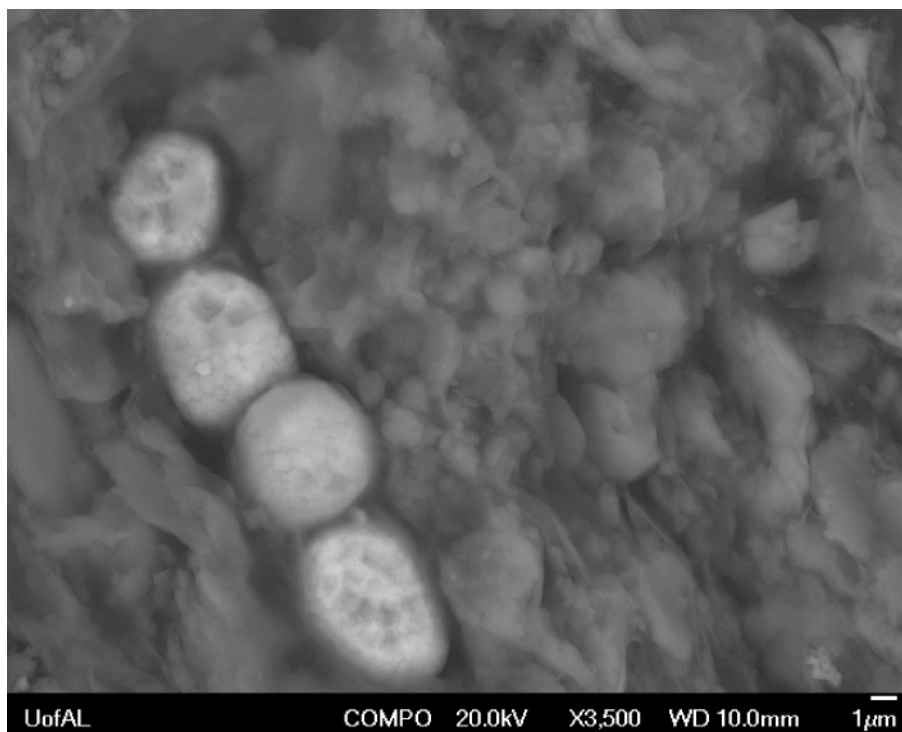


Figure 83.—Row of pyrite framboids with clay overgrowth in Neal shale, O'Bryant 6-15 #1 well, Pickens County, Alabama, 7,123.1 ft.

in several forms ranging from nodular agglomerations in the Chattanooga Shale (fig. 80) to rows of framboids in the Neal shale (fig. 83). Additional pyrite forms observed in the Neal include fibrous crystal arrays and pyritized pellets that have a jeweled appearance (fig. 84). Framboids are further a source of microporosity in shale, and the interstices between crystals even hosted crystalline illite growth (fig. 85).

Organic matter in gas shale takes many forms and has a varied expression in SEM images. Because kerogen is less dense than minerals, discrete kerogen particles, including vitrinite, liptinite, and inertinite, appear dark (fig. 86). Matrix bituminite coats virtually all surfaces within organic-rich black shale. These coatings are very thin and thus appear imperceptible in

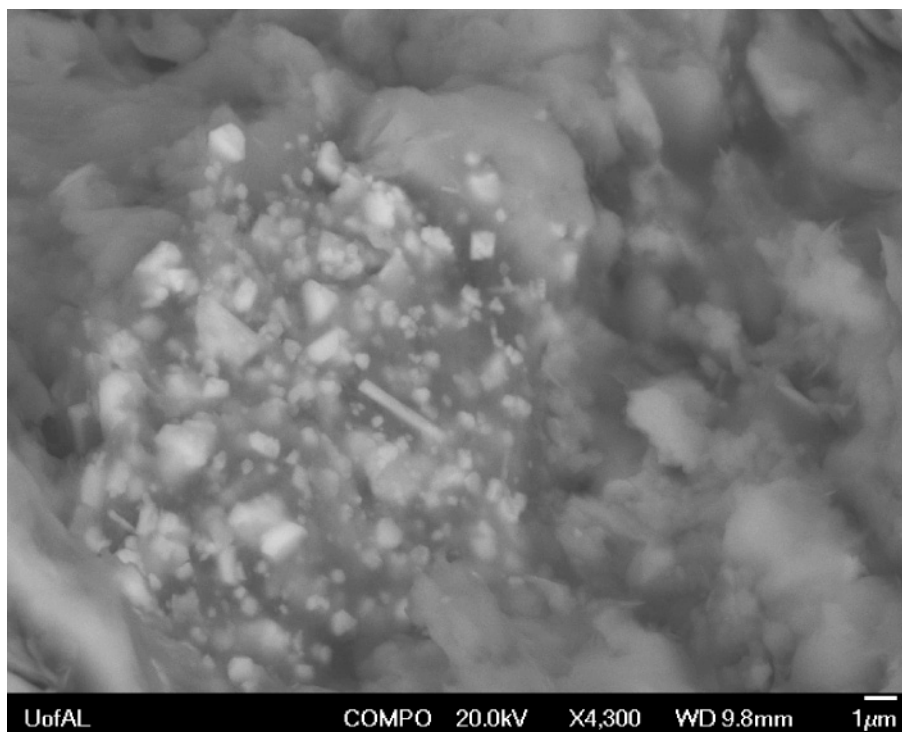


Figure 84.—Pyrite crystals lining peloid in Neal shale, O'Bryant 6-15 #1 well, Pickens County, Alabama, 7,123.3 ft.



Figure 85.—Porosity and pore-filling clay in pyrite framboid, Chattanooga Shale, Weyerhaeuser 2-43-2402 well, Greene County, Alabama, 8,211.9 ft.

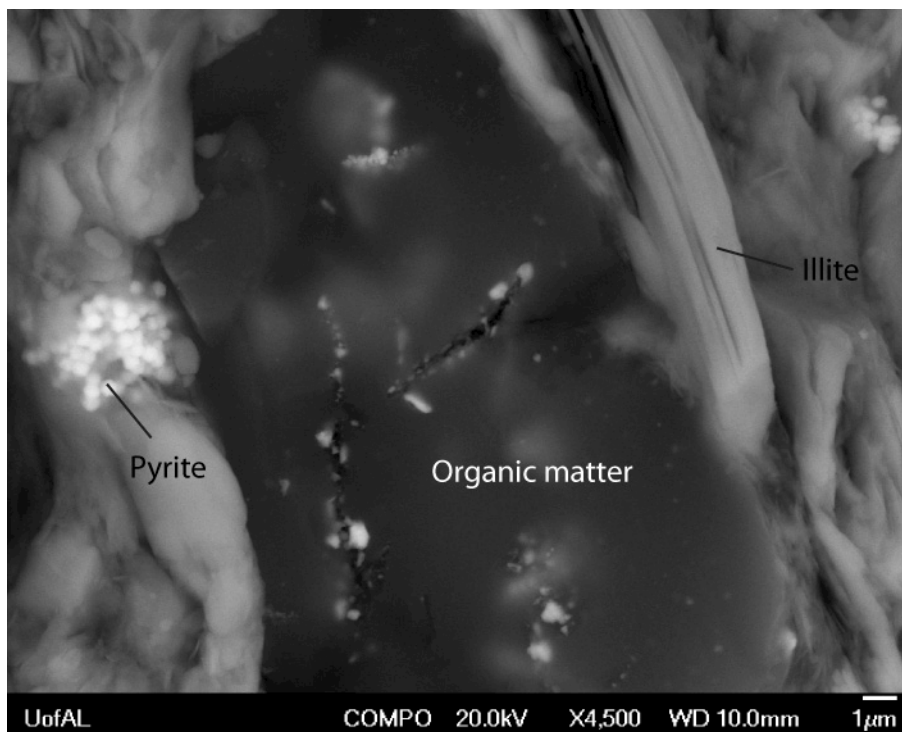


Figure 86.—Organic particle in Neal shale, Weyerhaeuser 2-43-2402 well, Greene County, Alabama, 8,034.9 ft.

SEM photomicrographs. However, the bituminite is readily vaporized by the scanning beam when employing the electron microprobe capabilities of the SEM used in this study.

Porosity is difficult to image using an SEM. The principal difficulty is the inability to distinguish plucked voids from dissolution voids. Accordingly, some of the most convincing microscopic evidence of porosity in shale comes from pores containing crystals that had to grow into open space. Soeder (1988) stated that interstitial porosity in Devonian shale of the Appalachian basin was dominated by the slot-like voids between and within clay flakes. Indeed pore throats in shale typically range in size from 0.1 to 0.0005  $\mu\text{m}$  and can thus approach or even overlap the size of gas and hydrocarbon molecules (e.g., Nelson, 2009). Our observations in Alabama support this contention. High-magnification SEM imagery (up to 75,000 times) has demonstrated that pores within and among illite flakes are bridged by delicate illite laths or tubes

that are 100 to several hundred nanometers long and a few tens to about 100 nanometers across (fig. 87). This kind of microporosity in shale appears to be widespread in Alabama Paleozoic shale, but SEM imaging allows only a qualitative analysis of porosity and the interconnectedness of pores. Accordingly, quantitative analysis of porosity, permeability, and gas storage is the focus of the next section of this report.

### **GAS STORAGE AND PERMEABILITY**

Shale has been recognized as a dual-porosity medium for storage of natural gas (e.g., Kuuskraa and others, 1992; Montgomery and others, 2005; Ross and Bustin, 2008). Gas is stored primarily in a free state in the interstitial porosity of the shale matrix and in an adsorbed state in the microporosity of the organic matter (fig. 88). Gas stored in a free state is expected to follow the pressure-volume-temperature relationships dictated by ideal gas law. Accordingly, assuming constant temperature, free gas mobility can be fairly constant across a broad range of reservoir pressure. By contrast, adsorbed gas is attracted to free surfaces by Van der Waals forces and can thus be characterized using Langmuir parameters. As such, adsorbed gas can be mobilized by small pressure changes at low reservoir pressure, where the Langmuir isotherm is steep. Larger pressure changes are required to mobilize gas at elevated pressure, where the isotherm is flat.

Regardless of storage mechanism, however, the permeability of shale is very low, typically on the order of  $0.1 \mu\text{D}$  (e.g., Soeder, 1988). Free gas is thought to flow primarily by Darcian processes and thus responds directly to pressure changes. Although adsorption is a pressure-sensitive phenomenon, gas flows in organic matrix primarily by Fickian processes, or diffusion, which is driven by concentration gradients rather than pressure. The contrasting storage and flow mechanisms in shale give rise to reservoirs with characteristics resembling a mix of tight



Figure 87.—Sub-micrometer scale illite bridges (arrows) demonstrating open porosity within the clay matrix of shale (Shell Burke well, depth = 1,037.8 ft.

sandstone and coal. Because of this, however, it is perhaps best to consider shale reservoirs on their own terms when developing exploration and development strategies.

### **Porosity and Permeability**

Even though the prospective shale-gas formations of the Black Warrior basin and Appalachian thrust belt are thermally mature and have exhausted their generative potential for hydrocarbons, results of core analysis demonstrate that the shale is capable of holding large volumes of natural gas (tables 10-13). Based on the Dawson 34-03-01 core (table 10), shale in the Conasauga Formation has effective porosity between 1.4 and 5.4 percent. On average, gas occupies 66.5 percent of this pore volume, and gas saturation increases with depth to a maximum

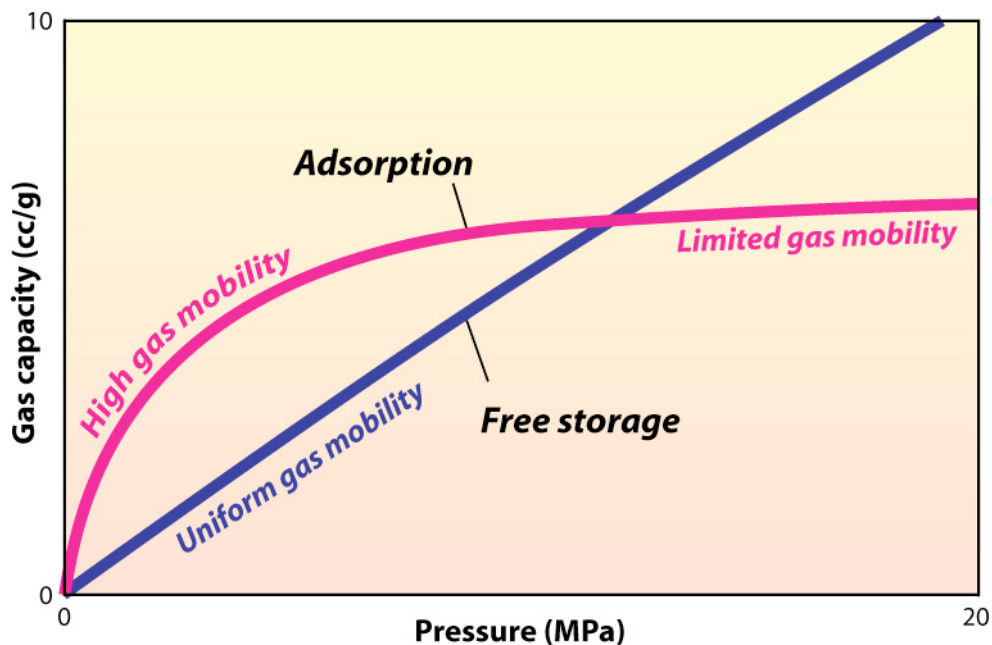


Figure 88.—Generalized diagram showing gas storage mechanisms and their effect on the mobility of gas in shale.

of 93.5 percent of pore volume. Water saturation is inversely related to gas saturation. Water saturation decreases from more than 52.6 percent of pore volume shallower than 900 feet to less than 24.3 percent at greater depth. Oil saturation averages 2.5 percent of pore volume and is fairly consistent throughout the core. Pressure-decay permeability ranges from 0.105 to 0.180  $\mu\text{D}$  and averages 0.133  $\mu\text{D}$ .

In the Greene-Hale synclinorium, Devonian shale of the Bayne Etheridge 36-9 #1 well has effective porosity between 1.2 and 2.5 percent, and about 79 percent of this pore volume is gas-filled (table 11). Irreducible water saturation averages 15.1 percent, but is as high as 26.3 percent within the calcareous gray shale facies. Oil saturation averages 7.6 percent and is thus substantially higher than in Conasauga shale. Permeability ranges from 0.111 to 0.188  $\mu\text{D}$  and averages 0.144  $\mu\text{D}$ .

Table 10. Basic reservoir properties of Conasauga shale as determined by core analysis.

Well	Depth (ft)	Effective porosity (%)	Gas-filled porosity (%)	Gas Saturation (%)	Water Saturation (%)	Oil saturation (%)	Permeability ( $\mu$ D)
Dawson 34-3-1	578	5.4	2.5	45.8	52.6	1.6	0.180
Dawson 34-3-1	844	3.5	1.5	43.7	53.8	2.5	0.147
Dawson 34-3-1	853	3.5	1.2	33.5	64.0	2.5	0.107
Dawson 34-3-1	873	3.1	1.1	34.1	63.1	2.8	0.125
Dawson 34-3-1	904	4.4	1.5	32.7	65.3	2.0	0.133
Dawson 34-3-1	910	1.4	1.1	78.9	17.7	3.4	0.137
Dawson 34-3-1	947	1.8	1.7	92.9	2.2	4.9	0.134
Dawson 34-3-1	950	2.6	1.8	72.3	24.3	3.4	0.152
Dawson 34-3-1	1178	4.1	3.8	92.0	5.9	2.1	0.158
Dawson 34-3-1	1204	4.3	3.7	86.4	11.6	2.0	0.112
Dawson 34-3-1	1220	4.6	4.3	91.8	7.1	1.0	0.105
Dawson 34-3-1	1307	4.0	3.7	93.5	4.2	2.2	0.110
<b>Statistics</b>							
n		12	12	12	12	12	12
Mean		3.6	2.3	66.5	31.0	2.5	0.133
Minimum		1.4	1.1	32.7	2.2	1.0	0.105
Maximum		5.4	4.3	93.5	65.3	4.9	0.180
Standard deviation		1.1	1.2	25.0	25.2	1.0	0.022

The Chattanooga Shale of the Lamb 1-3 #1 well has much greater effective porosity, between 1.6 and 5.6 percent (table 12). Roughly 73 percent of this pore volume is gas-filled, and an average of 23 percent of pore space is occupied by irreducible water. Oil saturation ranges from 1.0 to 8.8 percent and averages 3.3 percent. Permeability ranges from 0.087  $\mu$ D to 0.393  $\mu$ D and averages 0.237  $\mu$ D. Hence, the Chattanooga Shale in the Lamb well is significantly more permeable than the other shale units analyzed during this investigation. With values between 2.3 and 7.7 percent, effective porosity appears to be greatest in the Neal shale of the Lamb 1-3 #1 well (table 13). Gas saturation ranges from 27.8 to 76.5 percent of pore volume, and gas-filled porosity accounts for an average 1.9 percent of bulk volume. Irreducible water saturation is

Table 11. Basic reservoir properties of Devonian shale in the Greene-Hale synclinorium as determined by core analysis.

Well	Depth (ft)	Effective porosity (%)	Gas-filled porosity (%)	Gas Saturation (%)	Water Saturation (%)	Oil saturation (%)	Permeability ( $\mu$ D)
Bayne-Etheridge 36-9 #1	8318	2.0	1.7	87.6	8.1	4.3	0.188
Bayne-Etheridge 36-9 #1	8328	2.0	1.7	84.5	11.1	4.4	0.176
Bayne-Etheridge 36-9 #1	8341	1.3	1.0	76.0	17.2	6.8	0.140
Bayne-Etheridge 36-9 #1	8429	1.5	1.0	67.8	26.3	5.9	0.112
Bayne-Etheridge 36-9 #1	8438	1.3	0.9	72.0	20.8	7.2	0.120
Bayne-Etheridge 36-9 #1	8451	2.5	1.9	77.5	15.5	7.0	0.185
Bayne-Etheridge 36-9 #1	8461	1.3	1.1	82.9	10.1	7.0	0.124
Bayne-Etheridge 36-9 #1	8471	1.2	1.0	80.7	11.8	7.6	0.111
<b>Statistics</b>							
n		8	8	8	8	8	8
Mean		1.6	1.3	78.6	15.1	6.3	0.144
Minimum		1.2	0.9	67.8	8.1	4.3	0.111
Maximum		2.5	1.9	87.6	26.3	7.6	0.188
Standard deviation		0.4	0.4	6.2	5.7	1.2	0.031

highest in the Neal shale, with an average value of 45.8 percent and a range of 17.8 to 71.1 percent. Hence, a large portion of the pore space contains bound water when compared to the other shale formations. Oil saturation also ranges greatly from 0.3 to 6.9 percent in Neal shale. Permeability ranges from 0.073 to 0.227  $\mu$ D and averages 0.146  $\mu$ D, which is typical of Alabama gas shale.

Based on 77 core analyses, the average effective porosity of Alabama gas shale is 3.5 percent and has a standard deviation of 1.3 percent. Gas saturation averages 68 percent of pore volume and has a standard deviation of 17.1 percent. Water saturation averages 28.6 percent and has a standard deviation of 18.2 percent, whereas oil saturation averages 3.3 percent and has a standard deviation of 2.3 percent.

Table 12. Basic reservoir properties of Chattanooga shale as determined by core analysis.  
Table continued next page.

Well	Depth (ft)	Effective porosity (%)	Gas-filled porosity (%)	Gas Saturation (%)	Water Saturation (%)	Oil saturation (%)	Permeability ( $\mu$ D)
Lamb 1-3 #1	9135	3.5	3.0	86.0	7.3	6.7	0.230
Lamb 1-3 #1	9135	4.2	2.6	63.0	36.0	1.0	0.259
Lamb 1-3 #1	9137	3.8	2.2	58.6	40.3	1.1	0.304
Lamb 1-3 #1	9137	2.6	2.1	77.7	13.4	8.8	0.181
Lamb 1-3 #1	9139	4.3	2.7	63.5	35.5	1.0	0.341
Lamb 1-3 #1	9141	2.6	1.9	73.6	19.7	6.7	0.212
Lamb 1-3 #1	9142	3.6	2.2	61.1	36.7	2.2	0.113
Lamb 1-3 #1	9142	2.0	1.5	72.9	18.6	8.6	0.149
Lamb 1-3 #1	9143	3.9	2.5	64.5	33.5	2.0	0.109
Lamb 1-3 #1	9144	3.1	1.8	57.6	39.8	2.6	0.087
Lamb 1-3 #1	9147	3.4	2.5	73.0	25.7	1.3	0.202
Lamb 1-3 #1	9148	3.1	2.7	88.0	6.5	5.6	0.233
Lamb 1-3 #1	9150	3.8	2.6	68.7	30.2	1.2	0.140
Lamb 1-3 #1	9152	2.5	1.3	51.2	45.7	3.2	0.130
Lamb 1-3 #1	9152	2.6	1.3	51.8	45.1	3.1	0.136
Lamb 1-3 #1	9154	3.3	2.3	70.8	27.9	1.4	0.096
Lamb 1-3 #1	9154	3.6	2.3	62.2	36.6	1.2	0.154
Lamb 1-3 #1	9156	3.2	1.9	60.1	37.5	2.4	0.196
Lamb 1-3 #1	9157	2.3	2.0	84.6	8.1	7.3	0.230
Lamb 1-3 #1	9159	1.6	1.5	89.8	5.4	4.8	0.114
Lamb 1-3 #1	9161	3.4	2.2	66.2	32.6	1.3	0.209
Lamb 1-3 #1	9163	4.0	2.8	70.5	27.6	1.9	0.331
Lamb 1-3 #1	9165	4.0	2.6	65.9	32.1	1.9	0.221
Lamb 1-3 #1	9167	1.6	1.4	89.5	5.5	5.0	0.107
Lamb 1-3 #1	9170	4.6	3.7	80.4	18.0	1.6	0.393
Lamb 1-3 #1	9171	3.6	2.7	75.1	23.7	1.2	0.338
Lamb 1-3 #1	9173	4.3	2.9	67.6	30.6	1.8	0.292
Lamb 1-3 #1	9174	4.0	2.7	69.0	27.2	3.8	0.354
Lamb 1-3 #1	9178	4.7	4.1	87.7	10.7	1.6	0.390

Table 12 (continued). Basic reservoir properties of Chattanooga shale as determined by core analysis.

Well	Depth (ft)	Effective porosity (%)	Gas-filled porosity (%)	Gas Saturation (%)	Water Saturation (%)	Oil saturation (%)	Permeability ( $\mu\text{D}$ )
Lamb 1-3 #1	9181	4.5	3.5	79.2	19.1	1.7	0.254
Lamb 1-3 #1	9182	2.9	2.6	91.4	2.9	5.8	0.293
Lamb 1-3 #1	9183	3.3	2.5	75.7	23.0	1.3	0.343
Lamb 1-3 #1	9185	2.7	2.5	93.0	0.7	6.3	0.275
Lamb 1-3 #1	9186	3.2	2.7	85.4	13.3	1.3	0.287
Lamb 1-3 #1	9187	5.6	4.1	71.9	25.5	2.6	0.379
Lamb 1-3 #1	9188	2.8	2.6	93.7	0.3	5.9	0.294
Lamb 1-3 #1	9190	4.6	2.9	63.1	35.4	1.6	0.259
Lamb 1-3 #1	9191	2.7	2.4	88.2	5.5	6.2	0.228
Lamb 1-3 #1	9191	4.2	3.3	78.5	19.8	1.8	0.341
Lamb 1-3 #1	9193	4.0	2.7	66.7	31.4	1.9	0.258
<b>Statistics</b>							
n		40	40	40	40	40	40
Mean		3.4	2.5	73.4	23.3	3.2	0.237
Minimum		1.6	1.3	51.2	0.3	1.0	0.087
Maximum		5.6	4.1	93.7	45.7	8.8	0.393
Standard deviation		0.9	0.7	11.6	12.9	2.3	0.088

Pressure-decay permeability values from the shale units fall within a narrow range. Average permeability is  $0.191 \mu\text{D}$ ; minimum and maximum values are  $0.073$  and  $0.393 \mu\text{D}$ , respectively. The standard deviation of these analyses is only  $0.085 \mu\text{D}$ , indicating high consistency. These porosity and permeability values are typical of producing shale gas reservoirs in other regions, and so all units studied have commercial reservoir properties in terms of free gas storage and permeability.

Table 13. Basic reservoir properties of Neal shale as determined by core analysis.

Well	Depth (ft)	Effective porosity (%)	Gas-filled porosity (%)	Gas Saturation (%)	Water Saturation (%)	Oil saturation (%)	Permeability ( $\mu$ D)
Lamb 1-3 #1	9013	4.3	2.1	48.1	47.9	4.0	0.170
Lamb 1-3 #1	9014	7.7	2.1	27.8	71.1	1.0	0.084
Lamb 1-3 #1	9016	5.9	2.8	47.4	51.3	1.3	0.151
Lamb 1-3 #1	9017	3.2	2.0	63.5	31.2	5.2	0.218
Lamb 1-3 #1	9018	5.4	1.7	31.1	67.5	1.5	0.077
Lamb 1-3 #1	9020	5.7	2.2	38.1	61.1	0.8	0.110
Lamb 1-3 #1	9021	2.5	1.4	55.6	37.4	6.9	0.179
Lamb 1-3 #1	9022	5.5	2.5	46.4	52.2	1.4	0.095
Lamb 1-3 #1	9023	3.0	2.3	76.5	17.8	5.7	0.225
Lamb 1-3 #1	9024	5.4	3.3	60.7	37.9	1.4	0.208
Lamb 1-3 #1	9024	2.6	1.8	70.5	23.0	6.5	0.224
Lamb 1-3 #1	9025	4.9	2.4	49.4	49.1	1.5	0.227
Lamb 1-3 #1	9058	3.5	1.8	49.9	49.9	0.3	0.108
Lamb 1-3 #1	9059	2.6	1.3	48.8	48.1	3.1	0.073
Lamb 1-3 #1	9059	3.7	1.9	51.6	47.2	1.2	0.085
Lamb 1-3 #1	9060	2.3	1.4	63.4	32.9	3.7	0.076
Lamb 1-3 #1	9061	5.5	2.5	45.9	52.5	1.6	0.171
<b>Statistics</b>							
n		17	17	17	17	17	17
Mean		4.3	2.1	51.5	45.8	2.8	0.146
Minimum		2.3	1.3	27.8	17.8	0.3	0.073
Maximum		7.7	3.3	76.5	71.1	6.9	0.227
Standard deviation		1.5	0.5	12.4	14.0	2.1	0.058

### Adsorption

Adsorption isotherms were run for methane on shale samples at reservoir temperature as estimated from bottom-hole temperature observations. Results from the Black Warrior basin and the Appalachian thrust belt indicate that adsorption capacity varies greatly (fig. 89; tables 14-17). The performance of the samples analyzed can be characterized in terms of Langmuir volume and Langmuir pressure. Langmuir volume is the adsorption capacity at infinite pressure. Langmuir pressure, by comparison, is the pressure at which adsorption capacity is 50 percent of

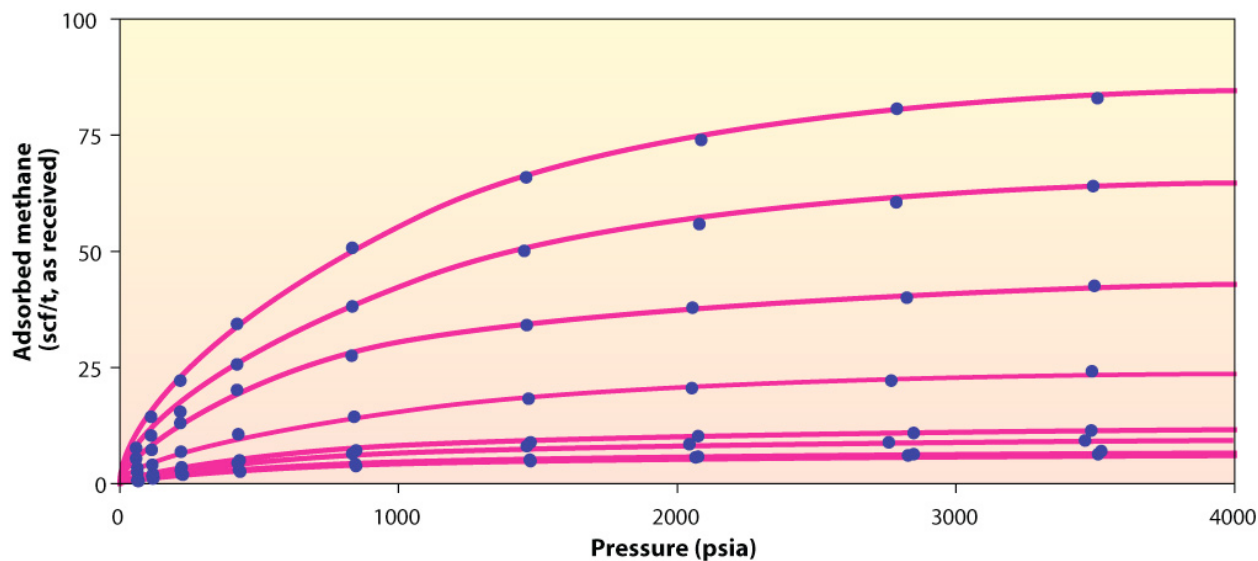


Figure 89.—Absolute methane adsorption isotherms from Devonian shale in the Bayne-Etheridge 36-9 #1 well, Greene County, Alabama.

Langmuir volume. Langmuir pressure is a measure of isotherm shape. Isotherms with low Langmuir pressure are very steep at low pressure and flatten greatly at high pressure; those with high Langmuir pressure tend to maintain slope at elevated pressure.

In Conasauga shale from the Dawson 34-03-01 core, Langmuir volume is very low, ranging from 9 to 29 standard cubic feet per ton (scf/t) (table 14). Langmuir pressure ranges from 526 to 670 absolute pounds per square inch (psia). In the Devonian shale of the Bayne-Etheridge 36-9 #1 well from the Greene-Hale synclinorium, Langmuir volume ranges from 8 to 101 scf/t. (fig. 78) (table 15), and Langmuir pressure is higher than that in the Conasauga, ranging from 712 to 840 psia. In the Lamb 1-3 #1 well, which is in the southeastern Black Warrior basin of Greene County, the Chattanooga Shale has Langmuir volume ranging from 52 to 127 scf/t, and the Neal shale has Langmuir volume ranging from 56 to 88 scf/t (tables 16, 17). Langmuir pressure in the Chattanooga ranges from 676 to 885 psia. Langmuir pressure is slightly higher in the Neal, ranging from 922 to 1,012 psia. Langmuir volume correlates directly with TOC content (fig. 90),

Table 14. Summary results of adsorption isotherm analysis in the Conasauga Formation.

Well name	Depth	TOC (%)	V <sub>L</sub> (scf/t)	V <sub>p</sub> (psia)
Dawson 34-3-1	578	0.3	12	555
Dawson 34-3-1	844	0.3	11	535
Dawson 34-3-1	853	0.2	9	573
Dawson 34-3-1	873	0.2	10	615
Dawson 34-3-1	904	0.2	12	590
Dawson 34-3-1	910	1.8	29	665
Dawson 34-3-1	947	0.6	19	670
Dawson 34-3-1	950	0.6	19	641
Dawson 34-3-1	1178	0.4	16	596
Dawson 34-3-1	1204	0.2	11	526
Dawson 34-3-1	1220	0.4	15	550
Dawson 34-3-1	1307	0.3	11	625
<b>Statistics</b>				
n		12	12	12
Mean		0.5	14	595
Minimum		0.2	9	526
Maximum		1.8	29	670
Standard deviation		0.4	5	47

V<sub>L</sub> = Langmuir volume; V<sub>p</sub> = Langmuir pressure

Table 15. Summary results of adsorption isotherm analysis in Devonian shale of the Greene-Hale synclinorium.

Well name	Depth	TOC (%)	V <sub>L</sub> (scf/t)	V <sub>p</sub> (psia)
Bayne Etheridge 36-9 #1	8318	4.9	101	752
Bayne Etheridge 36-9 #1	8328	3.7	79	841
Bayne Etheridge 36-9 #1	8341	1.3	29	748
Bayne Etheridge 36-9 #1	8429	0.4	11	725
Bayne Etheridge 36-9 #1	8438	0.3	8	805
Bayne Etheridge 36-9 #1	8451	2.5	51	712
Bayne Etheridge 36-9 #1	8461	0.7	14	808
Bayne Etheridge 36-9 #1	8471	0.3	8	827
<b>Statistics</b>				
n		8	8	8
Mean		1.7	38	777
Minimum		0.3	8	712
Maximum		4.9	101	841
Standard deviation		1.7	33	46

Table 16. Summary results of adsorption isotherm analysis in Chattanooga shale.

Well name	Depth	TOC (%)	V <sub>L</sub> (scf/t)	V <sub>P</sub> (psia)
Lamb 1-3 #1	9135	7.6	128	773
Lamb 1-3 #1	9137	6.3	107	835
Lamb 1-3 #1	9141	3.4	59	795
Lamb 1-3 #1	9142	2.9	50	783
Lamb 1-3 #1	9148	3.8	66	709
Lamb 1-3 #1	9157	3.3	56	738
Lamb 1-3 #1	9182	5.8	102	676
Lamb 1-3 #1	9185	5.9	103	700
Lamb 1-3 #1	9188	6.3	106	885
Lamb 1-3 #1	9191	3.1	52	830
<b>Statistics</b>				
n		10	10	10
Mean		4.8	83	772
Minimum		2.9	50	676
Maximum		7.6	128	885
Standard deviation		1.6	27	63

Table 17. Summary results of adsorption isotherm analysis in Neal shale.

Well name	Depth	TOC (%)	V <sub>L</sub> (scf/t)	V <sub>P</sub> (psia)
Lamb 1-3 #1	9013	2.3	56	989
Lamb 1-3 #1	9017	4.0	88	1012
Lamb 1-3 #1	9021	2.8	62	953
Lamb 1-3 #1	9023	3.8	85	952
Lamb 1-3 #1	9024	3.8	87	922
<b>Statistics</b>				
n		5	5	5
Mean		3.3	75	966
Minimum		2.3	56	922
Maximum		4.0	88	1012
Standard deviation		0.7	14	31

indicating that sorbed gas is stored primarily in the organic fraction of most shale samples. The Neal regression line is not particularly well constrained, especially at low TOC values, but those for Devonian and Chattanooga shale have positive y-intercepts of 2.3 and 0.8 scf/t, respectively.

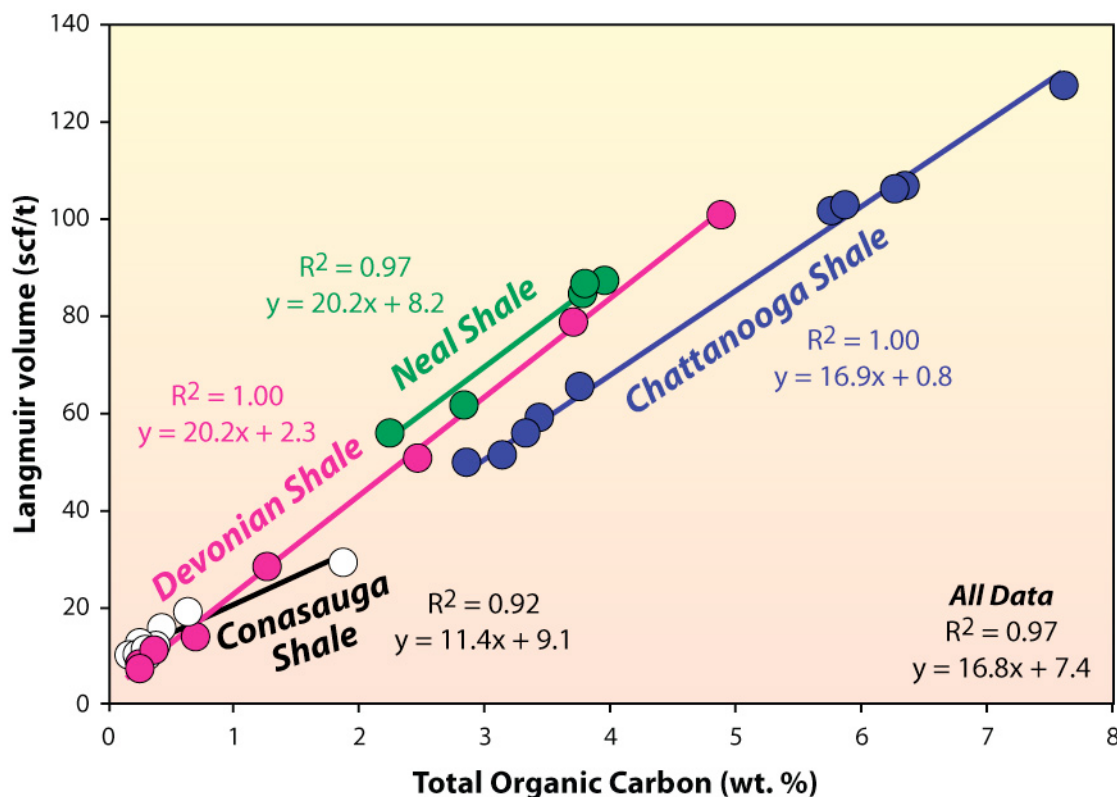


Figure 90.—Correlation between Langmuir volume and TOC content in Alabama gas shale.

This suggests that a small percentage of the gas is adsorbed on surfaces in the inorganic matrix, probably in clay. The effect of clay sorption appears to be greatest in the Conasauga shale, which contains relatively little TOC. The y-intercept of the Conasauga regression line is at 9.1 scf/t, suggesting that 31 to 97 percent of the gas is adsorbed on clay.

Langmuir pressure values from the shale samples are relatively high, ranging from 526 to 1,012 psia and averaging 740 psia (tables 14-17). This contrasts sharply with Langmuir volume in coalbed methane reservoirs of the Black Warrior basin, which ranges from 260 to 880 psia and indicates much flatter isotherms than in the shale reservoirs (Pashin, 2010b). In general, the Langmuir pressure values in shale show high consistency, although values in the Conasauga Formation tend to be slightly lower than those in the other stratigraphic units. High Langmuir pressure, moreover, helps promote the mobility of adsorbed gas at elevated pressure.

Another consideration in the analysis of adsorption in shale gas reservoirs is temperature. Simply stated, the adsorption capacity of organic matter decreases as reservoir temperature increases (Yang and Saunders, 1985; Zhou and others, 2000; Gasem and others, 2009) (fig. 91). The data presented here come from deep, warm reservoirs in the southeastern Black Warrior basin and the Greene-Hale synclinorium. In the shallow, cool reservoirs of Blount and Cullman Counties, low reservoir pressure places the reservoirs in a steeper part of the isotherm, and low reservoir temperature should facilitate higher adsorption capacity.

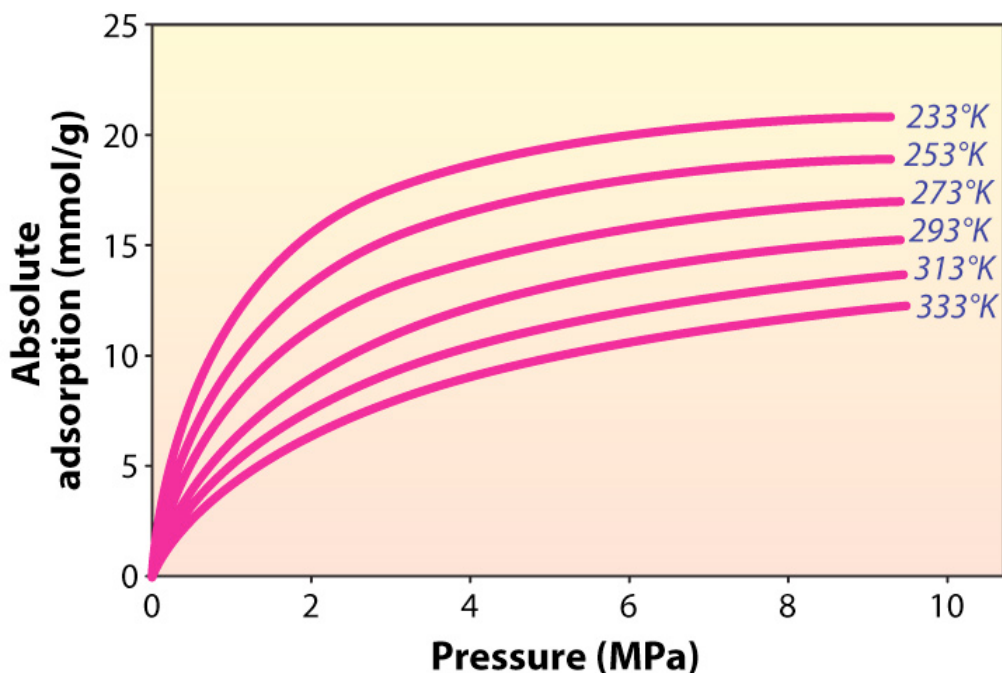


Figure 91.—Effect of temperature on methane adsorption in activated carbon (modified from Zhou and others, 2000).

### SHALE GAS RESOURCES AND RESERVES

Core analyses and adsorption isotherms indicate that the capacity of the target shale formations to store natural gas is significant. The areal extent, thickness, depth, and temperature of the shale units studied herein vary greatly. In addition, the proportions of free and adsorbed

gas can vary greatly, as can the mobility of each gas fraction. As stated in the discussion of analytical methods, determination of OGIP for each target is based on a simple volumetric model in which free gas volume was estimated based on fundamental pressure-volume-temperature relationships assuming normal hydrostatic pressure gradients. Sorbed gas volume was estimated at Langmuir volume. Accordingly, estimates of free gas volume can be considered as conservative values, considering the evidence for high gas pressure in some formations. By contrast, estimates of sorbed gas volume can be considered as upper resource limits.

Applying this approach to the Conasauga Formation in the Gadsden, Palmerdale, and Bessemer MUSHWADs indicates that an enormous natural gas resource base exists in Cambrian shale of the Appalachian thrust belt (table 18; fig. 92). Free gas resources are estimated to approach 524 trillion cubic feet (Tcf), whereas sorbed gas resources are estimated at more than 101 Tcf. Accordingly, the total gas resource in the area evaluated may exceed 625 Tcf and constitutes gas that is stored mainly in a free state. Mapping OGIP in the MUSHWADs indicates that resource concentration follows isopach trends and locally exceeds 1,000 billion cubic feet per square mile (Mcf/mi<sup>2</sup>) (figs. 36, 92). Considering that additional resources are projected to exist in undeformed strata of the eastern Black Warrior basin and within deformed strata of the Appalachian thrust belt in northeast Alabama and northwest Georgia (e.g., Cook and Thomas, 2010), the Conasauga is unquestionably a vast exploration target.

The volume and distribution of natural gas in Devonian shale differs significantly from that in Cambrian shale (table 18, fig. 93). The Chattanooga Shale of the Black Warrior basin is estimated to contain a free gas resource of about 22 Tcf and a sorbed resource of about 38 Tcf. Hence, adsorbed gas apparently forms the majority of the Chattanooga resource base, which is estimated to exceed 60 Tcf. However, the Chattanooga has limited development potential in

Table 18. Estimates of original gas in place and reserve potential based on deterministic volumetric analysis of prospective Alabama shale formations.

Formation	Age	Area (mi <sup>2</sup> )	Free gas (Bcf)	Sorbed gas (Bcf)	Total Gas (Bcf)	Total Gas (Tcf)	10% recovery (Tcf)	20% recovery (Tcf)
Conasauga	Cambrian	1,703	523,827	101,165	624,992	625.0	62.5	125.0
Chattanooga	Devonian	9,930	22,506	38,020	60,526	60.5	6.1	12.1
North area		1,049	4,042	6,467	10,509	10.5	1.1	2.1
South area		798	4,595	7,350	11,945	11.9	1.2	2.4
North + South		1,847	8,637	13,817	22,454	22.5	2.2	4.5
Unnamed	Silurian-Devonian	250	12,673	21,578	34,250	34.3	3.4	6.9
Floyd (Neal)	Mississippian	2,583	38,080	62,515	100,595	100.6	10.1	20.1
North area		1,552	19,762	32,628	52,390	52.4	5.2	10.5
South area		1,031	18,318	29,887	48,205	48.2	4.8	9.6

most of the Black Warrior basin, where it is thinner than 30 feet and can hold less than 8 Bcf/mi<sup>2</sup> (figs. 20, 93). This leaves two primary areas of interest from a development perspective (fig. 93). The northern area, which includes the productive reservoirs of Blount and Cullman Counties, contains an estimated gas resource of more than 10 Tcf and locally supports more than 15 billion cubic feet per square mile (Bcf/mi<sup>2</sup>) (table 18, fig. 93). The southern interest area, which contains the thickest Chattanooga Shale, contains an estimated gas resource of nearly 12 Tcf and supports gas concentrations as high as 25 Bcf/mi<sup>2</sup>. Thus OGIP in parts of the Chattanooga Shale that are considered favorable for development is interpreted to exceed 22 Tcf (table 18).

An even larger resource base appears to exist in the thick, unnamed Silurian-Devonian shale of the Greene-Hale synclinorium (table 18, fig. 93). The extent of the synclinorium is currently unknown and may be substantially greater than the 250 square miles used to estimate OGIP in this study. The three wells that constrain reservoir thickness indicate that resource concentration

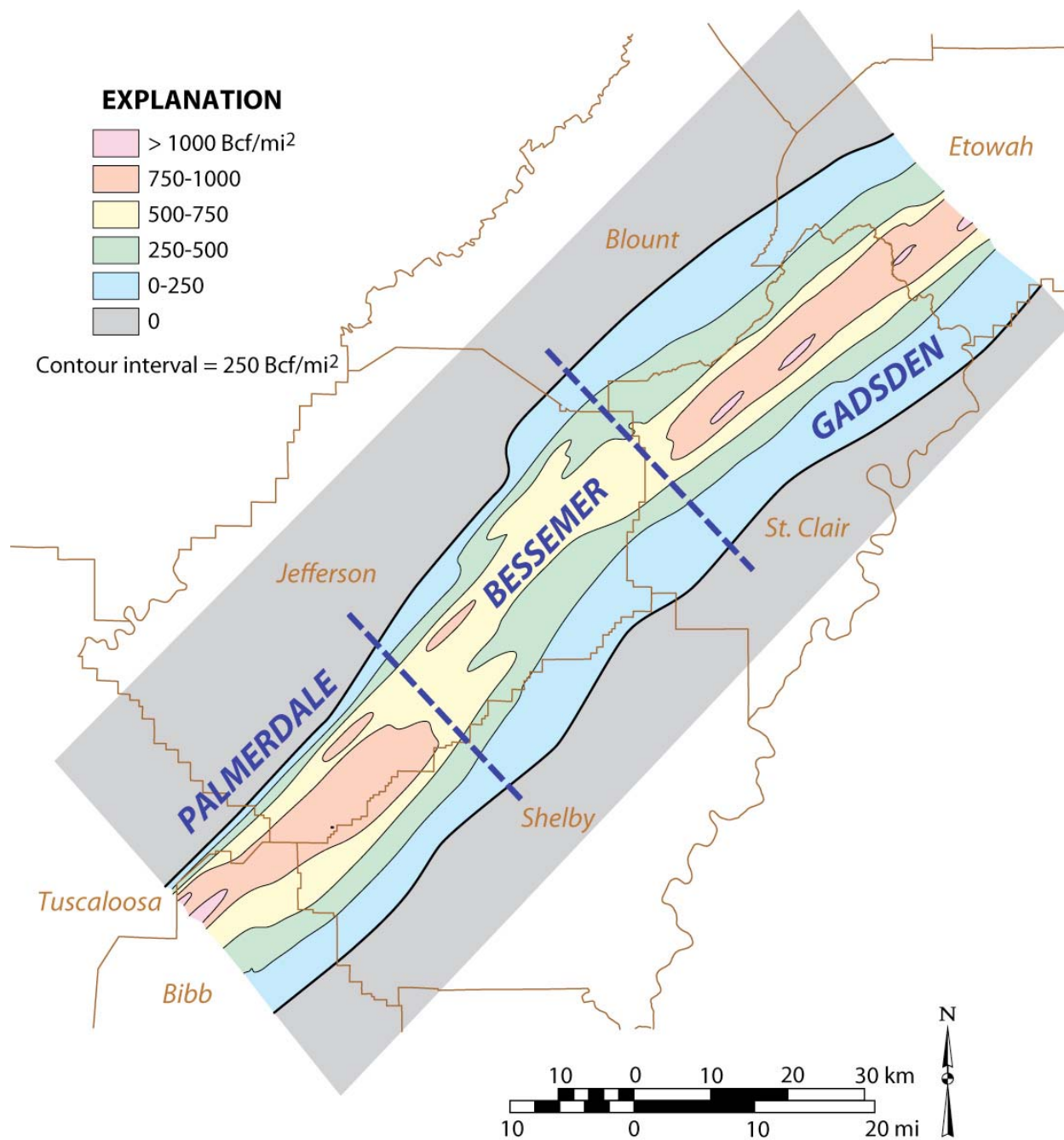


Figure 92.—Map of estimated original gas-in-place within the deformed Conasauga shale masses of the southern Appalachian thrust belt.

ranges at least from 86 to 206 Bcf/mi<sup>2</sup> and increases toward the southwest (fig. 93). More than 12 Tcf of gas is projected to be stored in a free state, and more than 21 Tcf is projected to be stored in an adsorbed state (table 18). Hence, the resource potential of the Greene-Hale

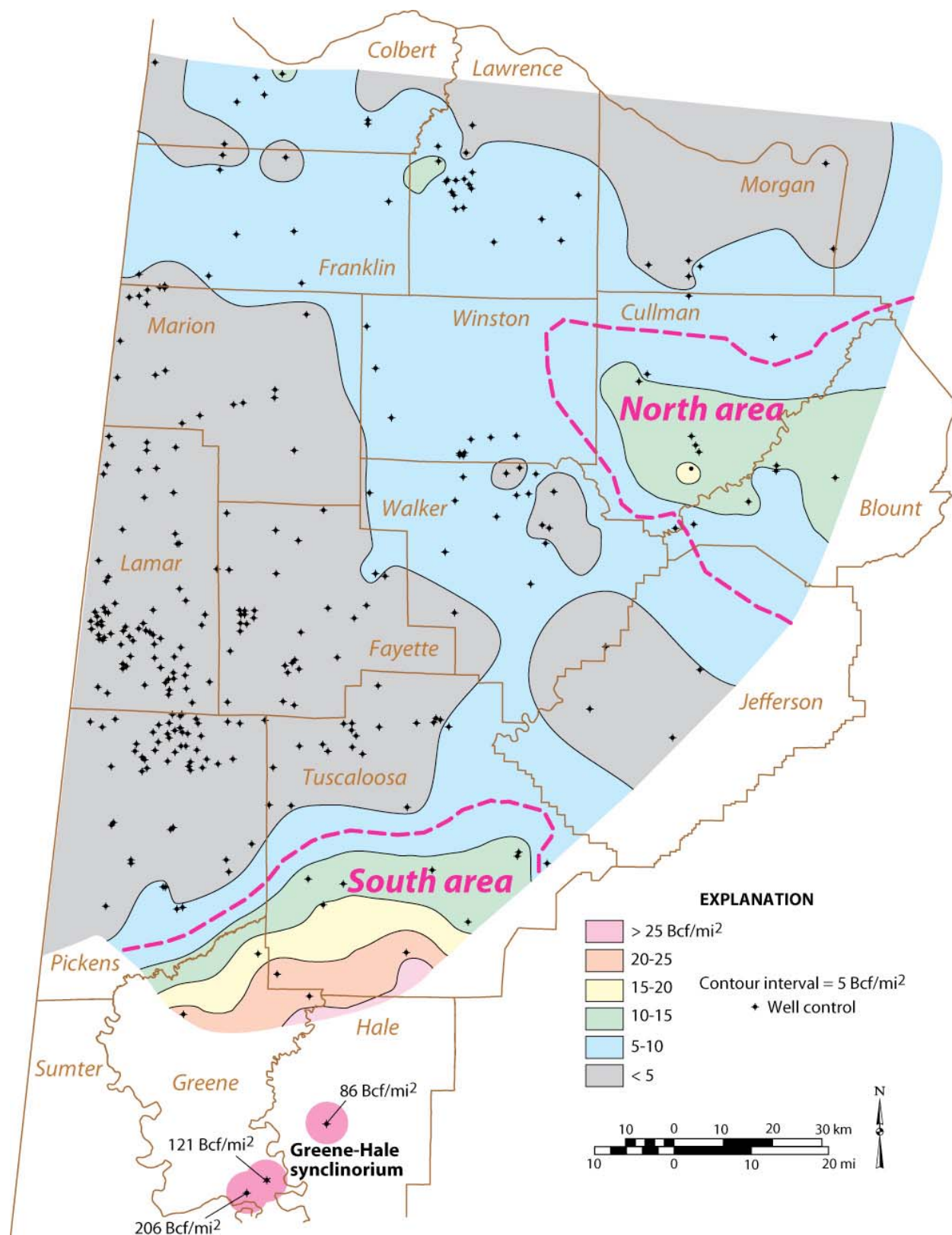


Figure 93.—Map of estimated original gas-in-place in the Chattanooga shale of the Black Warrior basin and the unnamed Silurian-Devonian shale of the Greene-Hale synclinorium.

synclinorium is projected to be at least 34 Tcf and may be much larger depending on the lateral extent of the synclinorium and the Silurian-Devonian black shale deposits contained therein.

The Neal shale extends throughout the southwestern part of the Black Warrior basin and potentially holds a natural gas resource greater than 100 Tcf in Alabama (table 18, fig. 94). Of this, about 38 Tcf is estimated to be stored as free gas, and more than 62 Tcf is estimated to be adsorbed. Gas concentrations are potentially greatest in the clinofom shale in the northern part of the study area, where the shale can support 50 to 80 Bcf/mi<sup>2</sup> (fig. 94). However, much of the shale in the northern part of the study area is submature with respect to major thermogenic gas generation (fig. 75). Accordingly, shale in the northern part of the map area may be undersaturated with gas and may thus have limited development potential. In the southern interest area, where reservoirs have adequate thermal maturity, estimated OGIP is generally between 20 and 60 Bcf/mi<sup>2</sup> (fig. 94). Here, the shale has estimated OGIP exceeding 48 Tcf, of which about 18 Tcf is stored as free gas and nearly 30 Tcf is stored as adsorbed gas (table 18).

The results of volumetric analysis indicate that OGIP in the Alabama shale gas formations is probably greater than 820 Tcf (table 18). Of this, a resource base of more than 695 Tcf is thought to have significant development potential. Estimating natural gas reserves in Alabama shale gas reservoirs is a difficult proposition because information on well performance is limited and because distinct technical challenges exist for drilling and completion in each formation (Pashin, 2008, 2009). Indeed, reserve estimation is difficult in the major shale plays that have already been developed because the response of wells to multiple stimulation treatments is highly variable, the long-term decline characteristics of producing wells has yet to be determined (Seidle, and O'Connor, 2011). The Energy Information Administration currently carries no

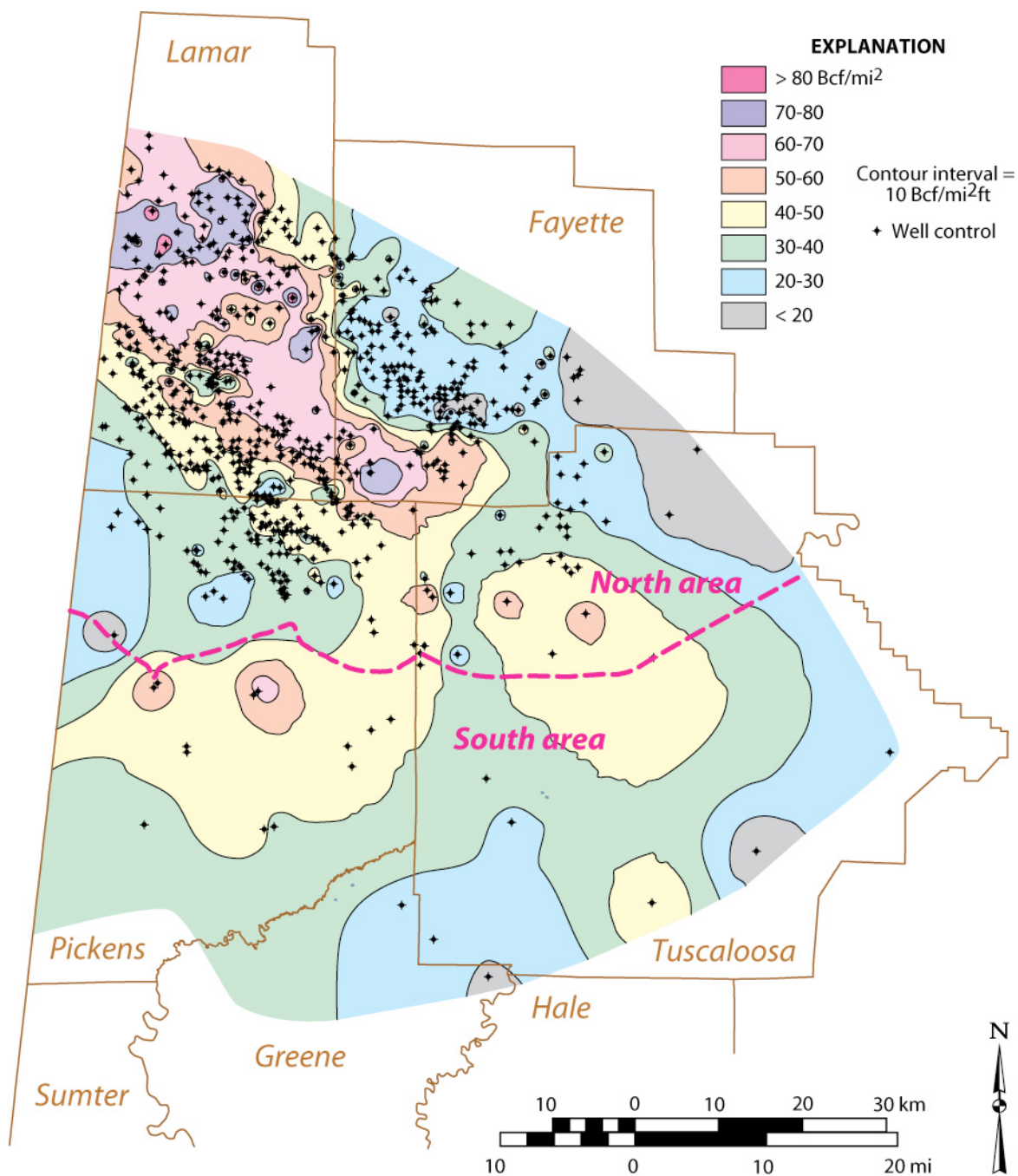


Figure 94.—Map of estimated original gas-in-place in the Neal shale of the Black Warrior basin.

proven shale gas reserves in Alabama and carried a maximum proven reserve estimate of only 2 Bcf in 2008. Alternatively, Geomet considers recoverable reserves within their 64,000-acre lease position in the Chattanooga Shale of Blount and Cullman Counties to be at least 1 Tcf (Haynes

and others, 2010). This estimate is consistent with the generalized 10 to 20 percent of OGIP values used to estimate technically recoverable gas in this study. The remainder of this discussion, then, focuses on these estimates and the implications for resource development.

The amount of gas that is technically recoverable from the Conasauga Formation is estimated to be between 62 and 125 Tcf in the Gadsden, Palmerdale, and Bessemer MUSHWADs (table 18), and additional gas may be recoverable from other areas in the Appalachian thrust belt and the Black Warrior basin. Therefore, Conasauga shale constitutes a giant target for resource development, although efforts to date have proven challenging because of well control and completion problems related to gas pressure and tectonic deformation. Volumetric analysis indicates that more than 80 percent of OGIP is stored in a free state, which indicates that the quantity of gas per unit volume of rock effectively increases linearly with depth. The sorbed gas resource is limited by low TOC content, and low Langmuir pressure relative to the other shale formations indicates reduced mobility of the sorbed gas fraction at elevated reservoir pressure. Hence, development efforts should perhaps focus on the free gas fraction, which has mobility at elevated pressure and is most highly concentrated in deep reservoirs. The key challenge for transforming the vast Conasauga resource base into reserves is learning how to produce from tectonically deformed shale masses. Moreover, additional information is needed on the prospectivity of the thick, gently deformed Conasauga shale that lies northwest of the Appalachian thrust belt.

Recoverable gas volumes in the Chattanooga Shale of the Black Warrior basin are estimated to be between 2.2 and 4.5 Tcf (table 18). Nearly 60 percent of OGIP is in an adsorbed state, and the mobility of the adsorbed fraction is much greater in the shallow, cool reservoirs of northern interest area than in the deep, warm reservoirs of the southern area. In the northern interest area,

where reservoirs sit in the steep part of the adsorption isotherm, it may be possible to produce from reservoirs that are undersaturated with gas, provided that hydrostatic pressure can be lowered below critical desorption pressure. Co-production of significant volumes of water in this area indicates that dewatering can facilitate production of the adsorbed fraction. In areas where large volumes of adsorbed gas can be mobilized, wells may behave similarly to coalbed methane wells, which commonly require long-term depressurization to achieve peak production rate and begin long-term exponential or hyperbolic decline. In the southern interest area, high gas pressure may be requisite for economic production, because deep, warm reservoir conditions favor the mobility of free gas. However, elevated Langmuir pressure in Devonian shale indicates that part of the sorbed gas fraction may remain mobile at elevated reservoir pressure. The same follows for the Silurian-Devonian shale of the Greene-Hale synclinorium, where recoverable gas volumes may be between 3.4 to 6.9 Tcf.

In the Neal shale, the amount of recoverable gas may be 10 to 20 Tcf. Development potential is highest in the southern interest area, where recoverable gas is estimated to be between 4.8 and 9.6 Tcf. The ratio of free to sorbed gas is similar to that in Devonian shale, and so many of the observations put forth for the Devonian also apply to the Neal. Production efforts in the Neal shale have to date been unsuccessful. All wells have been sited near older exploration wells that were drilled into structural highs along faults. Chances of success may be greater if exploration efforts focus on the interiors of large fault blocks, where leakoff of fracturing fluid into natural fracture networks can be better controlled (Bowker, 2007; Pashin, 2008, 2009). Another caveat in developing Neal reservoirs is a general lack of gas shows in existing wells, which may indicate undersaturation. However, exploration of deep Neal shale in structural lows has yet to

take place, yet it is in these areas where prospects for saturated reservoirs with structural continuity may be greatest.

The total amount of gas that may be recoverable from Alabama shale reservoirs is estimated to be between 82 and 164 Tcf, and all formations analyzed during this investigation have significant potential for development. The areas that are considered to have high potential for development may contain 70 to 139 Tcf of technically recoverable gas. However, all prospective formations face challenges that must be confronted so that economic development can take place. In the Conasauga Formation and the Silurian-Devonian shale of the Appalachian thrust belt, the technological frontier lies in achieving economic production from faulted and folded shale masses, where existing fracture networks may act as thief zones for stimulation fluid. In the Chattanooga Shale, the principal challenge is in developing reservoirs with limited pay thickness in what has proven to be a challenging economic climate. In the Neal shale, keys to success appear to include verifying the amount of gas-in-place and developing coherent structural panels between major faults. Reservoir volumetrics indicate that the Alabama shale formations represent large objectives for shale gas exploration, and meeting the challenges posed by these formations can add greatly to domestic natural gas reserves.

## **SUMMARY AND CONCLUSIONS**

Shale gas reservoirs in the Black Warrior basin and Appalachian thrust belt are diverse, occurring in Cambrian, Silurian, Devonian, and Mississippian strata. Development in this area has been affected by uncertainty about best practices for reservoir evaluation, exploration, and completion. Indeed, an integrated, multidisciplinary approach is required to evaluate shale and is the focus of this study. Key geologic variables to be considered when exploring shale reservoirs,

are stratigraphy, sedimentation, structure, hydrodynamics, geothermics, petrology, geochemistry, gas storage, and permeability.

Many characteristics of shale gas reservoirs are determined in the original depositional environment, thus stratigraphy and sedimentation are critical variables. Shale gas reservoirs in Alabama were deposited on the North American craton as organic-rich mud in euxinic sedimentary basins. These basins formed in extensional and compressional tectonic settings contemporaneously with Iapetan rifting and Appalachian-Ouachita foreland basin development. Processes within the euxinic basins were varied and were influenced by the development of coeval carbonate ramps and siliciclastic coastal plains and shelves. In all formations studied, black shale deposition was highly dynamic, reflecting changing redox conditions, variable sediment and nutrient flux, and reworking by storms. The result of these processes was a complex stratigraphic architecture that gave rise to heterogeneous facies and reservoir quality.

Geologic structure affects the geometry, continuity, and permeability of shale gas reservoirs. Extensional faults are common in the Black Warrior basin and reflect a multiphase tectonic development that spanned Paleozoic time. The faults are developed above multiple detachments, including a thick-skinned, mid-crustal detachment and thin-skinned detachments at the top of the Cambrian shale section, and within the Carboniferous synorogenic clastic wedge. These faults pose significant risk for leakoff of stimulation fluid during well completion, so careful mapping is required to define coherent structural panels favorable for shale gas development. Thrust belt structures in Alabama include giant antiformal stacks in Cambrian Conasauga shale and ramp-flat structure in younger strata. Structural deformation in the antiformal stack has resulted in shale accumulations thicker than 12,000 feet but poses challenges for drilling and completion. Fold hinges in ramp-flat structures may be associated with productivity sweet spots, but can also

be sources of co-produced water that must be managed responsibly. Fracture networks, including joints and shear zones, are common in the shale gas reservoirs and appear to form important hydraulic conduits in shallow shale reservoirs. Fractures in deep reservoirs are cemented, and petrologic analysis indicates that the fractures have hosted fluids that have alternated between alkaline and acidic and included carbonate scavenged by dissolution of older sediment and rock. Major shear zones can be associated with significant gas shows, but caution should be applied because of the potential for leakoff of stimulation fluid.

Hydrodynamics and geothermics are strong determinants of shale reservoir characteristics. Fluid chemistry and reservoir pressure are influenced strongly by recharge along the Appalachian frontal structures. Significant gas pressure, by contrast, exists in the deep parts of the Black Warrior basin and the Appalachian thrust belt and resulted in a blowout in the Conasauga shale. Modern reservoir temperatures are related to the depth of target formations, and geothermal gradients in the region are generally between 9 and 15°F per thousand feet. Shallow shale reservoirs in the frontal Appalachians can be classified as shallow, cool reservoirs, whereas those in the deep subsurface are substantially warmer and thus have different gas reservoir properties. Petrologic evidence indicates that the shale reservoirs were substantially warmer in the geologic past than they are today, and burial history modeling indicates that major thermogenic gas generation was associated with synorogenic tectonic subsidence during Carboniferous and Permian time.

Petrology and geochemistry are critical determinants of reservoir quality. Detrital minerals are dominated by clay, quartz, and carbonate. Authigenic minerals include pyrite, calcite, dolomite, silica, and illite. SEM analysis was used to evaluate shale fabric, which represents a network of detrital minerals, authigenic minerals, organic matter, and porosity. As such, the rock

fabric is the product of sedimentation, compaction, diagenesis, and hydrocarbon generation. Weak alignment of platy clay minerals in Cambrian shale appears to reflect overpressuring related to formation of the giant antiformal stacks. Devonian shale is distinctive because it contains biogenic silica formed by radiolarians and sponges that may help contribute to the brittleness of the shale and may thus facilitate effective hydraulic fracture treatments. Organic matter in the shale gas reservoirs is dominated by matrix bituminite and includes minor amounts of vitrinite, sporinite, and inertinite. Most of the prospective reservoirs can be classified as type III to type IV source rocks. Geochemical evidence points toward an evolution from sapropelic source material toward thermally mature kerogen that has exhausted most if not all of its generative potential. Although the generative potential is largely exhausted, the shale is capable of storing large volumes of natural gas.

Shale is a dual-porosity reservoir in which some gas is stored in a free state, and some is adsorbed on organic matter and minerals with high surface area. Effective porosity in Alabama gas shale is between 1.2 and 7.7 percent, and about 68 percent of the pore volume is capable of free gas storage. Pressure-decay permeability averages  $0.191 \mu\text{D}$  and is locally as high as  $0.393 \mu\text{D}$ . Adsorption isotherms indicate that Langmuir volume is as high as 128 scf/t, and adsorption capacity correlates directly with TOC content. Langmuir pressure in the Paleozoic shale units is between 526 and 1,012 psia, which indicates significant sorbed gas mobility at elevated initial reservoir pressure. Free gas is mobile across a spectrum of pressure-temperature conditions. Sorbed gas, by contrast, has greatest mobility at low reservoir pressure, where the isotherm is steep. In addition, the adsorption capacity of organic matter decreases as reservoir temperature increases. Therefore, the adsorbed gas fraction is most mobile in shallow, cool geologic settings, which are common in the frontal Appalachians. OGIP in the Alabama shale formations is

estimated to be about 826 Tcf. Technically recoverable resources in areas with significant development potential are estimated to be between 70 and 139 Tcf. Hence, the prospective shale formations contain enough natural gas to have a major impact on domestic gas reserves.

Important technical hurdles that must be overcome to bring these resources to market include the development of completion technologies for giant, tectonically deformed shale masses, as well as development strategies for thin shale formations.

### **ACKNOWLEDGMENTS**

Funding for this project is provided by RPSEA through the “Ultra-Deepwater and Unconventional Natural Gas and Other Petroleum Resources” program authorized by the U.S. Energy Policy Act of 2005. RPSEA (<http://www.rpsea.org>) is a nonprofit corporation whose mission is to provide a stewardship role in ensuring the focused research, development and deployment of safe and environmentally responsible technology that can effectively deliver hydrocarbons from domestic resources to the citizens of the United States. RPSEA, operating as a consortium of premier U.S. energy research universities, industry, and independent research organizations, manages the program under a contract with the U.S. Department of Energy’s National Energy Technology Laboratory.

The project team at the Geological Survey of Alabama would like to thank Keith Greaves of Terra Tek, who ran adsorption isotherms and determined basic reservoir properties of core samples. We would also like to thank Albert Maende of Weatherford Laboratories for donating analyses of Conasauga shale to this project. Discussions with Marc Bustin, Andrew Goodliffe, Rick Groshong, Delores Robinson, and Bill Thomas were invaluable for characterizing the regional geologic framework and interpreting basic reservoir data. Publications and other

materials related to this project can be downloaded from the web site of the Geological Survey of Alabama at <http://www.gsa.state.al.us/gsa/shalegas.html>.

### REFERENCES CITED

- Aigner, T., 1985, Storm depositional systems: Berlin, Springer-Verlag, Lecture Notes in Earth Sciences, v. 3, 174 p.
- Astini, R. A., Thomas, W. A., and Osborne, W. E., 2000, Sedimentology of the Conasauga Formation and equivalent units, Appalachian thrust belt in Alabama, *in* Osborne, W. E., Thomas, W. A., and Astini, R. A., eds., The Conasauga Formation and equivalent units in the Appalachian thrust belt in Alabama: Tuscaloosa, Alabama Geological Society 31st Annual Field Trip Guidebook, p. 41-71.
- Ayers, W. B., Jr., and Kaiser, W. A., eds., 1994, Coalbed methane in the Upper Cretaceous Fruitland Formation, San Juan Basin, Colorado and New Mexico: Texas Bureau of Economic Geology Report of Investigations 218, 216 p.
- Bailey, R. M., 2007, Seismic interpretation and structural restoration of a seismic profile through the southern Appalachian thrust belt under Gulf Coastal Plain sediments: Tuscaloosa, University of Alabama, unpublished Master's thesis, 71 p.
- Bowker, K. A., 2007, Barnett Shale gas production, Fort Worth basin: Issues and Discussion: American Association of Petroleum Geologists Bulletin, v. 91, p. 525-533.
- Burchard, B., and Lewan, M. D., 1990, Reflectance of vitrinite-like macerals as a thermal maturity index for Cambrian-Ordovician Alum Shale, southern Scandinavia: American Association of Petroleum Geologists Bulletin, v. 74, p. 394-406.
- Butts, Charles, 1910, Description of the Birmingham Quadrangle, Alabama: U.S. Geological Survey Geologic Atlas, Folio 175, 24 p.
- \_\_\_\_\_, 1926, The Paleozoic rocks, *in* Adams, G. I., Butts, Charles, Stephenson, L. W., and Cooke, C. W., Geology of Alabama: Alabama Geological Survey Special Report 14, p. 40-230.
- \_\_\_\_\_, 1927, Bessemer-Vandiver folio: U.S. Geological Survey Geologic Atlas, Folio 221, 22 p.
- Carroll, R. E., Pashin, J. C., and Kugler, R. L., 1995, Burial history and source-rock characteristics of Upper Devonian through Pennsylvanian strata, Black Warrior basin, Alabama: Alabama Geological Survey Circular 187, 29 p.
- Cates, L. M., and Groshong, R. H., Jr., 1999, Confirmation of regional thin-skinned extension in the eastern Black Warrior Basin, Alabama, *in* Pashin, J. C. and Carroll, R. E., eds., Geology of the Cahaba coalfield: Alabama Geological Society 36th Annual Field Trip Guidebook, p. 49-57.
- Cleaves, A. W., 1983, Carboniferous terrigenous clastic facies, hydrocarbon producing zones, and sandstone provenance, northern shelf of Black Warrior basin: Gulf Coast Association of Geological Societies Transactions, v. 33, p. 41-53.

- Cleaves, A. W., and Broussard, M. C., 1980, Chester and Pottsville depositional systems, outcrop and subsurface, in the Black Warrior basin of Mississippi and Alabama: Gulf Coast Association of Geological Societies Transactions, v. 30, p. 49-60.
- Conant, L. C., and Swanson, V. E., 1961, Chattanooga Shale and related rocks of central Tennessee and nearby areas: U.S. Geological Survey Professional Paper 357, 91 p.
- Cook, B. S., and Thomas, W. A., 2010, Ductile duplexes as potential natural gas plays: an example from the Appalachian thrust belt in Georgia, USA: Geological Society of London Special Publication 348, p. 57-70.
- Debajyoti, P. and Skrzypek, G., 2007, Assessment of carbonate-phosphoric acid analytical technique performed using GasBench II in continuous flow isotope ratio mass spectrometry: International Journal of Mass Spectrometry, v. 262, p. 180-186.
- Engelder, T., Lash, G. G., and Uzcátegui, R. S., 2009, Joint sets that enhanced production from Middle and Upper Devonian gas shales of the Appalachian basin: American Association of Petroleum Geologists Bulletin, v. 95, p. 857-889.
- Engelder, T., and Whitaker, A., 2006, Early jointing in coal and black shale: Evidence for an Appalachian-wide stress field as a prelude to the Alleghanian orogen: *Geology*, v. 34, p. 581-584.
- Espitalié, J., Laporte, J. L., Madec, M., Marquis, F., Leplat, P., Paulet, J., and Boutefeu, A., 1977, Methode rapide de caracterisation des roches mares, et de leur potentiel petrolier et de leur degre d'evolution: *Revue de l'Institut Francais du Petrole*, v. 32, p. 23-42.
- Ettensohn, F. R., 1985, Controls on the development of Catskill Delta complex basin-facies: Geological Society of America Special Paper 201, p. 65-77.
- Ettensohn, F. R., Miller, M. L., Dillman, S. B., Elam, T. D., Geller, K. L., Swager, D. R., Markowitz, G., Woock, R. D., and Barron, L. S., 1988, Characterization and implications of the Devonian-Mississippian black shale sequence, eastern and central Kentucky, U.S.A.: pycnoclines, transgression, regression, and tectonism, in McMillan, N. J., Embry, A. F., and Glass, D. J., eds., *Devonian of the World, Proceedings of the Second International Symposium on the Devonian System*: Canadian Society of Petroleum Geologists Memoir 14, v. 2, p. 323-345.
- Farrell, S. G., and Eaton, S., 1987, Slump strain in the Tertiary of Cyprus and the Spanish Pyrenees: definition of palaeoslopes and soft-sediment deformation, in Jones, M. E., and Preston, R. M. F., eds., *Deformation of Sediments and Sedimentary Rocks*: London Geological Society Special Publication 29, p. 181-196.
- Fortey, R. A. and Theron, J., 1994, A new Ordovician arthropod *Soomaspis* and the agnostid problem: *Palaeontology*, v. 37, p. 841-61.
- Friedman, I., and O'Neil, J. R., 1977, Compilation of stable isotope fractionation factors of geochemical interest, in Fleischer, M., ed., *Data of Geochemistry*, 6th ed.: U.S. Geological Survey Professional Paper 440-KK, 12 p.
- Gale, J. F. W., Reed, R. M., and Holder, John, 2007, Natural fractures in the Barnett Shale and their importance for hydraulic fracture treatments: American Association of Petroleum Geologists Bulletin, v. 91, p. 603-622.

- Gasem, K. A. M., Pan, Z., Mohammad, S., and Robinson, R. L., Jr., 2009, Two-dimensional equation of state modeling of adsorbed coalbed methane gases: *American Association of Petroleum Geologists Studies in Geology* 59, p. 475-497.
- Gates, M. G., 2006, Structure of the Wills Valley anticline in the vicinity of Mentone, Alabama: Tuscaloosa, University of Alabama, unpublished Master's thesis, 46 p.
- Groshong, R. H., Jr., 2005, Listric-thrust kinematic model for thin-skinned, highly asymmetric, Wills Valley anticline, southern Appalachians: *Geological Society of America Abstracts with Programs*, v. 37, no. 7, p. 234.
- \_\_\_\_\_, 2006, 3-D structural geology—A practical guide to quantitative surface and subsurface map interpretation: New York, Springer, 400 p.
- Groshong, R. H., Jr., Hawkins, W. B., Jr., Pashin, J. C., and Harry, D. L., 2010, Extensional structures of the Alabama promontory and Black Warrior foreland basin: Styles and relationship to the Appalachian fold-thrust belt, *in* Tollo, R.P., Bartholomew, M.J., Hibbard, J.P., and Karabinos, P.M., eds., *From Rodinia to Pangea: Geological Society of America Memoir* 206, p. 579-605.
- Groshong, R. H., Jr., Pashin, J. C., McIntyre, M. R., 2009, Structural controls on fractured coal reservoirs in the southern Appalachian Black Warrior foreland basin: *Journal of Structural Geology*, v. 31, p. 874-886, doi:10.1016/j.jsg.2008.02.017.
- Haynes, C. D., Malone, P. G., and Camp, B. S., 2010, Exploration of the shallow Chattanooga Shale in north central Alabama: Tuscaloosa, Alabama, University of Alabama, College of Continuing Studies, 2010 International Coalbed & Shale Gas Symposium Proceedings, paper 1015, 16 p.
- Heckel, P. H. and Witzke, B. J., 1979, Devonian world palaeogeography determined from distribution of carbonates and related lithic palaeoclimatic indicators, *in* House, M. R., Scrutton, C. T. and Bassett, M. G., eds., *The Devonian System: A Palaeontological Association International Symposium; Special Papers in Palaeontology* 23, p. 99-123.
- Hill, R. J., and Jarvie, D. M., eds., 2007, Barnett Shale: *American Association of Petroleum Geologists Bulletin*, v. 91, p. 399-622.
- Hunt, J. M., 1979, *Petroleum geochemistry and geology*: San Francisco, Freeman, 617 p.
- Kidd, J. T., 1975, Pre-Mississippian stratigraphy of the Warrior Basin: *Gulf Coast Association of Geological Societies Transactions*, v. 25, p. 20-39.
- Kuuskraa, V. A., Wicks, D. E., and Thurber, J. L., 1992, Geologic and reservoir mechanisms controlling gas recovery from the Antrim Shale: *Society of Petroleum Engineers, Annual Technical Conference and Exhibition, SPE Paper* 24883, p. 209-224.
- Kvale, E. P., Archer, A. W., and Johnson, H. R., 1989, Daily, monthly, and yearly tidal cycles within laminated siltstones of the Mansfield Formation (Pennsylvanian) of Indiana: *Geology*, v. 17, p.365–368.
- Laubach, S. E., Marrett, R. A., Olson, J. E., and Scott, A. R., 1998, Characteristics and origins of coal cleat: A review: *International Journal of Coal Geology*, v. 35, p. 175-207.

- Laubach, S. E., Reed, R. M., Olson, J. E., Lander, R. H., and Bonnell, L. M., 2004, Coevolution of crack-seal texture and fracture porosity in sedimentary rocks: cathodoluminescence observations of regional fractures: *Journal of Structural Geology*, v. 26, p. 967-982.
- Lorant, F., Prinzhover, A., Behar, F., and Huc, A. Y., 1998, Carbon isotopic and molecular constraints on the formation and the expulsion of thermogenic hydrocarbon gases: *Chemical Geology*, v. 147, p. 249-264.
- Maher, C. A., 2002, Structural deformation of the southern Appalachians in the vicinity of the Wills Valley anticline, northeast Alabama: Tuscaloosa, University of Alabama, unpublished Master's thesis, 45 p.
- Markello, J. R., and Read, J. F., 1981, Carbonate ramp to deeper shelf transitions of an Upper Cambrian intrabasin shelf, Nolichucky Formation, southwest Virginia Appalachians: *Sedimentology*, v. 28, p. 573-597.
- \_\_\_\_\_, 1982, Upper Cambrian intrashelf basin, Nolichucky Formation, southwest Virginia Appalachians: *American Association of Petroleum Geologists Bulletin*, v. 28, p. 860-878.
- Mars, J. C., and Thomas, W. A., 1999, Sequential filling of a late Paleozoic foreland basin: *Journal of Sedimentary Research*, v. 69, p. 1191-1208.
- Martin, J. P., 2009, Marcellus Shale natural gas: the resources: New York State Energy Research and Development Authority, unpublished PDF of PowerPoint presentation, 19 p.
- Martini, A. M., Walter, L. M., Budai, J. M., Ku, T. C. W., Kaiser, C. J., and Schoell, M., 1998, Genetic and temporal relations between formation waters and biogenic methane: Upper Devonian Antrim Shale, Michigan basin, USA: *Geochimica et Cosmochimica Acta*, v. 62, p. 1699-1720.
- Martini, A. M., Walter, L. M., and McIntosh, J. C., 2008, Identification of microbial and thermogenic gas components from Upper Devonian black shale cores, Illinois and Michigan basins: *American Association of Petroleum Geologists Bulletin*, v. 92, p. 327-339.
- Mittenthal, M. D., and Harry, D. L., 2004, Seismic interpretation and structural validation of the southern Appalachian fold and thrust belt, northwest Georgia: *Georgia Geological Guidebook*, v. 42, p. 1-12.
- Montgomery, S. L., Jarvie, D. M., Bowker, K. A., and Pollastro, R. M., 2005, Mississippian Barnett Shale, Fort Worth Basin, north-central Texas: Gas shale play with multi-trillion cubic foot potential: *American Association of Petroleum Geologists Bulletin*, v. 89, p. 155-175.
- Muller, K. J., and Walossek D., 1987, Morphology, ontogeny and life habit of *Agnostus pisiformis* from the Upper Cambrian of Sweden: *Fossils and Strata*, v. 19, p. 1-124.
- National Energy Technology Laboratory, 2002, U.S. National Brine Wells Database: U.S. Department of Energy, National Energy Technology Laboratory, unpaginated CD-ROM.
- Nelson, P. H., 2009, Pore-throat sizes in sandstones, tight sandstones, and shales: *American Association of Petroleum Geologists Bulletin*, v. 93, p. 329-340.
- Nuttall, B. C., Drahovzal, J. A., Eble, C. F., and Bustin, R. M., 2009, Regional assessment of organic-rich gas shales for carbon sequestration: an example from the Devonian shales of the

- Illinois and Appalachian basins, Kentucky: American Association of Petroleum Geologists Studies in Geology 59, p. 173-190.
- Olson, J. E., Laubach, S. E., and Lander, R. H., 2009, Natural fracture characterization in tight gas sandstones: integrating mechanics and diagenesis: AAPG Bulletin, v. 93, p. 1535-1549.
- Ortiz, I., Weller, T. F., Anthony, R. V., Frank, J., Linz, D., and Nakles, D., 1993, Disposal of produced waters: Underground injection option in the Black Warrior Basin, 1993 International Coalbed Methane Symposium Proceedings, p. 339-364.
- Osborne, W. E., Thomas, W. A., Astini, R. A., and Irvin, G. D., 2000, Stratigraphy of the Conasauga Formation and equivalent units, Appalachian thrust belt in Alabama, *in* Osborne, W. E., Thomas, W. A., and Astini, R. A., eds., The Conasauga Formation and equivalent units in the Appalachian thrust belt in Alabama: Tuscaloosa, Alabama Geological Society 31st Annual Field Trip Guidebook, p. 1-17.
- Pashin, J. C., 1993, Tectonics, paleoceanography, and paleoclimate of the Kaskaskia sequence in the Black Warrior basin of Alabama, *in* Pashin, J. C., ed., New Perspectives on the Mississippian System of Alabama: Alabama Geological Society 30th Annual Field Trip Guidebook, p. 1-28.
- \_\_\_\_\_, 1994a, Cycles and stacking patterns in Carboniferous rocks of the Black Warrior foreland basin: Gulf Coast Association of Geological Societies Transactions, v. 44, p. 555-563.
- \_\_\_\_\_, 1994b, Flexurally influenced eustatic cycles in the Pottsville Formation (Lower Pennsylvanian), Black Warrior basin, Alabama, *in* Dennison, J. M., and Ettensohn, F. R. eds., Tectonic and Eustatic Controls on Sedimentary Cycles: Society of Economic Paleontologists and Mineralogists Concepts in Sedimentology and Paleontology, v. 4, p. 89-105.
- \_\_\_\_\_, 1998, Stratigraphy and structure of coalbed methane reservoirs in the United States: an overview: International Journal of Coal Geology, v. 35, p. 207-238.
- \_\_\_\_\_, 2004, Cyclothems of the Black Warrior basin in Alabama: eustatic snapshots of foreland basin tectonism, *in* Pashin, J. C., and Gastaldo, R. A., eds., Sequence stratigraphy, paleoclimate, and tectonics of coal-bearing strata: American Association of Petroleum Geologists Studies in Geology 51, p. 199-217.
- \_\_\_\_\_, 2005, Coalbed methane exploration in thrust belts: experience from the southern Appalachians, USA: Tuscaloosa, Alabama, University of Alabama, College of Continuing Studies, 2005 International Coalbed Methane Symposium Proceedings, paper 0519, 14 p.
- \_\_\_\_\_, 2007, Hydrodynamics of coalbed methane reservoirs in the Black Warrior Basin: key to understanding reservoir performance and environmental issues: Applied Geochemistry, v. 22, p. 2257-2272.
- \_\_\_\_\_, 2008, Gas shale potential of Alabama: Tuscaloosa, Alabama, University of Alabama, College of Continuing Studies, 2008 International Coalbed & Shale Gas Symposium Proceedings, paper 0808, 13 p.
- \_\_\_\_\_, 2009, Shale gas plays of the southern Appalachian thrust belt: Tuscaloosa, Alabama, University of Alabama, College of Continuing Studies, 2009 International Coalbed & Shale Gas Symposium Proceedings, paper 0907, 14 p.

- \_\_\_\_ 2010a, Mature coalbed natural gas reservoirs and operations in the Black Warrior basin of Alabama, *in* Reddy, K. J., ed., *Coalbed Natural Gas: Energy and Environment*: Haupage, New York, Nova Science Publishers.
- \_\_\_\_ 2010b, Variable gas saturation in coalbed methane reservoirs of the Black Warrior basin: implications for exploration and production: *International Journal of Coal Geology*, v. 82, p. 135-146, doi:10.1016/j.coal.2009.10.017.
- Pashin, J. C., Carroll, R. E., McIntyre, M. R., and Grace, R. L. B., 2010, Geology of unconventional gas plays in the southern Appalachian thrust belt: Society for Sedimentary Geology (SEPM) Guidebook, Field Trip 7, American Association of Petroleum Geologists Annual Conference and Exposition, New Orleans, Louisiana, 86 p.
- Pashin, J. C., and Ettensohn, F. R., 1992, Paleogeology and sedimentology of the dysaerobic Bedford fauna (Late Devonian), Ohio and Kentucky (USA): *Palaeogeography, Palaeoclimatology, and Palaeoecology*, v. 91, p. 21-34.
- Pashin, J. C., and Ettensohn, F. R., 1995, Reevaluation of the Bedford-Berea sequence in Ohio and adjacent states: forced regression in a foreland basin: *Geological Society of America Special Paper 298*, 68 p.
- Pashin, J. C., Grace, R. L. B., and Kopaska-Merkel, D. C., 2010, Devonian shale plays in the Black Warrior basin and Appalachian thrust belt of Alabama: Tuscaloosa, Alabama, University of Alabama, College of Continuing Studies, 2010 International Coalbed & Shale Gas Symposium Proceedings, paper 1016, 20 p.
- Pashin, J. C., and Groshong, R. H., Jr., 1998, Structural control of coalbed methane production in Alabama: *International Journal of Coal Geology*, v. 38, p. 89-113.
- Pashin, J. C., and Hinkle, Frank, 1997, Coalbed methane in Alabama: Alabama Geological Survey Circular 192, 71 p.
- Pashin, J. C., and Kugler, R. L., 1992, Delta-destructive spit complex in Black Warrior basin: facies heterogeneity in Carter sandstone (Chesterian), North Blowhorn Creek oil unit, Lamar County, Alabama: *Gulf Coast Association of Geological Societies Transactions*, v. 42, p. 305-325.
- Pashin, J. C., and McIntyre, M. R., 2003, Temperature-pressure conditions in coalbed methane reservoirs of the Black Warrior basin, Alabama, U.S.A: implications for carbon sequestration and enhanced coalbed methane recovery: *International Journal of Coal Geology*, v. 54, p. 167-183.
- Pashin, J. C., and Payton, J. W., 2005, Geological sinks for carbon sequestration in Alabama, Mississippi, and the Florida panhandle: Alabama Geological Survey, Final Report to Southern States Energy Board, Subgrant SSEB-NT41980-997-GSA-2004-00, unpaginated CD-ROM.
- Pashin, J. C., Ward, W. E., II, Winston, R. B., Chandler, R. V., Bolin, D. E., Richter, K. E., Osborne, W. E., and Sarnecki, J. C., 1991, Regional analysis of the Black Creek-Cobb coalbed-methane target interval, Black Warrior basin, Alabama: Alabama Geological Survey Bulletin 145, 127 p.

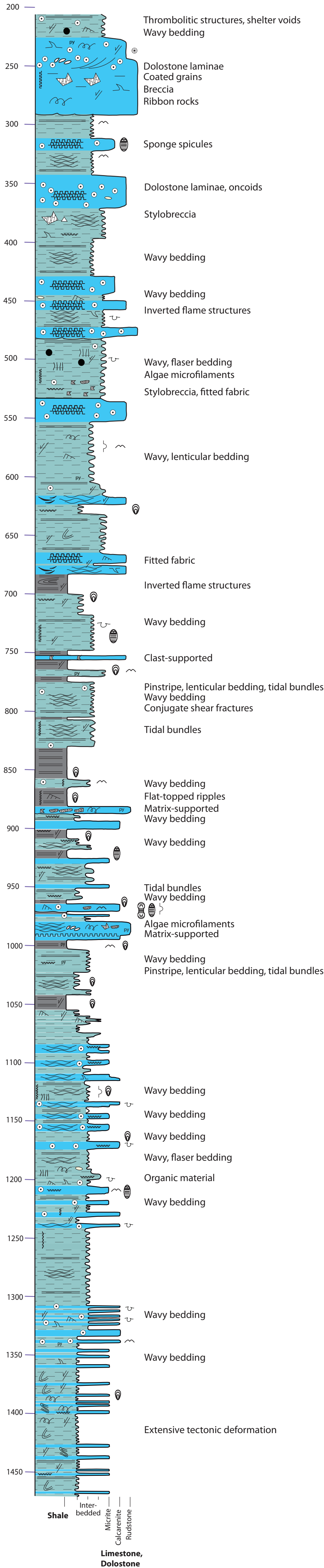
- Pitman, J. K., Pashin, J. C., Hatch, J. R., and Goldhaber, M. B., 2003, Origin of minerals in joint and cleat systems of the Pottsville Formation, Black Warrior basin, Alabama: implications for coalbed methane generation and production: *American Association of Petroleum Geologists Bulletin*, v. 87, p. 713-731.
- Rheams, K. F., and Neathery, T. L., 1988, Characterization and geochemistry of Devonian oil shale, north Alabama, northwest Georgia, and south-central Tennessee (a resource evaluation): *Alabama Geological Survey Bulletin* 128, 214 p.
- Rich, J. L., 1951, Three critical environments of deposition and criteria for recognition of rocks deposited in each of them: *Geological Society of America Bulletin*, v. 62, p. 1-20.
- Rodgers, John, 1950, Mechanics of Appalachian folding as illustrated by the Sequatchie anticline, Tennessee and Alabama: *American Association of Petroleum Geologists Bulletin*, v. 34, p. 672-681.
- Ross, D. J. K., and Bustin, R. M., 2008, Characterizing the shale gas resource potential of Devonian-Mississippian strata in the Western Canada sedimentary basin: Application of an integrated formation evaluation: *American Association of Petroleum Geologists Bulletin*, v. 92, p. 87-125.
- Sawlowicz, Z., 1993, Pyrite framboids and their development: a new conceptual mechanism: *Geologische Rundschau*. v. 82, p. 148-156.
- Schieber, J., 1994, Evidence for episodic high energy events and shallow water deposition in the Chattanooga Shale, Devonian, central Tennessee, U.S.A.: *Sedimentary Geology*, v. 93, p. 193-208.
- \_\_\_\_\_, 2011, Marcasite in black shales—a mineral proxy for oxygenated bottom waters and intermittent oxidation of carbonaceous muds: *Journal of Sedimentary Research* v. 81, p. 447-458.
- Schieber, J., Zimmerle, W., and Sethi, P. S., 1998, *Shales and Mudstones*, Vols. I and II: Stuttgart, Germany, E. Schweizerbart Verlagsbuchhandlung, 680 p.
- Scott, A. R., 2002, Hydrogeologic factors affecting gas content distribution in coal beds: *International Journal of Coal Geology*, v. 50, p. 363-387.
- Seidle, John, and O'Connor, Leslie, 2011, Well performance & economics of selected U.S. shales: Amelia Island, Florida, Society of Petroleum Evaluation Engineers Annual Meeting Proceedings, 31 p.
- Soeder, D. J., 1988, Porosity and permeability of eastern Devonian gas shale: *SPE Formation Evaluation*, March 1988, p. 116-124.
- SPEE, in press, Guidelines for the practical evaluation of undeveloped reserves in resource plays: *Society of Petroleum Evaluation Engineers Monograph* 3.
- Telle, W. R., Thompson, D. A., Lottman, L. K., and Malone, P. G., 1987, Preliminary burial-thermal history investigations of the Black Warrior basin: implications for coalbed methane and conventional hydrocarbon development: Tuscaloosa, Alabama, University of Alabama, 1987 Coalbed Methane Symposium Proceedings, p. 37-50.

- Thomas, W. A., 1972, Mississippian stratigraphy of Alabama: Alabama Geological Survey Monograph 12, 121 p.
- \_\_\_\_\_, 1977, Evolution of Appalachian-Ouachita salients and recesses from reentrants and promontories in the continental margin: *American Journal of Science*, v. 277, p. 1233-1278.
- \_\_\_\_\_, 1985, Northern Alabama sections, in Woodward, N. B., ed., Valley and Ridge thrust belt: balanced structural sections, Pennsylvania to Alabama: University of Tennessee Department of Geological Sciences Studies in Geology 12, p. 54-60.
- \_\_\_\_\_, 1988, The Black Warrior basin, in Sloss, L. L., ed., Sedimentary cover—North American craton: Geological Society of America, *The Geology of North America*, v. D-2, p. 471-492.
- \_\_\_\_\_, 2001, Mushwad: Ductile duplex in the Appalachian thrust belt in Alabama: *American Association of Petroleum Geologists Bulletin*, v. 85, p. 1847-1869.
- Thomas, W. A., Astini, R. A., Osborne, W. E., and Bayona, G., 2000, Tectonic framework of deposition of the Conasauga Formation, in Osborne, W. E., Thomas, W. A., and Astini, R. A., eds., *The Conasauga Formation and equivalent units in the Appalachian thrust belt in Alabama*: Tuscaloosa, Alabama Geological Society 31st Annual Field Trip Guidebook, p. 19-40.
- Thomas, W. A., and Bayona, G., 2005, The Appalachian thrust belt in Alabama and Georgia: thrust-belt structure, basement structure, and palinspastic reconstruction: *Alabama Geological Survey Monograph 16*, 48 p.
- Thomas, W. A., and Mack, G. H., 1982, Paleogeographic relationship of a Mississippian barrier-island and shelf-bar system (Hartselle Sandstone) in Alabama to the Appalachian-Ouachita orogenic belt: *Geological Society of America Bulletin*, v. 93, p. 6-19.
- Whiticar, M. J., 1994, Correlation of natural gases with their sources: *American Association of Petroleum Geologists Memoir 60*, p. 261-283.
- Wignall, P. B., and Newton, R., 1998, Pyrite framboid diameter as a measure of oxygen deficiency in ancient mudrocks: *American Journal of Science*, v. 298, p. 537-552.
- Wilkin, R. T., and Barnes, H. L., 1997, Pyrite formation in an anoxic estuarine basin: *American Journal of Science*, v. 297, p. 620-650.
- Williams, Peggy, 2007, Conasauga Saga: Oil and Gas Investor, September 6, 2007, unpaginated PDF document.
- Yang, R. T., and Saunders, J. T., 1985, Adsorption of gases on coals and heat-treated coals at elevated temperature and pressure: *Fuel*, v. 64, p. 616-620.
- Zhou, L., Zhou, Y., Li, M., Chen, P., and Wang, Y., 2000, Experimental modeling study of the adsorption of supercritical methane on a high surface activated carbon: *Langmuir*, v. 16, p. 5955-5959.

**GRAPHIC CORE LOG OF CONASAUGA FORMATION, BIG CANOE CREEK FIELD**

By Ann C. Arnold  
2011

Dawson 34-03-01 Exploratory Core  
Sec. 34, T. 13 S., R. 4 E., 865 FNL, 2346 FWL  
33.864° N. lat., 86.21191 W. long.  
Big Canoe Creek Field  
St. Clair County



**EXPLANATION**

**Rock types**

-  Dolomitic limestone (dominantly peloidal)
-  Interbedded limestone and shale
-  Shale (fissile, laminated)

**Textures**

-  Nodular
-  Stylonodular
-  Conglomeratic
-  Oil stained

**Sedimentary structures**

-  Cross-beds
-  Ripple cross-laminae
-  Horizontal laminae
-  Convolute bedding
-  Flame structures
-  Shale chips
-  Imbricate clasts
-  Coated grains
-  Fenestrae
-  Synaeresis cracks
-  Stylolite (vertical, horizontal)
-  Chert nodule
-  Pyrite (disseminated and nodular)

**Biological structures**

-  Burrows (horizontal, vertical)
-  Lingulid brachiopod
-  Ptychoparioid Trilobite
-  Agnostid trilobite
-  Trilobite fragments
-  Echinoderm ossicles

**Tectonic structures**

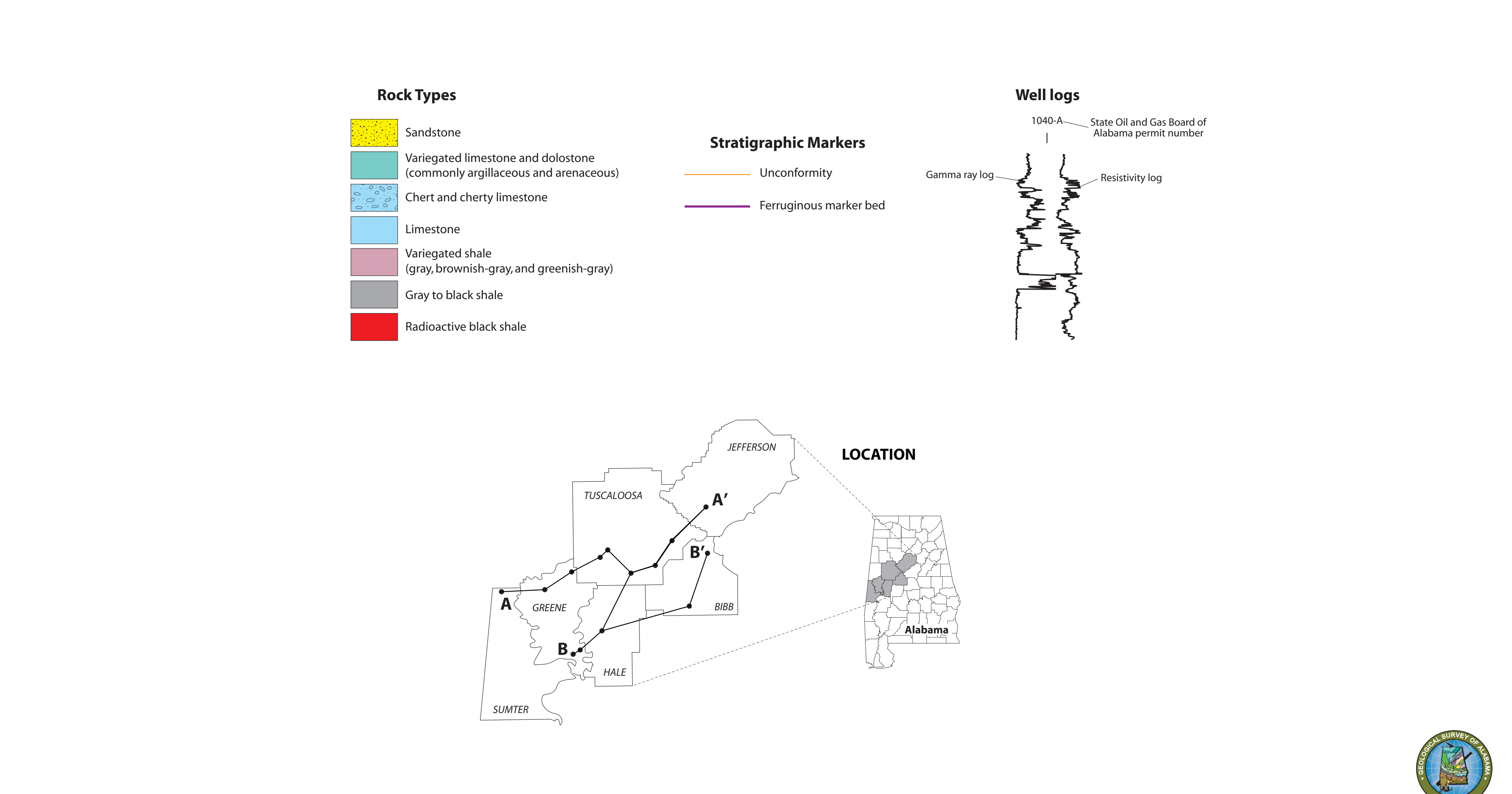
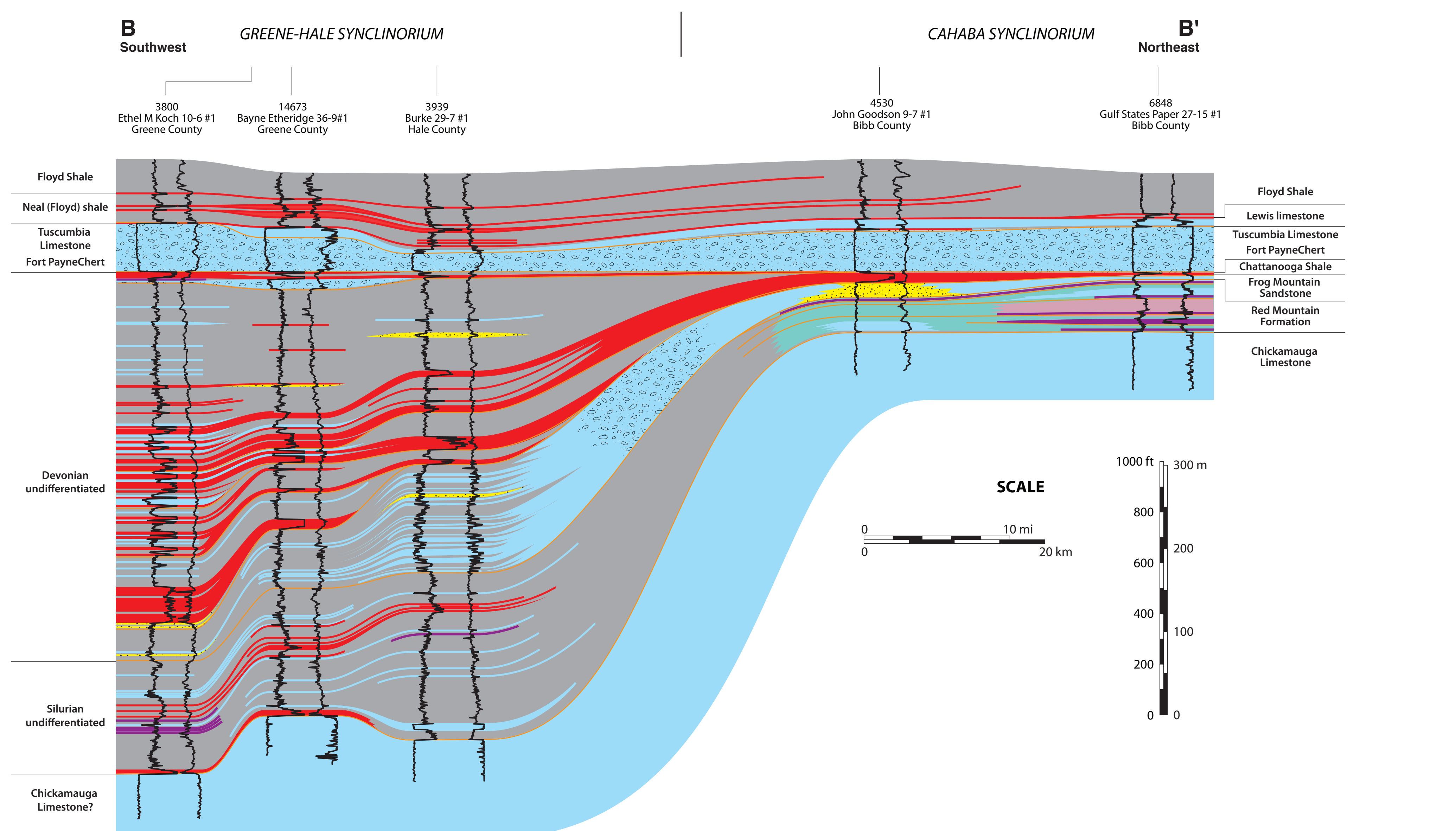
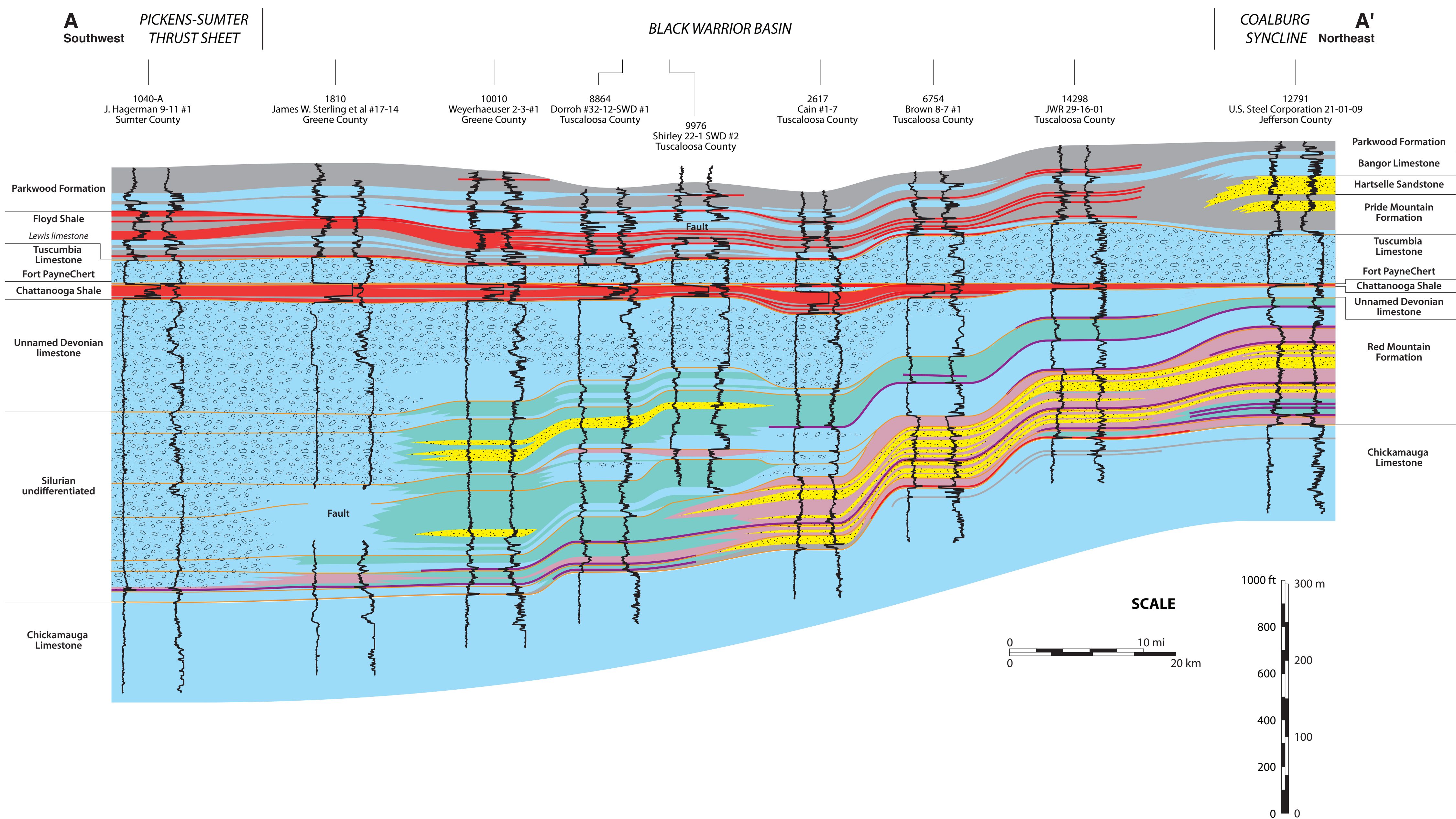
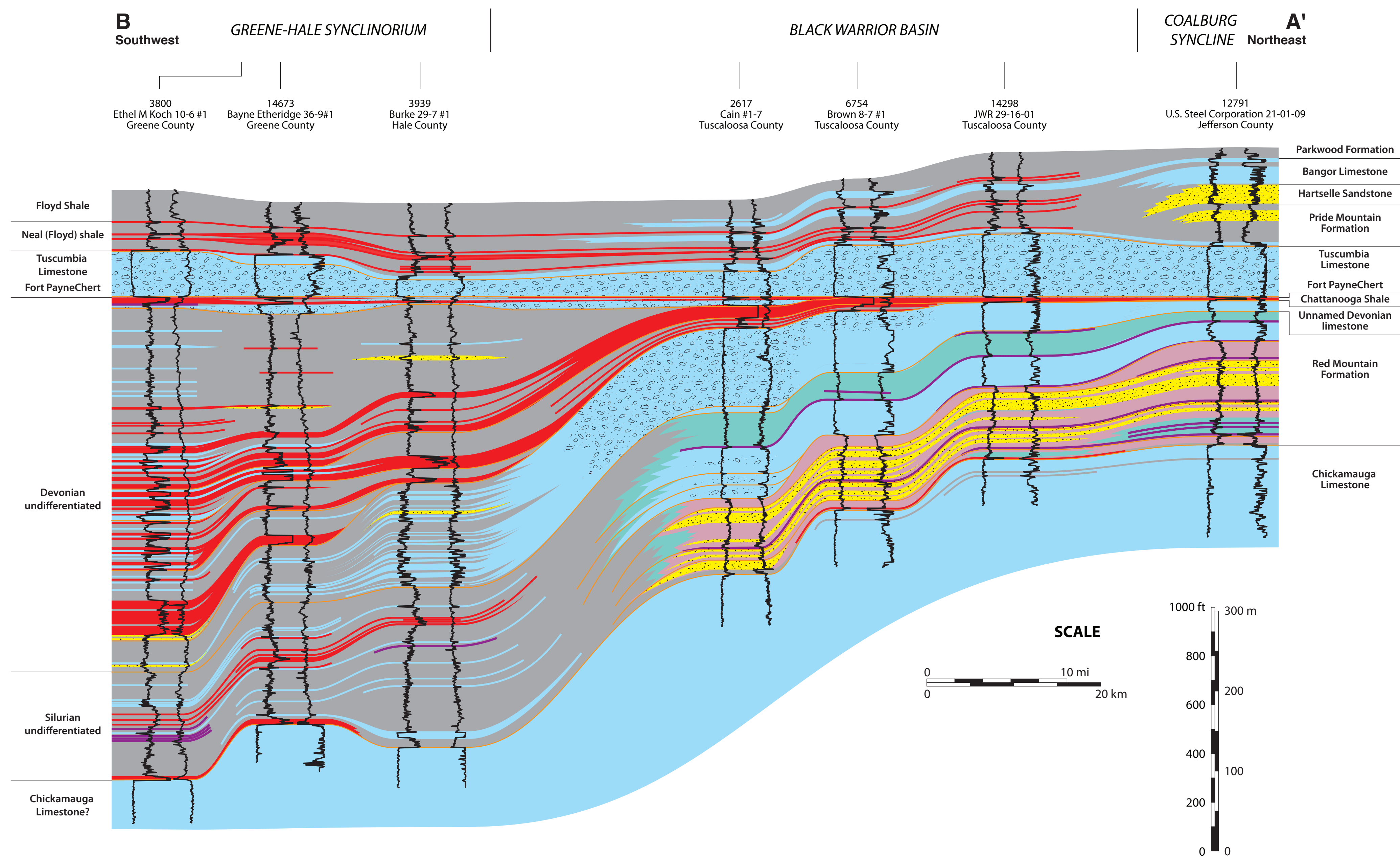
-  Faults and microfaults
  -  Recumbent fold
  -  Open fold
  -  Isoclinal fold
- Note: calcite veins abundant throughout core



Berry H. Tew, Jr.  
State Geologist

STRATIGRAPHIC CROSS SECTIONS OF ORDOVICIAN-MISSISSIPPIAN STRATA IN THE BLACK WARRIOR BASIN AND APPALACHIAN THRUST BELT

by Jack C. Pashin  
2010



STRATIGRAPHIC CROSS SECTION OF DEVONIAN-MISSISSIPPIAN STRATA IN THE BLACK WARRIOR BASIN

by Jack C. Pashin and Denise J. Hills  
2010

A  
North

A'  
South

FRANKLIN COUNTY

MARION COUNTY

LAMAR COUNTY

PICKENS COUNTY

